THE PETROLOGY AND GEOCHEMISTRY OF THE MIDDLE RIVER AREA, CAPE BRETON ISLAND, NOVA SCOTIA

by

Pierre Doucet

Submitted in partial fulfillment of the requirements for the Degree of Master of Science at Dalhousie University, Halifax, Nova Scotia

September 1983

DALHOUSIE UNIVERSITY

FACULTY OF GRADUATE STUDIES

The undersigned hereby certify that they have read and recommend to the Faculty of Graduate Studies for acceptance a thesis entitled " THE PETROLOGY AND GEOCHEMISTRY OF THE MIDDLE RIVER AREA, CAPE BRETON ISLAND, NOVA SCOTIA "

by Pierre Doucet

in partial fulfillment of the requirements for the degree of Master of Science.

Dated September 8, 1983

External Examiner _

Research Supervisor _

Examining Committee _

DALHOUSIE UNIVERSITY

Date September 12, 1983

Author Pierre Doucet

Title THE PETROLOGY AND GEOCHEMISTRY OF THE MIDDLE RIVER AREA, CAPE BRETON ISLAND, NOVA SCOTIA

Department or School GEOLOGY

Degree M.Sc. Convocation FALL Year 1983

Permission is herewith granted to Dalhousie University to circulate and to have copied for non-commercial purposes, at its discretion, the above title upon the request of individuals or institutions.

Signature of Author

TABLE OF CONTENTS

	PAGE
TABLE OF CONTENTS	i
LIST OF MAPS	vi
LIST OF FIGURES	vii
LIST OF TABLES	x
LIST OF PLATES	xii
ABSTRACT	xiv
ACKNOWLEDGEMENTS	xvi
CHAPTER 1 - INTRODUCTION	1
1.1 PRECAMBRIAN ROCKS OF THE CAPE BRETON HIGHLANDS	1
1.2 PREVIOUS WORK IN THE MIDDLE RIVER AREA	10
1.3 OBJECTIVES OF THE STUDY	13
1.4 APPROACH	14
1.5 LOCATION AND ACCESS	15
CHAPTER 2 - LITHOLOGY AND FIELD RELATIONS	17
2.1 INTRODUCTION	17
2.2 MIDDLE RIVER UNIT	18
2.2.1 Metasedimentary Schists and Phyllites	18
2.2.2 Metaconglomerate	21
2.2.3 Metabasite	25
2.2.4 Pelitic and Semipelitic Schists and Gneisses	33
2.2.5 Marble	36

PAGE

2.2.6 Meta-rhyolite and Meta-tuff 42

2.3 EGYPT HIGHLAND UNIT 45

2.3.1 Fine-grained Foliated Granitic Rock 45

2.3.2 Coarse-grained Foliated Granitic Rock 45

2.4 IGNEOUS ROCKS 49

2.4.1 Granodiorite 49

2.4.2 Monzogranite 52

2.4.3 Pegmatite 52

2.4.4 Dykes 55

2.5 CARBONIFEROUS SEDIMENTARY ROCKS 56

2.6 SUMMARY 58

CHAPTER 3 - STRUCTURE 61

3.1 INTRODUCTION 61

3.2 METAMORPHIC FABRIC ELEMENTS 62

3.3 DEFORMATION 65

3.4 SHEARING AND FAULTING 74

3.5 RELATIONSHIP BETWEEN THE FABRIC ELEMENTS 77

3.6 STRUCTURAL MODELS 79

3.7 THRUSTING VERSUS HIGH-ANGLE FAULTING 85

3.8 SUMMARY AND STRUCTURAL SYNTHESIS 90

CHAPTER 4 - PETROGRAPHY 94

4.1 MIDDLE RIVER UNIT 94

4.1.1 Metasedimentary Schists and Phyllites 94

4.1.2 Metaconglomerate 98

4.1.3 Metabasite 101

PAGE

4.1.4 Pelitic and Semipelitic Schists and Gneisses 105
4.1.5 Marble 110
4.1.6 Meta-rhyolite and Meta-tuff 110

4.2 EGYPT HIGHLAND UNIT 112

4.2.1 Fine-grained Foliated Granitic Rock 112
4.2.2 Coarse-grained Foliated Granitic Rock 113

4.3 IGNEOUS ROCKS 115

4.3.1 Granodiorite 115
4.3.2 Monzogranite 117
4.3.3 Pegmatite 119
4.3.4 Dykes 120

4.4 SUMMARY 121

CHAPTER 5 - GEOCHEMISTRY OF THE METABASITES AND METASEDIMENTARY AND GRANITIC ROCKS 124

5.1 INTRODUCTION 124

5.2 GEOCHEMISTRY OF THE METABASITES 124

5.3 GEOCHEMISTRY OF THE METASEDIMENTARY ROCKS 140

5.4 GEOCHEMISTRY OF THE GRANITIC ROCKS 144

CHAPTER 6 - MINERAL CHEMISTRY 153

6.1 INTRODUCTION 153

6.2 CHLORITE ANALYSES 153

6.3 CHLORITOID ANALYSES 157

6.4 MUSCOVITE ANALYSES 163

6.5 BIOTITE ANALYSES 168

6.6 GARNET ANALYSES 178

PAGE

6.7 PLAGIOCLASE ANALYSES 200

6.8 AMPHIBOLE ANALYSES 210

6.9 CALCITE ANALYSES 223

6.10 STAUROLITE, KYANITE AND SILLIMANITE ANALYSES 227

6.11 SUMMARY 230

CHAPTER 7 - METAMORPHISM 235

7.1 METAMORPHIC ASSEMBLAGES 235

7.2 CONDITIONS OF METAMORPHISM 243

7.2.1 Petrologic Data 243

7.2.2 Geothermometry 257

A. Calcite-Dolomite Geothermometry 259

B. Garnet-Biotite Geothermometry 264

7.3 ORIGIN OF THE MIGMATITES AND PEGMATITES 274

7.4 TIMING OF METAMORPHISM 278

7.5 RELATIONSHIP BETWEEN METAMORPHISM AND DEFORMATION 283

7.6 SUMMARY 286

CHAPTER 8 - ECONOMIC GEOLOGY 288

8.1 INTRODUCTION 288

8.2 SECOND GOLD BROOK GOLD MINE 288

8.2.1 History, Development and Production 288

8.2.2 Recent Work 289

8.2.3 Geology and Structure 294

8.2.4 Mineralization 295

PAGE

8.2.5 Metallogenesis 296

8.3 NILE BROOK COPPER PROSPECT 298

8.3.1 Introduction 298
8.3.2 Geology 300
8.3.3 Mineralization 300
8.3.4 Metallogenesis 301

8.4 SARACH BROOK MINERALIZATION 302

8.5 REGIONAL ECONOMIC SIGNIFICANCE 302

CHAPTER 9 - CONCLUSIONS AND RECOMMENDATIONS FOR FUTURE WORK 305

9.1 CONCLUSIONS 305

9.2 RECOMMENDATIONS FOR FUTURE WORK 309

REFERENCES 311

APPENDIX I - ANALYTICAL METHODS 324

APPENDIX II - PETROGRAPHIC SUPPLEMENT 327

LIST OF MAPS

STRUCTURAL MAP	in the back pocket
SAMPLE LOCATION MAP	in the back pocket
GEOLOGICAL MAP	in the back pocket

LIST OF FIGURES

		PAGE
Figure 1.1	Distribution of the "George River Group" in the Cape Breton Highlands	3
3.1	a) Stereoplot of L_{GB1}	66
	b) Stereoplot of L_{GB2}	66
3.2	Stereoplot of D_3 fold and kink axes	71
3.3	a) Stereoplot of S_{GB1} defining an antiform west of Second Gold Brook	72
	b) Stereoplot of S_{GB1} defining an antiform along the western margin of the study area	72
	c) Stereoplot of S_{EHU} defining a synform near Fielding Road	73
3.4	Alternative models for the structure of the Middle River area	80
3.5	Postulated structural model for the Middle River area	84
3.6	Distribution of the Middle River unit illustrating the southward displacement of the complex	89
5.1	Plot of K_2O+Na_2O versus (K_2O/K_2O+Na_2O)	131
5.2	Plot of Niggli c versus mg	134
5.3	Part of the 100mg, c and (al+alk) triangular diagram	136
5.4	Plot of Niggli k versus mg	138
5.5	Delineated compositional fields for chloritoid-bearing metapelites	146

LIST OF FIGURES

(CONTINUED)

		PAGE
6.1	Microprobe traverse across a garnet from sample 8130	190
6.2	Plot of CaO+MnO versus FeO+MgO in garnets	198
6.3	Plot of TiO_2 in hornblende versus TiO_2 in metabasites	222
7.1	Metamorphic map of the Middle River area	242
7.2	Thompson AFM diagrams:	
	a) CHL-BT or CHL-CHLT assemblages	252
	b) CHL-BT-GNT or CHL-CHLT-GNT assemblages	252
	c) BT-GNT assemblage	253
	d) BT-GNT-ST-KY assemblage	253
	e) BT-GNT-KY assemblage	253
7.3	Postulated P-T paths of the southern and central belts of the Middle River complex	258
7.4	Graf and Goldsmith (1955) calcite-dolomite geothermometer	261
7.5	Goldsmith and Newton (1969) calcite-dolomite geothermometer	262
7.6	Thompson (1976) garnet-biotite geothermometer	266
7.7	Goldman and Albee (1977) garnet-biotite geothermometer	267
7.8	Ferry and Spear (1978) garnet-biotite geothermometer	269

LIST OF FIGURES

(CONTINUED)

		PAGE
7.9	$^{40}Ar/^{39}Ar$ age spectra for biotite and hornblende from sample 81120	281
7.10	Inferred relative timing of deformation and metamorphism	284
8.1	Plan section of Second Gold Brook gold mine	290
8.2	Vertical section of Second Gold Brook gold mine	291
8.3	Geology and structure in the area of the Nile Brook copper prospect	299

LIST OF TABLES

			PAGE
Table	4.1	Modes of the Bothan Brook granodiorite and West Branch North River monzogranite	116
	5.1	Major element composition of the metabasites	126
	5.2	Modes of the metabasites	129
	5.3	Major element composition of metasedimentary rocks	142
	5.4	Modes of the pelitic schists and metasedimentary phyllite	143
	5.5	Major and trace element composition of the Egypt Highland unit granitic rocks	148
	5.6	Major and trace element composition of the Bothan Brook granodiorite	149
	5.7	Major and trace element composition of the West Branch North River monzogranite	150
	6.1	Microprobe analyses of chlorites	154
	6.2	Microprobe analyses of chloritoids	159
	6.3	Microprobe analyses of muscovites	164
	6.4	Microprobe analyses of biotites	169
	6.5	Microprobe analyses of garnets	179
	6.6	Microprobe analyses across a garnet from sample 8130	191

LIST OF TABLES

(CONTINUED)

		PAGE
6.7	Microprobe analyses of plagioclase	201
6.8	Microprobe analyses of amphiboles	211
6.9	Microprobe analyses of calcites	224
6.10	Microprobe analyses of staurolites, kyanites and sillimanite	228
6.11	Fe/Fe+Mg ratios of coexisting rocks and minerals	233
7.1	Metamorphic mineral assemblages of the Middle River unit	238
7.2	Calculated equilibrium temperatures from calcite-dolomite geothermometers	263
7.3	Calculated equilibrium temperatures from garnet-biotite geothermometers	271
8.1	Gold production at the Second Gold Brook gold mine	292

LIST OF PLATES

		PAGE
Plate 1.	Polished sample of metasedimentary phyllite	20
2.	Outcrop of metaconglomerate	24
3.	Polished sample of metabasite	27
4.	Contact between a metabasite sheet and surrounding metasedimentary phyllite	30
5.	Contact between medium- and coarse-grained metabasites	32
6.	Polished sample of pelitic schist	35
7.	Polished samples of pure marble	39
8.	Marble samples after staining	39
9.	Polished sample of impure marble	41
10.	Polished sample of flow banded meta-rhyolite	44
11.	Polished sample of foliated granitic rock from the Egypt Highland unit	48
12.	Polished sample of the least deformed rocks of the Egypt Highland unit	48
13.	Polished sample of the Bothan Brook granodiorite	51
14.	Polished sample of the West Branch North River monzogranite	54
15.	Photomicrograph of S_{MR1} enclosed by the dominant S_{MR2}	64

LIST OF PLATES

(CONTINUED)

		PAGE
16.	Mesoscopic kinks in metasedimentary schist	70
17.	Mesoscopic open fold in semipelitic gneiss	70
18.	Photomicrograph of preferentially aligned syntectonic chlorite porphyroblasts	97
19.	Photomicrograph of syntectonic idioblastic chloritoid porphyroblast	97
20.	Photomicrograph of highly poikiloblastic chloritoid porphyroblasts	100
21.	Photomicrograph of preferentially aligned hornblende porphyroblasts	103
22.	Photomicrograph of pre-tectonic kyanite porphyroblast breaking down to fine-grained muscovite	108
23.	Photomicrograph of garnet porphyroblast from sample 8130	188
24.	Photomicrograph of kyanite/staurolite porphyroblast	250

ABSTRACT

The Middle River area of the southern Cape Breton Highlands is underlain by a sequence of interlayered metasedimentary and metavolcanic rocks. The Middle River unit, in the south, consists of two distinct east-west belts. Low- to medium-grade schists and phyllites with thin metabasite sheets form the "underlying" southern belt while high-grade paragneisses form the "overlying" central belt. The Egypt Highland unit, composed of foliated granitic rocks grading into a less deformed granite, makes up a third belt in the northern part of the area.

Four phases of deformation are recognized. The first is associated with a poorly preserved enclosed schistosity found only in the central belt. The second is represented by the principal fabric of the rocks of the Middle River and Egypt Highland units and by east- and west-plunging folds possibly related to the "stacking" of the belts along shear zones. The third and fourth phases are represented by north-trending small- and large-scale folds respectively. A southward and upward movement of the complex along a northeast-southwest mylonite zone and parallel north-south faults produced the observed structural configuration of the Middle River complex.

The grade of metamorphism increases rapidly northward in the southern belt from the biotite zone to the staurolite-kyanite zone. Peak metamorphic conditions reached the kyanite zone in the central belt during D_1 but were subsequently overprinted by garnet zone conditions during D_2. Calculated temperatures from calcite-dolomite and garnet-biotite geothermometers cluster between 500°C and 600°C and reflect these overprinting conditions. $^{40}Ar/^{39}Ar$ ages of 377 ± 9 Ma for biotite and 386 ± 9 Ma for coexisting hornblende from a metabasite sheet in the central belt apparently ascribe the cooling of the sequence during uplift following D_2 to the Middle Devonian Acadian orogeny.

The study area is enclosed by Mississippian sedimentary rocks to the west, a granodiorite of uncertain age to the east, a Devonian monzogranite to the northeast, and deformed volcanic and volcaniclastic rocks to the southeast.

ACKNOWLEDGEMENTS

My sincere thanks go to Dr. Becky Jamieson for originally suggesting this project, and for her advise, support and encouragement throughout its evolution. I wish to thank Drs. Robert Raeside, Clint Milligan and Peter Reynolds for their constructive criticism of this thesis. Discussions with Drs. Dave Craw, Gunter Muecke and A.K. Chatterjee are much appreciated.

I am extremely grateful to Mr. G. Brown for the preparation of thin and polished sections, Mr. R.M. MacKay for his guidance at the electron microprobe, Mr. S. Parich for his assistance in the laboratory and Dr. P. Reynolds and Mr. K. Taylor for their vigil at the argon radiometric clock.

I would like to thank Keith Johnston and Debbie Conrod for their assistance during field work, Doug Meggison for his steady hands at the drafting table, and Norma McKeigan for her help in typing the thesis.

I have the pleasure of acknowledging the hospitality of Mrs. Margaret Arsenault of East Margaree and Mr. and Mrs. Richard Brett (and Dave) for their gracious hospitality during the last few weeks of my stay in Halifax.

Nova Scotia Forest Industries kindly provided access to their extensive road network.

Funding for the research was provided by grants from the Geological Survey of Canada, EMR and NSERC awarded to Dr. R.A. Jamieson; while I was supported by a Dalhousie Graduate Fellowship.

Numerous friends have made my stay at Dalhousie pleasant and memorable. I would like to thank Dave Bailey, Mike Cullen, Marten Douma, Brian Todd, Marie-Claude Blanchard, Mark Williamson and Kathy Gillis for their friendship. I would also like to thank June, Martha, Dave, Mario, Jennifer, Angie, Keith and Doug and a score of other students for all the good times.

Finally, this work is dedicated to my parents, for their love and support, and to June.

CHAPTER 1

INTRODUCTION

1.1 PRECAMBRIAN ROCKS OF THE CAPE BRETON HIGHLANDS

The Cape Breton Highlands form a large block of plutonic and metamorphic rocks centrally located in the Canadian Appalachian belt, yet their geology is poorly understood, and, in fact, much of the Highlands remain classified as undivided gneiss in recent compilations (see Keppie, 1979). Although poor exposure and structural complexity are partly responsible for this lack of understanding, the root of the problem probably arises from the arbitrary assignment of metasedimentary rocks to the George River Group and of metavolcanic rocks to the Fourchu Group.

The George River Group originally referred to crystalline limestone, quartzites and greywackes and their metamorphic equivalents occurring in the Boisdale Hills of central Cape Breton Island, but the designation has expanded to include all unfossiliferous metasedimentary rocks containing crystalline limestone (Kelley, 1967). Weeks (1954) proposed the name Fourchu Group for an assemblage of variously metamorphosed volcanic and

sedimentary rocks underlying the Lower Cambrian (?) Morrison River Formation in southeastern Cape Breton Island. In more recent studies, metamorphosed felsic to intermediate volcanic and volcaniclastic rocks, considered to overlie the George River Group in a number of areas on Cape Breton Island, have been tentatively correlated with the Fourchu Group (Kelley, 1967; Wiebe, 1972; Helmstaedt and Tella, 1972 and 1973). Areas of the Cape Breton Highlands underlain by metasedimentary and metavolcanic rocks that have been ascribed to the George River and Fourchu Groups include the Crowdis Mountain-Middle River area (Kelley, 1967; Milligan, 1970), the Ingonish River-Clyburn Brook region (Wiebe, 1972; Murray, 1977), and the Cape North area (Neale and Kennedy, 1975; Macdonald and Smith, 1980) (Figure 1.1). Unfortunately, the incautious assignment of metasedimentary rocks to the George River Group and of metavolcanic rocks to the Fourchu Group has resulted in a great deal of confusion in the literature when relationships between the metasedimentary and metavolcanic rocks, and between low- and high-grade rocks in the metasedimentary assemblages, are examined.

Although the researchers agree that these metasedimentary and metavolcanic rocks are certainly pre-Middle Cambrian in age, their relative ages and the

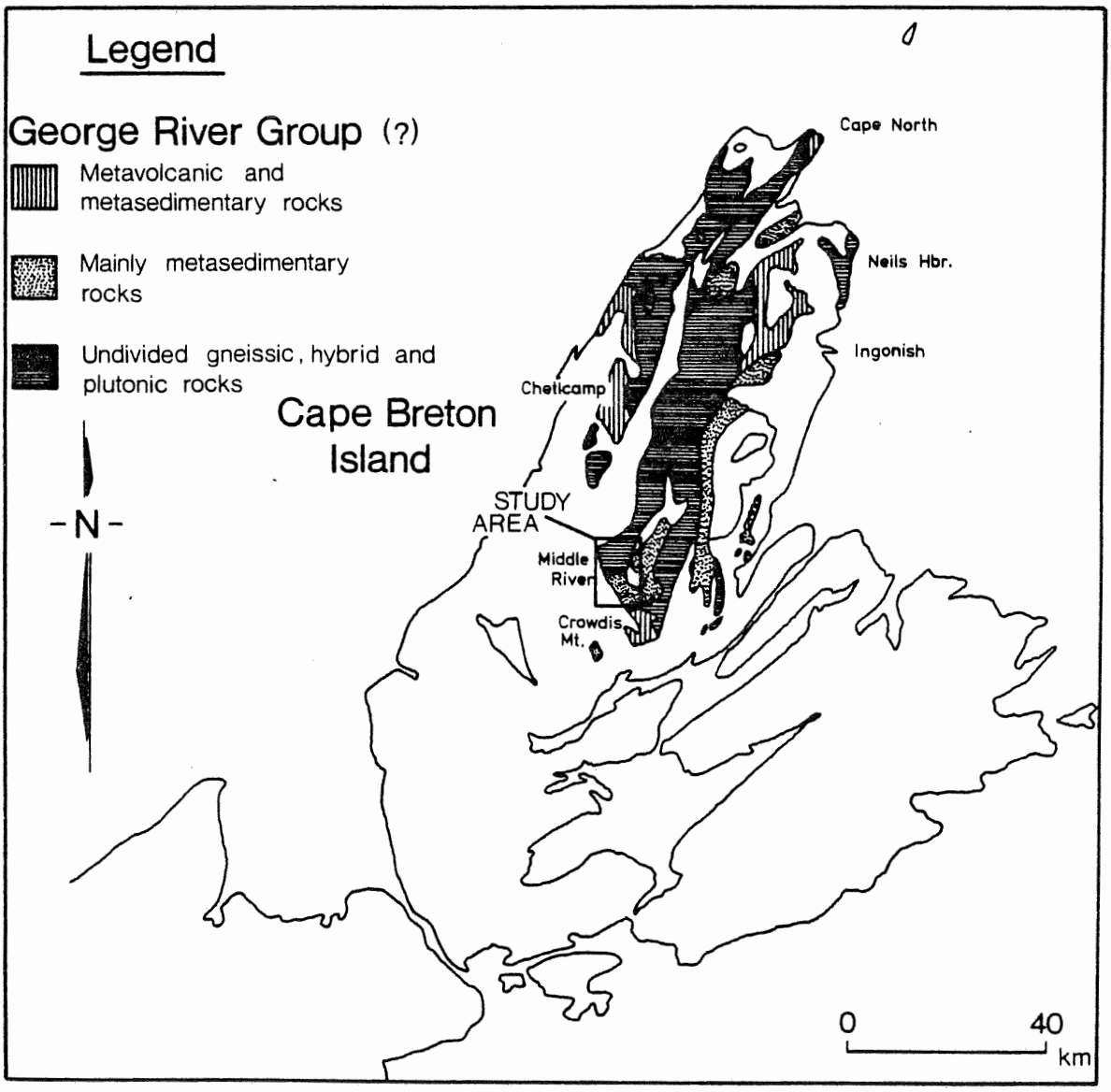

Figure 1.1 Geological map of the Cape Breton Highlands showing the distribution of metasedimentary and metavolcanic rocks arbitrarily assigned to the George River Group in recent studies (modified from Macdonald and Smith, 1980).

structural relationships between them is still unresolved. Weeks (1954) noted the presence of an unconformity between Middle Cambrian rocks and the older George River Group in southern Cape Breton but could not determine a clear structural relationship between George River and Fourchu rocks. In the Ingonish area, Wiebe (1972) showed that "George River" metasedimentary rocks had been deformed, metamorphosed and intruded by mafic to intermediate rocks before the accumulation of "Fourchu Group" metavolcanics.

Milligan (1970) did not recognize any significant structural break between the George River and Fourchu Groups. Helmstaedt and Tella (1972 and 1973), working in southeastern Cape Breton, indicated that the Coxheath volcanics, which they tentatively correlated with the Fourchu Group, were deposited during George River Group sedimentation. Helmstaedt and Tella (1972 and 1973) concluded that the George River and Fourchu Groups are not greatly separated in time, and that they are possibly time equivalents representing different depositional environments.

Wiebe (1973) examined the evidence put forward by Milligan (1970) and Helmstaedt and Tella (1972 and 1973) and considered it "inadequate and unconvincing" and

reasserted his view that the George River Group was deformed, metamorphosed and intruded by igneous rocks prior to the accumulation of the Fourchu Group. On the other hand, Murray (1977) detected no major structural break between the metasedimentary (George River ?) and metavolcanic (Fourchu ?) rock units in the Ingonish River-Clyburn Brook area, and the evidence presented by Wiebe (1972) for an angular unconformity could not be substantiated. The trace of the unconformity coincided instead with a major dip-slip fault with a rotational component (Murray, 1977).

Macdonald and Smith (1980) described a sequence of metasedimentary and metavolcanic rocks in the Cape North area and tentatively interpreted these as equivalent to the George River and Fourchu Groups respectively. They did not recognize an unconformable contact which had been proposed by Neale and Kennedy (1975) but suggested that a conformable relationship exists between the two assemblages.

The relationship between low-grade metasedimentary rocks and higher grade paragneisses in the Cape Breton Highlands is another question confused by the indiscriminant assignment of metasedimentary rocks to the George River Group. Although possible relationships have only

been investigated in a few of the more recent studies, two contrasting conclusions have already been formulated.

Macdonald and Smith (1980) examined low- to medium-grade schistose volcanic and sedimentary rocks (Money Point Group) abutting against medium- to high-grade paragneisses (Cape North Group) in the Cape North area. The apparently older Cape North Group consists of banded semipelitic gneisses, with a distinctive graphitic marble layer and adjacent pelitic gneiss, while the apparently younger Money Point Group consists of pelitic and semi-pelitic schists and pyroclastic and volcanic schists. Macdonald and Smith (1980) documented a rapid increase in the metamorphic grade toward the west, from biotite to kyanite and sillimanite zones, and two episodes of penetrative deformation affecting both the Money Point and Cape North units, with the peak of metamorphism attained during the second phase of deformation. Macdonald and Smith (1980) concluded that the two Groups appear essentially conformable, with no evidence of any erosional or tectonic break between them, and were affected by the same sequence of events.

Currie (1975 and in press) examined a sequence of metasedimentary and metavolcanic rocks in the Cheticamp region but, considering a correlation with George River

and Fourchu rocks too tenuous, assigned regional names to the three assemblages he delineated. The older sequence, the Pleasant Bay complex, consists of a series of biotitic, amphibolitic and granodioritic gneisses with minor marble and anorthosite, and is almost everywhere at amphibolite grade. East of Cheticamp, these rocks are cut by a highly fractured but unfoliated granodiorite complex, termed the Corney Brook complex (Currie, 1975) (Cheticamp pluton in Barr et al., 1979) for which a Rb-Sr isochron age of 530 ± 44 million years has been obtained (Cormier, 1972; recalculated by Keppie and Smith, 1978). The peak of metamorphism of the Pleasant Bay complex, represented by relict kyanite grains encased in muscovite, took place during the emplacement of the Corney Brook complex (Currie, in press). However, the Corney Brook (Cheticamp) pluton has no penetrative fabric (Jamieson, pers. comm., 1983) and therefore was more likely emplaced after the peak of metamorphism of the Pleasant Bay complex.

A younger sequence, consisting of basal bimodal volcanics overlain by black pelite and capped by greywacke, unconformably overlies the granodiorite. These rocks, termed the Jumping Brook complex (Currie, in press), range from sub-greenschist to upper amphibolite facies and have been complexly folded and faulted.

Both the Pleasant Bay and Jumping Brook assemblages had been included in the "George River Series" by Milligan (1970). Currie (1975 and in press) indicated that the Pleasant Bay complex had undergone metamorphism, tensional deformation and dyke intrusion before the emplacement of the granodiorite pluton, and assigned an undetermined but definitely Precambrian age to the Pleasant Bay complex. Dykes cutting the 530 Ma granite and interpreted as feeding basal rhyolite flows of the Jumping Brook complex yielded a U-Pb discordia age of 439 ± 7 Ma (Currie et al., 1982), apparently indicating a Late Ordovician or Silurian emplacement.

Craw (in press) investigated relationships between rocks of different metamorphic grades in the Cheticamp River area. He delineated three north-south belts of metabasic and quartzofeldspathic schists and gneisses with a west-to-east increase in metamorphic grade, and noted a single phase of penetrative deformation in the low-grade western belt as compared to two phases in the medium- and high-grade central and eastern belts. According to Craw (in press), the low-grade belt was farther removed from the medium- and high-grade belts, which followed roughly similar metamorphic paths, than at present, and the sequence in fact represents a stacked assemblage with the low-grade rocks at the bottom. Craw (in press) wrote that the stacking process is probably responsible for the

pervasive fabric in the low-grade belt and the overprinting second fabric in the medium- and high-grade belts, and that peak metamorphic conditions, represented by syn- and post-tectonic kyanite and staurolite, were contemporaneous with the stacking of the three belts. Based on strong similarities between rock types between low- and high-grade belts, and on the parallel and continuous deformational histories of the belts, Craw (in press) indicates that it is highly unlikely that basement rocks are present in the area and he concludes that the three belts represent one or more slices of a single protolithic package.

Whether the paragneisses are high-grade equivalents of adjacent low-grade metasedimentary rocks, as indicated by Milligan (1970), Macdonald and Smith (1980) and Jamieson and Craw (1983), or whether the low-grade rocks rest unconformably on a higher grade "basement complex", as suggested by Neale and Kennedy (1975) and Currie (1975 and in press) may never be resolved.

Work by Kelley (1967), Milligan (1970) and Jamieson (1981) showed that in the Middle River area low-grade metasedimentary rocks, correlated with the George River Group (Kelley, 1967; Milligan, 1970), are closely associated with high-grade metamorphic rocks. A detailed

investigation was undertaken to study the geology of this region and to determine if an unconformable or gradational boundary exists between the low- and high-grade rocks near Middle River. Also, since the Second Gold Brook gold mine is located within the study area, an understanding of the surrounding geology may provide some useful information on the deposit; however, it must be emphasized that this study is not a "metallogenic" investigation of the Second Gold Brook gold and sulphide mineralization.

1.2 PREVIOUS WORK IN THE MIDDLE RIVER AREA

Milligan (1970) investigated the George River Series beginning in 1962. In the Middle River region, he reported a sequence of sedimentary and low-grade metasedimentary rocks which grade into quartz-feldspar-biotite gneisses, the boundary between these arbitrarily set at the garnet isograd. Milligan (1970) described augen gneisses and a red "granitic" rock, occurring farther north, which he suggested were just the para-gneisses with a red feldspar or hematite alteration added. He also noted that the contact between the George River rocks and low-lying Mississippian rocks to the west more or less followed topographic contour lines,

suggesting that the contact may be a nearly horizontal thrust plane very similar to another thrust fault observed in Christopher McLeod Brook about 16 kilometers east of Middle River. Although Milligan's work proved to be a valuable source of information, the region north of Sarach Brook and east of Fionnar Brook was not explored, and rocks above the garnet isograd were lumped together as a single rock type.

Delahay (1979) examined in detail the section along Second Gold Brook and Falls Brook across the southern limit of the Middle River area to determine, among other things, the grade of metamorphism of the assemblage and to examine the evidence presented by Milligan (1970) for a large-scale low-angle thrust fault underlying the region. His investigation showed a gradational regional metamorphic grade from upper greenschist facies in the southeast to middle amphibolite facies in the northwest, and he detected no evidence of any major thrust fault in the section.

Jamieson (1981) carried out reconnaissance mapping in the Crowdis Mountain-Middle River region to examine relationships between the low- and high-grade rocks and to define a basis for correlation between the Cape Breton Highlands and southeastern Cape Breton. She recognized

four units: a southern and eastern volcano-sedimentary sequence, a western and central zone of schists and amphibolites, a northern area of granitic gneisses, and various granitic plutons. Preliminary investigations, centered on the volcano-sedimentary sequence, suggested that these rocks are not part of the George River Group, as indicated by Milligan (1970), and are lower Paleozoic rather than Precambrian in age (Jamieson, 1981).

Jamieson's examination of the schists, amphibolites and gneisses farther north confirmed the northward increase in metamorphic grade and structural complexity of the sequence. Jamieson (unpub. rep., 1981) suggested two contrasting interpretations for the Middle River assemblage: the rocks could be a single sequence with the change in grade attributable to a regional metamorphic gradient increasing toward the northwest, or the low grade rocks in the south could be separated from the higher grade rocks in the north by an as yet unrecognized structural break or unconformity. The first interpretation was favored because of the continuity of the sequence in the Gold Brooks area. Jamieson (unpub. rep., 1981) also compared the Middle River rocks to George River Group sections in the Craignish Hills, Boisdale Hills and Kelly's Mountain regions. Her work showed very few lithological similarities between the Middle River

area and the George River Group and she suggested that the Middle River rocks be considered as a distinct unit until more detailed studies determine some basis for correlation. Jamieson's work forms the basis for this study.

1.3 OBJECTIVES OF THE STUDY

Since the metamorphic rocks of the Middle River area cover a wide range of metamorphic grades, a detailed investigation of the geology of the region may shed some light on the problem of the relationship between these low- and high-grade rocks and those found elsewhere in the Cape Breton Highlands and discussed in section 1.1. The objectives of the present study are:

1. To contribute detailed petrological and geochemical data on metasedimentary and metavolcanic rocks covering a wide range of metamorphic grades in the Middle River area.

2. To establish the relationship between a low-grade schistose assemblage in the south and an adjacent medium- to high-grade gneissic assemblage to the north. Specifically, to determine if the two assemblages form a continuous sequence or are separated by a structural break.

3. To delineate the structural and metamorphic events which have affected the assemblages.

1.4 APPROACH

To meet the objectives of the study, mapping of the area was carried out by the author during the 1981 and 1982 field seasons to define the various lithologies present and to document structural features in the area. Mapping was done at a scale of four inches to the mile (1:15000) using maps derived from aerial photographs. Since the Cape Breton Highlands plateau is essentially devoid of outcrops, traverses were restricted to stream valleys and roads. The final geological map was reduced to a more manageable scale of 1:25000.

About 175 samples, encompassing all the rock types identified, were collected for thin sectioning and detailed petrographic examination. Thirty-two polished sections were obtained from the freshest samples of the major lithologies for microprobe analysis of the various mineral phases. Particular attention was paid to minerals with variable compositions (chlorite, biotite, muscovite, garnet, amphibole and plagioclase) and to calcite for calcite-dolomite geothermometry.

Major element whole-rock compositions for 34 samples, again encompassing the major rock types, were obtained, as were the trace element makeups of the various granitic

rock types present.

Calcite-dolomite and garnet-biotite geothermometers were applied to appropriate samples to define the pressure and temperature conditions of metamorphism. Biotite and hornblende mineral separates were obtained from a metabasite sample for radiometric dating to determine the age of metamorphism.

1.5 LOCATION AND ACCESS

The study area is shown in Figure 1.1. It is located between longitudes 60° 48' and 61° 00' west and latitudes 46° 13' and 46° 23' north on maps 11K2 and 11K7 of the National Topographic System. The region lies at the southwestern edge of the Cape Breton Highlands which rise steeply from the relatively flat farmlands of the Margaree valley. The study area is bounded by Second Gold Brook in the south, Middle River in the east, Lake O'Law in the west and Fielding Road in the north.

The Cabot Trail provides access to the area from the Trans-Canada Highway via exit 7, 10 kilometers west of Baddeck. Two major Nova Scotia Forest Industries gravel roads, used for pulp wood haulage, branch off the Cabot Trail south and north of the study area. Highland

Road, which intersects the Cabot Trail near Hunters Mountain, is situated along the highlands between Middle River and North Baddeck River. It joins Fielding Road at the northeast corner of the study area and continues north; Fielding Road links with the Cabot Trail in Margaree Valley. These roads, capable of withstanding the abuse of large lumbering operations, are regularly maintained and are in excellent condition. Secondary gravel roads, including Egypt Highland Road, form a network along the mountaintops, but these are not as well maintained and are eroded or grown over in certain parts.

CHAPTER 2

LITHOLOGY AND FIELD RELATIONS

2.1 INTRODUCTION

The area bounded by Second Gold Brook in the south, Middle River in the east, Lake O'Law in the west, and Fielding Road in the north is underlain by a complex of metamorphic rocks. These can be divided into two major assemblages, informally referred to in this study as the Middle River unit and the Egypt Highland unit. This broad division reflects major differences in rock types only and has no stratigraphic implications.

The Middle River unit, in the south, comprises low- to high-grade metasedimentary rocks with thin metabasite layers. The Egypt Highland unit, in the north, is composed of foliated granitic rocks. These rocks appear to grade into less deformed rocks near Fielding Road. The Middle River unit is intruded in the east by an elongate granodiorite body. The Egypt Highland unit is cut along its eastern margin by a small monzogranite to granodiorite pluton.

Both units are cut by numerous thin diabase and

rhyolite dykes and are faulted against lower grade metavolcanic rocks and Carboniferous sedimentary rocks to the west. The order of descriptions which follows reflects the general lithological distribution in the study area from south to north.

2.2 MIDDLE RIVER UNIT

2.2.1 Metasedimentary Schists and Phyllites

These rocks are the dominant lithologies in the vicinity of Second Gold Brook, where they are best exposed. In outcrop, they are usually light grey to brown although distinctly greenish casts, indicative of chlorite or green biotite, are present. The rocks consist typically of quartz, chlorite, muscovite (which gives the characteristic silvery sheen to the phyllites), and biotite. They are dominantly fine-grained except for certain distinct layers within the sequence where porphyroblasts of chlorite, biotite, chloritoid and garnet, up to 2 mm in size, are concentrated (Plate 1).

The schists and phyllites exhibit a strongly developed phyllitic schistosity striking east-west and dipping at a shallow to moderate angle to the north. This fabric may be locally deformed, resulting in the formation of open to close mesoscopic folds and kinks

Plate 1. Polished sample of fine-grained porphyroblastic metasedimentary phyllite, with disseminated garnet (reddish-brown) and biotite porphyroblasts, found at the mouth of Second Gold Brook.

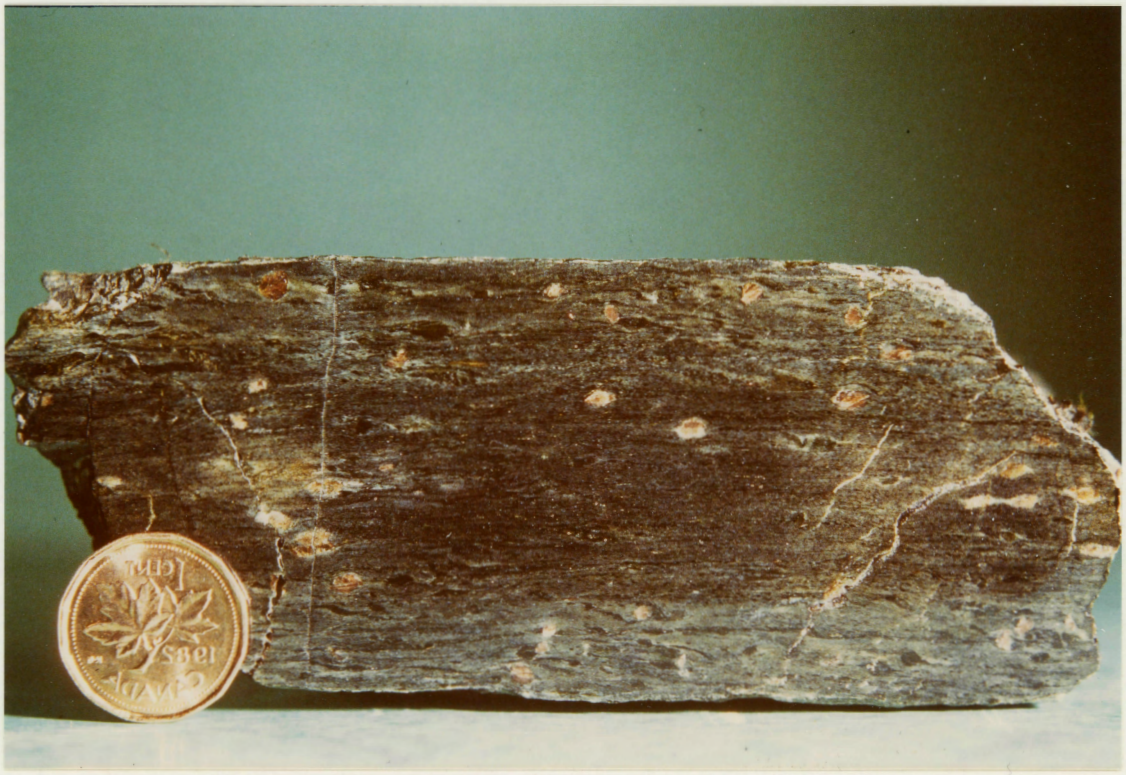

plunging moderately to steeply to the north. Minor fabric elements, best observed along Second Gold Brook, include a northeast-trending, shallowly-plunging chloritic mineral lineation and a very fine crenulation cleavage and associated intersection lineation which also plunge at a shallow angle to the northeast. Although the layering produced by the concentration of porphyroblastic minerals probably represents compositional differences in the original sediments, no definite primary bedding or sedimentary facing directions have been detected in these rocks.

The overall thickness of the assemblage is about 1 km and although the possibility of increased thickness due to folding or faulting exists, the presence of a single layer of metaconglomerate and a single layer of marble (albeit represented by one outcrop near the mouth of Second Gold Brook) suggests that the sequence is not repeated by folding.

2.2.2 Metaconglomerate

Near the northern end of Second Gold Brook, in scattered outcrops along the road leading to the old gold mine, and along Middle River, is a distinctive metaconglomerate layer. The strong deformation of the conglo-

merate is seen in the densely packed and clearly aligned pebbles producing a well-developed northeast-trending lineation. Pebble size is highly variable, from 1 to 5 cm in lenght, although longest dimensions of individual clasts can exceed 15 cm on exposed surfaces (Plate 2). The pebbles make up 40 to 60 percent of the rock and consist of quartzite, siltstone and granite in a fine-grained matrix of quartz, muscovite and biotite. Although masked by the numerous closely spaced pebbles, the schistosity of the matrix is nonetheless visible and is concordant with the foliation of the surrounding schists and phyllites. The reddish elongate granitic pebbles produce a marked red-brown patch or streak on the outcrop surface contrasting sharply with the dark grey to green matrix.

Contact between the metaconglomerate and the adjacent schists and phyllites is gradational and marked by a decrease in the size and number of clasts. A zone in the metasedimentary schists, about 30 m above and below the metaconglomerate layer, is characterized by fine rounded blue quartz grains measuring up to 5 mm in diameter. Milligan (1970) interpreted this zone as representing a transition from a slaty sandstone to the conglomerate proper. The thickness of the metaconglomerate layer is approximately 10 meters.

Plate 2. Highly deformed metaconglomerate occurring along Middle River west of Second Gold Brook. The densely packed pebbles include quartzite (white to pale grey), siltstone (dark grey) and granite (orange to red). Note the small kink in the foliation in the upper right corner.

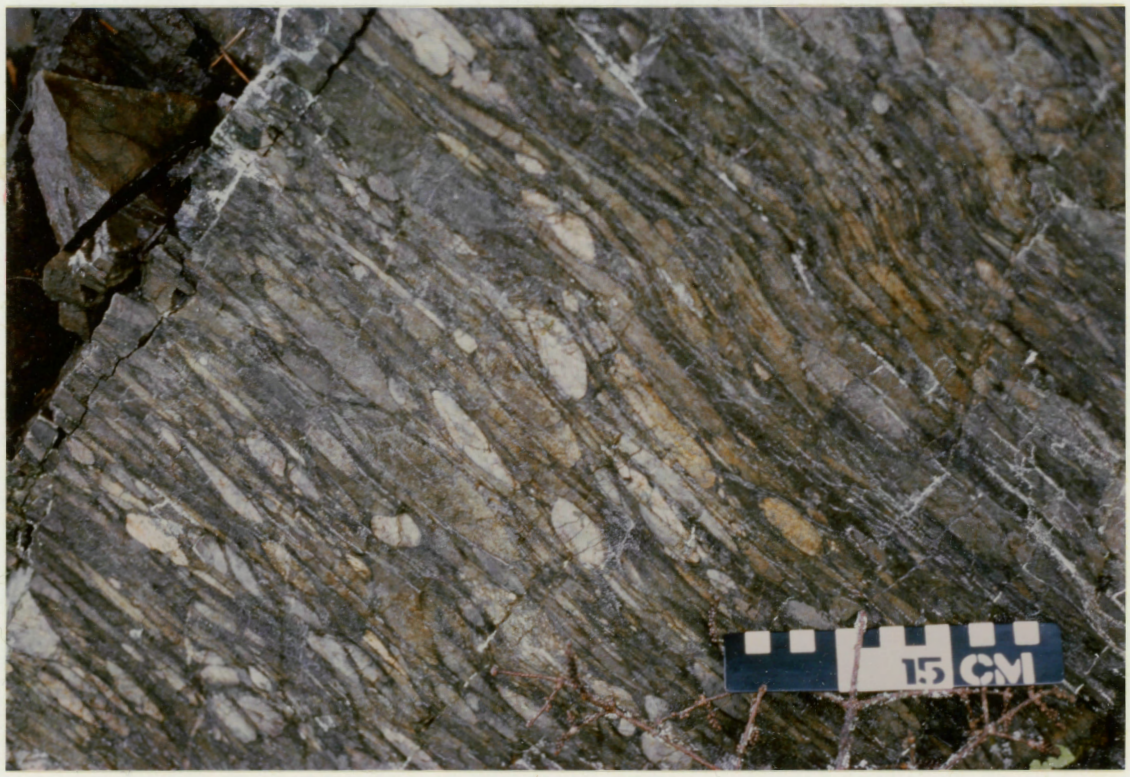
1.5 CM

2.2.3 Metabasite

A series of distinct and seemingly separate metabasite sheets occurs within the metasedimentary sequence. The five southernmost sheets, located between Second and Third Gold brooks, are between 5 and 15 meters thick. A sequence of thick metabasite sheets interlayered with thin metasedimentary layers, with a total thickness of about 800 meters, occurs between Third and Fourth Gold brooks. A number of thin metabasite layers, less than a few meters thick, are present in the pelitic and semipelitic schists and gneisses north of Fourth Gold Brook.

The metabasites, composed of hornblende, quartz and plagioclase, occur as fine- to coarse-grained equigranular rocks having no fabric whatsoever (Plate 3) or, more rarely, as fine-grained porphyroblastic rocks with a pronounced foliation produced by the planar arrangement of large hornblende crystals, which locally define a mineral lineation plunging at a shallow angle to the northeast. All metabasites weather greenish-grey while fresh surfaces are dark greenish black and locally marked by black spots where coarse hornblende crystals occur. Observed contacts between the metabasite sheets and adjacent metasedimentary rocks are sharp and conformable

Plate 3. Polished sample of medium-grained unfoliated metabasite, from Middle River between Second and Third Gold brooks, consisting predominantly of hornblende and intergranular quartz and plagioclase.

with the dominant schistosity (Plate 4).

Milligan (1970) noted definite pillowed structures in one exposure along Fourth Gold Brook but careful examination of the area by this author revealed no such structures. Primary volcanic features, such as phenocrysts or vesicular patterns, have not been detected in the metabasites. The lack of such primary features, coupled with the apparent uniformity of the sheets along strike would indicate that the metabasites represent either decarbonated calcareous or dolomitic shales, very thin basic sills intruded in the metasedimentary sequence, or basic flows or mafic tuffs deposited intermittently between clastic sediment layers.

At one locality along Middle River, between Falls Brook and Third Gold Brook, two distinct metabasites, one coarse-grained and the other medium-grained, are in contact with one another. The contact, which is at a high angle to the dominant fabric of the surrounding metasedimentary rocks, is marked by what appears to be a chilled margin in the finer grained metabasite (Plate 5). The two metabasites may replesent separate sills or perhaps a sill intruded into a consolidated sediment or flow or tuff layer.

Plate 4. Contact between a fine-grained metabasite sheet (bottom) and the metasedimentary phyllite (top), from an outcrop along Middle River between Second Gold and Falls brooks. The contact, marked by vegetation in the centre of the picture, is concordant to the foliation of the phyllite.


15 CM

Plate 5. Contact between a coarse-grained metabasite (right) and a medium-grained metabasite (left), from Middle River between Falls Brook and Third Gold Brook. The contact is apparently marked by a chilled margin in the medium-grained metabasite. The metabasites may represent separate sills or flows or a sill intruded into a consolidated sediment or mafic flow or tuff layer.

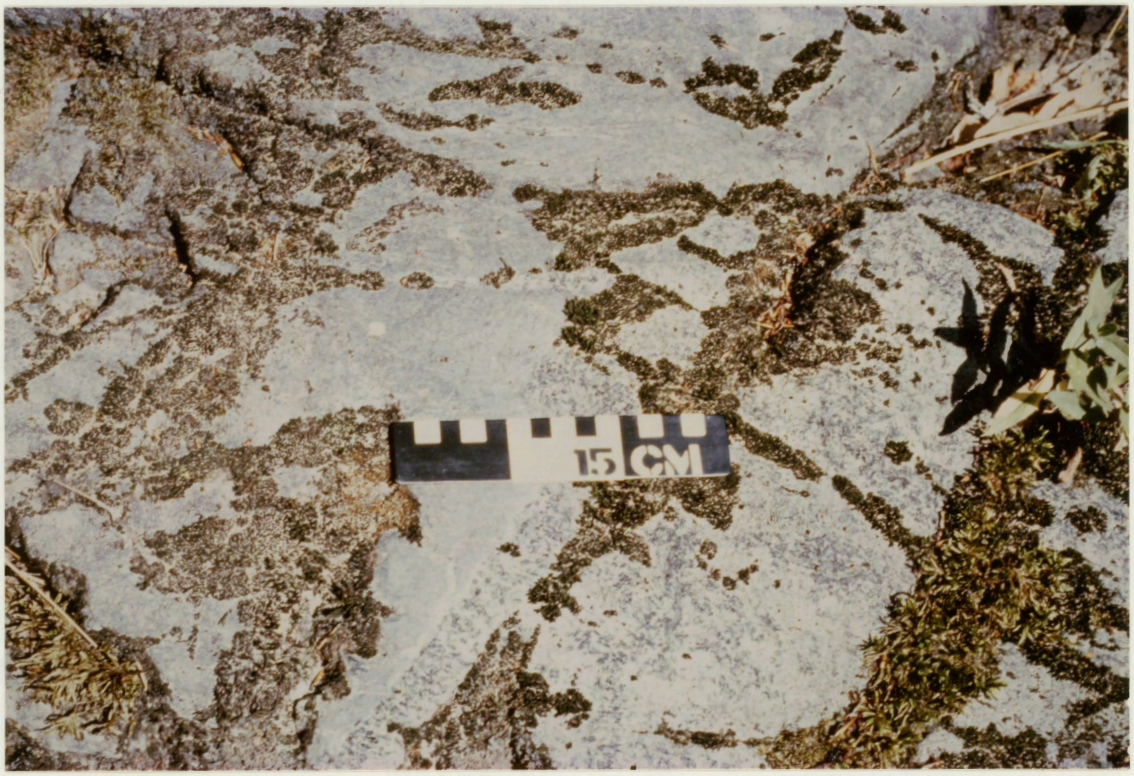
15 CM

2.2.4 Pelitic and Semipelitic Schists and Gneisses

Dominating the northern half of the Middle River unit is a sequence of interlayered pelitic and semipelitic rocks. Two distinct types occur within this assemblage which is best exposed along Middle River north of Fourth Gold Brook. The first type is a dark brown medium-grained quartz-biotite-muscovite-plagioclase schist. Numerous large garnets, up to 1.5 cm in diameter, are present in many layers (Plate 6) and the presence or absence of garnet appears to reflect compositional variations on a small scale. The second type is a black and white, slightly foliated, fine-grained gneiss composed of quartz, plagioclase and biotite. Contact relationships between the two rock types are nowhere seen but are probably sharp because of the different mineralogy of the two rock types.

Compositional banding, with individual mafic and felsic layers measuring between 0.5 and 5 cm thick, is best observed in the coarser grained schists, and was interpreted by Milligan (1970) as original compositional layering in the sediment. Polyphase deformation, metamorphic recrystallization, and the presence of pegmatite lenses and laminae within the foliation suggest that the layering is actually secondary and the result of meta-

Plate 6. Polished sample of medium-grained pelitic schist (sample 8247), from Middle River between Fourth Gold and Duncan brooks. The quartz-biotite-muscovite-plagioclase schist contains large garnet porphyroblasts (red) as well as disseminated kyanite and staurolite grains.

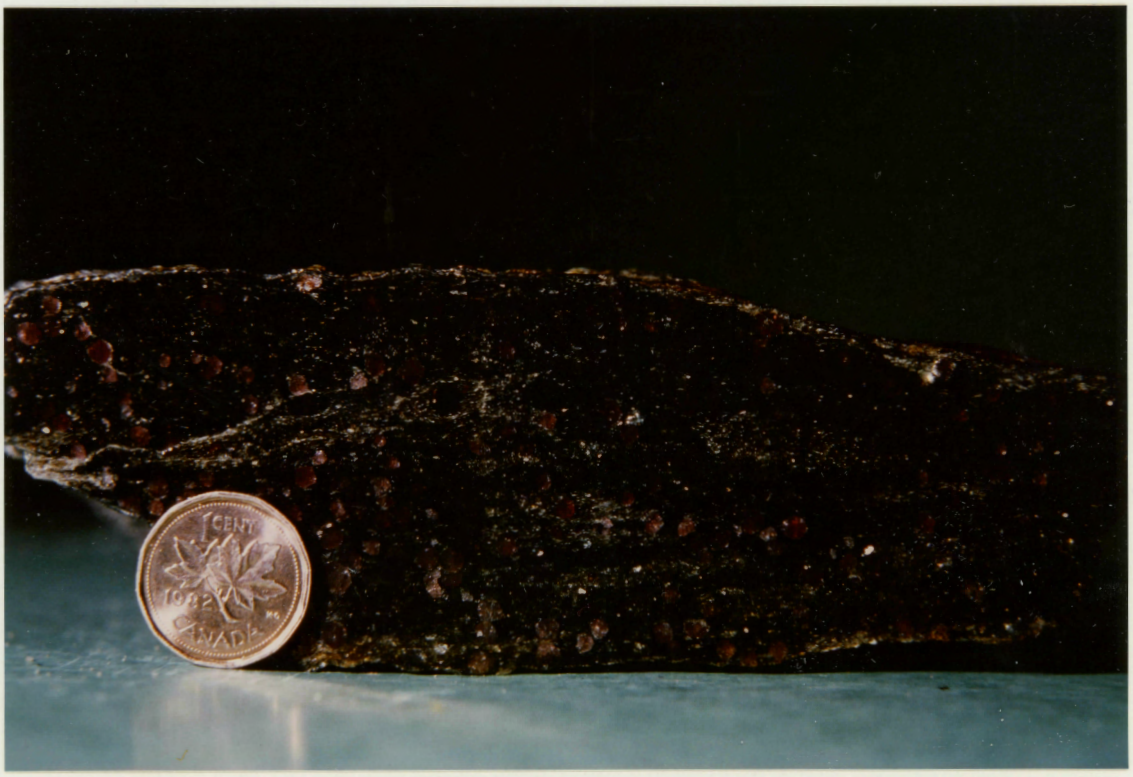
CENT
1982
CANADA

morphic segregation.

The major fabric, represented in these rocks by a schistose or gneissic foliation, strikes east-west and dips moderately to the north. Mesoscopic open to close folds and kinks are not as common as in the metasedimentary schists and phyllites but, where present, plunge moderately to the northeast. Three close synformal and antiformal folds, several tens of meters wide, plunging at shallow angles to the east and west, have been recognized.

Contact between the gneissic rocks and the schists and phyllites is nowhere observed and the two assemblages are separated by a zone of coarse-grained granitic pegmatite along Middle River north of Fourth Gold Brook. The measured thickness of the sequence is about 5.3 km but the presence of small- and large-scale folding indicates tectonic repetition has thickened the original sequence to an unknown extent.

2.2.5 Marble

A thin, east-west trending marble layer is located within the gneisses along Middle River north of Sarach Brook. The marble is snow white, pure, coarse-grained,

with individual crystals of calcite and dolomite up to 5 mm in size visible on fresh surfaces (Plate 7). Proportions of calcite and dolomite are approximately equal and staining with Alizarin red S (following the procedure described in Friedman, 1959) shows that the two minerals occur in discrete bands (Plate 8), concordant with the foliation of the surrounding gneisses, that may represent primary compositional layering or, more probably, metamorphic segregation. The thickness of the marble layer is about 15 meters. Numerous thinner layers of marble, ranging in thickness from a few centimeters up to a few meters, are found adjacent to the main layer and in the upper part of Fionnar Brook.

Along Middle River, near Second Gold Brook, is a single outcrop of fine-grained impure marble. Unlike its counterpart in the north, this marble is pink with faint discontinuous greyish streaks and swirls (Plate 9). Its thickness is about 1.5 meters.

Contacts between the gneiss and marble layers, both thick and thin, and between the phyllites and marble near Second Gold Brook are sharp and concordant with the major foliation of the surrounding lithologies.

Plate 7. Polished samples of pure coarse-grained dolomitic marble from the thick layer along Middle River north of Sarach Brook.

Plate 8. Dolomitic marble samples after staining with alazarin red S. Distinct layers of calcite (red) and dolomite (white) are concordant to the foliation of the surrounding metapelites but most likely result from metamorphic segregation rather than primary compositional bedding.

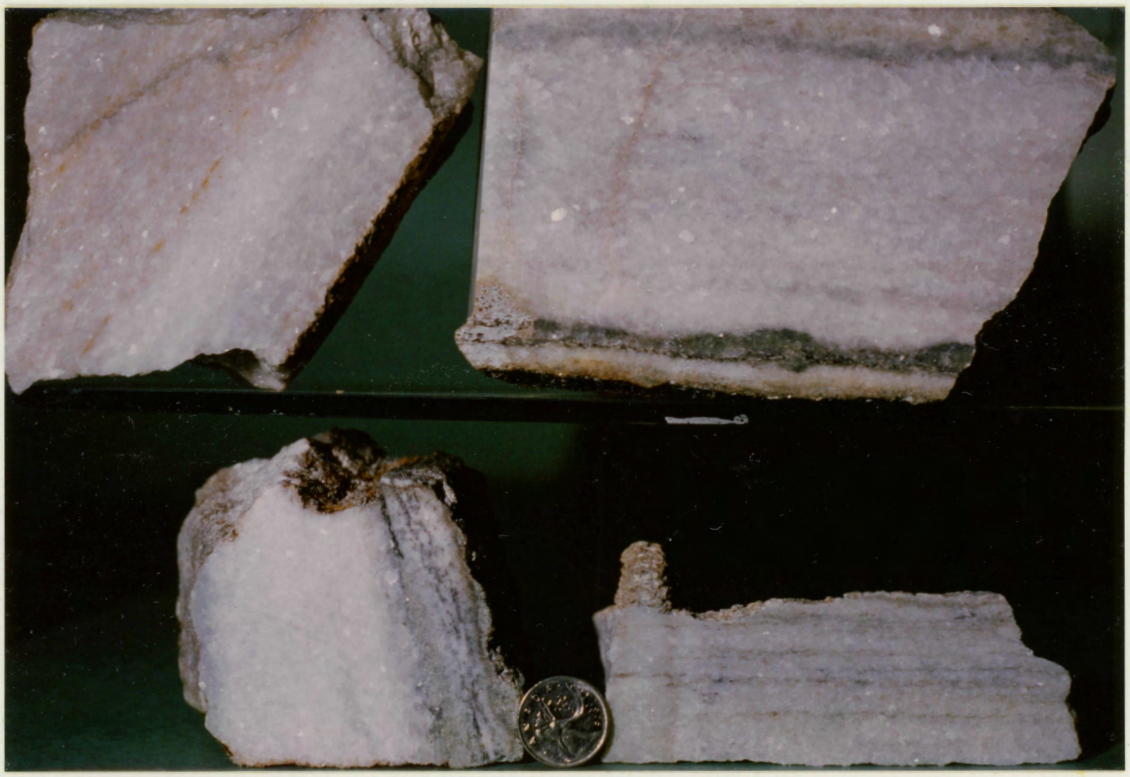

Plate 9. Polished sample of impure marble from the outcrop along Middle River near Second Gold Brook. The marble is composed of fine-grained calcite and dolomite with minor quartz, muscovite and magnetite.


1982
CANADA

2.2.6 Meta-rhyolite and Meta-tuff

A distinctive siliceous rock, believed to be a deformed rhyolite flow, is found along a small unnamed brook draining into First Lake O'Law, about 3.4 km north of Fortune Brook. The meta-rhyolite is dark pink to brown in color, on both fresh and weathered surfaces, with very thin flow banding, and is composed of fine-grained quartz with small disseminated plagioclase and quartz phenocrysts (Plate 10). Although the flow banding is in places highly contorted, its overall orientation follows the general east-west strike and moderate to steep northerly dip of the surrounding metabasites.

Contact relationships between the meta-rhyolite and the adjacent metabasites are not observed. The thickness of the flow could not be determined because of poor exposure, possible repetition by folding and the roughly parallel-to-strike nature of the traverse along that particular brook. A thickness of about 95 m can be deduced in the field but the flow may be much thicker.

Throughout the Middle River unit are thin concordant layers of felsic meta-tuffs (?). Typically, they are fine-grained, with small quartz and plagioclase phenocrysts, massive although locally finely laminated, and

Plate 10. Polished sample of flow banded meta-rhyolite, from the unnamed brook located about 3.4 km north of Fortune Brook, composed of fine-grained quartz and disseminated quartz and plagioclase phenocrysts. The sample shows both flow banding and shearing (near the bottom of the sample).


1 CENT
1982
CANADA

commonly strongly jointed. The rock weathers white, pink or buff but is very resistant to erosion. The layers are usually less than one meter thick and are in sharp contact with the adjacent phyllites, schists or gneisses.

2.3 EGYPT HIGHLAND UNIT

2.3.1 Fine-grained Foliated Granitic Rock

A fine-grained, pale pink, potessium feldspar-quartz-plagioclase-biotite rock is the principal lithology north of South Nile Brook where it is best exposed. A slight schistosity in the rock is defined by thin discontinuous bands of fine biotite flakes and is much better defined than in interlayered coarse-grained augen-rich rocks. Contact relationships between the granitic rocks of the Egypt Highland unit and the gneisses of the Middle River unit to the south are not observed because of poor exposure. However, as will be discussed in Chapter 3, the two units are believed to be separated by a major tectonic break.

2.3.2 Coarse-grained Foliated Granitic Rock

Making up the remainder of the Egypt Highland unit is a medium- to coarse-grained, dark red, potassium feldspar-quartz-plagioclase rock with distinctive

K-feldspar augen up to 1 cm in diameter (Plate 11). The medium-grained quartz and plagioclase, with trace amounts of biotite, produce a poorly developed fabric which wraps around the subrounded to angular augen. This foliation gradually diminishes northward until it is no longer visible near Fielding Road (Plate 12). Although occurring as relatively thin bands throughout the Egypt Highland unit, the augen-rich rock is best observed in the northern section of Nile Brook where it forms a broad continuous band. Contacts between the fine- and coarse-grained granitic rocks are gradational over a thickness of a few meters.

The Egypt Highland unit strikes roughly east-west and dips steeply to the north except near Fielding Road where the foliation swings to the northwest in the west and to the northeast in the east, forming a concentric structure encircling the least deformed granitic rocks. Both rock types are cut by numerous narrow zones of greyish-black, very fine-grained micaceous schist that may represent small shear zones. Concentrated along Nile Brook, the zones, usually less than 5 meters thick, generally strike north to northeast and dip steeply. The thickness of the Egypt Highland unit is about 5 km but repetition by folding and faulting is probable.

Plate 11. Polished sample of the foliated rocks of the Egypt Highland unit, from Nile Brook. The sample contains medium- to coarse-grained K-feldspar augen wrapped around by the poorly-developed foliation defined by recrystallized quartz and biotite.

Plate 12. Polished sample of the least deformed rocks of the Egypt Highland unit, from the northern section of Nile Brook near Fielding Road. The quartz-plagioclase-K-feldspar-biotite rock is fractured yet not foliated.


1 CENT
1982
CANADA


1 CENT
1982
CANADA

Milligan (1970) suggested that these granitic rocks resulted from the alteration of the grey paragneisses by red feldspar or hematite, based on the presence of red alteration adjacent to fractures and large feldspar porphyroblasts forming a halo around granodioritic dykes cutting the gneisses. Detailed petrographic examination of the foliated granitic rocks, described in Chapter 4, reveals that these rocks are deformed intrusions rather than "granitized" metasedimentary rocks.

2.4 IGNEOUS ROCKS

2.4.1 Granodiorite

A distinctive north-south trending granodiorite occupies the eastern margin of the study area and is informally termed the Bothan Brook granodiorite. It is medium-grained, salmon pink and white, and composed of equigranular quartz, plagioclase and minor potassium feldspar with few mafic minerals (Plate 13). The granodiorite appears to intrude the Middle River unit to the west but no definite contact relationship is detected and the possibility that the two are fault-bounded cannot be dismissed. Although the feldspars are highly altered, giving the rock its uncharacteristic reddish color, the rock does not show any metamorphic foliation and appears undeformed except for a narrow mylonite band along its

Plate 13. Polished sample of the Bothan Brook granodiorite (sample 8248), from the upper reaches of Fourth Gold Brook. The granodiorite is composed of medium-grained plagioclase (pink, the anomalous color due to extensive hematization), quartz and minor K-feldspar and chloritized biotite.

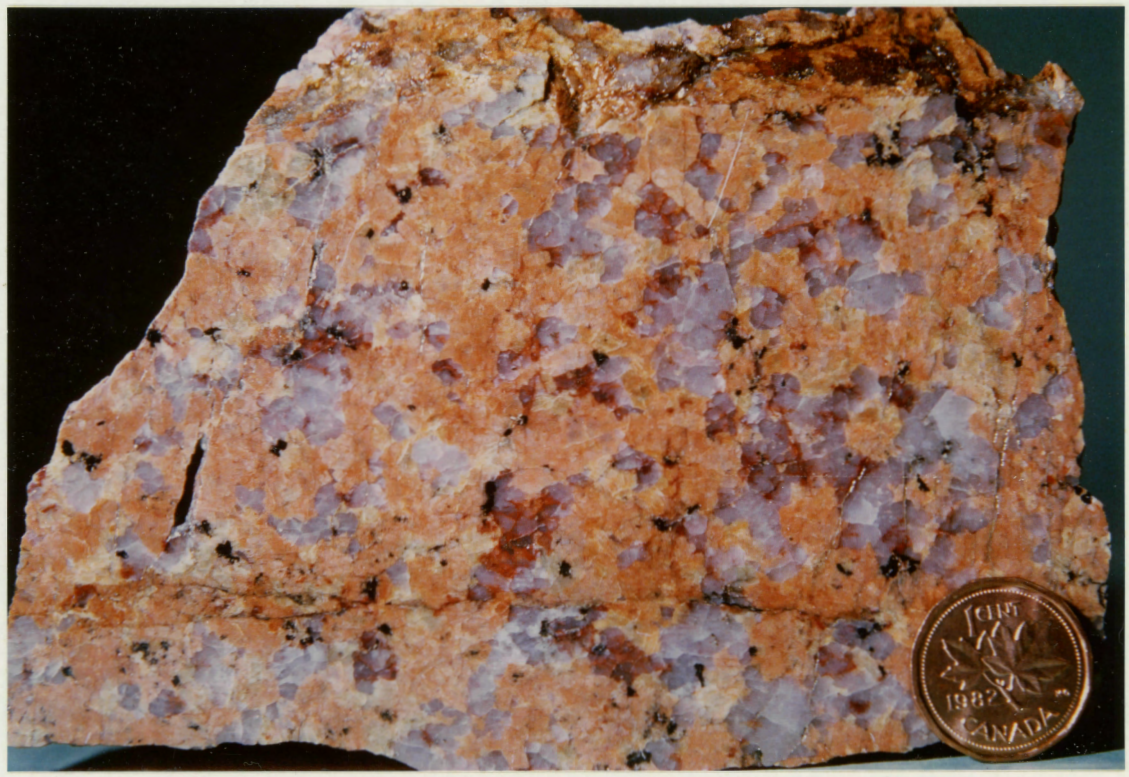
1982
CANADA

northeastern edge.

2.4.2 Monzogranite

Near the intersection of Fielding and Highland roads is a black and white monzogranite to granodiorite, informally termed the West Branch North River monzogranite. It is composed of disseminated K-feldspar crystals in a medium-grained groundmass of plagioclase, hornblende, boitite and quartz (Plate 14). The monzogranite does not show any metamorphic fabric in the study area. However, a measurable northeast-striking foliation has been observed east of Highland Road (Jamieson, pers. comm., 1983). Although no contact relationships are observed, the monzogranite appears to be, at least locally, in fault contact with the granitic rocks of the Egypt Highland unit. Contact between the West Branch North River monzogranite and the Bothan Brook granodiorite is nowhere detected because of very poor exposure but the two appear to be separated by a narrow mylonite zone.

2.4.3 Pegmatite

Late granitic pegmatite veins and pockets are found throughout the study area north of Third Gold Brook but their concentration clearly increases toward the north

Plate 14. Polished sample of the West Branch North River monzogranite, from Fielding Road near Highland Road. The monzogranite is made up of medium-grained quartz, plagioclase, hornblende and biotite with minor disseminated K-feldspar (pale red). Although dominantly unfoliated, the West Branch North River pluton rarely shows a slight fabric.

as the granitic rocks of the Egypt Highland unit are approached. The pegmatites are pale pink and composed of plagioclase, quartz, potassium feldspar and scarce muscovite books up to 2 cm in diameter.

The pegmatites vary considerably in size and texture. The smallest, only a few centimeters thick, are medium-grained equigranular stringers or layers concordant with the gneissossity of the surrounding rocks or, less commonly, cutting across the foliation. The largest, up to 10 meters thick, form medium- to coarse-grained dykes and pockets at the confluence of Sarach Brook and Middle River where pegmatite is the dominant rock type.

These late medium- to coarse-grained granitic pegmatite veins and pockets are not to be confused with thin, concordant or ptygmatically folded, fine-grained, white, quartz-plagioclase leucosomes derived from metamorphic segregation found within the gneisses of the Middle River unit.

2.4.4 Dykes

A number of late dykes cut across the region in a north-south to northeast-southwest direction. Fine-grained, equigranular, dark green to black diabase dykes,

up to 3 meters thick, dominate. A medium-grained, equigranular, black, ultramafic dyke, measuring less than 1 meter thick, intrudes the gneisses of the Middle River unit 3 km south of Ryan Brook. A pale red porphyritic rhyolite dyke, less than 1 meter thick, cuts across the West Branch North River monzogranite along Middle River about 2.5 km south of Fielding Road. The rhyolite dyke may be related to the large granite plutons of the area but very poor exposure in the immediate vicinity of the dyke precludes confirmation of any relationship. The various dykes are apparently undeformed but they may be altered.

2.5 CARBONIFEROUS SEDIMENTARY ROCKS

The western margin of the study area, between the Cabot Trail and the edge of the Cape Breton Highlands, is underlain by rocks belonging to the Horton Group. Of the various lithologies making up the Horton Group (see Kelley, 1967), only red conglomerate and red sandstone are present in the study area. The conglomerate, best exposed along the lower section of Fortune Brook, is composed of rounded to subangular cobbles of granite, quartzite and limestone, up to 20 cm in diameter, in a red to brown matrix containing fine granules of quartz and feldspar. The sandstone, best exposed along an

unnamed brook 1.5 km south of Ryan Brook, consists of fine rounded to subrounded grains of quartz bound by a red iron-stained quartz cement. Both the conglomerate and the sandstone are flat-lying, or dip very slightly to the north.

Contacts between Mississippian sedimentary rocks and older rocks in other parts of the Cape Breton Highlands are steep faults, rare thrusts (Currie, 1977) or unconformities. Milligan (1970) indicated that the metamorphic complex of the Middle River area may be thrust over the Mississippian rocks but his work yielded conflicting evidence and he could not formulate a definite relationship. Delahay (1979) found no evidence of a thrust plane in the Second Gold Brook area but since the brook is far removed from the contact, a low-angle fault plane would pass at some depth under it and would not be detectable.

The evidence gathered during this study (discussed in Chapter 3) indicates that a high-angle fault occurs near the edge of the Highlands in the Middle River area. The presence of such a fault suggests that a low-angle thrust plane under this part of the Highlands is unlikely. Whether the very edge of the Highlands is marked by a second high-angle fault or whether the Horton Group

rocks unconformably overlie the Middle River complex cannot be definitely resolved. However, the relative straightness of the Highlands plateau, the abruptness of the rise in elevation between the Margaree valley and the plateau and the low-lying attitude of the sedimentary rocks all point to the first interpretation.

2.6 SUMMARY

The study area is underlain by a complex of metamorphic rocks which have been divided into two assemblages. The Middle River unit in the south consists of low- to medium-grade metasedimentary rocks with thin metabasite layers. Fine-grained schists and phyllites with a distinct metaconglomerate layer are found in the vicinity of Second Gold Brook while medium-grained mica-rich schists and gneisses dominate to the north. Fine- to medium-grained, equigranular or rarely porphyroblastic, metabasite sheets, fine-grained massive meta-tuff layers (?) and a deformed rhyolite flow make up the remainder of the Middle River unit. A thin marble layer occurs within the gneisses along Middle River north of Sarach Brook. Isolated outcrops of marble also occur along Middle River near Second Gold Brook and in the upper part of Fionnar Brook. Contacts between these various lithologies are sharp except for the metacon-

glomerate layer which grades into the surrounding phyllites.

The Egypt Highland unit in the north is made up of a thick sequence of granitic rocks. Two types can be distinguished: a fine-grained pale pink moderately foliated rock and a coarser grained dark red poorly foliated rock with distinctive K-feldspar augen. Contacts between the two types are gradational. The rocks appear to grade into less deformed granitic rocks near Fielding Road. The Egypt Highland unit is cut by numerous zones of fine-grained dark grey schist that may be small shear zones.

Contact between the Middle River and Egypt Highland units is nowhere seen but is believed to be a major tectonic break. Both units strike roughly east-west and dip moderately to steeply north, except near Fielding Road where the foliation forms a concentric structure around the least deformed granitic rocks. A large-scale fold along Middle River west of Second Gold Brook plunges moderately to the north. A number of large-scale synformal and antiformal folds, plunging at shallow angles to the east and west, have been recognized in the gneisses of the Middle River unit. Mesoscopic folds and kinks plunging moderately to steeply to the north deform

all lithologies but are best developed in the schists and phyllites. Minor fabrics, which include a northeast-trending mineral lineation and a crenulation cleavage, are best observed along Second Gold Brook. No sedimentary facing direction has been identified.

The Middle River unit is cut along its eastern margin by a medium-grained salmon pink granodiorite, informally termed the Bothan Brook granodiorite. In the northeast corner of the study area, near the junction of Fielding and Highland roads, is a medium-grained monzogranite, informally termed the West Branch North River monzogranite. It appears to be, at least locally, in fault contact with the Egypt Highland unit. Numerous diabase and rare rhyolite and ultramafic dykes, trending northeast-southwest, cut all rock types.

The western margin of the study area is underlain by Horton Group conglomerates and sandstones.

CHAPTER 3

STRUCTURE

3.1 INTRODUCTION

The structure of the Middle River area is fairly complex despite the apparently simple outcrop distribution. This distribution pattern, where outcrops are essentially restricted to stream valleys and scattered roadside occurrences, results in poor overall exposure and makes correlation, even across short distances, difficult. The fact that many of the brooks appear to be fault-controlled further hinders any attempts to interpret the structure of the area.

Six separate phases of deformation have been identified in the study area although they are best observed in the south of the region where early structures are preserved. Two major north-south trending faults are located along the eastern and western margins of the metamorphic complex. A narrow shear zone, the Sarach Brook mylonite zone, cuts across the Bothan Brook granodiorite in a northeast-southwest direction. Minor faults, joints and small localized shear zones trend north-south to northeast-southwest across the east-west structural

fabric.

3.2 METAMORPHIC FABRIC ELEMENTS

The principal planar element is a strongly developed micaceous foliation ranging from a phyllitic schistosity in the south, S_{GB1}, to a gneissic foliation in the north, S_{MR2}. In a few isolated occurrences in the pelitic and semipelitic rocks in the north, the gneissic foliation wraps around and encloses an early isoclinally folded schistosity, S_{MR1} (Plate 15). The Middle River unit strikes east-west and dips moderately, in the south, to steeply, in the north, north to northwest (see the Structural Map in the back pocket). The poorly-developed foliation of the Egypt Highland unit rocks, S_{EHU1}, strikes northwest in the west and northeast in the east and dips steeply to the north. The scatter in orientation, especially in the extreme south and north, is due to the effect of later small- and large-scale folding.

A well-developed lineation, defined by the elongated pebbles in the metaconglomerate, plunges moderately to the northeast. Alignment of chlorite crystals in the schists and phyllites and of hornblende porphyroblasts in the metabasites produces a mineral lineation, L_{GB1}, that plunges slightly to moderately to the northeast

Plate 15. Photomicrograph of the early isoclinally folded schistosity, S_{MR1}, wrapped around by the dominant foliation, S_{MR2} (vertical schistosity at right), in a pelitic schist of the Middle River unit. (Magnification x25; crossed nicols.)

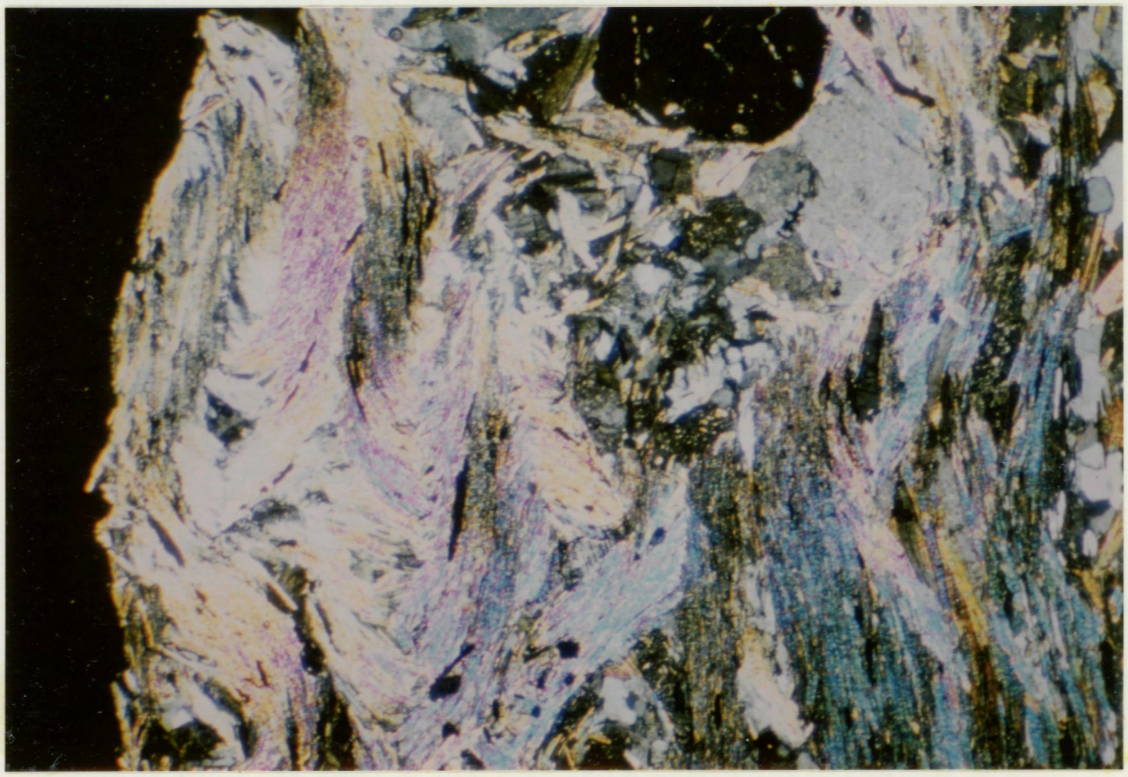

(Figure 3.1a). Since the minerals that define the mineral lineation are syn- to post-tectonic to the foliation of the host rocks, the pebble lineation and the mineral lineation are structurally associated. A very fine crenulation cleavage, S_{GB2}, and associated intersection lineation, L_{GB2}, plunging at a shallow angle to the northeast (Figure 3.1b), round up the fabric elements detected in the rocks of the Middle River unit. The crenulation cleavage and intersection lineation are not observed in the schists and phyllites north of Second Gold Brook, nor are they seen in the metabasites and gneisses farther north.

3.3 DEFORMATION

Four phases of deformation can be identified in the study area. The first, D_1, is represented by the development of the early, poorly-preserved enclosed schistosity, S_{MR1}, and the isoclinal folds affecting it. Where observed, the schistosity is isoclinally folded with strongly attenuated limbs. Because of the scarcity and small scale of the folds, the symmetry, or asymmetry, of the folds could not be determined and no information regarding their orientation was obtained.

The second phase, D_2, includes the principal fo-

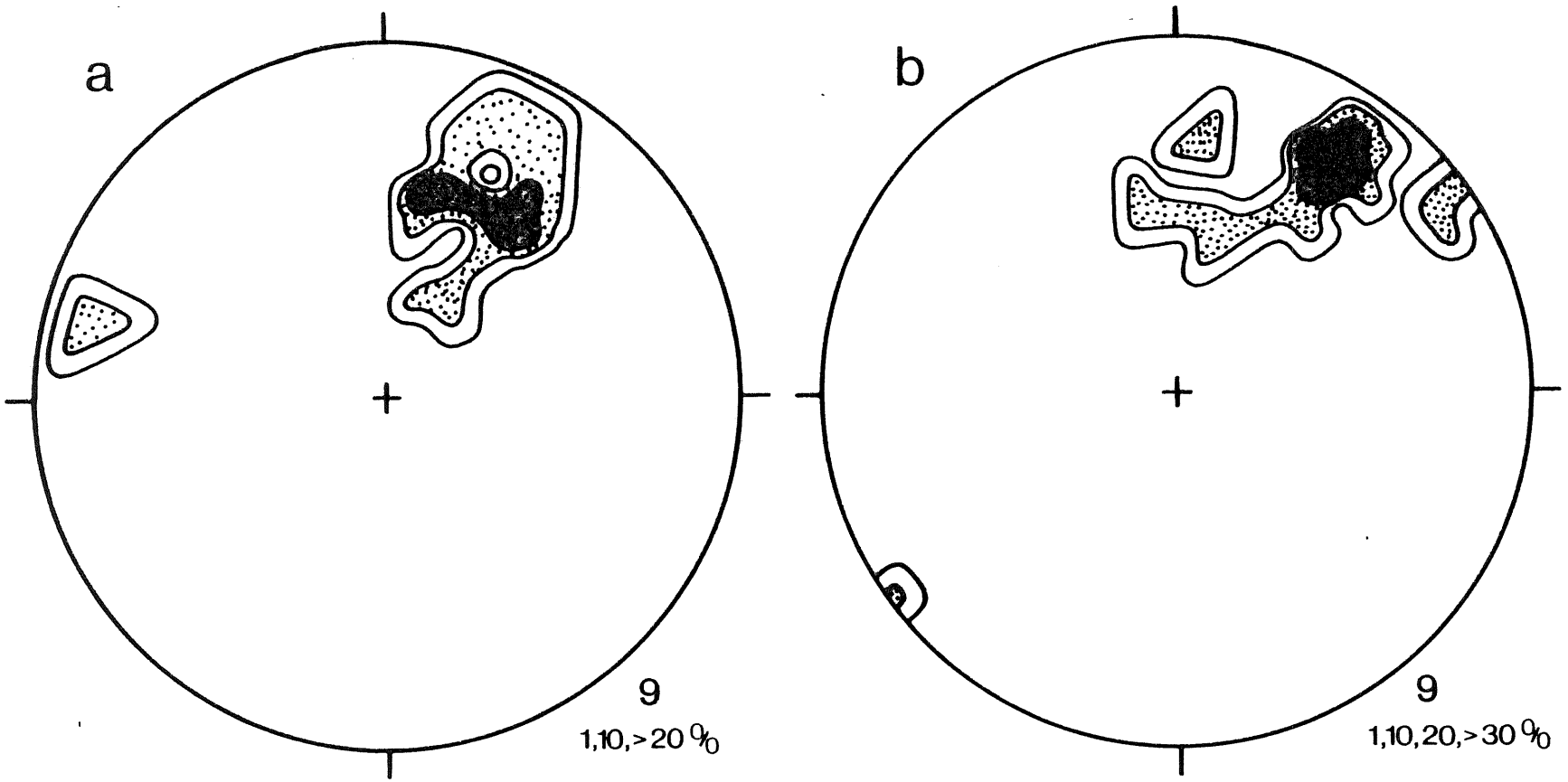

Figure 3.1 Stereoplots illustrating (a) chlorite and hornblende mineral lineation, L_{GB1}, and (b) intersection lineation, L_{GB2}, resulting from the intersection of the major schistosity, S_{GB1} and a fine crenulation cleavage, S_{GB2}. Numbers at lower right of plots correspond to numbers of data points and to contour values (percent per unit area).

liations of the Middle River and Egypt Highlands units: S_{GB1} in the schists and phyllites, S_{MR2} in the gneisses, and S_{EHU1} in the granitic rocks. It also includes the lineation formed by the alignment of the pebbles in the metaconglomerate and the syn- to post-tectonic chlorite and hornblende mineral lineation, L_{GB1}. This deformational phase would be associated with the "stacking" or juxtaposition of the three belts postulated in the second and final structural models presented in the later part of this chapter.

A small number of tight synformal and antiformal folds, which plunge at shallow angles to the east or west, are believed to be related to the "stacking" event. Although only three folds, which measure several tens of meters across, have been identified (two along Fionnar Brook and a third in the northwest corner of the area) and represented on the Structural Map, other similar folds may be present but were not located due to restricted exposure. The folds deform the gneissic foliation, S_{MR2}, but since similar folds have not been detected farther south, their relationship to S_{GB1} is not known.

The third phase of deformation, D_3, is represented by numerous mesoscopic folds and kinks. They are best

developed in the metasedimentary schists and phyllites (Plate 16) but can also be observed in the gneisses (Plate 17) and granitic rocks of the Egypt Highland unit. The folds and kinks are open to tight, affect all three major foliations, and plunge moderately to steeply to the north and northwest (Figure 3.2). The folds and kinks are probably responsible, to some degree, for the slight scatter in the orientation of the mineral lineation, L_{GB1}. The folds and kinks may also affect the crenulation cleavage but since the crenulation cleavage is restricted to outcrops along Second Gold Brook and since the folds and kinks occur farther north, a definite relationship can not be established.

The fourth phase, D_4, includes three large folds measuring up to several kilometers across. A broad antiformal fold, located along Middle River west of Second Gold Brook, plunges moderately to the north (Figure 3.3a). The fold deforms the phyllitic schistosity, S_{GB1}, and is probably responsible for some of the scatter in the orientation of the mineral lineation, L_{GB1}. The fold may also affect the crenulation cleavage, but again, restricted exposure hinders the definition of a precise relationship. The fold appears to be gradually attenuated northward but the absence of outcrop in the central region of the study area north of Fourth Gold Brook prevents an accurate definition of the attitude of the fold north

Plate 16. Mesoscopic kinks in metasedimentary schist representing D_3, from an outcrop along Middle River near Second Gold Brook. The kink axes plunge moderately to the northeast.

Plate 17. Mesoscopic open fold in semipelitic gneiss representing D_3, from an outcrop along a road in Margaree Valley. The fold axis plunges at a shallow angle to the northeast.


15 CM

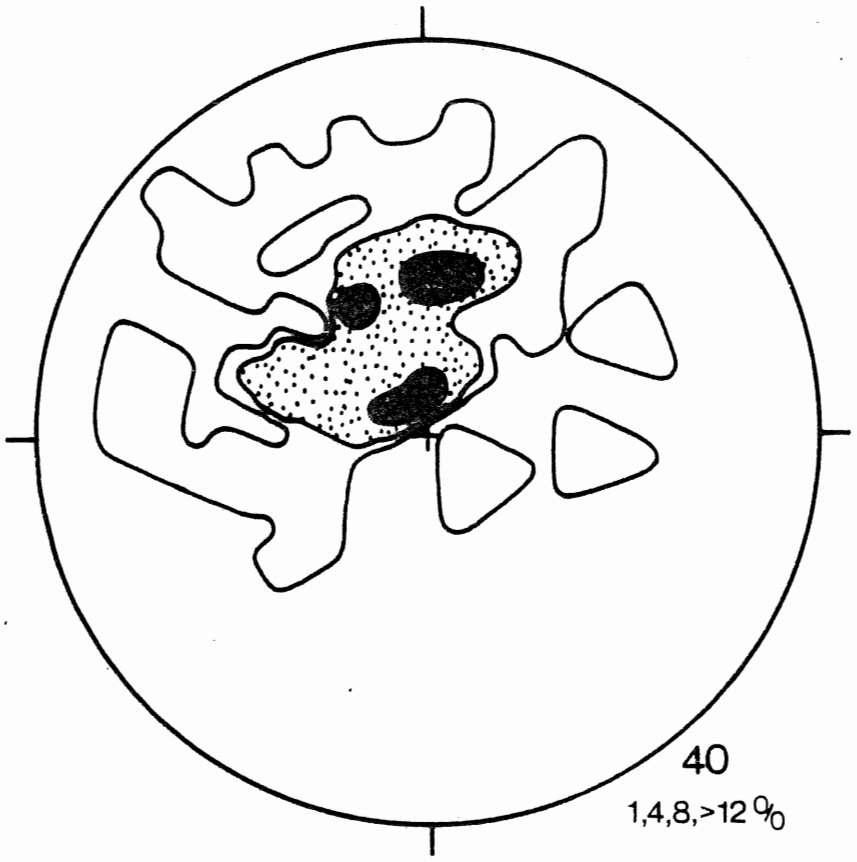

Figure 3.2 Stereoplot illustrating the orientation of D_3 structural data, the orientation of mesoscopic fold and kink axes. (Refer to Figure 3.1 for explanation of captions to stereoplot.)

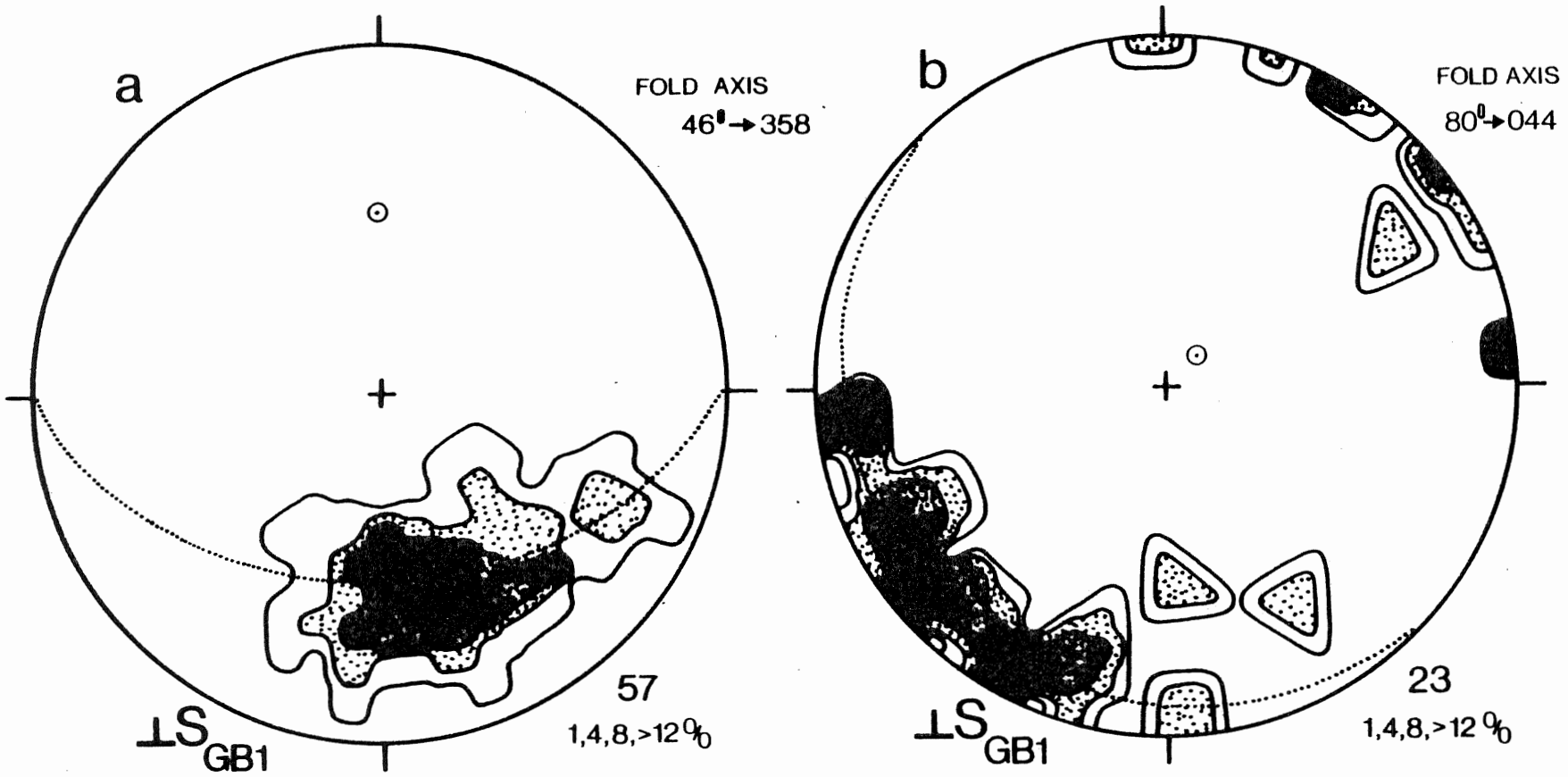

Figure 3.3 Stereoplots illustrating (a) S_{GB1} foliation defining a broad antiformal fold along Middle River west of Second Gold Brook, and (b) S_{GB1} foliation defining a broad fold. (Refer to Figure 3.1 for explanation of captions to stereoplots.)

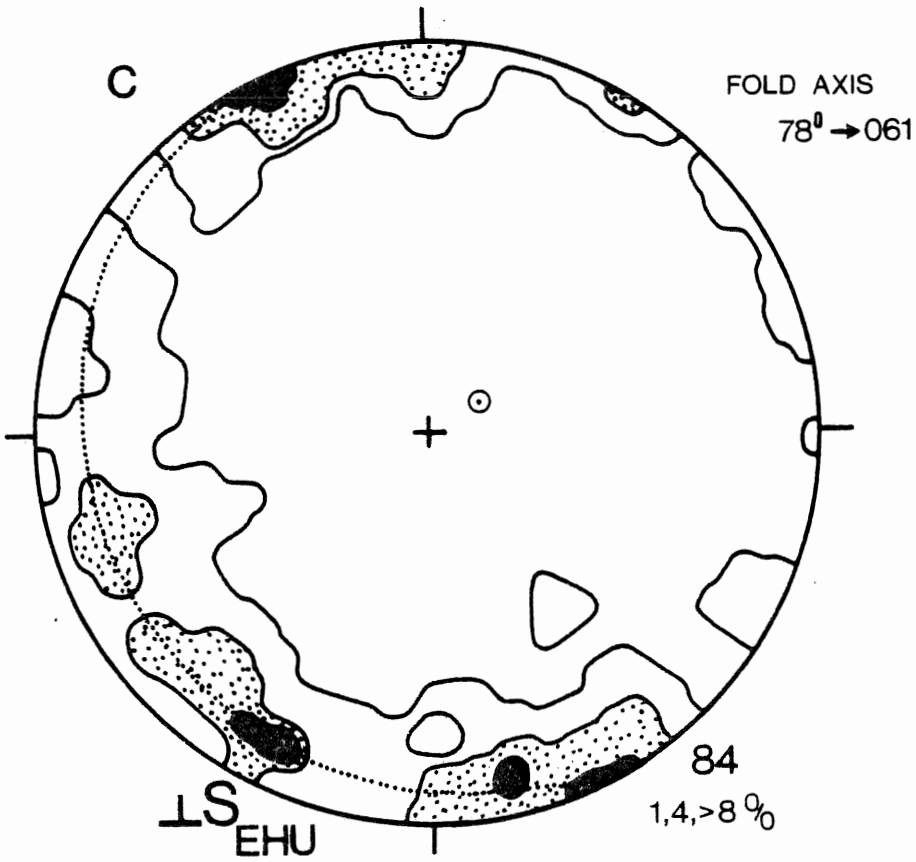

Figure 3.3 (continued) Stereoplot illustrating (c) S_{EHU} defining a broad synformal fold around the least deformed granitic rocks near Fielding Road. (Refer to Figure 3.1 for explanation of captions to stereoplot.)

of Middle River.

A second fold, also antiformal, is defined on the western margin of the area, in a narrow sliver separated from the main central block by a major north-south trending fault. The fold, which deforms the principal foliation, S_{GB1}, in the thin sliver, plunges steeply to the northeast (Figure 3.3b).

The third fold, this one synformal in character, is formed in the north where the major foliation, S_{EHU1}, swings to the northwest in the west and to the northeast in the east, producing a concentric structure around the least deformed granitic rocks near Fielding Road. Although exposure is concentrated along the western and central sections of the fold, enough data were gathered to show a northeast-trending stteply plunging fold axis (Figure 3.3c).

3.4 SHEARING AND FAULTING

A band of mylonite rocks, informally referred to as the Sarach Brook mylonite, trends northeast-southwest through the Bothan Brook granodiorite. The mylonite zone varies between 100 and 500 meters wide, extends from Bothan Brook along Sarach Brook and continues for some

distance in a northeasterly direction. It may appear again in the south end of Second Gold Brook in the form of small shear zones. The Sarach Brook mylonite consists predominantly of greenish-grey deformed pyroclastic rocks. Stretched ash fragments define a down-dip lineation that locally plunges obliquely across the dip and rarely has a shallow plunge, with the Middle River metamorphic complex moving south relative to volcanic rocks located southeast of the study area (Jamieson and Doucet, 1983).

Two major north-south trending faults and numerous small shear zones and faults are observed in the study area. As mentioned previously, a narrow sliver of Middle River unit metasedimentary schists and metabasites occurs near the western edge of the study area and is separated from the main central block by a north-south fault dipping steeply to the east. Another parallel to subparallel fault probably marks the edge of the Cape Breton Highlands and separates this sliver from the low-lying Carboniferous rocks to the west.

The other north-south trending fault separates, at least locally, the West Branch North River monzogranite from the Egypt Highland unit. The fault appears to predate the intrusion of the Bothan Brook granodiorite but

very poor exposure in the area makes this structural interpretation sketchy at best and the fault may extend farther south, separating the Bothan Brook granodiorite from the Middle River unit.

A large number of narrow zones of very fine-grained dark grey schists cut across the structural grain of the area and probably represent localized shear zones or faults. Usually less than a few meters wide, these shear zones or faults generally trend northeast-southwest, dip steeply to the east or west, and are responsible for localized retrograde metamorphism and, as best exemplified in the Nile Brook copper showing, restricted sulphide concentration.

Finally, two post-Mississippian faults have been recognized in the region. Both are inferred from apparent displacements of the contact between the Mississippian Horton Group sedimentary rocks and the Middle River metamorphic complex. The first fault, located along Middle River in the southwest corner of the study area, has an estimated horizontal left-handed displacement of one kilometer. The second, located along Ryan Brook in the northwest corner of the region, shows a left-handed horizontal displacement of approximately 500 meters. The dips of the fault planes are unknown.

3.5 RELATIONSHIP BETWEEN THE FABRIC ELEMENTS

Two possible relationships can be defined between the southern phyllitic schistosity, S_{GB1}, and the gneissic foliation, S_{MR2}, when the enclosed isoclinally folded schistosity, S_{MR1}, is considered:

$$S_{GB1} = S_{MR1} \quad \text{or} \quad S_{GB1} = S_{MR2}.$$

In the first case, where the phyllitic schistosity is equivalent, structurally and "chronologically", to the enclosed schistosity, one must conclude that the principal foliations S_{GB1} and S_{MR2} are very different despite their similar orientation. This relationship implies that the first phase of penetrative deformation produced a pervasive foliation (S_{GB1} and S_{MR1}) in a thick sedimentary and volcanic sequence; that the sequence was subsequently separated into two "belts" with only one of them affected by a second phase of penetrative deformation (producing S_{MR2}); and that the two belts were finally brought together to their present configuration.

In the second case, where the phyllitic schistosity is structurally and "chronologically" equivalent to the gneissic foliation, one must conclude that the principal foliation is pervasive throughout the Middle River unit.

This relationship implies that a sedimentary and volcanic sequence was affected by a first phase of penetrative deformation (producing S_{MR1}); that this assemblage was brought up against an essentially undeformed sequence of similar sedimentary and volcanic rocks; and that during this "stacking" of the two belts, the overprinting fabric in the northern belt (S_{MR2}) and the principal fabric in the southern belt (S_{GB1}) were developed.

As mentioned previously, minor fabric elements are only observed in the south. Their absence in the north can be related to the two relationships discussed above. If the mineral lineation and crenulation cleavage were developed after S_{GB1}-S_{MR1} and before S_{MR2}, then they were totally destroyed in the northern belt during the second phase of penetrative deformation. Conversely, if the lineation and crenulation cleavage were developed after S_{GB1} and S_{MR2} (as per the second relationship), they are still present in the north but may be less well developed and/or hidden by the coarser grain size of the gneisses.

There can be no doubt that the lineation produced by the elongated pebbles in the metaconglomerate is related to the development of the phyllitic schistosity which clearly wraps around and encloses the pebbles.

Uncertainty resides in the relation between the above lineation and the one resulting from the alignment of syn- to post-tectonic chlorite and hornblende crystals. Since all three have a similar orientation, it appears that they are related to some degree, but poor exposure and limited data make this relationship tentative.

The crenulation cleavage, S_{GB2}, and associated intersection lineation, L_{GB2}, deform, and therefore post-date, the phyllitic schistosity.

3.6 STRUCTURAL MODELS

Using the structural information presented thus far, two models, representing extremes, can be proposed. Both are illustrated in Figure 3.4. Assuming that repetition of the various lithologies by folding and faulting is minimal, that no major tectonic break separates the metasedimentary schists and phyllites and metabasites from the gneissic rocks, that the northward increasing metamorphic grade is continuous over these rocks, and the Egypt Highland unit and Middle River unit are not separated by any major tectonic break, it is concluded that the entire metamorphic complex represents a single unit (Figure 3.4a).

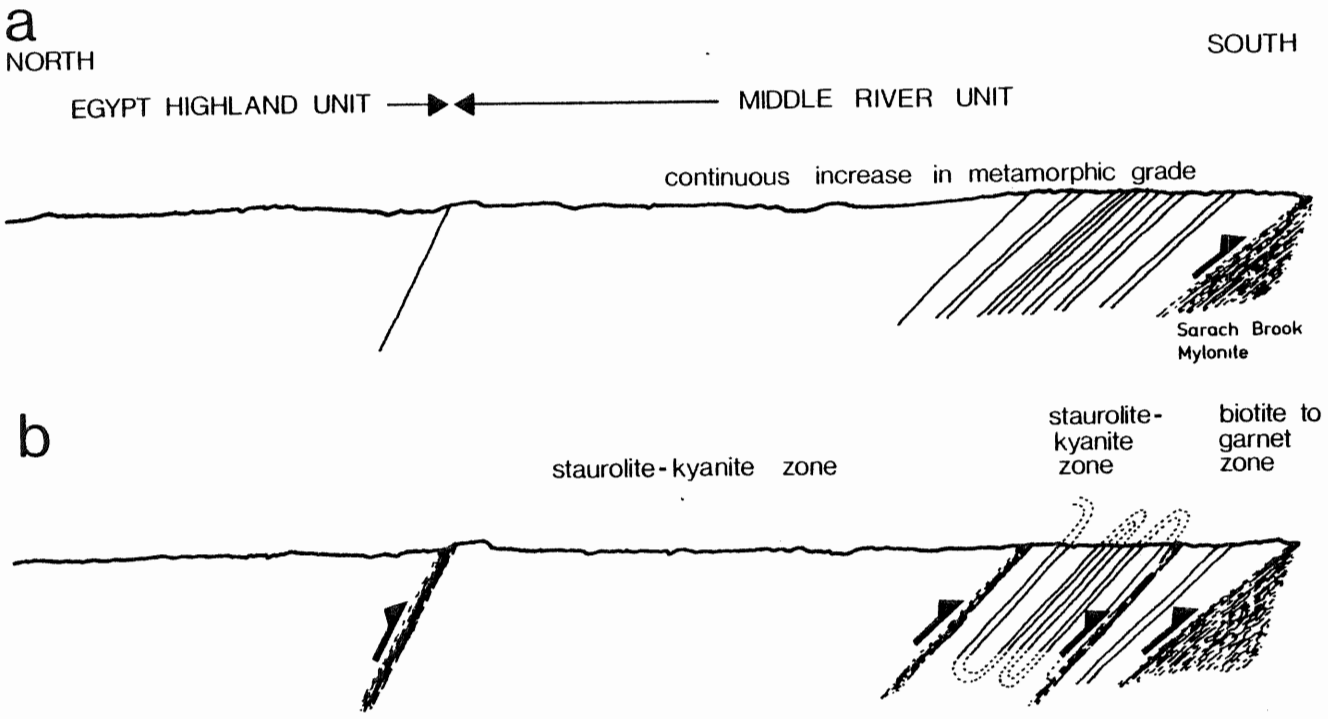

Figure 3.4 Alternative structural models for the Middle River area (a) assuming minimum repetition by folding with the complex working as a single block, and (b) assuming repetition by folding with complex moving as a series of "stacked" slabs.

On the other hand, if repetition of the lithologies (especially the metabasites and the gneisses of the Middle River unit) is considerable, if there is a major break within the Middle River unit itself, if the northward increasing metamorphic grade is not continuous but occurs as separate slices of uniform grade abutting against other slices of different grade, and if the apparently unfolded Egypt Highland unit abuts against the highly folded Middle River unit, it is concluded that the metamorphic complex represents a series of thin slabs faulted against one another (Figure 3.4b). As mentioned above, these two interpretations are extremes and a number of intermediate models can also be possible.

The first structural model is supported by the following evidence:

1. No major east-west faults or shear zones have been detected in the study area.
2. The presence of a single thin layer of metaconglomerate and a single layer of marble in the Second Gold Brook area and the isolated occurrence of flow banded rhyolite in the narrow sliver along the western margin confirm that at least these sections are apparently not repeated by folding.
3. Textural variations and differences in major element composition (especially titanium) in the metabasite

sheets indicate that they are most probably distinct sheets rather than a single sheet repeated by folding.

4. The metamorphic grade appears to increase steadily from the greenschist facies in the metasedimentary schists and phyllites to the amphibolite facies in the pelitic and semipelitic gneisses.

The second structural model is supported by the following evidence:

1. Although only three major east- and west-trending folds have been inferred from field measurements, other similar folds may be present but have not been identified.
2. The rapid increase in metamorphic grade over a very short horizontal distance may indicate an extremely high geothermal gradient or, more probably, suggests that a break in the sequence may be present. This break would separate the apparently continuous low- to medium-grade sequence south of Fourth Gold Brook from the high grade gneisses farther north. The break would therefore be located just north of Fourth Gold Brook.
3. The presence of two metamorphic fabrics in the northern rocks of the Middle River unit (S_{MR1} and S_{MR2}) as compared to one in the south (S_{GB1}) suggests different deformation histories for the two assemblages and thus implies a major tectonic break between

them.

Another factor which must be considered is the poor exposure throughout the study area. Even though, as mentioned above, no major east-west faults or shear zones have been recognized in the area, such features are present farther south (Jamieson and Doucet, 1983), and it is very possible that east-west faults or shear zones exist in the study area but are not exposed.

Taking all these factors into consideration, it would appear that an acceptable representation of the study area resides in a model intermediate to the two extremes described. Such a model, illustrated in Figure 3.5, incorporates the following:

1. A southern belt, containing the metasedimentary schists and phyllites and metabasite sheets of the Middle River unit. This belt is characterized by a single major penetrative fabric, S_{GB1}, is transitional between the greenschist and amphibolite facies, and is not tectonically repeated by folding.
2. A central belt, containing the pelitic and semipelitic gneisses of the Middle River unit. This belt is characterized by two penetrative fabrics, S_{MR1} and S_{MR2}, is in the upper amphibolite facies, and is repeated, to some degree, by tight east- and

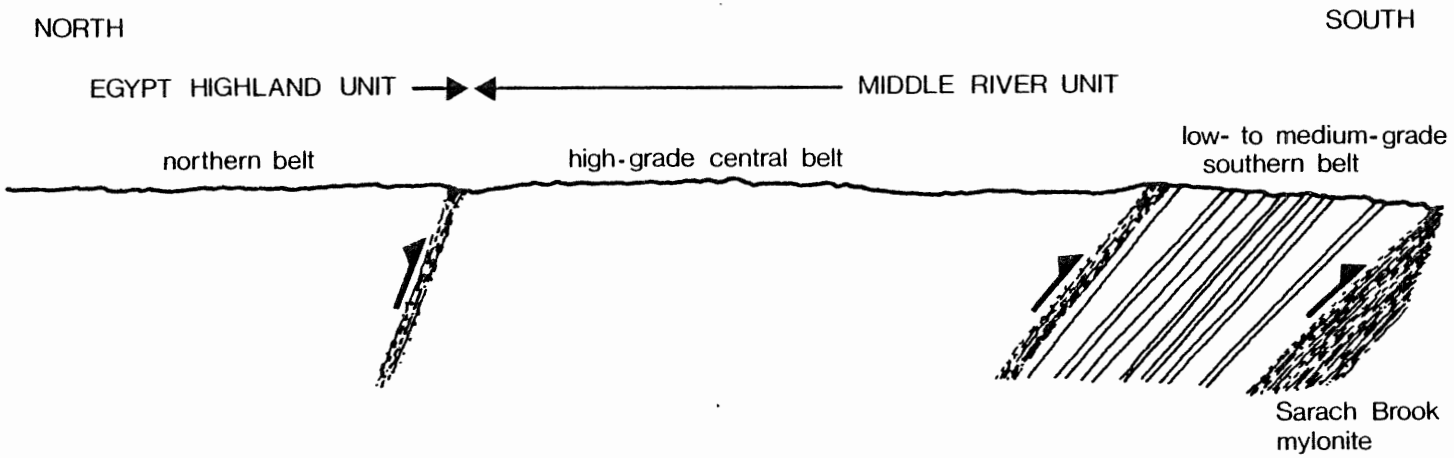

Figure 3.5 Postulated structural model for the Middle River area comprising a low-to medium-grade belt in the south, a central high-grade belt, and the Egypt Highland unit forming a third belt in the north.

west-plunging folds.

3. A northern belt containing the granitic rocks of the Egypt Highland unit.

These three east-west belts are stacked against one another with the southern low-grade belt at the bottom of the sequence. The "stacking" of the three belts probably occurred along shear zones rather than brittle faults, since the "stacking" or juxtaposition was more likely a ductile deformational process. In the model, the Egypt Highland unit may represent the "basement complex" of the sequence, but further work to the north of Fielding Road would be required to confirm this relationship.

3.7 THRUSTING VERSUS HIGH-ANGLE FAULTING

In order to explain a number of anomalous geological features he encountered during his study of the area, Milligan (1970) proposed that a large-scale, low-angle thrust fault, observed in Christopher McLeod Brook about 16 km east of the area, be extended into the Middle River-Crowdis Mountain region. Milligan (1970) noted that the contact between low-lying Mississippian sedimentary rocks and George River rocks (Middle River unit) more or less followed topographic contour lines,

suggesting that the contact may be a nearly horizontal thrust plane. The overthrust hypothesis, he indicated, would also explain an area of anomalously low metamorphic grade in the schists near the gold mine, only one hundred meters from an alaskite intrusion at the head of Second Gold Brook (the southernmost exposure of the Bothan Brook granodiorite as reported in this study), which would represent a "window" through the thrust plane.

Milligan (1970) also presented two features which contradict his hypothesis. He noted that if a thrust fault was present in the area, George River rocks should occur on a number of hilltops in the region but, in fact, they have not been reported at these localities. Milligan (1970) also wrote that the thrust plane itself, and possibly Horton Group sedimentary rocks underlying it, should be found some distance up Middle River but that, in fact, no such features were observed. Delahay (1979), working along the Second Gold Brook-Falls Brook section, found no evidence to support the thrust fault theory.

The evidence gathered during this study does not support the hypothesis of a low-angle thrust plane at the base of the Middle River complex. No visible thrust plane or outcrops of Horton Group rocks were detected along Middle River and the absence of any visible thrust

plane along Second Gold Brook suggest that no major post-Horton thrust fault exists in the area. These pieces of negative evidence are based on the assumption that the thrust plane is nearly horizontal; if, on the other hand, the postulated thrust fault angles under the Highlands, it would not occur along Middle River and would be at some depth under Second Gold Brook.

As will be discussed in Chapter 7, the anomalous low-grade metamorphic assemblage near the gold mine mentioned by Milligan (1970) is not anomalous but is part of a sequence which exhibits a more or less continuous increase in metamorphic grade toward the north.

Finally, the north-south trending steeply-dipping fault near the western margin of the area and the parallel to sub-parallel fault inferred for the edge of the Highlands severely limits the probability of a low-angle fault occurring directly underneath this section of the Cape Breton Highlands.

The observed structural configuration of the Middle River area is instead interpreted to be the result of a large-scale southward movement of the entire sequence along sub-parallel north-south trending steeply dipping faults. A component of uplift may also have been involved.

The interpretation of a southward and upward movement of the central block is based on the following features illustrated schematically in Figure 3.6:

- the distribution of metasedimentary schists and metabasites farther north in the narrow sliver making up the western margin of the area
- the presence of pelitic and semipelitic rocks on the eastern side of the eastern north-south fault
- a combination of lateral and vertical displacement inferred by the stretched ash fragments of the Sarach Brook mylonite, with the Bothan Brook granodiorite and Middle River metamorphic complex moving south relative to an assemblage of volcanic and volcaniclastic rocks located to the southeast of the study area (Jamieson and Doucet, 1983).

The total horizontal displacement of the central block may never be accurately determined but a conservative estimate can be derived from the fact that the schists and metabasites of the Middle River unit in the thin sliver lie about 5 km farther north than any of their counterparts in the central block.

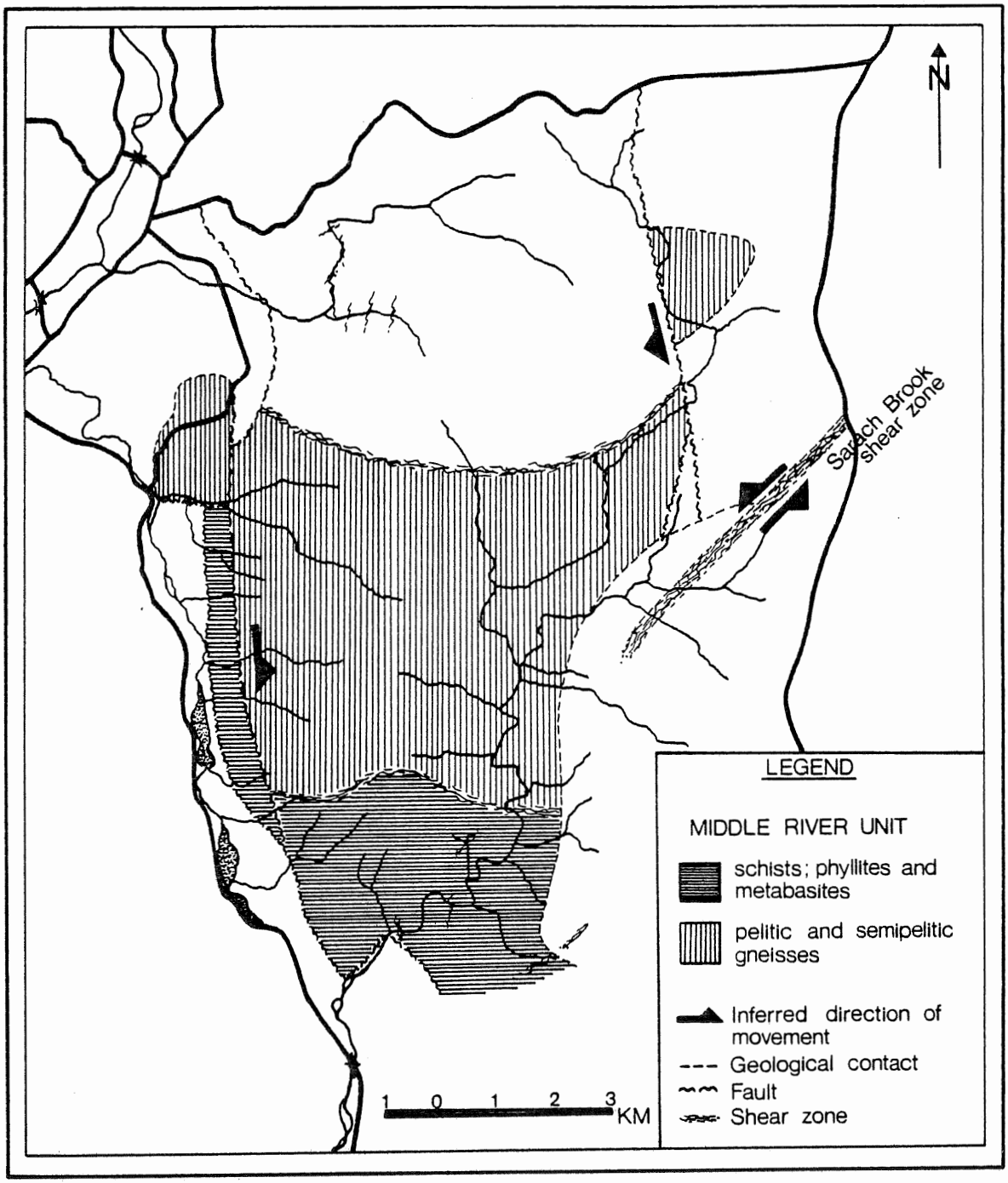

Figure 3.6 Distribution of Middle River unit rocks with respect to the two major north-south faults illustrating the postulated southward movement of the central block.

3.8 SUMMARY AND STRUCTURAL SYNTHESIS

The Middle River area is divided into three major east-west belts. The southern belt, which is composed of the metasedimentary schists and phyllites and metabasites, is characterized by a pervasive phyllitic schistosity with a related mineral lineation and a later fine crenulation cleavage restricted to outcrops along Second Gold Brook.

The central belt, which is made up of the pelitic and semipelitic gneisses of the Middle River unit, is characterized by a well-developed gneissic foliation which overprints an earlier schistosity. The mineral lineation and crenulation cleavage have not been detected in these coarser grained rocks.

The northern belt consists of the granitic rocks of the Egypt Highland unit. These rocks are characterized by a moderately- to poorly-developed foliation which gradually deminishes northward.

Four phases of deformation have affected the rocks of the Middle River complex. The first appears to be restricted to the central belt and is associated with the early enclosed schistosity. The second phase produced

the principal foliation of each belt and includes the "stacking" of the three belts. Large-scale east- and west-plunging folds are believed to be associated with this second phase of deformation.

The third phase is represented by numerous folds and kinks affecting all three belts. The fourth phase includes three large-scale folds: an antiform along Middle River west of Second Gold Brook, a second antiform in the narrow sliver along the western margin of the area, and a synform near Fielding Road surrounding the least deformed granitic rocks of the Egypt Highland unit. These small- and large-scale folds are responsible for the scatter in the earlier mineral lineation and crenulation cleavage in the southern belt.

The Sarach Brook mylonite zone cuts across the Bothan Brook granodiorite in a northeast-southwest direction. A southward movement of the Middle River complex along this shear zone is postulated. Two major north-south faults occur along the eastern and western margins of the Middle River metamorphic complex, and numerous small faults and shear zones are found throughout the region. Two post-Mississippian faults are detected in the southwest and northwest corners of the area.

The structural configuration of the Middle River

metamorphic complex is believed to have resulted from the following sequence of events:

1. Metamorphism of a sedimentary and volcanic assemblage to produce an early fabric, S_{MR1}.
2. "Stacking" of this assemblage against an essentially undeformed sedimentary and volcanic sequence, and "stacking" of the Egypt Highland granitic rocks against these two assemblages. The development of the major foliations of the three belts, S_{GB1} (and associated lineation, L_{GB1}), S_{MR2} and S_{EHU}, and the formation of large-scale east- and west-plunging folds, is believed to be related to this "stacking" process.
3. Lateral shortening of the complex resulted in the formation of small-scale folds and kinks and large-scale synforms and antiforms affecting all three belts.
4. Southward and upward movement of the metamorphic complex occurred along the Sarach Brook mylonite zone. Since the structural grain of the Middle River sequence is more or less perpendicular to the general north-south orientation of structures in other areas of the Cape Breton Highlands, a rotation of the complex must be explained. Movement along the north-east-southwest Sarach Brook mylonite zone and east-west shear zones situated south of the area probably

produced the rotation from an early north-south configuration to the present east-west orientation.

5. Finally, a southward movement of the central section of the complex occurred along two north-south steeply-dipping faults.

CHAPTER 4

PETROGRAPHY

4.1 MIDDLE RIVER UNIT

4.1.1 Metasedimentary Schists and Phyllites

The most abundant mineral in these rocks is quartz. It occurs as granoblastic crystals ranging in size from .05 to 0.5 mm and makes up between 20 and 55 percent of the rock. Larger grains commonly show strained extinction. No crystallographic preferred orientation is observed. Very fine plates of muscovite, between .05 and 0.1 mm in size, occur either disseminated or as densely packed layers up to 1 mm thick, make up about 15 to 25 percent of the schists and phyllites and, in conjunction with chlorite, produce the phyllitic schistosity characteristic of these rocks. Fibrous chlorite makes up 5 to 30 percent of the rock and gives it its greyish green to green color. Angular disseminated magnetite grains, up to 0.1 mm in diameter, make up less than 1 percent of these rocks.

Four minerals occur as porphyroblasts found in distinct layers in the metasedimentary sequence. Fine chlorite blades, up to 1 mm in length, cut across the

schistosity and show a distinct preferred orientation with respect to their long crystallographic axes (Plate 18). Commonly twinned, the chlorite porphyroblasts can only be found in certain layers south of the gold mine along Second Gold Brook.

Medium-grained biotites, up to 3 mm in diameter, occur in a number of thin layers along the northern section of Second Gold Brook. The biotites contain numerous minute inclusions of quartz, zircon and magnetite. The biotite grains show corroded margins and they are wrapped around by the phyllitic schistosity.

Medium-grained rounded garnet porphyroblasts are found in the schists near the mouth of Second Gold Brook and farther north. These fractured and corroded garnets, between 0.1 and 0.5 mm in size, are also enclosed by the foliation.

Fine- to medium-grained chloritoid crystals are found in a thin layer within the phyllites near the gold mine along Second Gold Brook. Measuring up to 2.5 mm in length, the crystals are commonly idioblastic and twinned and show the characteristic bow tie inclusion pattern (Plate 19). Although the majority of chloritoid grains are aligned with the schistosity, others are

Plate 18. Photomicrograph of chlorite porphyroblasts in a sample of metasedimentary phyllite. The porphyroblasts are commonly parallel to the foliation (from lower left to upper right) and rarely at an angle to the fabric. (Magnification x25; crossed nicols.)

Plate 19. Photomicrograph of idioblastic chloritoid porphyroblast in metasedimentary phyllite sample 8220. The crystal shows the characteristic bow tie inclusion pattern and contains ilmenite needles oriented parallel to matrix ilmenites, a reflection of the syn- to post-tectonic nature of the chloritoids. (Magnification x25; plane polarized light.)

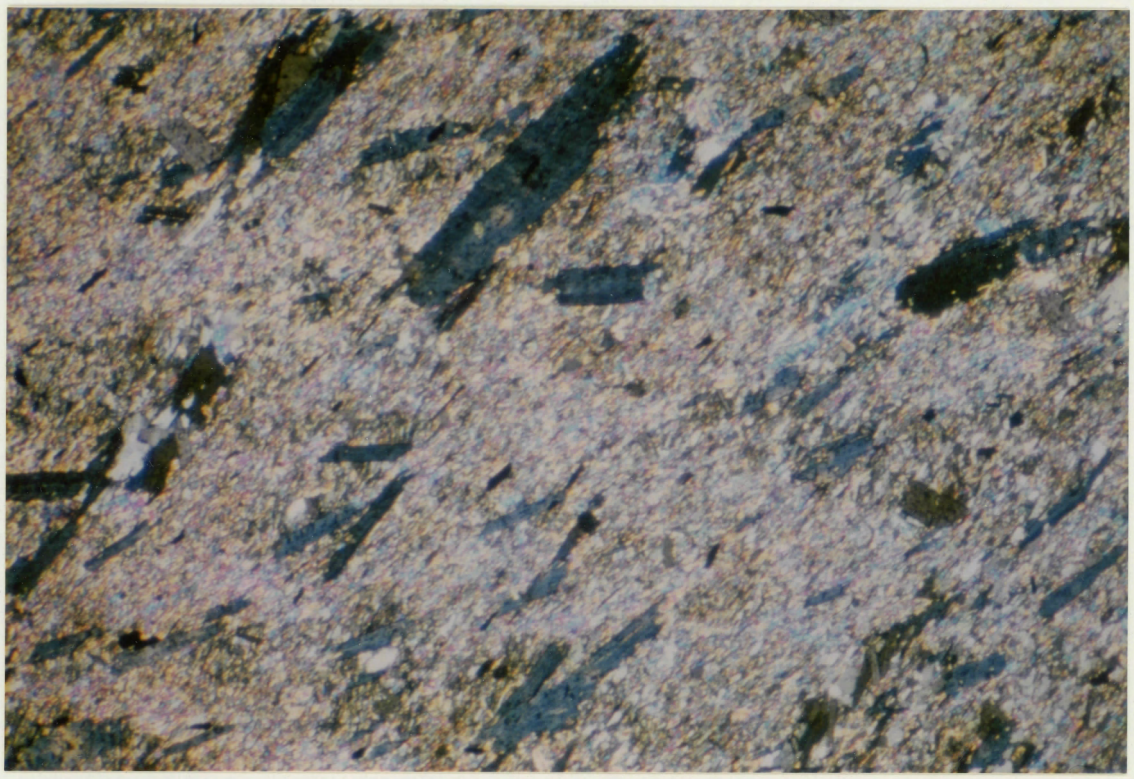

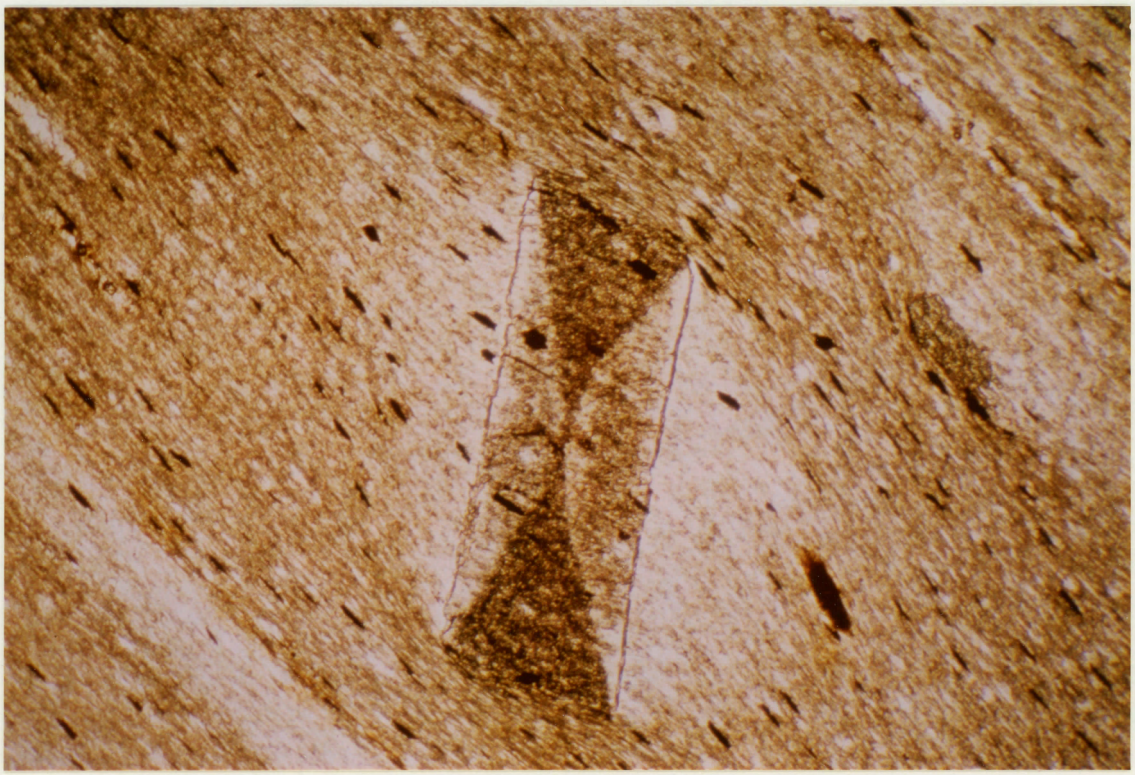

rotated, yet contain fine ilmenite blades concordant with matrix ilmenites, a reflection of the syntectonic nature of these crystals. Chloritoid occurs in one other location in the study area, in an outcrop about 300 m east of where two small brooks converge to form Fortune Brook. Unlike their Second Gold Brook counterparts, these medium-grained chloritoid crystals are very poorly developed and have a spongy, highly poikiloblastic texture (Plate 20). The grains contain relatively straight inclusion trails of quartz and ilmenite and can be up to 2 mm in length.

4.1.2 Metaconglomerate

The very fine phyllitic matrix of the metaconglomerate is identical in every aspect to the metasedimentary schists and phyllites except for the absence of porphyroblasts and the presence of fine blue-colored quartz granules in the grit layers adjacent to the conglomerate. The quartz granules range from 1 to 3 mm in diameter, are subangular to rounded, and are composed either of a single grain of strained quartz or of an aggregate of small quartz crystals. Also occurring in the grit are fine- to medium-grained rounded to subrounded relict plagioclase grains and chert fragments between 0.5 and 2 mm in diameter. Pebbles in the metaconglomerate

Plate 20. Photomicrograph of spongy, highly poikiloblastic chloritoid porphyroblasts from sample 81108. The crystals are either parallel to or at an angle to the schistosity (left to right). (Magnification x25; plane polarized light.)

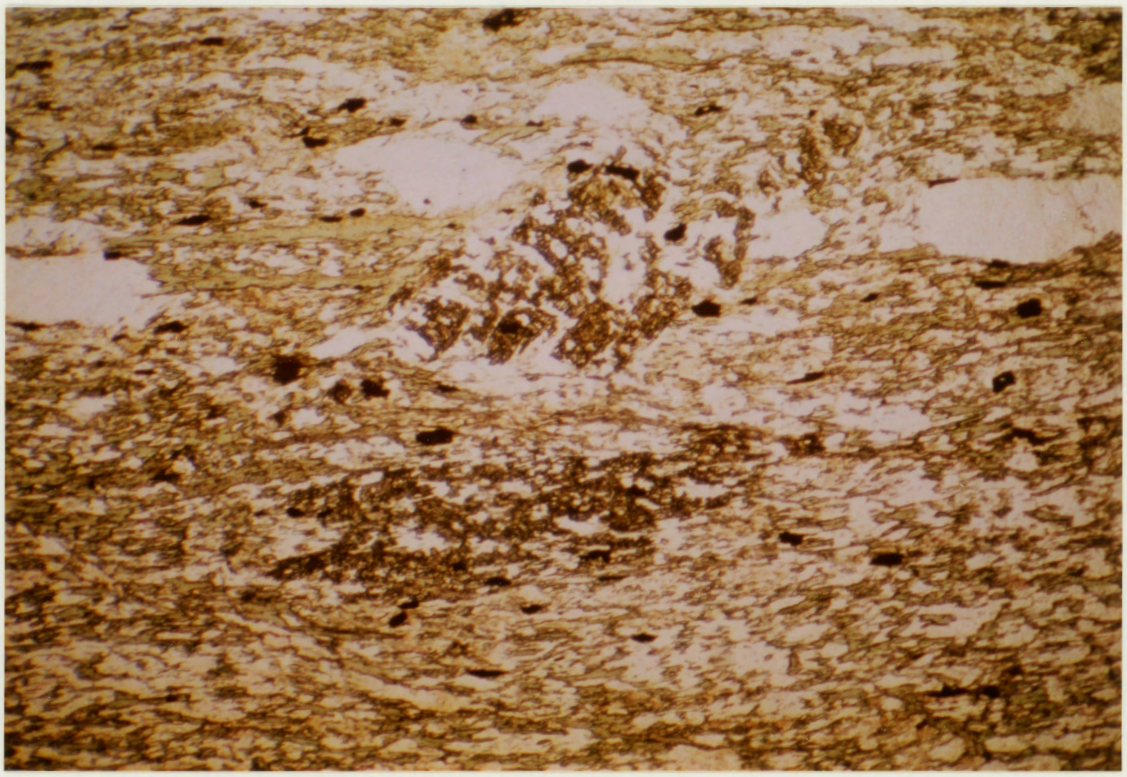

include: quartzite, which consist almost exclusively of very fine-grained polycrystalline quartz, up to 0.1 mm in size, with a few minute disseminated magnetite grains; siltstone, which closely resemble the quartzite pebbles in that they are composed mostly of quartz, the major differences reside in the slightly finer grain size of the quartz in the siltstone pebbles and the occurrence of fine muscovite flakes in the siltstone; and granitic pebbles composed of fine-grained quartz, showing strained extinction and the development of subgrains, microcline and sericitized plagioclase.

4.1.3 Metabasite

Hornblende forms 20 to 80 percent of this lithology. It occurs either as very fine prismatic crystals, between 0.1 and 1 mm in size, or as medium to coarse xenoblastic grains or idioblastic porphyroblasts up to 3 mm in length (Plate 21). Where a foliation is present in a particular metabasite sheet, it is produced by a preferred orientation of the hornblende crystals. Where porphyroblastic, the metabasites show a slight mineral lineation resulting from the alignment of hornblendes along their c crystallographic axes. Hornblendes are rarely rimmed by retrograde actinolite and chloritization is essentially nonexistent. Polygonal quartz

Plate 21. Photomicrograph of fine- to coarse-grained subidioblastic to idioblastic hornblende porphyroblasts. Although a number of crystals are aligned with the foliation (left to right), the greater part are preferentially aligned at an angle to the fabric. (Magnification x25; plane polarized light.)

makes up to 40 percent of the rock. Although generally showing very slight undulose extinction, the quartz crystals, ranging in size from 0.2 to 2 mm, reflect good textural equilibrium with straight grain boundaries. No crystallographic preferred orientation of the quartz is observed. Plagioclase makes up 5 to 25 percent of the metabasites. The crystals, between .02 and 2 mm in size, commonly show well-developed albite twinning, do not exhibit zoning, and compositions of single grains range between An 19 and An 42. Alteration of plagioclase to sericite varies from slight to extensive.

Clinozoisite, characterized by its anomalous Berlin blue interference color, is the principal accessory mineral. It occurs as disseminated rounded to angular grains up to .75 mm in diameter. Other accessory minerals include: brown biotite, occurring as fine flakes, up to 1 mm in length, showing various degrees of retrograde alteration to chlorite along cleavage traces and grain boundaries; sphene, consisting of rounded to angular grains rarely containing, and replacing, opaque cores (ilmenite ?) and, when large enough, showing good cleavage or parting; carbonate, found both in tiny veinlets cutting across the rock and as disseminated crystals up to 0.5 mm in size; fine- to medium-grained rounded garnet porphyroblasts containing minute inclusions of

quartz, plagioclase and sphene; opaque minerals, identified in reflected light as ilmenite and minor pyrite, occur as fine angular grains disseminated throughout the rock; and apatite and rutile, found rarely, and in minor amounts, as tiny angular to rounded grains no more than 0.1 mm in size. Accessory minerals form up to 10 percent of the metabasites.

4.1.4 Pelitic and Semipelitic Schists and Gneisses

Quartz is the dominant mineral in the felsic gneisses. It is fine- to medium-grained, with crystals up to 3 mm in length, shows slight to moderate strained extinction and subgrain development, and makes up 25 to 55 percent of the rock. Both biotite and muscovite are major constituents of the schists; their preferred orientation produces the principal foliation (S_{MR2}). Occurring as rectangular flakes between 0.1 and 1.5 mm in length, brown biotite makes up 10 to 40 percent of the rock while muscovite ranges between 10 to 35 percent. Retrograde chloritization of biotite grains varies in any given sample from nonexistent to total. The micas are spatially related to a number of other minerals in the pelitic schists; both biotite and muscovite can surround, abut against, or, in rare cases, be included within large garnet, staurolite and kyanite crystals.

Fine- to medium-grained plagioclase, slightly to moderately altered to sericite, shows good albite twinning and makes up 15 to 50 percent of the felsic gneisses but is found only in minor amounts in the schistose rocks. The plagioclase crystals are not zoned and individual grains vary in composition from An 22 to An 45 in both the schists and gneisses. Garnet porphyroblasts, ranging from 0.1 to 1 cm in diameter only occur within certain layers of the pelitic schists and make up to 15 percent of the rock. Commonly poikiloblastic, the garnets may contain various amounts of fine quartz, sphene and opaques that can form either random or complex helicitic inclusion patterns, none of which are continuous with the matrix. High grade minerals, found only in a few schist samples, include: kyanite, occurring as fractured crystals up to 3 mm in length, commonly containing randomly distributed inclusions of quartz, muscovite and biotite, and rarely breaking down to sericite along grain boundaries and cleavage planes (Plate 22); staurolite, found as subrounded fine- to coarse-grained fractured crystals, also containing minute inclusions of quartz and biotite and also breaking down to sericite; and minor sillimanite (fibrolite) occurring as bundles of very fine needles within large muscovite flakes.

Plate 22. Photomicrograph of pre-tectonic kyanite porphyroblasts breaking down to fine-grained muscovite. The porphyroblasts are wrapped around by the schistosity and contain inclusions of syntectonic biotite and muscovite. (Magnification x25; plane polarized light.)

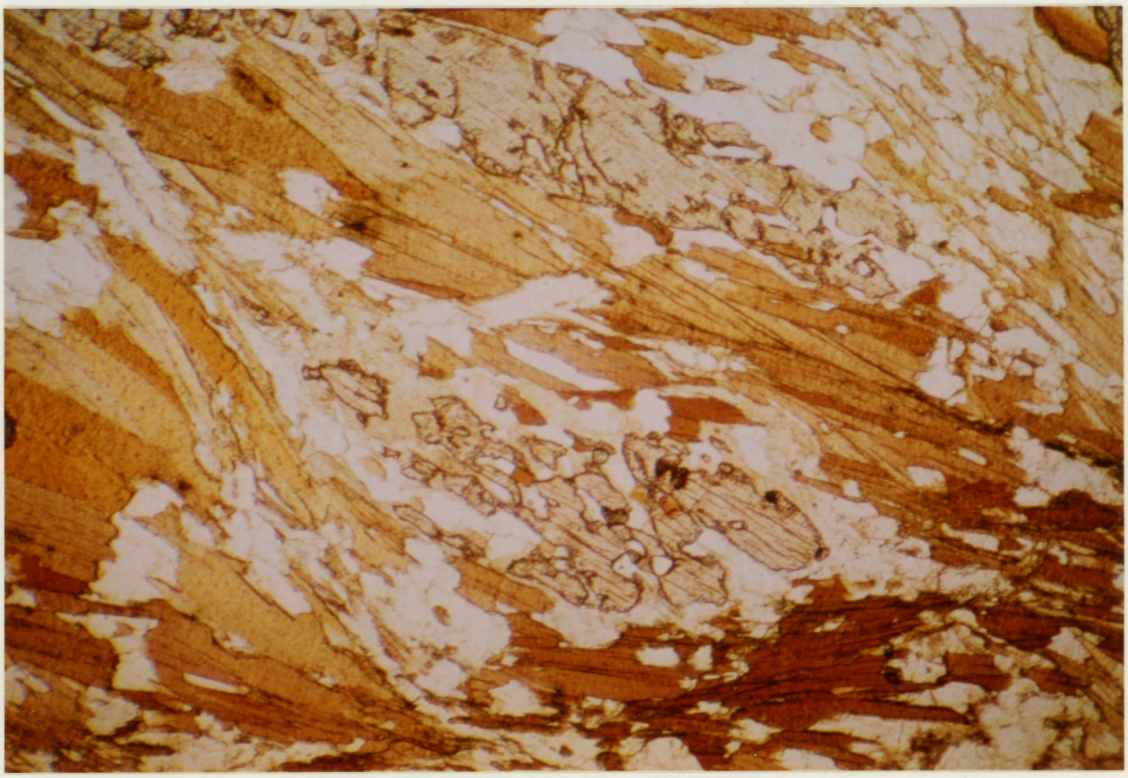

The textural relationships between the micas and the various high grade minerals clearly show that the well-developed biotite, muscovite and garnet are syn-tectonic to the principal foliation, S_{MR2}, while moderately preserved kyanite and staurolite are unstable and breaking down to sericite and are apparently pre-tectonic to the micaceous foliation.

Pyrite, with lesser chalcopyrite and pyrrhotite, is the dominant accessory mineral found in both the felsic gneisses and schists. Occurring as fine to medium disseminated angular grains up to 3 mm in size, these sulphides make up to 5 percent of the rock. Very fine- to fine-grained rounded crystals of apatite and sphene are also found in small amounts in both rock types. Medium-grained hornblende crystals, up to 1 mm in length, are concentrated in thin distinct layers in some of the samples showing compositional layering. Fine disseminated zoned idioblastic tourmaline crystals can be seen in a small number of schist samples.

Compositional layering in the micaceous rocks is reflected by the presence of concentrations of biotite or garnet or, as mentioned above, on the presence of hornblende. In the gneisses, metamorphic segregation has resulted in the formation of thin concordant or ptyg-

matically folded white leucosomes composed of fine-grained quartz and plagioclase (see section 7.3).

4.1.5 Marble

The white marble layer located along Middle River north of Sarach Brook is composed of about equal amounts of magnesian calcite and dolomite in distinct layers a few centimeters thick. Both calcite and dolomite occur as medium-grained xenoblastic crystals, up to 4 mm in size, with well-developed cleavage traces and straight to curved grain boundaries. The marble layer is separated from the surrounding pelitic rocks by a very thin veneer of talc and phlogopite (on the pelitic margin) and tremolite and diopside (on the marble margin), probably reflecting metasomatic zoning between the two rock types (Vidale, 1969; Brock, 1972; Thompson, 1975).

The pink and grey marble outcrop situated along Middle River near Second Gold Brook is composed of fine-grained xenoblastic calcite and dolomite, often showing bent cleavage traces, and minor amounts of disseminated fine-grained quartz, muscovite and granular magnetite.

4.1.6 Meta-rhyolite and Meta-tuff

Quartz makes up approximately 90 percent of the flow

banded meta-rhyolite. It occurs as very fine- to fine-grained polygonal crystals, up to 0.5 mm in size, with strained extinction, in thin and tightly folded bands. Subangular to angular plagioclase phenocrysts, up to 1 mm in length, make up 5 percent of the rock. Only very slightly altered to sericite, the plagioclase grains are generally fractured and show poor to good albite twinning. The phenocrysts are not zoned and were identified optically as andesine (An 32). Disseminated very fine angular magnetite, fine muscovite flakes aligned with the flow banding, and chlorite, perhaps derived from the alteration of preexisting biotite, make up the remaining 5 percent of the meta-rhyolite.

The thin meta-tuff (?) layers, found throughout the Middle River unit, are dominantly composed of minute quartz grains no more than 0.5 mm in size. Subrounded to angular, slightly sericitized, commonly fractured plagioclase grains up to 1 mm in longest dimension, and trace amounts of disseminated granular magnetite and fine-grained chloritized biotite and muscovite flakes make up the remainder of the rock and give it a faint layering.

4.2 EGYPT HIGHLAND UNIT

4.2.1 Fine-grained Foliated Granitic Rock

Quartz, occurring as fine- to medium-grained polygonal crystals exhibiting slight to moderate strained extinction and various degrees of subgrain development, makes up 15 to 30 percent of the fine-grained foliated granitic rocks. The crystals, which can measure up to 1.0 mm in size, show no crystallographic preferred orientation.

Fine- to medium-grained plagioclase makes up between 25 and 55 percent of the rock. The grains are not zoned and individual crystals were identified optically as oligoclase or andesine (An content between 25 and 32). Alteration to sericite varies from slight to extensive and red hematite alteration, superimposed on the sericitization, can be seen adjacent to small fractures found throughout this lithology. Poorly-developed myrmekite, composed of medium-grained plagioclase crystals and fine vermicular to bleb-like quartz patches, is present in small amounts in several samples. The myrmekite appears unrelated to the foliation of the rock but since the myrmekite is poorly-developed, this interpretation is uncertain.

Microcline, with poor to well defined cross-hatched twinning, makes up 5 to 30 percent of the fine-grained granitic rocks. It is found as fine-grained crystals, between 0.1 and 0.5 mm in size, that are only slightly altered to sericite. Fine rectangular flakes of muscovite, associated with chlorite, resulting from the retrograde alteration of biotite, produce the foliation observed on the hand sample and outcrop scales. Muscovite and chlorite rarely exceed 0.5 mm in size and together make up about 5 to 15 percent of the rock. Accessory minerals include rounded sphene and apatite grains, angular magnetite, disseminated grains of garnet, and a few zoned, twinned and highly altered grains of allanite (?). These minerals rarely compose more than 5 percent of the rock.

4.2.2 Coarse-grained Foliated Granitic Rock

Microcline, showing well-developed cross-hatched twinning, is the dominant mineral of this lithology. Making up 20 to 35 percent of the rock, it occurs as medium-grained crystals in the "matrix" and as large porphyroclasts, up to 2 cm in diameter. producing the augen texture described in Chapter 2. Quartz crystals, between 0.1 and 1.5 mm in size, show slight to moderate strained extinction and good subgrain development.

Quartz makes up 15 to 30 percent of the rock. Fine- to medium-grained plagioclase, measuring up to 1 mm in size, makes up 15 to 25 percent of the rock. Although alteration to sericite can be extensive and is commonly accompanied by hematite staining near small fractures, albite twinning is preserved and optical identification shows that the plagioclase is oligoclase (An 28).

Muscovite and brown biotite, occurring as fine flakes up to 0.5 mm in length, in association with chlorite derived from the partial retrograde alteration of biotite, produce the wrap-around foliation of this lithology. Muscovite can make up to 5 percent of the rock, biotite 5 to 15 percent, and chlorite up to 15 percent. Accessory minerals include: sphene, which can rarely show good cleavage or parting; apatite, garnet and epidote, occurring as fine rounded grains; and fine angular to subangular magnetite. Disseminated throughout the augen-rich rock, these minerals rarely make up more than a few percent of the mineralogy.

The apparent gradation from fine-grained moderately foliated granitic rocks in the area of Nile Brook, through medium-grained poorly foliated augen-rich rocks, to less deformed granitic rocks near Fielding Road would suggest that the foliated rocks of the Egypt Highland

unit are metamorphosed plutonic rocks rather than "granitized" paragneisses as proposed by Milligan (1970). The large microcline augen in these rocks are more readily explained as relict fragments of a coarse-grained granitic intrusion which have survived deformation, while the quartz, plagioclase and rare mafic minerals have fractured or recrystallized to finer grains, rather than as recrystallized potassium feldspar derived from high grade regional metamorphism.

4.3 IGNEOUS ROCKS

4.3.1 Granodiorite

The modal composition for a sample of the Bothan Brook granodiorite is given in Table 4.1 Column A. Fine- to coarse-grained plagioclase, with crystals up to 5 mm in size, dominates. Although moderately to extensively sericitized, cleavage traces and albite twinning are preserved in some crystals. Microprobe analyses from the Bothan Brook granodiorite reveal that the plagioclase is albite, with anorthite content of individual grains ranging between 2 and 9 percent. These compositions may be primary but are more likely the result of alteration processes as indicated by the sericitization mentioned previously.

TABLE 4.1

MODES OF THE BOTHAN BROOK GRANODIORITE

AND THE WEST BRANCH NORTH RIVER MONZOGRANITE

	A Bothan Brook granodiorite	B West Branch North River monzogranite
Quartz	34.8	11.8
Plagioclase[+]	48.2	63.0
Microcline	12.4	0.6
Biotite	-	13.3
Muscovite	0.3	-
Hornblende	-	8.7
Epidote	-	1.3
Chlorite	1.4	0.1
Sphene	-	0.8
Opaques	2.9	0.4
Total	100.0	100.0
[+] Composition	An 2 - 9	An 25 - 30

Quartz, occurring either as fine rounded grains or as coarse polygonal crystals up to 4 mm in size, shows moderate strained extinction and poor subgrain development and can form poorly-developed myrmekitic intergrowths with adjacent plagioclase grains. Microcline crystals, ranging in size from 0.2 to 3 mm, show extensive sericitization and poorly developed cross-hatched twinning. Accessory minerals include fine rounded apatite and sphene grains and fine fibrous chlorite probably resulting from the retrograde alteration of pre-existing biotite.

Although the rock has been deformed to some degree, as evident from strained quartz crystals, and hydrothermally altered, as indicated by the ubiquitous sericitization and reddening of the plagioclase, no penetrative metamorphic fabric has been detected in the Bothan Brook granodiorite.

4.3.2 Monzogranite.

The modal mineral composition of a sample of the West Branch North River monzogranite is listed in Table 4.1 Column B. However, the results given categorize the rock as a quartz diorite; this is because the results are not representative of the whole intrusion since outside

the study area the rock ranges locally from granodiorite to aplite and pegmatite.

Medium- to coarse-grained plagioclase is the dominant mineral. The crystals, up to 5 mm in size, do not show zoning, and composition of individual grains, determined optically, ranges between An 25 and An 30. Alteration to sericite is slight to moderate and many grains show bent or kinked albite twins. Fine- to medium-grained brown biotite makes up more than 50 percent of the mafic mineralogy of this rock. The larger flakes, which can be up to 3 mm in length, are commonly bent or kinked and contain randomly distributed minute inclusions of apatite, zircon and magnetite. Retrograde alteration to chlorite is minimal.

Minor medium-grained quartz is interstitial to the plagioclase. The quartz crystals show strained extinction and poorly-developed subgrains. Hornblende, between .05 and 2 mm in length, makes up the remainder of the mafic phase of the monzogranite. The grains show slight alteration to chlorite along fractures and grain boundaries.

Microcline, showing poorly-developed cross-hatched twinning, occurs as disseminated crystals ranging in size from 0.1 to 1 mm. Accessory minerals include fine rounded

apatite, zircon and magnetite (mentioned above), and medium-grained sphene.

Although the West Branch North River monzogranite is clearly deformed, as shown by strained quartz grains and bent or kinked plagioclase and biotite crystals, and has been hydrothermally altered, the rock does not show any metamorphic fabric in the study area. However, Jamieson (pers. comm., 1983) indicated that, in at least one locality east of Highland Road, the monzogranite has a weak foliation.

4.3.3 Pegmatite

Although the mineralogy of the late pegmatite veins and pockets is highly variable, plagioclase, determined by optical methods to be oligoclase (An 28 to An 30), is generally dominant. Composing between 25 and 55 percent of the pegmatite, it occurs as extensively sericitized fine- to medium-grained crystals up to 3 mm in size. Fine- to medium-grained quartz shows strained extinction and makes up between 20 and 50 percent of the rock. Fine- to medium-grained microcline, showing good cross-hatched twinning, makes up 20 to 35 percent of individual pegmatite samples. Fine to medium flakes of muscovite, disseminated throughout the rock, generally comprise less than 2 percent of any given sample but rarely form

large muscovite books several centimeters in size. Minor chlorite, probably resulting from the alteration of preexisting biotite, can be found in small amounts in a few samples.

4.3.4 Dykes

The diabase dykes are typically composed of plagioclase, clinopyroxene, olivine and minor biotite and opaques. Plagioclase, which can make up to 70 percent of an individual sample, occurs as subhedral laths, up to 1 mm in length, showing no preferred orientation. Although twinning is more or less preserved, extensive sericitization prevents optical determination of the plagioclase composition. Interstitial angular augite and rounded olivine rimmed by magnetite, are between 0.1 and .75 mm in size, and compose up to 45 percent and 10 percent of the rock respectively. Brown biotite, occurring as very fine flakes, rarely exceeding 0.1 mm in length, can be found in small amounts in some of the dykes. In others, only retrograde chlorite, derived from the biotite, is observed. Magnetite occurs as fine granular alteration rims surrounding olivine grains.

The ultramafic dyke, located 3 km south of Ryan Brook, is composed of fine-grained anhedral hypersthene

crystals, up to 0.5 mm in size, making up 60 percent of the dyke; very fine- to medium-grained anhedral to subhedral hornblende crystals, composing 20 percent of the rock; very fine to medium angular magnetite grains, making up the remaining 20 percent; and a few disseminated grains of sphene. The dyke is cut by a thin fine-grained quartz-plagioclase veinlet lined on either side by hornblende crystals.

The rhyolite dyke, situated along Middle River about 2.5 km south of Fielding Road, consists of fine- to coarse-grained phenocrysts in a very fine-grained, almost cryptocrystalline, groundmass of totally sericitized plagioclase microlites. The phenocrysts, up to 2 cm in diameter, make up about 45 percent of the dyke and include euhedral crystals of potassium feldspar (?), rounded grains of quartz commonly showing strained extinction, and subhedral to anhedral plagioclase crystals showing very poor albite and pericline twinning. Alteration to sericite proved too extensive for an optical determination of the plagioclase composition.

4.4 SUMMARY

The following is a summary of the findings obtained

from the petrographic examination of the rocks of the Middle River area:

1. The overall grain size increases from very fine- to fine grained in the phyllitic and schistose metasedimentary rocks in the south to medium- to coarse-grained in the pelitic and semipelitic schists and gneisses and granitic rocks in the north.
2. Textural equilibrium is poorly developed in all lithologies except for isolated instances such as samples containing idioblastic hornblende and chloritoid porphyroblasts.
3. Porphyroblast mineralogy changes from low-grade minerals (chlorite and chloritoid) in the schists and phyllites to higher grade minerals (garnet, staurolite and kyanite) in the gneisses.
4. In the low grade rocks, the porphyroblasts are syntectonic to post-tectonic to the development of the schistosity; in the high grade rocks, staurolite and kyanite porphyroblasts are pre-tectonic to the gneissossity while garnet crystals are pre- or syn- to post-tectonic to the gneissic foliation.
5. Alteration of hornblende to actinolite in the metabasite sheets and the breakdown of staurolite and kyanite to muscovite and biotite in the high-grade metapelites appear to reflect pervasive retrograde metamorphism of the Middle River complex.

6. Retrograde chloritization of biotite, hornblende and garnet and sericitization and hematization of plagioclase and microcline are highly variable and probably reflect localized hydrothermal activity associated with minor faults and shear zones found throughout the area.

CHAPTER 5

GEOCHEMISTRY OF THE METABASITES AND METASEDIMENTARY AND GRANITIC ROCKS

5.1 INTRODUCTION

The major element makeup of the metabasite sheets, phyllites and pelitic schists of the Middle River unit is determined by whole-rock analysis. Twelve samples of metabasites, four samples of pelitic schists and a sample of metasedimentary phyllite were selected for analysis using the electron microprobe technique (see Appendix I). The major and trace element makeup of three samples of the coarse-grained augen-rich granitic rocks of the Egypt Highland unit, four samples of Bothan Brook granodiorite and five samples of West Branch North River monzogranite was determined by X-ray fluorescence at the University of Ottawa. Five additional samples of West Branch North River monzogranite were analyzed using the electron microprobe technique.

5.2 GEOCHEMISTRY OF THE METABASITES

Analyses of metabasite samples were carried out to determine if any gradational change in major element

composition could be detected. Any such change could be used as evidence that the metabasite sheets are distinct and separate as opposed to being a single layer repeated by folding. It is also hoped that the data, in conjunction with lithological and petrographic observations discussed in Chapters 2 and 4 respectively, may lead to the determination of the protolith of these mafic rocks.

The whole-rock chemical analyses of the metabasites are listed in Table 5.1. The mineral assemblages present in each sample and their modal percentages are listed in Table 5.2.

Before any attempt at interpreting the major element composition of the metabasites is undertaken, one must first consider the degree of alteration affecting the rocks. Alteration processes that have affected, to some degree, the metabasites are: chloritization of biotite and, to a lesser extent, hornblende; sericitization of plagioclase; breakdown of hornblende to actinolite; and introduction of calcite and minor hematite in veinlets and fractures. Variable, and in some cases relatively high, water content and ferric to ferrous iron ratios also reflect alteration of particular samples. Another indication of alteration, in terms of alkali metasomatism, is shown in Figure 5.1, where more than half the

TABLE 5.1

MAJOR ELEMENT COMPOSITION OF THE METABASITES

The samples are arranged geographically from south to north.

	8106	8118B	8103	8113	8114A
SiO_2	51.27	54.90	48.11	48.57	48.76
TiO_2	.77	.92	1.82	2.71	2.75
Al_2O_3	15.41	15.62	15.31	15.64	14.38
Fe_2O_3	4.96	3.96	3.26	3.16	2.41
FeO	7.73	7.73	8.78	10.00	10.45
MnO	.23	.20	.38	.47	.29
MgO	5.92	5.39	9.18	6.68	5.40
CaO	6.52	5.44	9.31	7.40	9.81
Na_2O	3.74	3.08	3.43	2.91	3.94
K_2O	.62	1.49	.37	.21	.18
P_2O_5	.11	.02	.14	.25	.31
H_2O+	1.66	2.06	2.81	2.29	1.29
H_2O-	.18	.20	.17	.06	.29
CO_2	.38	.63	1.86	.31	.79
TOTAL	99.44	101.64	104.93	100.66	101.05
Q	2.27	7.80	-	1.55	-
Or	3.79	8.93	2.19	1.24	1.07
Ab	32.49	26.40	28.95	25.14	33.79
An	24.10	24.70	25.27	29.59	21.32
Ne	-	-	.02	-	-
Di	6.87	2.05	16.13	5.12	21.47
Hy	21.34	22.49	-	26.87	2.94
Ol	-	-	18.93	-	9.88
Mt	7.39	5.81	4.72	4.67	3.54
Il	1.50	1.77	3.46	5.24	5.30
Ap	.25	.05	.33	.58	.72
TOTAL	100.00	100.00	100.00	100.00	100.00

TABLE 5.1

MAJOR ELEMENT COMPOSITION OF THE METABASITES - (CONTINUED)

The samples are arranged geographically from south to north.

	8115	81109	8128	8129	81111
SiO_2	47.27	48.38	50.00	49.70	46.91
TiO_2	2.53	1.93	2.94	2.20	3.25
Al_2O_3	16.02	14.22	15.10	15.53	14.45
Fe_2O_3	1.98	2.14	.99	1.52	3.30
FeO	11.37	9.93	10.99	10.27	11.71
MnO	.20	.12	.19	.12	.37
MgO	7.34	7.50	5.13	6.40	6.94
CaO	9.27	10.30	8.23	8.78	9.24
Na_2O	3.29	3.06	4.17	2.79	2.55
K_2O	.21	.18	.49	.19	.19
P_2O_5	.30	.13	.36	.15	.38
H_2O+	1.46	1.57	1.70	1.61	1.48
H_2O-	.24	.12	.42	.14	.02
CO_2	.05	.45	2.46	.30	.20
TOTAL	101.53	100.03	103.17	99.70	100.99
Q	-	-	-	1.25	-
Or	1.24	1.07	2.96	1.12	1.12
Ab	27.94	26.42	35.75	24.21	21.76
An	28.36	25.11	21.36	30.00	27.60
Ne	-	-	-	-	-
Di	12.96	21.51	14.67	11.24	13.22
Hy	3.77	8.75	7.55	25.30	22.42
Ol	17.35	9.94	9.74	-	1.98
Mt	2.87	3.16	1.45	2.26	4.81
Il	4.81	3.74	5.66	4.27	6.21
Ap	.70	.30	.86	.35	.88
TOTAL	100.00	100.00	100.00	100.00	100.00

TABLE 5.1

MAJOR ELEMENT COMPOSITION OF THE METABASITES - (CONTINUED)

The samples are arranged geographically from south to north.

	81103	81120
SiO_2	46.54	49.12
TiO_2	1.40	1.13
Al_2O_3	16.06	17.26
Fe_2O_3	2.88	1.47
FeO	9.22	8.47
MnO	.19	.22
MgO	11.48	8.06
CaO	8.93	9.46
Na_2O	2.94	2.98
K_2O	.56	1.39
P_2O_5	-	-
H_2O+	2.81	2.16
H_2O-	.26	.18
CO_2	.13	.04
TOTAL	103.40	101.93
Q	-	-
C	3.32	8.29
Ab	21.33	23.34
An	28.94	29.72
Ne	1.88	1.07
Di	12.31	14.22
Hy	-	-
Ol	25.40	19.06
Mt	4.16	2.15
Il	2.66	2.15
Ap	-	-
TOTAL	100.00	100.00

TABLE 5.2

MODES OF THE METABASITES

	8106	8118b	8103	8113	8114a	8115
Hornblende	45.4	23.7	58.9	56.3	66.7	67.6
Quartz	24.7	32.2	10.3	23.6	10.9	20.0
Plagioclase	-	-	20.7	-	11.4	0.2
Biotite	17.1	29.7	1.4	-	-	-
Epidote	4.3	6.0	-	-	2.9	-
Opaques[+]	8.5	2.5	6.9	13.0	7.7	12.2
Rutile	-	-	-	-	-	-
Sphene	-	-	-	-	-	-
Calcite	-	-	1.8	-	0.4	-
Chlorite	-	5.9	-	7.1	-	-
Total	100.0	100.0	100.0	100.0	100.0	100.0

[+] Opaque minerals include magnetite with minor ilmenite and pyrite.

Secondary calcite in veinlets and minor disseminated calcite.

Retrograde chlorite after biotite and hornblende.

TABLE 5.2

MODES OF THE METABASITES - (CONTINUED)

	81109	8128	8129	81111	81103	81120
Hornblende	63.2	48.5	69.4	66.1	75.1	59.7
Quartz	1.7	31.1	18.3	19.4	4.3	0.6
Plagioclase	15.9	-	-	-	17.4	29.1
Biotite	-	1.3	-	-	0.7	6.7
Epidote	1.5	-	0.1	2.1	-	-
Opaques[+]	17.4	10.0	10.0	12.4	-	0.4
Rutile	-	-	-	-	2.5	-
Sphene	-	-	-	-	-	3.5
Calcite	0.3	8.0	0.8	-	-	-
Chlorite	-	1.1	1.4	-	-	-
Total	100.0	100.0	100.0	100.0	100.0	100.0

[+]Opaque minerals include magnetite with minor ilmenite and pyrite.

Secondary calcite in veinlets and minor disseminated primary(?) calcite.

Retrograde chlorite after biotite and hornblende.

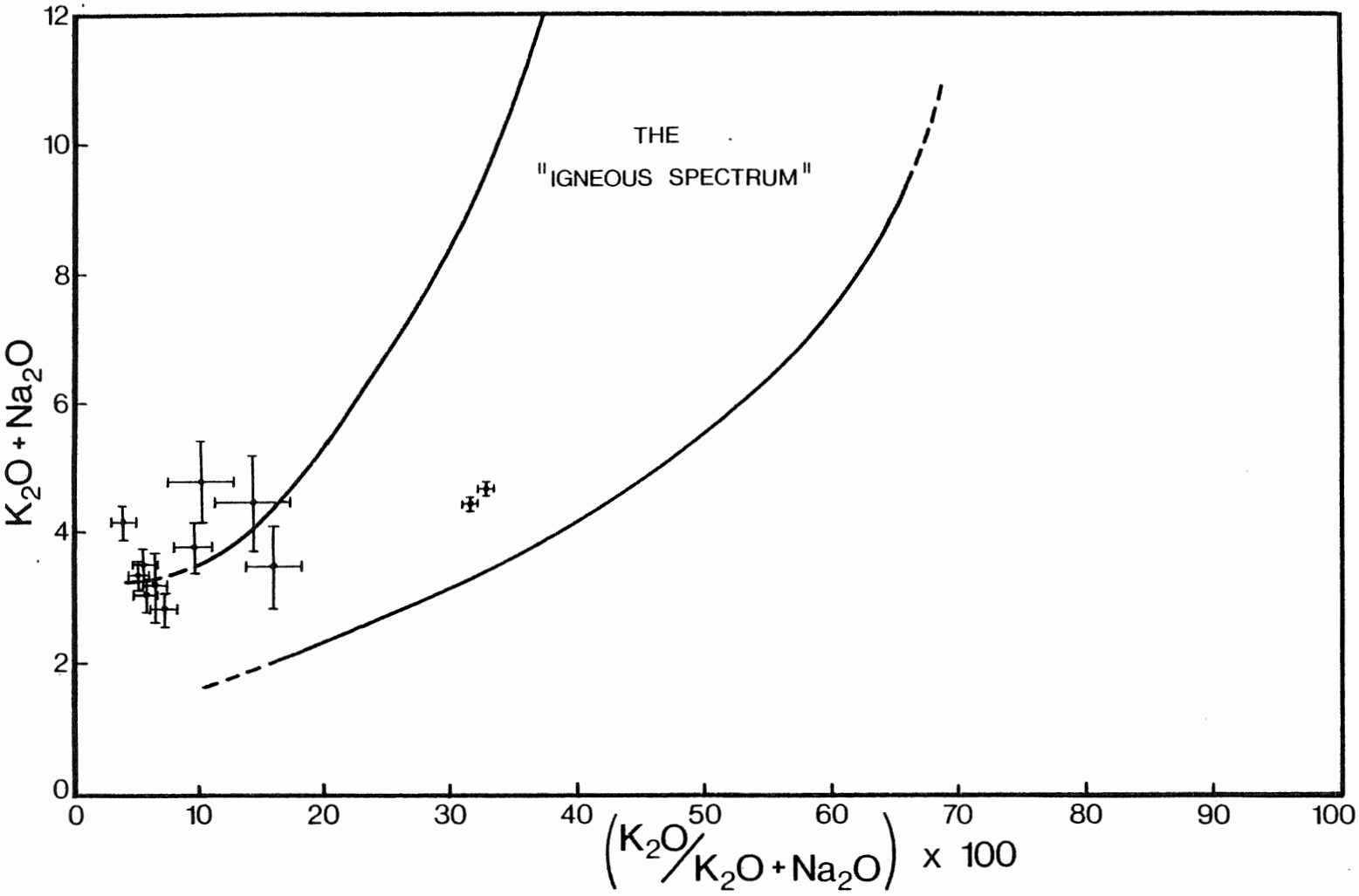

Figure 5.1 Plot of alkali parameters where the field of fresh volcanic rock compositions lies within the "igneous spectrum" (Hughes, 1973). Half of the Middle River metabasites plot outside the field, an indication of alteration through the loss of K_2O or the addition of Na_2O.

samples plot outside the normal "igneous spectrum" as defined by Hughes (1973). These alteration effects, and the polymetamorphic history of the area, have undoubtedly clouded all primary geochemical features of the metabasites and great care must therefore be exercised in interpreting their present major element makeup.

The origin of amphibolites, and the distinction between ortho- and para-amphibolites, is generally difficult to determine, especially in areas that have undergone high-grade metamorphism (see Evans and Leake, 1960; Leake, 1964; van de Kamp, 1970). Para-amphibolites result from the metamorphism of calcareous or dolomitic shale, whereas ortho-amphibolites are, typically, derived from basic igneous rocks (Leake, 1964).

The determination as to whether the metabasites of the Middle River unit are ortho- or para-amphibolites is hindered by a number of problems. Aside from a lack of exposure, the physical characteristics of the metabasite sheets is probably the greatest problem. The concordant contact relationship between the metabasites and the surrounding schists and phyllites supports a variety of modes of emplacement. Intrusion of thin sill-like sheets of basalt or diabase inconsolidated sedimentary rocks or

deposition of mafic tuffs or flows or of calcareous or dolomitic shales interlayered with clastic sediments could have resulted in the observed morphology of the metabasite sheets. The absence of primary igneous or sedimentary structures and the possibility that the parallel contacts could result from strain rather than representing original concordant contacts does not facilitate the task of determining the protolith of the metabasites.

To distinguish between ortho- and para-amphibolites, the study of differences between igneous and sedimentary compositional trends has proven more successful than the examination of individual major elements. The methods of Evans and Leake (1960) and Leake (1964), where major elements are converted to Niggli numbers (Niggli, 1954), are applied to the Middle River metabasites to determine whether they are of sedimentary or igneous origin.

The major difference between magmatic differentiation and sedimentary variation is seen when plotting Niggli c (CaO) versus mg ($MgO/MgO+FeO+MnO+2Fe_2O_3$) (Figure 5.2). In the early stages of crystallization, there is an increase in c with decrease in mg as the crystallization of olivine is secceeded by clinopyroxene and increasing amounts of calcic plagioclase. When plagioclase becomes more sodic, and the amount of clinopyroxene diminishes, c declines with lower mg (Leake, 1964). The trends given

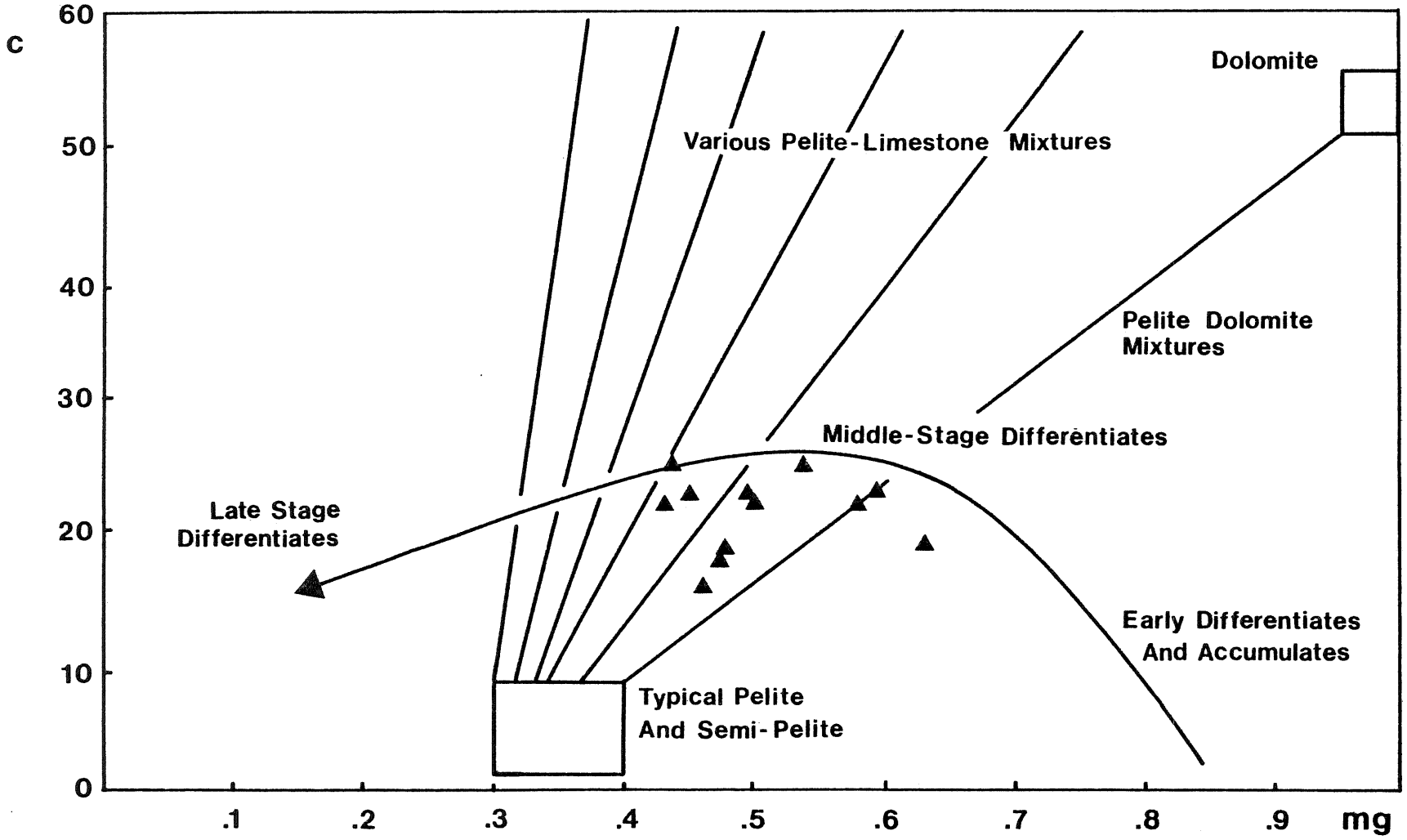

Figure 5.2 Niggli mg against c, where mg = MgO/FeO+MnO+2Fe_2O_3+MgO and c = CaO. Lines indicate various limestone-dolomite mixtures mixed with pelites and semipelites (from Leake, 1964). The Middle River metabasites follow the basic igneous differentiation trend but are shifted toward the pelite-semipelite region.

by mixtures of pelite and limestone or dolomite, or both, are approximately at right angles to the trend of basic igneous rocks. The metabasites of the Middle River unit, plotted on Figure 5.2, follow the magmatic differentiation trend of basic magmas yet are clearly shifted toward the pelite-semipelite region of the diagram, indicating a slight depletion of Ca in the rocks.

Another plot useful in distinguishing between igneous variations and those of pelite-limestone and pelite-dolomite mixtures is 100mg + c + (al+alk) = 100. The three variables are plotted on a triangular diagram according to Leake (1964) (Figure 5.3). The line joining dolomites and typical pelites and semipelites is at right angles to the variation of a typical basic igneous series while mixtures of pelites and semipelites plot in a totally different part of the diagram. The Middle River metabasites follow a trend similar to that of basic igneous rocks but, here also, are clearly shifted toward the pelite-semipelite region of the diagram, indicating an enrichment in Al, Na and K in the rocks. The shifts revealed in both diagrams are not altogether unexpected when considering the close stratigraphic relationship between the metabasite sheets and the surrounding metasedimentary rocks.

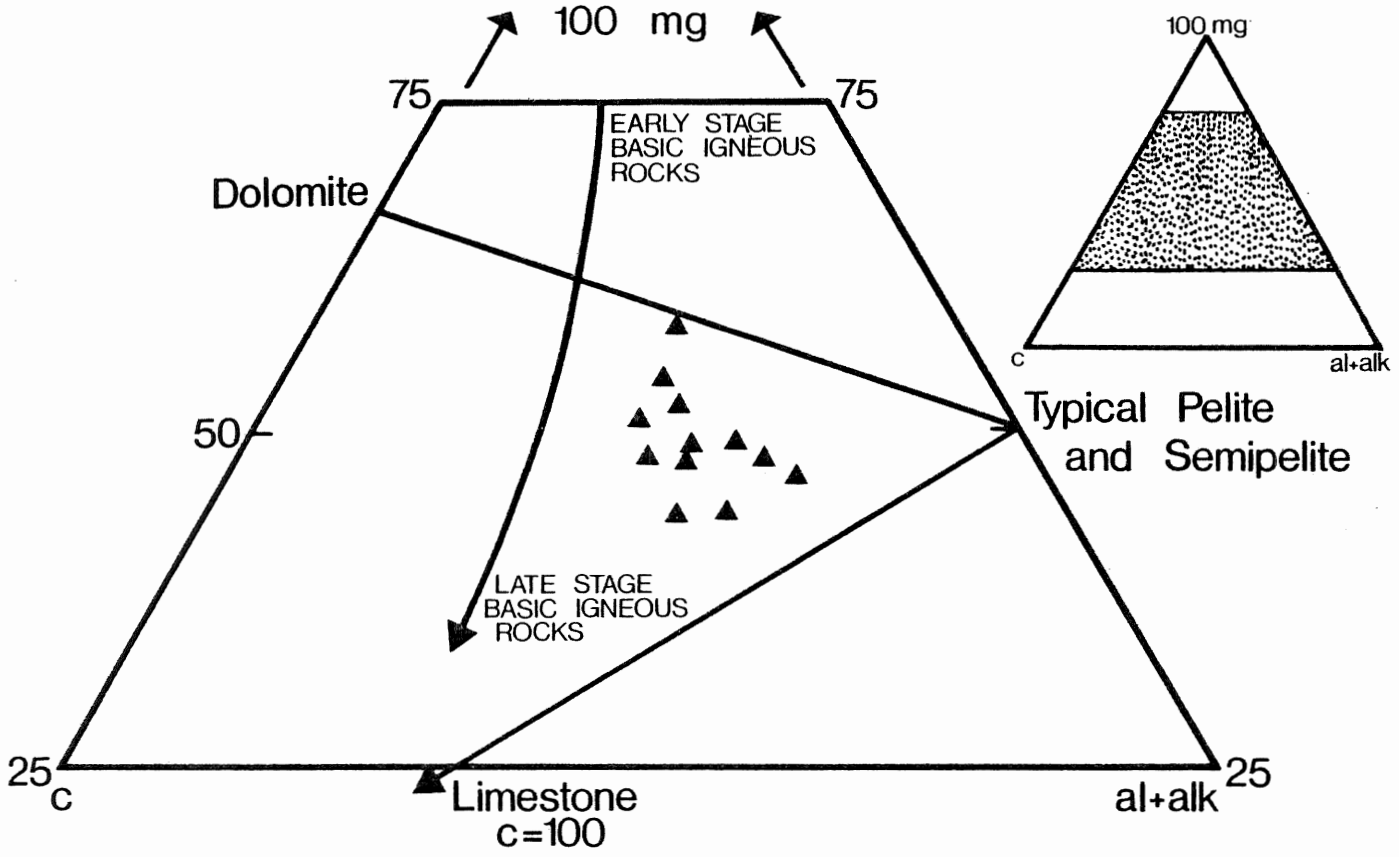

Figure 5.3 Part of the 100 mg, c and (al + alk) triangle (from Leake, 1960). The Middle River metabasites follow the basic igneous rock trend but are shifted toward the pelite-semipelite region.

Leake (1964) noted that ortho-amphibolites contained lower Niggli k ratios than para-amphibolites. A plot of Niggli k (K_2O/K_2O+Na_2O) versus mg (Figure 5.4) shows low k and moderate mg values for the metabasites, values that are characteristic of basic igneous rock suites (van de Kamp, 1970). Leake (1964) indicated that alkali metasomatism often disturbs the k ratio, but concluded that amphibolites having low k values are almost certainly igneous in origin while high k values can indicate either a sedimentary or igneous origin.

Based on these results, it is concluded that the metabasite sheets of the Middle River unit were derived from the metamorphism of basic igneous rocks as opposed to a carbonate-pelite mixture. The type of basic igneous rock (basalt, diabase, mafic tuff or flow) which could have produced the Middle River metabasites remains uncertain but the apparent continuity of the thin sheets over several kilometers along strike would favor the deposition of mafic tuffs or flows in a clastic sedimentary sequence rather than repeated intrusion of sills in consolidated sedimentary rocks. However, the "unconformable", and apparently "chilled", contact between two metabasites along Middle River (mentioned previously in Chapter 2) may represent two separate flows or a flow in contact with a tuff layer.

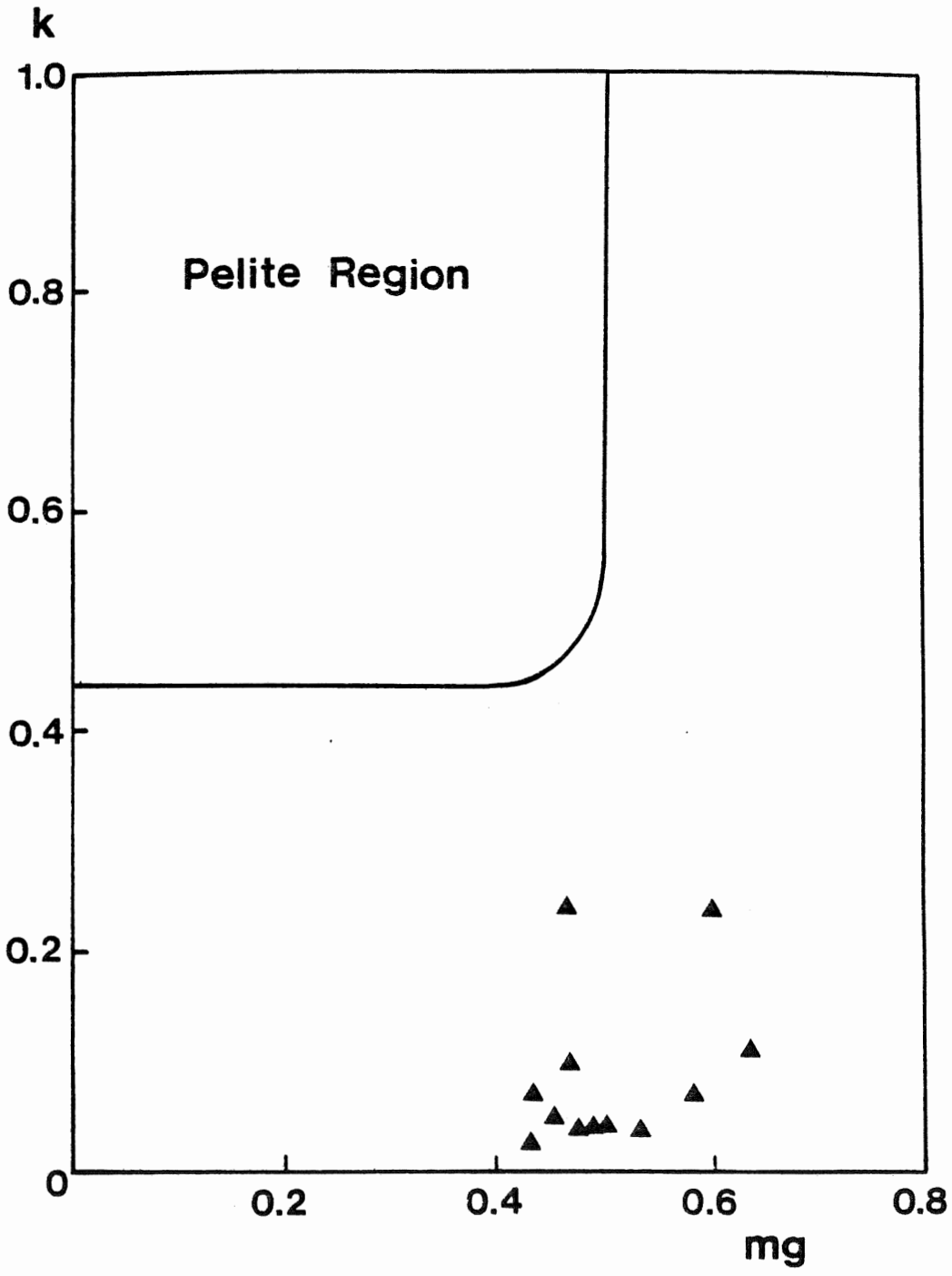

Figure 5.4 Niggli 1c (K_2O/K_2O+Na_2O) versus mg showing that the Middle River metabasites plot outside the delineated field for pelites (after van de Kamp, 1970).

A number of features of the metabasite analyses can be seen in Table 5.1. The metabasites have a narrow compositional range, with all samples being basaltic to andesitic (44-55 percent SiO_2). The silica saturation variability shown in the CIPW norms, with a few samples being silica oversaturated (Q and Hy in the norm), others being silica saturated (Ol and Hy in the norm), while still others being silica undersaturated (Ol and Ne in the norm) (Cox et al., 1979) even though all the metabasite samples appear to contain quartz. However, some of the "quartz" is so fine-grained that optical determination proved very difficult and the "quartz" may be plagioclase instead.

Another compositional feature of the metabasites is an increase in TiO_2 when traversing the sheets from south to north. This increase may represent compositional differences in the protolith, and may therefore be evidence that the metabasite sheets are distinct layers rather than a single layer repeated by folding. However, the small number of analyses and the irregular distribution of the samples makes this conclusion tentative at best.

Finally, the high CO_2 contents of samples 8103 and 8128, with correspondingly high total oxides contents,

reflects the high modal calcite contents of the two samples.

In their study of a similar metasedimentary and metavolcanic assemblage in the Cape North area of Cape Breton Island, Macdonald and Smith (1980) examined the major element composition of the metavolcanic rocks of the Money Point Group (intermediate and mafic tuffs, meta-basalts and amphibolites). Comparing the Money Point rocks to the metabasites of the Middle River unit reveals a high degree of similarity in the major element compositions of the two suites. These geochemical similarities are coupled with a broad lithological parallelism between the two assemblages. The two regions may be stratigraphically related but further comparative work between these and other lithologically similar areas in the Cape Breton Highlands is required before more concrete relationships are established.

5.3 GEOCHEMISTRY OF THE METASEDIMENTARY ROCKS

Whole-rock analyses were carried out on the four pelitic schist samples used for garnet-biotite geothermometry to determine if variations in the major element chemistry of the samples are substantial enough to invalidate a comparison of the temperatures obtained.

The metasedimentary phyllite, sample 81108, was analyzed because of its particular mineralogy and texture: the sample contains poorly developed chloritoid and garnet porphyroblasts in a chlorite-muscovite-quartz matrix. The analyses will also be used in Thompson AFM diagrams (in Chapter 7) to determine if equilibrium exists between the mineral assemblage and whole rock composition of each sample. The major element compositions of the schists and phyllite are listed in Table 5.3. Modal concentrations of the various minerals present in each sample are listed in Table 5.4.

The major element compositions of the four pelitic schists do not differ significantly except for higher SiO_2 in samples 81101 and 8150, which contain more modal quartz than the other two; and higher Al_2O_3 in samples 8123 and 8135, an enrichment that is reflected in the presence of kyanite in both samples and staurolite in 8135.

Based on the comparison of the bulk composition of chloritoid-bearing and chloritoid-free metapelites of the greenschist facies, Hoschek (1967) delineated compositional fields of chloritoid stability. In order for a rock to plot within these fields, its bulk composition requires a comparatively high Al_2O_3, low abundances of

TABLE 5.3

MAJOR ELEMENT COMPOSITION OF METASEDIMENTARY ROCKS

	8135	81101	8123	8150	81108
SiO_2	58.60	66.94	57.61	61.06	64.04
TiO_2	1.27	1.39	1.03	.85	.73
Al_2O_3	20.30	15.80	20.87	16.77	16.75
Fe_2O_3	3.16	2.10	1.89	1.86	.53
FeO	6.18	4.20	6.21	6.06	7.53
MnO	.09	.05	.10	.34	.13
MgO	3.56	2.16	3.71	4.01	2.66
CaO	1.17	1.55	1.56	3.22	2.26
Na_2O	1.51	2.77	2.64	1.92	2.97
K_2O	3.69	2.65	3.65	2.94	.76
P_2O_5	.18	.22	.11	.06	.21
TOTAL	99.71	99.83	99.38	99.09	98.57
Fe/Fe+Mg	.691	.715	.683	.661	.785

TABLE 5.4

MODES OF THE PELITIC SCHISTS
AND METASEDIMENTARY PHYLLITE

	8135	81101	8123	8150	81108
Quartz	30.6	59.6	29.4	36.3	45.8
Biotite	24.3	14.2	37.8	26.4	-
Muscovite	23.0	7.1	4.9	3.2	7.1
Plagioclase	6.3	17.7	18.4	16.9	-
Chlorite	-	-	-	-	34.2
Chloritoid	-	-	-	-	10.5
Garnet	9.2	1.2	5.2	12.7	1.0
Kyanite	3.0	-	4.3	-	-
Staurolite	1.6	-	-	-	-
Sphene	-	0.1	-	0.7	-
Opaques[+]	2.0	0.1	-	3.1	1.4
Total	100.0	100.0	100.0	100.0	100.0

[+] Opaque minerals include pyrite and chalcopyrite in samples 8135, 81101, 8123 and 8150; magnetite and ilmenite in sample 81108.

alkalies and CaO and a high FeO^T/FeO^T+MgO ratio. A number of workers (Liou and Chen, 1978; Atherton and Smith, 1979) have noted agreement between their results and the delineated fields, but some disagreements have been reported as well (see La Tour et al., 1980).

The major element composition of the chloritoid-bearing phyllite from this study plots in the delineated fields for chloritoid-bearing metasedimentary rocks (Figure 5.5) defined by Hoschek (1967) except for the Al_2O_3-CaO-($FeO+Fe_2O_3$) diagram where the sample plots just outside the field, indicating a slight enrichment in CaO. The high Al_2O_3 content of sample 81108 is an indication of the aluminous character of the original sediment, which was probably a clay-rich shale or mud-stone.

The bulk composition of sample 81108 resembles those of Atherton and Smith (1979) for chloritoid-biotite-bearing rocks from Perthshire, Scotland, but is higher in SiO_2, CaO and Na_2O and lower in Al_2O_3 and K_2O than those of Baltatzis (1979) for chloritoid-staurolite-bearing rocks from Stonehaven, Scotland.

5.4 GEOCHEMISTRY OF THE GRANITIC ROCKS

The major and trace element compositions of the

Figure 5.5 Empirically delineated bulk compositional fields (stippled) of chloritoid-bearing metapelites in the greenschist facies (from Hoschek, 1967). The bulk composition of sample 81108 plots within the delineated fields but is slightly enriched in CaO.

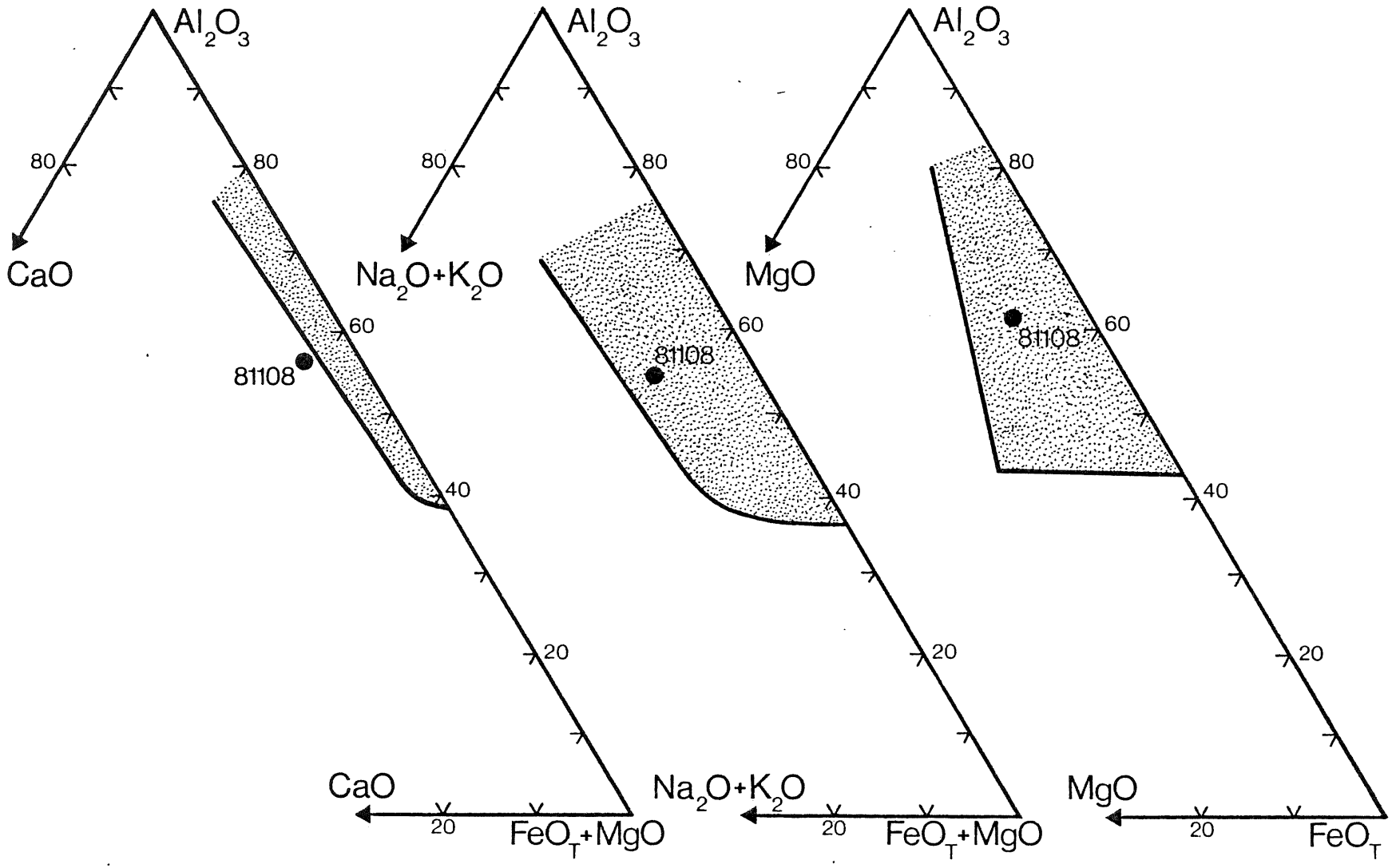
Al2O3
80
80
CaO
81108
60
40
20
CaO
20
FeOT+MgO
Al2O3
80
80
Na2O+K2O
81108
60
40
20
Na2O+K2O
20
FeOT+MgO
Al2O3
80
80
MgO
81108
60
40
20
MgO
20
FeOT

Egypt Highland unit granitic rocks, listed in Table 5.5, and of the Bothan Brook granodiorite, listed in Table 5.6, were obtained for a geochemical comparison of the two lithologically similar intrusions to determine if they could be geochemically and tectonically related. Although a comparison of the major element makeups is essentially meaningless since the augen-rich granitic rocks are deformed while the Bothan Brook granodiorite is undeformed, a comparison of the trace element compositions may prove more informative.

The major and trace element composition of the West Branch North River monzogranite, listed in Table 5.7, was obtained to establish a data base for future comparison and possible correlation with other similar rocks to the north of the study area. The modal mineralogy of a sample of Bothan Brook granodiorite and a sample of the West Branch North River monzogranite are listed in Table 4.1 Columns A and B respectively.

All the analyses are quartz normative and show various degrees of oxidation by the presence of normative hematite in the analyses obtained by X-ray fluorescence.

Comparison of the granitic rocks from the Egypt

TABLE 5.5

MAJOR AND TRACE ELEMENT COMPOSITION
OF THE EGYPT HIGHLAND UNIT GRANITIC ROCKS

	MR-092	MR-094	MR-007
SiO_2	76.73	79.09	77.58
TiO_2	.16	.11	.17
Al_2O_3	12.71	11.97	11.88
Fe_2O_3	1.93	1.42	1.99
MnO	.04	-	.01
MgO	.18	.07	.12
CaO	.41	.15	.25
Na_2O	3.47	2.86	2.59
K_2O	4.79	5.61	5.54
P_2O_5	-	-	-
S	-	-	.01
TOTAL	100.42	101.28	100.14
Ba	129	74	235
Cu	10	-	6
Zr	270	213	271
Sr	63	8	26
Rb	176	256	193
Y	42	65	43
La	64	62	-
Zn	16	-	9
Ni	18	15	4
K/Rb	226.68	181.82	238.31
Rb/Sr	2.77	31.95	7.52
Ba/Sr	2.03	9.24	9.15
La/y	1.53	.95	-
Q	36.89	40.02	40.52
C	1.06	.90	1.16
Or	28.21	32.77	32.72
Ab	29.24	23.89	21.88
An	2.03	.74	1.24
Ne	-	-	-
Di	-	-	-
Hy	.45	.17	.30
Ol	-	-	-
Mt	-	-	-
Il	.09	-	-
Ap	-	-	-
Hm	1.92	1.40	1.99
Ru	.11	.11	.17
Py	-	-	.12
TOTAL	100.00	100.00	100.00

TABLE 5.6

MAJOR AND TRACE ELEMENT COMPOSITION
OF THE BOTHAN BROOK GRANODIORITE

	MR-364	MR-139	MR-326	MR-328
SiO_2	76.10	76.35	76.01	76.42
TiO_2	.15	.21	.14	.13
Al_2O_3	13.31	13.50	13.20	13.45
Fe_2O_3	1.24	1.27	.96	1.05
MnO	-	.01	.01	.01
MgO	.19	.41	.18	.18
CaO	.36	.36	.35	.53
Na_2O	3.22	3.11	3.23	2.95
K_2O	5.58	5.18	5.66	5.89
P_2O_5	-	.02	-	-
S	-	-	-	-
TOTAL	100.15	100.42	99.74	100.56
Ba	420	458	277	249
Cu	-	14	-	-
Zr	114	106	84	95
Sr	161	155	120	122
Rb	137	161	143	144
Y	15	16	9	9
La	94	63	52	63
Zn	2	13	10	11
Ni	-	9	7	6
K/Rb	337.85	267.87	328.95	338.20
Rb/Sr	.85	1.04	1.19	1.18
Ba/Sr	2.61	2.96	2.31	2.03
La/y	6.27	3.80	5.50	6.82
Q	34.89	36.93	34.61	35.17
C	1.31	2.16	1.12	1.25
Or	32.96	30.51	33.57	34.65
Ab	27.20	26.20	27.40	24.82
An	1.78	1.65	1.74	2.61
Ne	-	-	-	-
Di	-	-	-	-
Hy	.47	1.02	.45	.32
Ol	-	-	-	-
Mt	-	-	-	-
Il	-	.02	.02	.02
Ap	-	.05	-	-
Hm	1.24	1.26	.96	1.04
Ru	.15	.20	.13	.12
TOTAL	100.00	100.00	100.00	100.00

TABLE 5.7

MAJOR AND TRACE ELEMENT COMPOSITION
OF THE WEST BRANCH NORTH RIVER MONZOGRANITE
(obtained by X-ray fluorescence)

	MR-104	MR-280	MR-283	MR-097	MR-284
SiO_2	61.84	64.65	70.49	58.26	73.46
TiO_2	.71	.69	.41	.88	.20
Al_2O_3	18.08	17.23	15.29	18.38	14.65
Fe_2O_3	4.28	4.15	2.46	5.63	1.57
MnO	.06	.07	.04	.09	.01
MgO	2.10	1.94	1.03	3.32	.45
CaO	3.64	3.26	1.49	4.83	.44
Na_2O	4.65	4.12	3.86	4.47	4.11
K_2O	2.77	3.07	4.34	2.13	5.01
P_2O_5	.29	.25	.12	.45	.05
S	-	-	.01	.01	-
TOTAL	98.42	99.43	99.54	98.45	99.95
Ba	1365	1322	1082	1216	754
Cu	22	9	5	42	3
Zr	320	321	201	255	106
Sr	879	794	327	1129	156
Rb	75	68	138	46	185
Y	19	15	9	21	20
La	97	108	82	64	61
Zn	51	52	17	64	5
Ni	33	28	12	57	28
K/Rb	304.58	373.87	262.67	382.79	224.29
Rb/Sr	.09	.09	.42	.04	1.19
Ba/Sr	1.55	1.66	3.31	1.08	4.83
La/y	4.99	6.99	9.11	3.06	3.09
Q	14.30	19.87	27.15	10.26	28.90
C	1.53	1.81	1.83	1.05	1.78
Or	16.65	18.26	25.79	12.80	29.65
Ab	39.98	35.06	32.81	38.42	34.79
An	16.42	14.62	6.64	21.30	1.86
Ne	-	-	-	-	-
Di	-	-	-	-	-
Hy	5.31	4.86	2.58	8.40	1.12
Ol	-	-	-	-	-
Mt	-	-	-	-	-
1l	.13	.15	.08	.20	.02
Ap	.68	.58	.28	1.06	.12
Hm	4.35	4.17	2.47	5.72	1.57
Ru	.65	.62	.37	.79	.19
TOTAL	100.00	100.00	100.00	100.00	100.00

TABLE 5.7

MAJOR AND TRACE ELEMENT COMPOSITION
OF THE WEST BRANCH NORTH RIVER MONZOGRANITE - (CONTINUED)
(obtained by the electron microprobe technique)

	MR-483	MR-484	MR-486	MR-489	MR-488
SiO_2	70.83	71.41	72.43	61.76	74.10
TiO_2	.31	.35	.31	1.00	.25
Al_2O_3	15.00	14.70	14.75	16.61	14.89
Fe_2O_3	.45	.70	.53	1.31	.36
FeO	1.07	1.09	1.08	3.86	.92
MnO	.03	.04	.04	.07	.03
MgO	.52	.59	.57	2.70	.33
CaO	1.48	1.54	1.54	3.46	1.35
Na_2O	3.94	3.97	3.94	3.98	3.70
K_2O	4.59	3.80	4.00	3.17	5.06
P_2O_5	.02	.04	.03	.35	.01
H_2O^+	.17	.41	.28	.85	.14
H_2O^-	.16	.36	.34	.35	.10
TOTAL	98.57	99.00	99.84	99.47	101.24
Q	26.38	29.80	29.85	14.22	29.07
C	.92	1.37	1.22	1.20	.88
Or	27.64	22.88	23.85	19.08	29.63
Ab	33.93	34.20	33.60	34.27	31.00
An	7.34	7.51	7.50	15.14	6.57
Ne	-	-	-	-	-
Di	-	-	-	-	-
Hy	2.48	2.44	2.55	11.40	1.84
Ol	-	-	-	-	-
Mt	.66	1.03	.77	1.93	.52
Il	.60	.68	.59	1.93	.47
Ap	.05	.09	.07	.83	.02
Hm	-	-	-	-	-
Ru	-	-	-	-	-
TOTAL	100.00	100.00	100.00	100.00	100.00

Highland unit and the Bothan Brook granodiorite reveals that the two "intrusions", although mineralogically similar, are different in both major and trace element makeup and are therefore geochemically and tectonically unrelated.

CHAPTER 6

MINERAL CHEMISTRY

6.1 INTRODUCTION

Following detailed petrographic examination of the various rock types, polished thin sections were prepared from 32 samples encompassing all the major lithologies of the study area. Electron microprobe analyses of several mineral phases were undertaken to determine their precise composition and, more specifically, to delineate compositional variations in hornblende across the sequence of metabasite sheets, to define compositional zoning in chloritoid and garnet, and for use in calcite-dolomite and garnet-biotite geothermometry. The location of the samples is shown on a Sample Location Map which can be found in the back pocket. The 32 samples are described in Appendix II.

6.2 CHLORITE ANALYSES

Table 6.1 is a compilation of chlorite analyses obtained from two metasedimentary schist samples (81108 and 8223) in which fine matrix chlorite grains were analyzed, a metabasite sample (8129) and two foliated granitic rock samples (8177 and 8191) in which chlorites

TABLE 6.1

MICROPROBE ANALYSES OF CHLORITES

	81108		8223		8129
	1	2	1	2	1
SiO_2	24.45	24.14	26.35	26.48	26.55
TiO_2	.08	.15	-	.09	.13
Al_2O_3	23.77	24.15	21.72	21.87	21.26
FeO*	29.08	29.10	21.07	21.52	22.77
MnO	.25	.17	.12	.20	.17
MgO	12.66	12.06	19.54	18.69	17.88
CaO	-	.05	-	.07	.08
Na_2O	-	-	-	-	-
K_2O	-	-	-	-	-
H_2O**	11.51	11.44	11.81	11.80	11.71
TOTAL	101.80	101.26	100.61	100.72	100.55
Si	5.092	5.055	5.348	5.378	5.434
Al^{IV}	2.908	2.945	2.652	2.622	2.566
Al^{VI}	2.925	3.014	2.543	2.612	2.561
Ti	.013	.024	-	.014	.020
Fe	5.065	5.096	3.576	3.655	3.897
Mn	.044	.030	.021	.034	.029
Mg	3.930	3.764	5.911	5.658	5.454
Ca	-	.011	-	.015	.018
Na	-	-	-	-	-
K	-	-	-	-	-
TOTAL CATIONS	19.977	19.939	20.051	19.988	19.979
Fe/Fe+Mg	.563	.575	.377	.392	.417
H	16.000	16.000	16.000	16.000	16.000
O	36.000	36.000	36.000	36.000	36.000
MINERAL NAME (AFTER HEY, 1954)	R I P I D O L I T E				

* Total iron as FeO.

** As computed from the program that derived the structural formulas.

TABLE 6.1

MICROPROBE ANALYSES OF CHLORITES - (CONTINUED)

	8129	8177		8191	
	2	1	2	1	2
SiO_2	26.09	27.18	27.10	28.23	28.23
TiO_2	-	-	.18	.17	-
Al_2O_3	22.25	16.50	16.95	18.57	18.42
FeO*	25.33	36.73	34.08	30.20	29.93
MnO	.21	.90	1.74	.97	.93
MgO	16.21	8.51	10.23	10.16	10.75
CaO	-	.16	-	.07	-
Na_2O	-	-	-	-	-
K_2O	-	.05	.08	.10	.04
H_2O**	11.73	10.95	11.10	11.20	11.20
TOTAL	101.82	100.98	101.46	99.67	99.50
Si_{IV}	5.331	5.950	5.850	6.078	6.039
Al^{IV}	2.669	2.050	2.150	1.962	1.961
Al^{VI}	2.687	2.207	2.161	2.718	2.682
Ti	-	-	.029	.027	-
Fe	4.328	6.724	6.152	5.402	5.354
Mn	.036	.167	.318	.176	.168
Mg	4.936	2.777	3.291	3.239	3.427
Ca	-	.038	-	.016	-
Na	-	-	-	-	-
K	-	.014	.022	.027	.011
TOTAL CATIONS	19.987	19.927	19.973	19.605	19.642
Fe/Fe+Mg	.467	.708	.651	.625	.610
H	16.000	16.000	16.000	16.000	16.000
O	36.000	36.000	36.000	36.000	36.000
MINERAL NAME (AFTER HEY, 1954)	RIPIDOLITE	BRUNSVIGITE		PYCNOCHLORITE	

* Total iron as FeO.

** As computed from the program that derived the structural formulas.

TABLE 6.1

MICROPROBE ANALYSES OF CHLORITES

(CONTINUED)

Rock type, sample location and minerals analyzed.

81108: Fine-grained metasedimentary phyllite from the east branch of Fortune Brook; fine-grained matrix chlorites.

8223: Fine-grained metasedimentary schist from the south end of Second Gold Brook; fine-grained matrix chlorites.

8129: Medium-grained metabasite from Fourth Gold Brook; fine-grained chlorites derived from the alteration of biotite.

8177: Medium-grained foliated granitic rock from upper Nile Brook near Fielding Road; fine-grained chlorites from the alteration of biotite.

8191: Medium-grained least deformed granitic rock from Nile Brook near Fielding Road; fine-grained chlorites from the alteration of biotite.

derived from the alteration of biotite were analyzed. The nomenclature of the chlorites, according to the scheme presented by Hey (1954) is included in Table 6.1.

The compositions of the chlorites from the two phyllites resemble those obtained by Atherton (1968), Mather (1970) and Ramsay (1973) from low-grade metapelites, although chlorites from sample 8223 are slightly enriched in magnesium and depleted in iron. Chlorites from sample 81108, which contains poorly-developed chloritoid and garnet porphyroblasts, have compositions very similar to those reported by Cruickshank and Ghent (1978), Baltatzis (1979) and Yardley et al. (1980) from chloritoid-bearing metasedimentary rocks.

The relatively high iron and low magnesium contents of the secondary chlorites from the granitic rocks are probably attributable to the pre-existing biotites from which the chlorites are derived but, unfortunately, because of pervasive chloritization, the compositions of these biotites could not be determined to verify this compositional relationship.

6.3 CHLORITOID ANALYSES

The analyses of chloritoids contained in two meta-

sedimentary schist samples are listed in Table 6.2. Sample 81108 contains medium-grained highly poikiloblastic crystals that are very poorly developed and have not reached textural equilibrium with the surrounding quartz-chlorite-muscovite matrix. Sample 8220 contains fine- to medium-grained, commonly idioblastic, twinned chloritoid crystals showing good hourglass inclusion patterns. Three large crystals were analyzed in sample 8220 to determine if any compositional zoning exists. As can be seen in Table 6.2, aluminum and magnesium increase from the core to the rim of the chloritoid crystals. The increase in magnesium is similar to that reported by Cruickshank and Ghent (1978) who also noted a decrease in manganese from core to rim, a trend not shown by the chloritoids of sample 8220. No major compositional differences are noted between the incipient and well-developed chloritoid crystals. The chloritoids of sample 8220 are characterized by slightly higher manganese and lower magnesium values and higher F/FM ratios and one of the three crystals contains titanium, which can be accounted for by the presence of fine ilmenite needles in many of the chloritoids in sample 8220.

The compositions of the chloritoids from both samples closely resemble those reported by Halferdahl (1961), Cruickshank and Ghent (1978), Baltatzis (1979)

TABLE 6.2

MICROPROBE ANALYSES OF CHLORITOIDS

	81108			8220	
	1	2	3	1	
				RIM	
SiO_2	23.94	23.91	24.26	24.20	24.66
TiO_2	-	-	-	-	-
Al_2O_3	39.92	39.97	39.72	40.94	41.12
FeO*	24.13	24.07	24.12	24.63	25.14
MnO	.40	.38	.31	.72	.78
MgO	2.87	2.85	2.55	2.25	2.29
CaO	.03	.02	-	-	-
Na_2O	-	-	-	-	-
K_2O	-	-	-	.04	-
TOTAL	91.29	91.20	90.96	92.78	93.99
Si	2.005	2.003	2.036	1.997	2.011
Al	3.941	3.948	3.930	3.984	3.954
Ti	-	-	-	-	-
Fe	1.690	1.687	1.693	1.700	1.715
Mn	.028	.027	.022	.050	.054
Mg	.358	.356	.319	.277	.279
Ca	.003	.002	-	-	-
Na	-	-	-	-	-
K	-	-	-	.004	-
TOTAL CATIONS	8.025	8.023	8.000	8.012	8.013
Fe/Fe+Mg	.825	.826	.841	.860	.860
O	12.000	12.000	12.000	12.000	12.000

* Total iron as FeO.

TABLE 6.2

MICROPROBE ANALYSES OF CHLORITOIDS - (CONTINUED)

	8220				
	1	CORE	RIM	2	
SiO_2	24.33	26.37	24.44	24.55	28.51
TiO_2	-	-	-	-	-
Al_2O_3	40.55	39.67	41.06	40.86	39.03
FeO*	24.82	25.11	24.58	24.70	24.25
MnO	.88	.76	.83	.87	.80
MgO	2.23	1.96	2.18	2.24	2.08
CaO	-	-	-	-	-
Na_2O	-	-	-	-	-
K_2O	-	-	-	.04	-
TOTAL	92.81	93.87	93.09	93.26	94.67
Si	2.011	2.146	2.009	2.016	2.279
Al	3.951	3.806	3.979	3.956	3.679
Ti	-	-	-	-	-
Fe	1.715	1.709	1.690	1.697	1.621
Mn	.062	.052	.058	.061	.054
Mg	.275	.238	.267	.274	.248
Ca	-	-	-	-	-
Na	-	-	-	-	-
K	-	-	-	.004	-
TOTAL CATIONS	8.014	7.951	8.003	8.008	7.881
Fe/Fe+Mg	.862	.878	.864	.861	.867
O	12.000	12.000	12.000	12.000	12.000

* Total iron as FeO.

TABLE 6.2

MICROPROBE ANALYSES OF CHLORITOIDS - (CONTINUED)

	8220 2		8220 3		
	CORE	RIM			CORE
SiO_2	27.66	24.30	24.28	24.65	27.29
TiO_2	-	.05	-	.06	.08
Al_2O_3	28.98	40.94	40.58	40.60	39.49
FeO*	24.14	24.89	25.04	25.21	24.68
MnO	.86	.83	.85	.77	.85
MgO	1.96	2.25	2.05	2.06	1.87
CaO	-	-	-	-	-
Na_2O	-	-	-	-	-
K_2O	-	.06	-	-	-
TOTAL	93.60	93.32	92.80	93.35	94.26
Si	2.241	1.998	2.009	2.026	2.203
Al	3.724	3.968	3.958	3.934	3.757
Ti	-	.003	-	.004	.005
Fe	1.636	1.711	1.733	1.732	1.663
Mn	.059	.058	.060	.054	.058
Mg	.237	.276	.253	.252	.225
Ca	-	-	-	-	-
Na	-	-	-	-	-
K	-	.006	-	-	-
TOTAL CATIONS	7.897	8.020	8.013	8.002	7.911
Fe/Fe+Mg	.873	.861	.873	.873	.881
O	12.000	12.000	12.000	12.000	12.000

*Total iron as FeO

TABLE 6.2

MICROPROBE ANALYSES OF CHLORITOIDS

(CONTINUED)

Rock type, sample location and minerals analyzed.

81108: Fine-grained metasedimentary phyllite from the east branch of Fortune Brook; medium-grained poorly-developed poikiloblastic (spongy) chloritoid porphyroblasts.

8220: Fine-grained metasedimentary phyllite from Second Gold Brook; medium-grained idioblastic chloritoid porphyroblasts.

and Yardley et al. (1980) for chloritoids in metapelites covering a wide range of metamorphic grades.

6.4 MUSCOVITE ANALYSES

Table 6.3 illustrates muscovite analyses obtained from six samples. Sample 8218, a low-grade metasedimentary phyllite, contains minute muscovite plates. Four samples from medium- to high-grade pelitic schists (8123, 8135, 8238 and 8247) contain abundant fine- to coarse-grained muscovite flakes up to 5 mm in length. Sample 8174, from the fine-grained foliated granitic rocks of the Egypt Highland unit, includes fine disseminated blades of muscovite interstitial to, or as inclusions within, plagioclase and microcline crystals, and the muscovite may therefore have resulted from the hydrothermal alteration of the feldspar.

Muscovite compositions from both the low- and high-grade metasedimentary rocks closely resemble those listed by Guidotti (1970 and 1974), Ramsay (1973), Baltatzis (1979), Yardley et al. (1980) and Mohr and Newton (1983) for metapelites although some of the Middle River muscovites are slightly enriched in titanium.

Ramsay (1973) noted that, in muscovites, the maximum

TABLE 6.3

MICROPROBE ANALYSES OF MUSCOVITES

	8218		8123		
	1	2	1	2	3
SiO_2	47.51	46.31	46.52	47.17	47.05
TiO_2	.29	.30	1.23	1.21	.91
Al_2O_3	34.57	34.25	34.98	34.80	35.26
FeO*	2.75	2.63	1.26	1.11	1.46
MnO	-	-	-	-	-
MgO	.56	.57	.73	.72	.88
CaO	-	.04	-	-	.05
Na_2O	.96	1.01	.26	.28	.30
K_2O	9.26	9.27	10.25	9.98	10.23
H_2O**	4.54	4.46	4.51	4.53	4.55
TOTAL	100.44	98.84	99.74	99.80	100.69
Si	6.275	6.227	6.127	6.236	6.190
Al^{IV}	1.725	1.773	1.823	1.764	1.810
Al^{VI}	3.656	3.653	3.651	3.658	3.656
Ti	.029	.030	.123	.120	.090
Fe	.304	.396	.140	.123	.161
Mn	-	-	-	-	-
Mg	.110	.114	.144	.142	.173
Ca	-	.006	-	-	.007
Na	.246	.263	.067	.072	.077
K	1.560	1.590	1.736	1.683	1.717
TOTAL CATIONS	13.905	13.952	13.861	13.798	13.881
Fe/Fe+Mg	.734	.722	.493	.464	.482
H	4.000	4.000	4.000	4.000	4.000
O	24.000	24.000	24.000	24.000	24.000
PHLO	26.629	27.864	50.802	53.620	51.790
ANN	73.371	72.136	49.198	46.380	48.210
MN	-	-	-	-	-
MARG	-	0.310	-	-	0.392
PARA	13.614	14.164	3.713	4.090	4.251
MUSC	86.386	85.526	96.287	95.910	95.358

* Total iron as FeO.

** As computed from the program that derived the structural formulas.

TABLE 6.3

MICROPROBE ANALYSES OF MUSCOVITES - (CONTINUED)

	8135		8238		8247
	1	2	1	2	1
SiO_2	46.82	46.86	46.83	47.51	46.56
TiO_2	.76	.65	1.78	1.80	.63
Al_2O_3	36.73	36.51	34.54	34.68	36.59
FeO*	.89	.89	1.39	1.26	1.18
MnO	-	-	-	-	-
MgO	.41	.36	.85	.75	.39
CaO	-	-	-	-	-
Na_2O	1.47	1.27	-	-	1.22
K_2O	9.02	9.07	10.62	10.82	9.09
H_2O**	4.59	4.56	4.54	4.58	4.56
TOTAL	100.69	100.17	100.55	101.40	100.22
Si	6.118	6.153	6.183	6.217	6.122
Al^{IV}	1.882	1.847	1.817	1.783	1.878
Al^{VI}	3.773	3.802	2.558	3.564	3.791
Ti	.075	.64	.177	.177	.062
Fe	.097	.098	.153	.138	.130
Mn	-	-	-	-	-
Mg	.080	.070	.167	.146	.076
Ca	-	-	-	-	-
Na	.372	.323	-	-	.311
K	1.503	1.519	1.789	1.806	1.524
TOTAL CATIONS	13.900	13.876	13.844	13.831	13.894
Fe/Fe+Mg	.548	.583	.478	.486	.631
H	4.000	4.000	4.000	4.000	4.000
O	24.000	24.000	24.000	24.000	24.000
PHLO	45.087	41.892	52.151	51.477	37.070
ANN	54.913	58.108	47.849	48.523	62.930
MN	-	-	-	-	-
MARG	-	-	-	-	-
PARA	19.854	17.549	-	-	16.944
MUSC	80.146	82.451	100.000	100.000	83.056

* Total iron as FeO.

** As computed from the program that derived the structural formulas.

TABLE 6.3

MICROPROBE ANALYSES OF MUSCOVITES - (CONTINUED)

	8247		8174		
	2	3	1	2	3
SiO_2	46.66	46.84	47.51	47.95	48.38
TiO_2	1.00	.83	.26	.10	.31
Al_2O_3	36.29	36.28	29.11	29.43	29.49
FeO*	.96	1.21	6.25	6.21	5.80
MnO	-	-	.06	.14	.14
MgO	.36	.46	1.34	1.39	1.53
CaO	-	-	.04	.07	-
Na_2O	1.22	1.23	-	-	-
K_2O	9.18	9.10	10.98	10.99	10.98
H_2O**	4.56	4.57	4.39	4.43	4.46
TOTAL	100.23	100.52	99.94	100.71	101.09
Si	6.133	6.139	6.484	6.489	6.505
Al^{IV}	1.867	1.861	1.516	1.511	1.495
Al^{VI}	3.754	3.743	3.165	3.183	3.177
Ti	.099	.082	.027	.010	.031
Fe	.106	.133	.713	.703	.652
Mn	-	-	.007	.016	.016
Mg	.071	.090	.273	.280	.307
Ca	-	-	.006	.010	-
Na	.311	.313	-	-	-
Ka	1.539	1.521	1.911	1.897	1.883
TOTAL CATIONS	13.870	13.882	14.102	14.099	14.066
Fe/Fe+Mg	.599	.596	.723	.715	.680
H	4.000	4.000	4.000	4.000	4.000
O	24.000	24.000	24.000	24.000	24.000
PHLO	40.061	40.390	26.629	28.059	31.457
ANN	59.939	59.610	73.371	70.335	66.907
MN	-	-	-	1.606	1.636
MARG	-	-	-	0.532	-
PARA	16.806	17.044	13.614	-	-
MUSC	83.194	82.956	86.386	99.468	100.000

* Total iron as FeO

** As computed from the program that derived the structural formulas.

TABLE 6.3

MICROPROBE ANALYSES OF MUSCOVITES

(CONTINUED)

Rock type, sample location and minerals analyzed.

8218: Fine-grained phyllite from the mouth of Second Gold Brook; fine-grained matrix muscovites.

8123: Medium-grained pelitic schist from Egypt Highland Road at the latitude of Ryan Brook; medium-grained muscovites defining S_{MR2}.

8135: Medium-grained pelitic schist from Middle River south of the mouth of the unnamed brook between Duncan Brook and Fourth Gold Brook; medium-grained muscovites defining S_{MR2}.

8238: Fine-grained semipelitic gneiss from Egypt Highland Road at the latitude of Duncan Brook; fine-grained muscovites defining S_{MR2}.

8247: Medium-grained pelitic schist from Middle River north of the mouth of the unnamed brook between Duncan Brook and Fourth Gold Brook; medium-grained muscovites defining S_{MR2}.

8174: Medium-grained foliated granitic rock from South Nile Brook; fine-grained muscovites, probably from the alteration of plagioclase feldspar.

Si content decreases, that Al^{vi} increases markedly at the expense of Mg and Fe, and that the Na/K ratio also increases with increasing metamorphic grade. A comparison between muscovites from the low-grade phyllite and those from the medium- to high-grade rocks reveals a slight decrease in Si and an increase in the Na/K ratio (except for sample 8123) while the Al^{vi} content varies irregularly even though the Fe content drops significantly.

The muscovites from sample 8174 are more iron- and magnesium-rich and aluminum-poor than their counterparts in the metasedimentary rocks and contain small concentrations of manganese. The compositions are very similar to those reported by Miller et al. (1981) for muscovites derived from the alteration of feldspar, supporting the postulated secondary nature of the muscovites from sample 8174.

6.5 BIOTITE ANALYSES

A compilation of biotite analyses is listed in Table 6.4. Six samples (8123, 8135, 8144, 8140 and 81101) are from pelitic and semipelitic schists. Samples 8123 and 8135 contain kyanite and the latter also contains minor staurolite. Sample 8144 contains scattered hornblende grains concentrated in thin layers. Three samples

TABLE 6.4

MICROPROBE ANALYSES OF BIOTITES

	8123				8135
	1	2	3	4	1
SiO_2	37.60	37.16	37.40	37.61	38.05
TiO_2	2.75	2.46	2.68	2.97	2.15
Al_2O_3	19.51	20.72	20.28	19.30	20.11
FeO*	16.53	16.17	16.89	17.23	17.44
MnO	.09	.08	.06	-	.05
MgO	11.09	10.57	10.71	10.93	11.04
CaO	-	-	-	-	-
Na_2O	-	.11	-	-	.11
K_2O	9.34	9.06	9.49	9.17	8.84
H_2O**	4.10	4.08	4.11	4.09	4.14
TOTAL	101.01	100.41	101.62	101.30	101.93
Si	5.506	5.454	5.453	5.503	5.517
Al^{IV}	2.494	2.546	2.547	2.497	2.483
Al^{VI}	.873	1.038	.938	.830	.953
Ti	.303	.272	.294	.327	.234
Fe	2.024	1.985	2.060	2.108	2.115
Mn	.011	.010	.007	-	.006
Mg	2.421	2.312	2.328	2.384	2.386
Ca	-	-	-	-	-
Na	-	.031	-	-	.031
K	1.745	1.696	1.765	1.711	1.635
TOTAL CATIONS	15.377	15.344	15.392	15.360	15.360
Fe/Fe+Mg	.455	.462	.469	.470	.479
H	4.000	4.000	4.000	4.000	4.000
O	24.000	24.000	24.000	24.000	24.000
PHLO	54.320	53.687	52.965	53.065	52.941
ANN	45.429	46.082	46.866	46.935	46.923
MN	0.251	0.231	0.169	-	0.136
MARG	-	-	-	-	-
PARA	-	1.812	-	-	1.856
MUSC	100.000	98.188	100.000	100.00	98.144

* Total iron as FeO.

** As computed from the program that derived the structural formulas.

TABLE 6.4

MICROPROBE ANALYSES OF BIOTITES - (CONTINUED)

	8135		8144		
	2	3	1	2	3
SiO_2	37.64	37.80	36.67	36.86	37.24
TiO_2	1.46	2.15	2.84	3.40	3.03
Al_2O_3	20.80	19.98	17.12	17.50	17.39
FeO*	17.83	17.76	21.55	12.37	21.46
MnO	-	-	.12	.11	.11
MgO	10.87	11.40	9.16	8.59	8.76
CaO	.08	-	-	.11	.09
Na_2O	.22	.18	-	-	-
K_2O	8.54	8.78	9.15	9.49	9.65
H_2O**	4.12	4.14	3.96	4.00	4.01
TOTAL	101.56	102.19	100.57	101.43	101.74
Si	5.480	5.479	5.545	5.527	5.568
Al^{IV}	2.520	2.521	2.455	2.473	2.432
Al^{VI}	1.048	.891	.585	.619	.632
Ti	.160	.234	.323	.383	.341
Fe	2.171	2.153	2.725	2.680	2.683
Mn	-	-	.015	.014	.014
Mg	2.359	2.463	2.064	1.920	1.952
Ca	.012	-	-	.018	.014
Na	.062	.051	-	-	-
K	1.586	1.623	1.765	1.815	1.840
TOTAL CATIONS	15.398	15.415	15.477	15.449	15.476
Fe/Fe+Mg	.479	.466	.569	.583	.579
H	4.000	4.000	4.000	4.000	4.000
O	24.000	24.000	24.000	24.000	24.000
PHLO	52.074	53.359	42.966	41.613	41.987
ANN	47.926	46.641	56.714	58.084	57.713
MN	-	-	0.320	0.303	0.300
MARG	0.752	-	-	0.964	0.777
PARA	3.740	3.022	-	-	-
MUSC	95.508	96.978	100.000	99,036	99.223

* Total iron as FeO.

** As computed from the program that derived the structural formulas.

TABLE 6.4

MICROPROBE ANALYSES OF BIOTITES - (CONTINUED)

	8140			8150	
	1	2	3	1	2
SiO_2	36.51	36.50	36.68	37.31	37.04
TiO_2	2.30	2.96	2.54	1.66	2.06
Al_2O_3	18.65	17.50	18.40	18.65	18.66
FeO*	19.53	20.89	19.75	15.90	16.02
MnO	.30	.05	.30	.56	.45
MgO	10.32	9.12	10.35	11.93	12.06
CaO	.09	-	.07	.19	-
Na_2O	-	-	-	-	-
K_2O	9.72	9.53	9.70	9.35	9.37
H_2O**	4.03	3.97	4.04	4.03	4.03
TOTAL	101.45	100.53	101.83	99.58	99.69
Si	5.437	5.515	5.446	5.553	5.509
Al^{IV}	2.563	2.485	2.554	2.447	2.491
Al^{VI}	.710	.633	.665	.824	.780
Ti	.258	.336	.284	.186	.230
Fe	2.432	2.640	2.452	1.979	1.993
Mn	.038	.006	.038	.071	.057
Mg	2.291	2.054	2.290	2.647	2.674
Ca	.014	-	.011	.030	-
Na	-	-	-	-	-
K	1.846	1.837	1.837	1.775	1.778
TOTAL CATIONS	15.589	15.506	15.577	15.512	15.512
Fe/Fe+Mg	.515	.562	.517	.428	.427
H	4.000	4.000	4.000	4.000	4.000
O	24.000	24.000	24.000	24.000	24.000
PHLO	48.116	43.701	47.913	56.355	56.609
ANN	51.089	56.163	51.298	42.142	42.191
MN	0.795	0.136	0.789	1.503	1.200
MARG	0.772	-	0.603	1.678	-
PARA	-	-	-	-	-
MUSC	99.228	100.000	99.397	98.322	100.000

* Total iron as FeO.

** As computed from the program that derived the structural formulas.

TABLE 6.4

MICROPROBE ANALYSES OF BIOTITES - (CONTINUED)

	8150	8110		
	3	1	2	3
SiO_2	38.16	36.01	37.26	36.94
TiO_2	1.54	2.19	3.16	2.49
Al_2O_3	18.79	19.76	19.86	20.05
FeO*	14.64	20.39	19.41	20.33
MnO	.35	.13	.11	.08
MgO	12.56	8.18	8.59	9.09
CaO	-	.28	.09	.06
Na_2O	-	.05	.13	-
K_2O	9.60	8.29	9.14	8.87
H_2O**	4.06	3.96	4.08	4.07
TOTAL	99.70	99.24	101.83	101.98
Si	5.625	5.454	5.480	5.439
Al^{IV}	2.375	2.546	2.520	2.561
Al^{VI}	.889	.981	.923	.918
Ti	.171	.249	.350	.276
Fe	1.805	2.583	2.388	2.503
Mn	.044	.017	.014	.010
MgO	2.760	1.847	1.883	1.995
Ca	-	.045	.014	.009
Na	-	.015	.037	-
K	1.805	1.602	1.715	1.666
TOTAL CATIONS	15.474	15.339	15.324	15.377
Fe/Fe+Mg	.395	.584	.559	.556
H	4.000	4.000	4.000	4.000
O	24.000	24.000	24.000	24.000
PHLO	59.886	41.535	43.954	44.251
ANN	39.165	58.090	55.726	55.528
MN	0.948	0.375	0.320	0.221
MARG	-	2.735	0.803	0.565
PARA	-	0.884	2.099	-
MUSC	100.00	96.382	97.098	99.435

* Total iron as FeO.

** As computed from the program that derived the structural formulas.

TABLE 6.4

MICROPROBE ANALYSES OF BIOTITES - (CONTINUED)

	8148		81103	
	1	2	1	2
SiO_2	38.68	38.47	39.32	39.19
TiO_2	2.01	2.31	1.47	1.48
Al_2O_3	17.48	17.51	17.47	17.54
FeO*	15.56	16.86	12.75	12.67
MnO	.09	.07	.15	.04
MgO	13.50	13.28	16.08	13.80
CaO	-	-	.10	.04
Na_2O	.05	-	.21	-
K_2O	9.89	9.66	9.70	9.72
H_2O**	4.14	4.13	4.17	4.14
TOTAL	102.40	102.29	101.42	100.62
Si_{IV}	5.641	5.587	5.654	5.671
Al^{IV}	2.359	2.413	2.346	2.329
Al^{VI}	.644	.583	.614	.661
Ti	.220	.252	.159	.161
Fe	1.898	2.048	1.533	1.533
Mn	.011	.009	.018	.005
Mg	2.934	2.875	3.446	3.408
Ca	-	-	.015	.006
Na	.014	-	.059	-
K	1.840	1.789	1.779	1.794
TOTAL CATIONS	15.561	15.556	15.623	15.568
Fe/Fe+Mg	.393	.416	.308	.310
O	4.000	4.000	4.000	4.000
H	24.000	24.000	24.000	24.000
PHLO	60.488	58.298	68.956	68.901
ANN	39.182	41.527	30.678	31.000
MN	0.230	0.175	0.366	0.099
MARG	-	-	0.831	0.344
PARA	0.763	-	3.160	-
MUSC	99.237	100.00	96.009	99.656

* Total iron as FeO.

** As computed from the program that derived the structural formulas.

TABLE 6.4

MICROPROBE ANALYSES OF BIOTITES - (CONTINUED)

	81117	
	1	2
SiO_2	36.56	38.64
TiO_2	2.13	2.52
Al_2O_3	17.94	17.58
FeO*	16.52	15,85
MnO	.04	.11
MgO	15.38	13.79
CaO	.08	-
Na_2O	-	.05
K_2O	7.98	9.64
H_2O**	4.09	4.15
TOTAL	100.72	102.33
Si	5.362	5.583
Al^{IV}	2.638	2.417
Al^{VI}	.463	.576
Ti	.235	.274
Fe	2.026	1.915
Mn	.005	.013
Mg	3.362	2.970
Ca	.013	-
Na	-	.014
K	1.493	1.777
TOTAL CATIONS	15.597	15.539
Fe/Fe+Mg	.376	.392
O	4.000	4.000
H	24.000	24.000
PHLO	62.339	60.627
ANN	37.569	39.098
MN	0.092	0.275
MARG	0.835	-
PARA	-	0.782
MUSC	99.165	99.218

* Total iron as FeO.

** As computed from the program that derived the stuctural formulas.

TABLE 6.4

MICROPROBE ANALYSES OF BIOTITES

(CONTINUED)

Rock type, sample location and minerals analyzed.

8123: Medium-grained pelitic schist from Egypt Highland Road at the latitude of Ryan Brook; medium-grained biotites defining S_{MR2}, very minor chloritization.

8135: Medium-grained pelitic schist from Middle River south of the mouth of the unnamed brook between Duncan Brook and Fourth Gold Brook; medium-grained biotites defining S_{MR2}, very minor chloritization.

8144: Medium-grained semipelitic gneiss from Middle River north of Sarach Brook; fine- to medium-grained biotites defining S_{MR2}, minor chloritization.

8140: Medium-grained semipelitic gneiss from Sarach Brook near the Bothan Brook granodiorite; fine- to medium-grained biotites defining S_{MR2}, minor chloritization.

8150: Medium-grained semipelitic gneiss from northern Middle River; fine- to medium-grained biotites defining S_{MR2}, very minor chloritization.

81101: Fine-grained semipelitic gneiss from an unnamed brook draining into First Lake O'Law; fine-grained biotites defining S_{MR2}, minor chloritization.

8148: Fine-grained metabasite from northern Middle River; fine-grained biotites intergranular to the dominant hornblende, minor chloritization.

TABLE 6.4

MICROPROBE ANALYSES OF BIOTITES

(CONTINUED)

81103: Fine-grained metabasite from Middle River near the mouth of Duncan Brook; fine-grained biotites intergranular to the dominant hornblende, minor chloritization.

81117: Fine-grained metabasite from the eastern reaches of Ryan Brook; fine-grained biotites intergranular to the dominant hornblende; minor chloritization.

(8148, 81103 and 81117) are from three metabasite sheets where biotite occurs as disseminated fine-grained flakes rarely more or less altered to chlorite.

A number of authors have examined the changes in the composition of biotites during progressive regional metamorphism of pelitic rocks. Atherton (1968) noted that the Mg/Mg+Fe ratio in biotite increases with grade. Ramsay (1973) observed an increase in the Al^{iv}/Si ratio while Guidotti (1974) and Yardley et al. (1980) noted a slight increase in TiO_2 with increasing metamorphic grade.

Since the six metasedimentary rock samples examined are located above the staurolite-kyanite isograd, compositional variations in the biotites due to changes in the metamorphic grade should be slight and more or less random. As can be seen in Table 6.4, the composition of the biotites from the metapelites varies only slightly and randomly although biotites from samples 8144, 8140 and 81101 have slightly higher FeO^T and correspondingly higher Fe/Fe+Mg and annite contents. In fact, the biotites from the Middle River metasedimentary rocks resemble those listed by Atherton (1968) for medium-grade pelitic rocks, by Ramsay (1973) for biotite zone metasedimentary rocks, and by Guidotti (1974) and Yardley et al. (1980) for staurolite to sillimanite zone meta-

pelites.

The biotites from the metabasites are slightly richer in magnesium and poorer in total iron compared to their counterparts in the pelitic rocks. The high MgO and low FeO^T concur with high magnesium and low total iron chlorites, derived from the alteration of biotite, in metabasite sample 8129 mentioned in section 6.1. However, great significance should not be given to this relationship since the chlorites and biotites are from different samples and from different metabasite sheets. Further work would be necessary to establish a definite correlation.

6.6 GARNET ANALYSES

Analyses of garnet porphyroblasts contained in one sample of low-grade phyllite (81108) and nine samples of medium- to high-grade pelitic schists are listed in Table 6.5. The garnets of sample 81108 are poorly developed, highly poikiloblastic, and have not reached textural equilibrium with the surrounding quartz-chlorite-muscovite matrix. The garnets of the higher grade schists can be either pre-tectonic or syntectonic to the biotites and muscovites that define the major foliation of these rocks (S_{MR2}). Distinction between the two garnet "popu-

TABLE 6.5

MICROPROBE ANALYSES OF GARNETS

	81108			8123	
	1	2	3	1	2
SiO_2	36.63	36.49	36.64	36.83	37.12
TiO_2	.02	-	.08	-	-
Al_2O_3	20.70	20.55	20.74	20.93	21.05
Fe_2O_3*	.13	.36	.46	2.01	1.25
FeO	33.03	31.31	32.21	30.50	31.44
MnO	4.29	5.46	5.07	2.94	2.56
MgO	1.59	1.55	1.65	4.31	4.30
CaO	2.84	3.17	2.83	2.28	2.13
Na_2O	-	-	-	-	-
K_2O	-	-	-	-	-
TOTAL	99.22	98.85	99.64	99.60	99.72
Si	5.994	5.994	5.976	5.931	5.957
Al	.006	.006	.024	.069	.043
Al	3.986	3.972	3.962	3.902	3.938
Ti	.002	-	.010	-	-
Fe^{3+}	.016	.044	.057	.244	.151
Fe	4.521	4.301	4.394	4.107	4.219
Mn	.595	.760	.700	.401	.348
Mg	.388	.380	.401	1.034	1.029
Ca	.498	.558	.495	.393	.366
Na	-	-	-	-	-
K	-	-	-	-	-
TOTAL CATIONS	16.006	16.015	16.019	16.081	16.051
Fe/Fe+Mg	.921	.919	.916	.799	.804
O	24.000	24.000	24.000	24.000	24.000
ALMD	75.34	71.67	73.52	69.18	70.74
ANDRA	.45	1.13	1.43	6.15	3.85
GROSS	7.81	8.18	6.61	.48	2.29
PYROPE	6.47	6.34	6.72	17.43	17.27
SPESS	9.93	12.68	11.72	6.76	5.84

* As computed from the program that derived the structural formulas.

TABLE 6.5

MICROPROBE ANALYSES OF GARNETS - (CONTINUED)

	8123		81101		8140
	3	4	1	2	
SiO_2	37.15	36.81	36.87	36.90	37.27
TiO_2	-	-	-	-	-
Al_2O_3	20.96	21.04	20.93	20.81	20.46
Fe_2O_3*	1.18	1.75	.57	.31	1.18
FeO	30.84	31.54	33.46	33.60	28.99
MnO	1.95	3.11	2.88	3.05	1.94
MgO	5.08	3.84	3.05	2.96	5.20
CaO	2.02	1.97	1.80	1.71	2.84
Na_2O	-	-	-	-	-
K_2O	-	-	-	-	-
TOTAL	99.06	99.88	99.50	99.41	97.14
Si	5.967	5.930	5.976	5.986	5.982
Al	.033	.070	.024	.014	.018
Al	3.934	3.924	3.974	3.984	3.917
Ti	-	-	-	-	-
Fe^{3+}	.142	.212	.069	.038	.145
Fe	4.142	4.249	4.536	4.559	3.597
Mn	.265	.424	.395	.419	.268
Mg	1.216	.922	.737	.716	1.265
Ca	.348	.340	.313	.297	.497
Na	-	-	-	-	-
K	-	-	-	-	-
TOTAL CATIONS	16.047	16.071	16.024	16.013	16.049
Fe/Fe+Mg	.773	.822	.860	.864	.758
O	24.000	24.000	24.000	24.000	24.000
ALMD	69.35	71.56	75.82	76.08	66.06
ANDRA	3.54	5.39	1.81	.98	3.69
GROSS	2.29	.35	3.43	3.98	4.62
PYROPE	20.38	15.55	12.33	11.96	21.15
SPESS	4.44	7.15	6.61	7.00	4.48

* As computed from the program that derived the structural formulas.

TABLE 6.5

MICROPROBE ANALYSES OF GARNETS - (CONTINUED)

	8144		8150		
	1	2	1	2	3
SiO_2	37.27	37.33	37.43	37.47	37.50
TiO_2	-	-	.13	-	-
Al_2O_3	20.92	20.90	21.14	21.13	21.16
Fe_2O_3*	1.05	1.34	1.79	2.35	1.66
FeO	27.84	27.02	17.93	17.97	18.57
MnO	1.47	1.44	7.99	6.87	6.54
MgO	2.55	2.49	2.18	2.74	2.88
CaO	8.37	9.18	11.71	11.74	11.36
Na_2O	-	-	-	-	-
K_2O	-	-	-	-	-
TOTAL	99.37	99.56	100.12	100.03	99.50
Si	5.978	5.974	5.936	5.933	5.953
Al	.022	.026	.064	.067	.047
Al	3.933	3.914	3.886	3.875	3.911
Ti	-	-	.016	-	-
Fe^{3+}	.127	.161	.213	.280	.198
Fe	3.735	3.615	2.378	2.379	2.465
Mn	.200	.195	1.073	.921	.879
Mg	.610	.594	.515	.647	.681
Ca	1.438	1.574	1.990	1.992	1.932
Na	-	-	-	-	-
K	-	-	-	-	-
TOTAL CATIONS	16.043	16.053	16.071	16.094	16.066
Fe/Fe+Mg	.860	.859	.822	.786	.784
O	24.000	24.000	24.000	24.000	24.000
ALMD	62.40	60.45	40.05	39.99	41.34
ANDRA	3.24	3.99	5.40	7.13	4.99
GROSS	20.82	22.36	27.77	26.45	27.47
PYROPE	10.20	9.94	8.68	10.91	11.44
SPRES	3.35	3.26	18.10	15.52	14.77

* As computed from the program that derived the structural formulas.

TABLE 6.5

MICROPROBE ANALYSES OF GARNETS - (CONTINUED)

	8135		8247		
	1	2	1	2	3
SiO_2	36.18	36.36	36.37	36.54	36.08
TiO_2	-	-	-	-	.06
Al_2O_3	20.34	20.74	21.13	21.06	20.98
Fe_2O_3*	.99	.63	.74	.72	1.14
FeO	33.22	33.20	35.01	35.18	33.35
MnO	1.28	1.09	.87	1.12	2.70
MgO	4.17	4.20	3.52	3.26	2.49
CaO	1.05	1.34	1.15	1.25	2.19
Na_2O	-	-	-	-	-
K_2O	-	-	-	-	-
TOTAL	97.13	97.50	98.82	99.06	98.78
Si	5.977	5.967	5.940	5.948	5.916
Al	.023	.033	.060	.052	.084
Al	3.937	3.977	3.995	3.988	3.970
Ti	-	-	-	-	.007
Fe^{3+}	.123	.078	.091	.089	.141
Fe	4.590	4.557	4.769	4.789	4.560
Mn	.179	.152	.120	.154	.375
Mg	1.027	1.027	.855	.791	.609
Ca	.186	.236	.201	.218	.385
Na	-	-	-	-	-
K	-	-	-	-	-
TOTAL CATIONS	16.042	16.027	16.031	16.029	16.047
Fe/Fe+Mg	.817	.816	.848	.858	.882
O	24.000	24.000	24.000	24.000	24.000
ALMD	76.66	76.29	80.20	80.45	76.89
ANDRA	3.11	2.04	2.35	2.19	3.57
GROSS	-	1.92	1.04	1.47	2.75
PYROPE	17.18	17.21	14.39	13.30	10.28
SPESS	2.99	2.55	2.02	2.59	6.33

* As computed from the program that derived the structural formulas.

TABLE 6.5

MICROPROBE ANALYSES OF GARNETS - (CONTINUED)

	8238		
	1	2	3
SiO_2	37.02	37.25	37.37
TiO_2	-	-	-
Al_2O_3	21.49	21.35	21.52
Fe_2O_3*	.66	.15	.79
FeO	30.38	31.18	30.67
MnO	3.40	3.32	3.39
MgO	4.17	3.83	4.28
CaO	2.38	2.50	2.33
Na_2O	-	-	-
K_2O	-	-	-
TOTAL	99.43	99.57	100.27
Si	5.940	4.974	5.948
Al	.060	.026	.052
Al	4.003	4.009	3.985
Ti	-	-	-
Fe^{3+}	.080	.018	.094
Fe	4.076	4.182	4.083
Mn	.462	.451	.457
Mg	.997	.916	1.015
Ca	.409	.430	.397
Na	-	-	-
K	-	-	-
TOTAL CATIONS	16.027	16.006	16.031
Fe/Fe+Mg	.803	.820	.801
O	24.000	24.000	24.000
ALMD	68.55	69.92	68.55
ANDRA	2.05	.45	2.35
GROSS	4.84	6.75	4.84
PYROPE	16.78	15.33	16.78
SPESS	7.78	7.55	7.78

* As computed from the program that derived the structural formulas.

TABLE 6.5

MICROPROBE ANALYSES OF GARNETS

(CONTINUED)

Rock type, sample location and minerals analyzed.

81108: Fine-grained metasedimentary phyllite from the east branch of Fortune Brook; medium-grained poorly-developed poikiloblastic (spongy) garnet porphyroblasts.

8123: Medium-grained pelitic schist from Egypt Highland Road at the latitude of Ryan Brook; medium-grained garnet porphyroblasts.

81101: Fine-grained semipelitic gneiss from an unnamed brook draining into First Lake O'Law; fine- to medium-grained garnet porphyroblasts.

8140: Medium-grained semipelitic gneiss from Sarach Brook near the Bothan Brook granodiorite; medium- to coarse-grained garnet porphyroblasts.

8144: Medium-grained semipelitic gneiss from Middle River north of Sarach Brook; medium- to coarse-grained garnet porphyroblasts.

8150: Medium-grained semipelitic gneiss from northern Middle River; medium- to coarse-grained garnet porphyroblasts.

8135: Medium-grained pelitic schist from Middle River south of the mouth of the brook between Duncan Brook and Fourth Gold Brook; medium- to coarse-grained garnet porphyroblasts.

TABLE 6.5

MICROPROBE ANALYSES OF GARNETS

(CONTINUED)

8247: Medium-grained pelitic schist from Middle River north of the mouth of the unnamed brook between Duncan Brook and Fourth Gold Brook; medium- to coarse-grained garnet porphyroblasts.

8238: Fine-grained semipelitic gneiss from Egypt Highland Road at the latitude of Duncan Brook; fine- to medium-grained garnet porphyroblasts.

lations" can be made on the basis of the relationship between the porphyroblasts and the adjoining matrix.

The garnets are classified as pre-tectonic when porphyroblasts are extensively fractured (with or without chloritization along these fractures), when they are penetrated by or contain large flakes of biotite and/or muscovite, and when the porphyroblasts are clearly wrapped around by the schistosity. The garnets are categorized as syntectonic when the porphyroblasts are only slightly fractured, or not at all, when they are free of biotite and/or muscovite inclusions, and when matrix biotite and muscovite blades abut against the porphyroblasts.

Inclusion patterns can also help in discriminating between garnets that are pre-, syn- or post-tectonic. Porphyroblasts devoid of inclusions and those containing inclusion trails concordant with the matrix can be either syn- or post-tectonic while porphyroblasts with inclusion trails discordant with the matrix are pre-tectonic (Spry, 1969). Finally, crystals with inclusion-filled cores and inclusion-free rims, such as those found in sample 8130 (Plate 23), may represent a polyphase growth of the garnet crystals.

Plate 23. Photomicrograph of a garnet porphyroblast from sample 8130. The textural anomaly differentiating the inclusion-filled core from the inclusion-free rim is postulated to represent a break in the metamorphic growth of this and similar garnets in this particular sample. Note the truncation of the inclusion pattern by the post-garnet foliation. (Magnification x25; plane polarized light.)

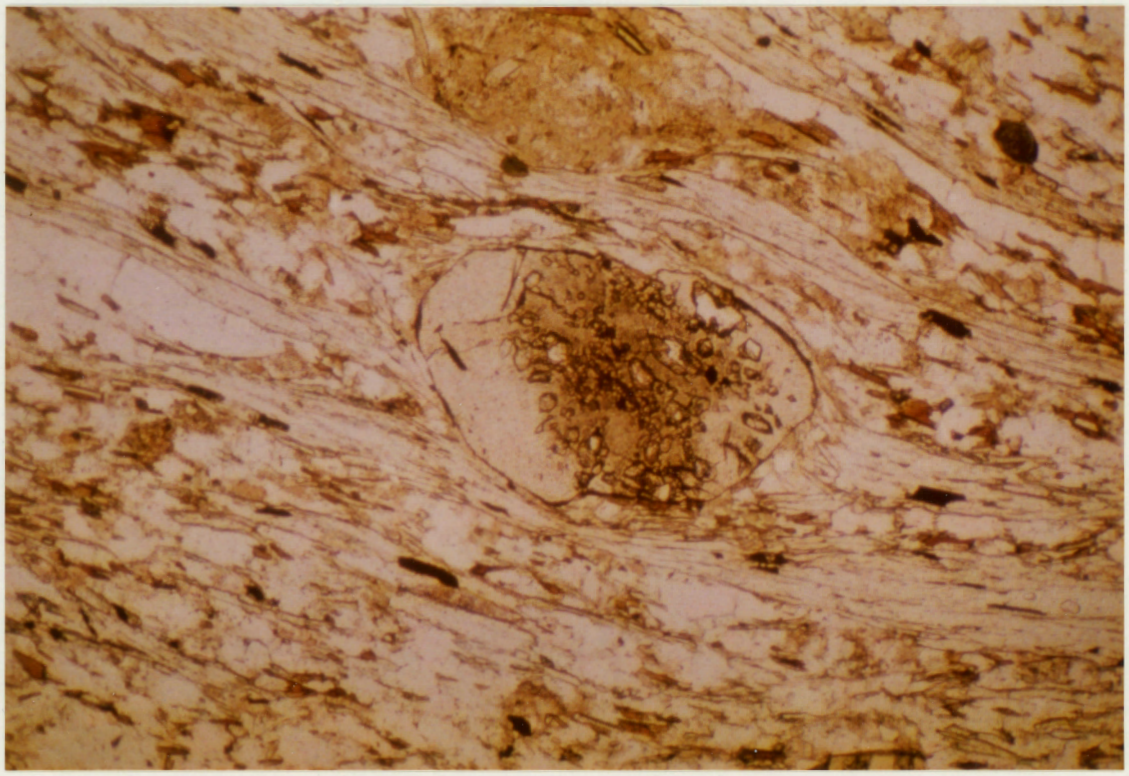

The garnets analyzed in the medium- to high-grade pelitic rocks are all classified as syntectonic crystals. Compositional zoning across a porphyroblast from sample 8130 (the grain illustrated in Plate 23), analyzed in an attempt to determined if any significant break in the gradual change in composition separates the inclusion-filled core from the inclusion-free rim, is shown in Figure 6.1. The complete mineral analyses are listed in Table 6.6.

The initial outward "normal" compositional zoning, characterized by a Ca- and Mn-rich core and a Fe- and Mg-rich rim (Hollister, 1966), is abruptly interrupted at the edge of the inclusion-filled core. The break is especially evident in the FeO and MnO traces if "ideal" bell-shaped curves (Hollister, 1966) are superimposed on the traces. "Normal" zoning resumes in the inclusion-free margin of the garnet. The break in the compositional zoning indicates that the garnet porphyroblast indeed grew in two stages.

In an attempt to explain variations in composition in garnets when considering element partitioning between the matrix and developing garnets, two models have been proposed. Hollister (1966) and Atherton (1968) showed that variations in MnO in zoned garnets could be ex-

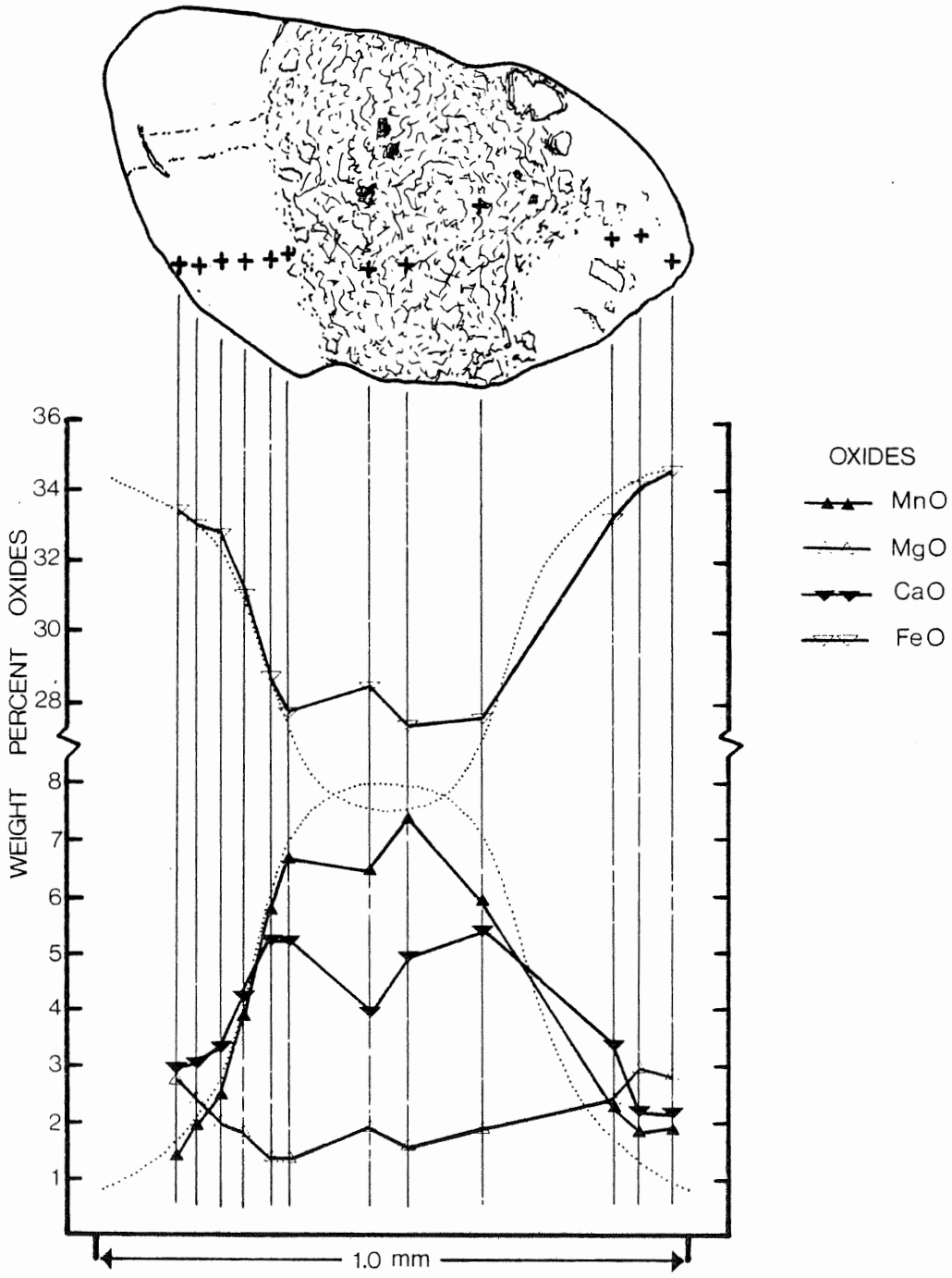

Figure 6.1 Microprobe traverse and trace of weight percent CaO, MnO, MgO and FeO across a garnet from sample 8130. "Ideal" bell-shaped curves are superimposed on the MnO and FeO traces to emphasize the break in the compositional zoning between the core and rim of the crystal.

TABLE 6.6

MICROPROBE ANALYSES ACROSS A GARNET
FROM SAMPLE 8130

	RIM		8130	
	1	2	3	4
SiO_2	36.51	36.25	36.26	36.33
TiO_2	.07	-	-	.13
Al_2O_3	20.28	20.60	20.46	20.53
Fe_2O_3*	.89	1.74	.79	1.00
FeO	33.49	33.02	32.77	31.01
MnO	1.46	1.96	2.54	3.91
MgO	2.78	2.48	2.08	1.82
CaO	2.99	3.09	3.39	4.20
Na_2O	-	-	-	-
K_2O	-	-	-	-
TOTAL	98.88	99.14	98.21	98.83
Si	5.956	5.938	5.978	5.957
Al	.044	.062	.022	.043
Al	3.950	3.914	3.952	3.924
Ti	.009	-	-	.016
Fe^{3+}	.109	.215	.098	.124
Fe	4.568	4.523	4.518	4.252
Mn	.202	.272	.355	.543
Mg	.676	.605	.511	.445
Ca	.523	.542	.599	.738
Na	-	-	-	-
K	-	-	-	-
TOTAL CATIONS	16.037	16.071	16.033	16.042
Fe/Fe+Mg	.871	.882	.898	.905
O	24.000	24.000	24.000	24.000
ALMD	76.69	76.10	75.49	71.10
ANDRA	2.79	5.38	2.48	3.16
GROSS	5.76	3.75	7.54	8.79
PYROPE	11.36	10.19	8.55	7.45
SPESS	3.40	4.58	5.94	9.09

* As computed from the program that derived the structural formulas.

TABLE 6.6

MICROPROBE ANALYSES ACROSS A GARNET
FROM SAMPLE 8130 - (CONTINUED)

	8130 CORE			
	5	6	7	8
SiO_2	36.49	36.40	36.42	36.67
TiO_2	-	-	-	-
Al_2O_3	20.57	20.40	20.61	20.60
Fe_2O_3*	1.71	1.12	1.48	1.65
FeO	28.68	27.67	28.50	27.19
MnO	5.82	6.63	6.43	7.41
MgO	1.38	1.38	1.93	1.60
CaO	5.18	5.24	4.01	4.95
Na_2O	-	-	-	-
K_2O	-	-	-	-
TOTAL	99.66	98.73	99.23	99.90
Si	5.951	5.978	5.952	5.958
Al	.049	.022	.048	.042
Al	3.904	3.925	3.921	3.903
Ti	-	-	-	-
Fe^{3+}	.210	.139	.182	.201
Fe	3.912	3.800	3.895	3.694
Mn	.804	.922	.890	1.020
Mg	.335	.338	.470	.387
Ca	.905	.922	.702	.862
Na	-	-	-	-
K	-	-	-	-
TOTAL CATIONS	16.070	16.046	16.060	16.067
Fe/Fe+Mg	.921	.918	.892	.905
O	24.000	24.000	24.000	24.000
ALMD	65.65	63.50	65.36	61.92
ANDRA	5.29	3.46	4.54	5.06
GROSS	9.91	11.96	7.26	9.41
PYROPE	5.63	5.65	7.90	6.50
SPESS	13.51	15.42	14.95	17.12

* As computed from the program that derived the structural forumulas.

TABLE 6.6

MICROPROBE ANALYSES ACROSS A GARNET
FROM SAMPLE 8130 - (CONTINUED)

	8130			RIM
	9	10	11	12
SiO_2	36.65	36.98	36.97	37.20
TiO_2	-	-	-	-
Al_2O_3	20.44	20.89	21.06	20.94
Fe_2O_3*	2.12	.75	1.19	.39
FeO	27.44	33.18	34.19	34.59
MnO	5.99	2.30	1.84	1.93
MgO	1.90	2.41	3.00	2.88
CaO	5.44	3.47	2.22	2.21
Na_2O	-	-	-	-
K_2O	-	-	-	-
TOTAL	99.77	99.91	100.35	100.11
Si	5.954	5.978	5.952	5.994
Al	.046	.022	.048	.006
Al	3.868	3.957	3.947	3.970
Ti	-	-	-	-
Fe^{3+}	.259	.092	.144	.048
Fe	3.729	4.486	4.603	4.662
Mn	.824	.315	.251	.263
Mg	.460	.581	.720	.692
Ca	.947	.601	.383	.382
Na	-	-	-	-
K	-	-	-	-
TOTAL CATIONS	16.087	16.032	16.048	16.017
Fe/Fe+Mg	.890	.885	.865	.871
O	24.000	24.000	24.000	24.000
ALMD	62.53	74.96	77.25	77.69
ANDRA	6.58	2.41	3.63	1.28
GROSS	9.33	7.64	2.81	5.10
PYROPE	7.73	9.72	12.10	11.54
SPESS	13.84	5.27	4.22	4.39

* As computed from the program that derived the structural formulas.

TABLE 6.6

MICROPROBE ANALYSES ACROSS A GARNET

FROM SAMPLE 8130

(CONTINUED)

Rock type, sample location and mineral analyzed.

8130: Fine-grained metasedimentary schist from the northern branch of Fourth Gold Brook; fine- to medium-grained garnet porphyroblast with inclusion-filled core and inclusion-free rim.

plained using a complete fractionation model assuming that:

1. There is no diffusion in garnet, that only the newly added growth layer is in equilibrium with the surrounding matrix.
2. Diffusion in the matrix is complete.
3. Fractionation of MnO between the new growth layer and the matrix is constant.

In this model, MnO would be concentrated in the core, and would thus be removed from the matrix, and subsequent growth layers would become poorer in MnO. According to Hollister (1966), the decrease in Mn must be accompanied by an increase in Fe and Mg to maintain the atomic balance in the garnet.

Miyashiro and Shido (1973) propose an alternative model where garnet would crystallize in complete equilibrium. The garnets are assumed to be homogeneous and in equilibrium with associated matrix minerals. In this model, the gradual breakdown of chlorite and biotite to produce garnet during increasing progressive metamorphism would gradually increase the amount of garnet without any substantial addition of MnO to the system, resulting in a progressive decrease in MnO in garnet. Similarly, the conversion of biotite to garnet causes an increase in the MgO content of garnet.

According to the two models, the compositional zoning pattern shown by the garnet porphyroblast in sample 8130 could result from an initial phase of "prograde" crystal growth (producing an inclusion-filled grain), which would be followed by a "retrograde" partial breakdown of the garnet down to the observed core-margin boundary, and which would be subsequently followed by a second phase of "prograde" crystal growth without the incorporation of inclusions.

Zoning reversals in garnet rims have been attributed to retrogressive effects by Evans and Guidotti (1966) and Tracy et al. (1976), and Karabinos (in press) proposed a prograde-retrograde-prograde sequence of crystal growth for garnets showing zoning patterns similar to that of the porphyroblast in sample 8130. Conversely, Thompson et al. (1977) indicated that textural unconformities and zoning reversals could result during continuous prograde metamorphism in that since garnet may participate in a series of prograde reactions, an intermediate reaction consuming garnet and a later reaction forming garnet could produce a zoning reversal. Thompson et al. (1977) also indicated that textural unconformities may result from tectonic events or polymetamorphism.

Sample 8130 is located just below the staurolite-

kyanite isograd and very near the postulated boundary between the southern low-grade belt and central medium- to high-grade belt. High grade minerals are not observed in the sample and there is therefore no evidence for garnet-consuming prograde reactions. It appears more likely that polyphase metamorphism, possibly involving retrograde garnet-consuming reactions, is responsible for the textural unconformity and zoning anomaly of the porphyroblast in sample 8130.

A number of researchers have linked the changes in the composition of garnets to the grade of progressive regional metamorphism. Miyashiro (1953) examined calcium-poor garnets and noted a progressive decrease in the MnO content with increasing grade. According to Sturt (1962), the CaO+MnO content in garnet decreases while FeO+MgO content increases with increasing metamorphic grade. This broad relationship was confirmed by Cooper (1972) in his study of garnets in metabasic rocks of southern New Zealand. Atherton (1968), working in the Scottish Dalradian, noted a decrease in MnO and CaO and an increase in FeO and MgO in garnets away from the garnet isograd toward higher grade rocks.

The garnets analyzed in this study are plotted on a CaO+MnO versus FeO+MgO diagram (Figure 6.2) taken from

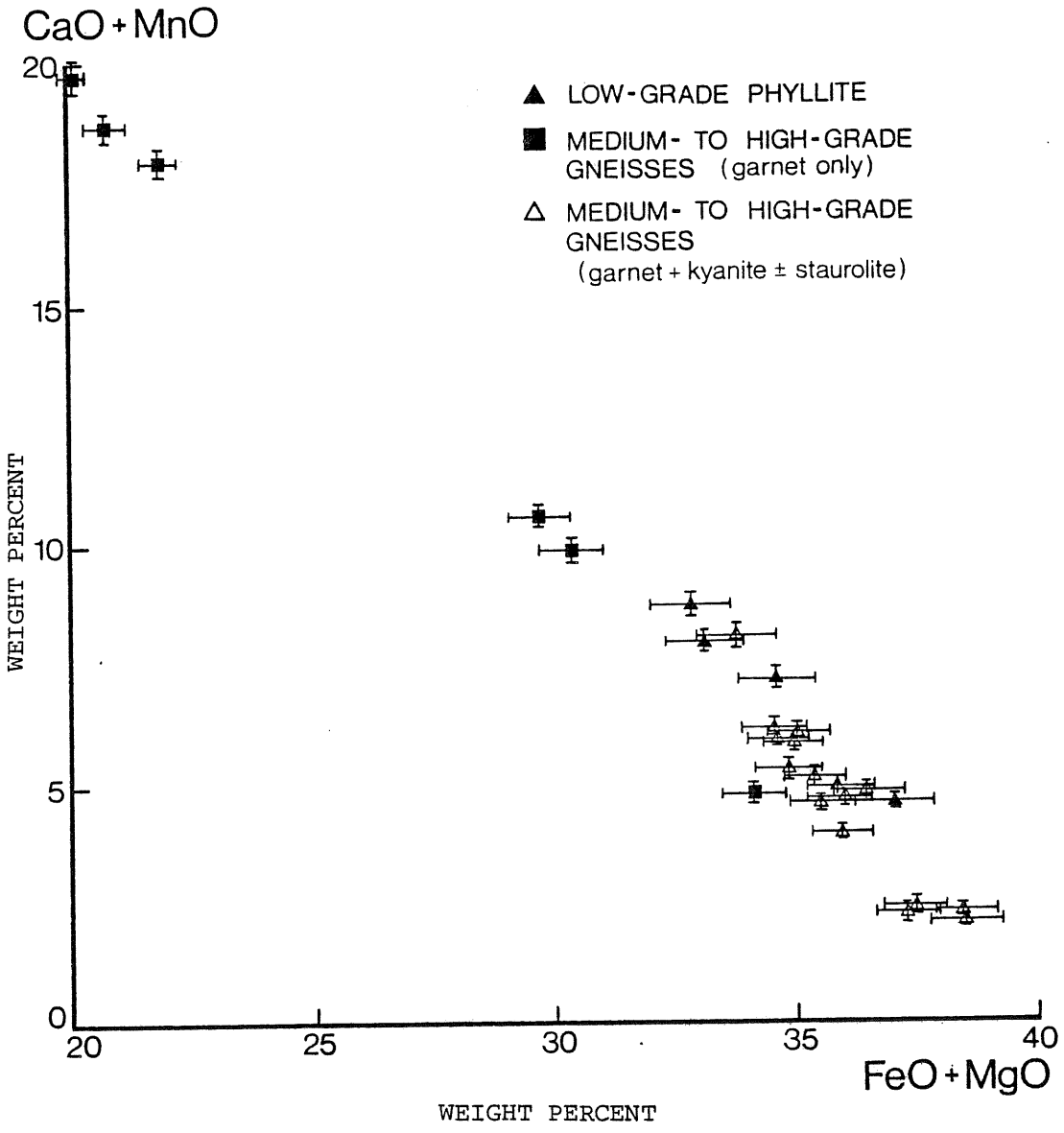

Figure 6.2 Plot of weight percent (CaO + MnO) against (FeO + MgO) for garnets of the Middle River until metapelites (after Sturt, 1962). The analyses follow the postulated decrease in (CaO + MnO) and increase in (FeO + MgO) with increasing metamorphic grade. The three "anomalous" garnets from sample 8150, which plot in the upper left corner, reflected relatively high CaO and MnO in the bulk composition of the sample.

Sturt (1962). The analyses cluster in the medium- to high-grade area of the diagram, in accordance with the medium- to high-grade metamorphic conditions postulated for these rocks (discussed in Chapter 7), except for the three analyses from sample 8150 which plot in the upper left corner of the diagram, the area reflecting chlorite zone metamorphic conditions according to the relationship noted by Sturt (1962). However, sample 8150 is located well above the staurolite-kyanite isograd and kyanite is observed in a sample taken from an outcrop less than 200 meters away. The discrepancy stems from the fact that the garnets from sample 8150 are enriched in CaO and MnO and depleted in FeO with respect to those of the other high-grade rocks. These differences in mineral composition are attributable to host rock compositional differences since sample 8150 is enriched in CaO and MnO relative to three other high-grade metapelites listed in Table 5.3. These whole rock differences may reflect a lithological difference or may be the result of metasomatic alteration.

The slight differences in the composition of the garnets listed in Table 6.5 are not altogether surprising since the element distribution pattern in garnet is a complex function of rock bulk composition, specific continuous reactions in which garnet is involved, P-T history of the rock, homogeneous diffusion rates within garnet,

and possibly also the availability of metamorphic fluids at the various stages of garnet growth (Tracy et al., 1976).

6.7 PLAGIOCLASE ANALYSES

The analyses of plagioclase feldspar contained in eleven samples are listed in Table 6.7. Four samples (8148, 81103, 81117 and 81120) from separate metabasite sheets and three samples from pelitic schists (8140, 8144 and 8150) contain oligoclase and andesine. Sample 8174, from the fine-grained foliated granitic rocks of the Egypt Highland unit, two samples from the least deformed granitic rocks near Fielding Road (8190 and 8191), and one sample from the Bothan Brook granodiorite (8248) contain albite. None of the plagioclase crystals analyzed are zoned. Alteration to sericite varies considerably from sample to sample and ranges from very slight in the pelitic schists, through moderate in the metabasites, to very extensive in the granitic rocks and it may be severe enough to produce erroneous results in these later rocks.

The anorthite contents of the plagioclase crystals analyzed from the metabasites are slightly higher than those listed by Laird and Albee (1981) for garnet and staurolite to kyanite grade mafic schists from Vermont.

TABLE 6.7

MICROPROBE ANALYSES OF PLAGIOCLASE

	8148	81103 1	81103 2	81117 1
SiO_2	63.43	59.56	59.91	61.49
TiO_2	-	-	-	-
Al_2O_3	23.18	25.36	25.68	24.15
FeO*	-	-	-	-
MnO	-	-	-	-
MgO	-	-	-	-
CaO	4.20	7.00	7.30	5.87
Na_2O	9.29	7.93	7.56	8.38
K_2O	.17	.07	-	.09
TOTAL	100.27	100.05	100.55	100.10
Si	11.186	10.630	10.624	10.916
Ti	-	-	-	-
Al	4.817	5.333	5.366	5.052
Fe	-	.019	.015	.018
Mn	-	-	-	-
Mg	-	-	-	-
Ca	.794	1.339	1.387	1.117
Na	3.176	2.744	2.599	2.884
K	.038	.016	-	.020
TOTAL CATIONS	20.011	20.081	19.991	20.007
O	32.000	32.000	32.000	32.000
Mol%				
Or	.954	.389	-	.507
Ab	79.247	66.952	65.206	71.728
An	19.799	32.659	34.794	27.765

* Total iron as FeO.

TABLE 6.7

MICROPROBE ANALYSES OF PLAGIOCLASE - (CONTINUED)

	81117		81120	
	2	3	1	2
SiO_2	61.20	61.59	57.43	58.76
TiO_2	.07	.07	-	-
Al_2O_3	24.04	24.23	26.82	26.22
FeO*	.08	.09	.10	.04
MnO	-	-	-	-
MgO	-	-	-	-
CaO	5.96	5.96	8.99	8.04
Na_2O	8.12	8.40	6.88	7.06
K_2O	.04	.08	.13	-
TOTAL	100.27	100.05	100.55	100.10
Si	10.919	10.900	10.279	10.483
Ti	.009	.009	-	-
Al	5.054	5.053	5.657	5.512
Fe	.012	.013	.015	.006
Mn	-	-	-	-
Mg	-	-	-	-
Ca	1.139	1.130	1.724	1.537
Na	2.809	2.882	2.388	2.442
K	.009	.018	.030	-
TOTAL CATIONS	19.951	20.009	20.093	19.980
O	32.000	32.000	32.000	32.000
Mol%				
Or	.230	.448	.717	-
Ab	70.980	71.513	57.653	61.375
An	28.79	28.039	41.631	38.625

* Total iron as FeO.

TABLE 6.7

MICROPROBE ANALYSES OF PLAGIOCLASE - (CONTINUED)

	8140		8144	
	1	2	1	2
SiO_2	60.84	61.66	60.95	59.93
TiO_2	-	-	-	-
Al_2O_3	24.48	24.05	24.86	25.54
FeO*	.13	.10	.06	.08
MnO	-	-	-	-
MgO	-	-	-	-
CaO	6.10	5.67	6.22	7.20
Na_2O	7.90	8.30	8.32	7.92
K_2O	.19	.12	.27	.16
TOTAL	99.64	99.90	100.68	100.83
Si	10.853	10.950	10.785	10.620
Ti	-	-	-	-
Al	5.146	5.033	5.183	5.333
Fe	.019	.015	.009	.012
Mn	-	-	-	-
Mg	-	-	-	-
Ca	1.166	1.079	1.179	1.367
Na	2.732	2.858	2.854	2.721
K	.043	.027	.061	.036
TOTAL CATIONS	19.959	19.962	20.071	20.089
O	32.000	32.000	32.000	32.000
Mol%				
Or	1.097	.686	1.488	.877
Ab	69.323	72.097	69.712	65.978
An	29.580	27.217	28.800	33.146

* Total iron as FeO.

TABLE 6.7

MICROPROBE ANALYSES OF PLAGIOCLASE - (CONTINUED)

	8150		8174	
	1	2	1	2
SiO_2	57.21	57.84	66.85	66.75
TiO_2	-	-	-	-
Al_2O_3	26.80	26.80	26.89	20.94
FeO*	.22	-	-	.09
MnO	-	-	-	-
MgO	-	-	-	-
CaO	9.09	8.79	1.63	2.06
Na_2O	6.19	6.33	10.51	10.43
K_2O	.13	.25	.17	.20
TOTAL	99.64	100.01	100.05	100.47
Si	10.296	10.349	11.710	11.669
Ti	-	-	-	-
Al	5.685	5.651	4.312	4.314
Fe	.033	-	-	.013
Mn	-	-	-	-
Mg	-	-	-	-
Ca	1.753	1.685	.306	.386
Na	2.160	2.196	3.569	3.535
K	.030	.057	.038	.045
TOTAL CATIONS	19.955	19.938	19.935	19.962
O	32.000	32.000	32.000	32.000
Mol%				
Or	.757	1.449	.971	1.125
Ab	54.785	55.761	91.212	89.146
An	44.458	42.790	7.817	9.730

* Total iron as FeO.

TABLE 6.7

MICROPROBE ANALYSES OF PLAGIOCLASE - (CONTINUED)

	8190		8191	
	1	2	1	2
SiO_2	68.50	68.39	67.16	66.68
TiO_2	-	-	.06	-
Al_2O_3	19.78	19.68	20.87	20.86
FeO*	.06	.09	.10	.10
MnO	-	-	-	-
MgO	-	-	-	-
CaO	.71	.45	1.79	2.00
Na_2O	11.18	11.49	10.50	10.50
K_2O	.15	.19	.18	.14
TOTAL	100.38	100.29	100.66	100.28
Si	11.931	11.933	11.705	11.677
Ti	-	-	.008	-
Al	4.060	4.046	4.286	4.304
Fe	.009	.013	.015	.015
Mn	-	-	-	-
Mg	-	-	-	-
Ca	.132	.084	.334	.375
Na	3.776	3.887	3.548	3.565
K	.033	.042	.040	.031
TOTAL CATIONS	19.941	20.005	19.936	19.995
O	32.000	32.000	32.000	32.000
Mol%				
Or	.846	1.054	1.020	.787
Ab	95.793	96.850	90.468	89.764
An	3.362	3.096	8.522	9.449

* Total iron as FeO.

TABLE 6.7

MICROPROBE ANALYSES OF PLAGIOCLASE - (CONTINUED)

	8248	
	1	2
SiO_2	68.94	68.87
TiO_2	-	-
Al_2O_3	19.47	19.45
FeO*	-	.25
MnO	-	-
MgO	-	-
CaO	.30	.06
Na_2O	11.70	11.76
K_2O	.09	.
TOTAL	100.54	100.39
Si	11.986	11.990
Ti	-	-
Al	3.989	3.990
Fe	-	.036
Mn	-	-
Mg	-	-
Ca	.056	.011
Na	3.944	3.970
K	.020	-
TOTAL CATIONS	19.995	19.997
O	32.000	32.000
Mol%		
Or	.497	-
Ab	98.113	99.719
An	1.390	.281

*Total iron as FeO.

TABLE 6.7

MICROPROBE ANALYSES OF PLAGIOCLASE

(CONTINUED)

Rock type, sample location and minerals analyzed.

8148: Fine-grained metabasite from northern Middle River; fine-grained plagioclase, slightly sericitized.

81103: Fine-grained metabasite from Middle River near the mouth of Duncan Brook; fine-grained plagioclase, very slightly sericitized.

81117: Fine-grained metabasite from the eastern reaches of Ryan Brook; fine-grained plagioclase, very slightly sericitized.

81120: Fine-grained metabasite from the eastern reaches of Ryan Brook; fine-grained plagioclase, very slightly sericitized.

8140: Medium-grained semipelitic gneiss from Sarach Brook near the Bothan Brook granodiorite; fine- to medium-grained plagioclase, slightly sericitized.

8144: Medium-grained semipelitic gneiss from Middle River north of Sarach Brook; medium-grained plagioclase, slightly sericitized.

8150: Medium-grained semipelitic gneiss from northern Middle River; fine- to medium-grained plagioclase, slightly sericitized.

TABLE 6.7

MICROPROBE ANALYSES OF PLAGIOCLASE

(CONTINUED)

8174: Medium-grained foliated granitic rock from South Nile Brook; medium-grained plagioclase, moderately sericitized.

8190: Medium-grained least deformed granitic rock from Nile Brook near Fielding Road; fine- to medium-grained plagioclase, extensively sericitized.

8191: Medium-grained least deformed granitic rock from Nile Brook near Fielding Road; fine- to medium-grained plagioclase, extensively sericitized.

8248: Medium-grained Bothan Brook granodiorite from the south branch of Fourth Gold Brook; fine- to medium-grained plagioclase, extensively sericitized.

Similarly, the An contents of the plagioclase from the three medium- to high-grade pelitic rocks are slightly higher than those reported by Guidotti (1970 and 1974) and Yardley et al. (1980) for upper staurolite to upper sillimanite grade metapelites, but more closely resemble those reported by Tracy (1978) for upper sillimanite pelitic schists.

The increase in the anorthite content of plagioclase accompanying an increase in metamorphic grade has been reported in both basic volcanic rocks (van de Kamp, 1970; Liou et al., 1974; Laird and Albee, 1981; Moody et al., 1983) and pelitic rock assemblages (Tracy, 1978). However, Guidotti (1970 and 1974) and Yardley et al. (1980) indicated that the average An content of plagioclase did not seem to rise with grade in their respective investigations of high-grade metapelites.

Unfortunately, the random distribution of the samples selected for plagioclase analysis and the small number of grains analyzed prevents a detailed documentation of any relationship between plagioclase composition and metamorphic grade in the Middle River rocks. However, there appears to be a general increase in the An content of the plagioclase in the four metabasite samples (from An 20 to An 42) and in the three metapelites (from An 27

to An 44) from south to north, parallel to the postulated increase in regional metamorphic grade. Since there is considerable difference in the degree of sericitization of the plagioclase, more data are required to thoroughly document the above relationship between the increasing An content in the plagioclase and the metamorphic grade in the Middle River area.

6.8 AMPHIBOLE ANALYSES

Table 6.8 is a compilation of amphibole analyses obtained from samples that are all, with one exception, from metabasites; sample 8144 is a pelitic gneiss containing amphibole-rich layers. The metabasite samples are roughly arranged according to geographical location, from south to north, parallel to the increasing grade of metamorphism.

Since the water plus halogen content of the amphiboles examined was not determined, the formulas are calculated on a water- and halogen-free basis of 23 (O) and 2 (OH, F, Cl) (Leake, 1978). The amphiboles analyzed fall within the calcic amphibole group, where $(Ca+Na)_B \geq 1.34$ and $Na_B < 0.67$, and their exact classification, according to the accepted nomenclature compiled by Leake (1978), is included in Table 6.8.

TABLE 6.8

MICROPROBE ANALYSES OF AMPHIBOLES

		8106				8118B
		1	2	3	4	1
SiO_2		43.31	42.97	42.32	43.25	42.53
Al_2O_3		14.09	14.23	13.31	13.92	14.52
Fe_2O_3		4.55	4.70	8.00	4.15	5.05
FeO		14.46	14.56	12.65	14.63	14.81
MgO		8.95	8.86	9.96	8.97	8.32
MnO		.36	.48	.40	.34	.41
TiO_2		.30	.40	.32	.31	.29
CaO		11.24	11.22	9.40	11.13	11.23
Na_2O		1.64	1.82	1.85	1.75	1.64
K_2O		.33	.34	.23	.27	.34
TOTAL		99.23	99.58	98.44	98.72	99.14
Z	Si_{IV}	6.357	6.303	6.261	6.379	6.277
	Al^{3+}	1.643	1.697	1.739	1.621	1.723
	Fe_{VI}	-	-	-	-	-
Y	Al^{3+}	.794	.763	.581	.798	.802
	Fe^{3+}	.503	.520	.892	.461	.562
	Ti	.033	.044	.036	.034	.032
	Fe	1.711	1.736	1.295	1.734	1.774
	Mn	-	-	-	-	-
	Mg	1.958	1.937	2.196	1.972	1.830
M_4	Mg_{2+}	-	-	-	-	-
	Fe^{2+}	.063	.050	.270	.070	.054
	Mn	.045	.060	.050	.042	.051
	Ca	1.768	1.763	1.490	1.759	1.776
	Na	.125	.127	.190	.129	.119
X	Ca	-	-	-	-	-
	Na	.342	.390	.341	.371	.350
	K	.062	.064	.043	.051	.064
OXYGEN		23.000	23.000	23.000	23.000	23.000
SUM Z		8.000	8.000	8.000	8.000	8.000
SUM Y		5.000	5.000	5.000	5.000	5.000
SUM M_4		2.000	2.000	2.000	2.000	2.000
SUM X		.404	.454	.384	.422	.414
MINERAL NAME		T S C H E R M A K I T I C H O R N B L E N D E S				
Fe/Fe+Mg		.475	.480	.416	.478	.500

TABLE 6.8

MICROPROBE ANALYSES OF AMPHIBOLES - (CONTINUED)

	8118B			81111	
	2	3	4	1	2
SiO_2	42.48	42.64	42.67	43.77	43.28
Al_2O_3	14.25	13.68	13.88	14.50	15.08
Fe_2O_3	6.50	4.25	3.45	2.80	3.35
FeO	13.09	15.09	15.49	13.45	13.43
MgO	8.92	8.24	8.24	9.58	9.26
MnO	.45	.45	.50	.28	.32
TiO_2	.24	.11	.34	.36	.47
CaO	10.51	11.02	11.06	11.25	11.03
Na_2O	1.66	1.57	1.69	1.63	1.70
K_2O	.34	.32	.31	.18	.19
TOTAL	98.44	97.37	97.63	97.81	98.11
Z Si	6.280	6.400	6.388	6.436	6.357
Al^{IV}	1.720	1.600	1.612	1.564	1.643
Fe^{3+}	-	-	-	-	-
Y Al^{VI}	.763	.819	.837	.949	.967
Fe^{3+}	.724	.481	.389	.310	.371
Ti	.027	.012	.038	.040	.052
Fe	1.520	1.844	1.897	1.599	1.583
Mn	-	-	-	-	-
Mg	1.966	1.843	1.839	2.102	2.027
M_4 Mg	-	-	-	-	-
Fe^{2+}	.098	.049	.042	.056	.066
Mn	.056	.057	.063	.035	.040
Ca	1.665	1.772	1.774	1.772	1.736
Na	.181	.121	.120	.137	.159
X Ca	-	-	-	-	-
Na	.295	.336	.370	.328	.325
K	.064	.061	.059	.034	.036
OXYGEN	23.000	23.000	23.000	23.000	23.000
SUM Z	8.000	8.000	8.000	8.000	8.000
SUM Y	5.000	5.000	5.000	5.000	5.000
SUM M_4	2.000	2.000	2.000	2.000	2.000
SUM X	.359	.397	.429	.362	.361
MINERAL NAME	TSCHERMAKITIC HORNBLENDES		FERROTSCHERM HORNBLENDES	TSCHERMAKITIC HORNBLENDES	
Fe/Fe+Mg	.451	.507	.513	.441	.449

TABLE 6.8

MICROPROBE ANALYSES OF AMPHIBOLES - (CONTINUED)

		81111		8129		
		3	4	1	2	3
SiO_2		44.02	43.72	42.39	42.47	43.23
Al_2O_3		13.94	14.01	16.32	16.87	15.25
Fe_2O_3		2.95	3.70	2.15	1.90	1.80
FeO		13.43	13.29	13.77	13.18	13.18
MgO		9.87	9.49	8.37	8.66	9.28
MnO		.18	.29	.24	.21	.25
TiO_2		.23	.29	.31	.33	.41
CaO		11.33	10.65	11.10	11.27	11.34
Na_2O		1.63	1.81	1.53	1.45	1.52
K_2O		.23	.14	.28	.31	.32
TOTAL		97.71	97.39	96.46	96.65	96.73
Z	Si	6.481	6.463	6.320	6.294	6.411
	Al^{IV}	1.519	1.537	1.680	1.706	1.589
	Fe^{3+}	-	-	-	-	-
Y	Al^{VI}	.900	.904	1.187	1.241	1.076
	Fe^{3+}	.327	.412	.242	.212	.201
	Ti	.025	.032	.035	.037	.046
	Fe	1.582	1.561	1.676	1.597	1.625
	Mn	-	-	-	-	-
	Mg	2.166	2.091	1.860	1.913	2.051
M_4	Mg	-	-	-	-	-
	Fe^{2+}	.071	.082	.040	.036	.028
	Mn	.022	.036	.030	.026	.031
	Ca	1.787	1.687	1.773	1.790	1.802
	Na	.119	.194	.157	.148	.139
C	Ca	-	-	-	-	-
	Na	.318	.324	.285	.269	.298
	K	.043	.026	.053	.059	.061
OXYGEN		23.000	23.000	23.000	23.000	23.000
SUM Z		8.000	8.000	8.000	8.000	8.000
SUM Y		5.000	5.000	5.000	5.000	5.000
SUM M_4		2.000	2.000	2.000	2.000	2.000
SUM X^4		.361	.350	.338	.328	.359
MINERAL NAME		T S C H E R M A K I T I C H O R N B L E N D E S				
Fe/Fe+Mg		.433	.440	.480	.461	.446

TABLE 6.8

MICROPROBE ANALYSES OF AMPHIBOLES - (CONTINUED)

		8122		8148		
		1	2	1	2	3
SiO_2		45.18	44.88	43.35	43.61	42.75
Al_2O_3		13.62	13.86	14.75	13.83	14.44
Fe_2O_3		.90	1.10	2.10	1.90	2.65
FeO		15.22	14.82	12.68	13.98	13.65
MgO		10.00	10.04	11.04	10.48	10.22
MnO		.24	.28	.23	.23	.15
TiO_2		.63	.84	1.14	.93	1.00
CaO		12.46	12.18	11.60	11.76	11.59
Na_2O		1.49	1.69	2.36	2.08	1.98
K_2O		.39	.38	.54	.55	.53
TOTAL		100.13	100.07	99.79	99.35	98.96
Z	Si_{IV}	6.524	6.480	6.264	6.361	6.264
	Al^{3+}_{IV}	1.476	1.520	1.736	1.639	1.736
	Fe^{3+}_{IV}	-	-	-	-	-
Y	Al^{3+}_{VI}	.842	.839	.776	.738	.757
	Fe^{3+}_{VI}	.098	.120	.229	.209	.293
	Ti	.068	.091	.124	.102	.110
	Fe	1.838	1.790	1.494	1.673	1.608
	Mn	.002	-	-	-	-
	Mg	2.152	2.161	2.378	2.278	2.232
M_4	Mg^{3+}	-	-	-	-	-
	Fe	-	-	.038	.033	.064
	Mn	.028	.034	.028	.028	.019
	Ca	1.928	1.884	1.796	1.838	1.819
	Na	.045	.082	.138	.101	.098
X	Ca	-	-	-	-	-
	Na	.373	.391	.523	.487	.465
	K	.072	.070	.100	.102	.099
OXYGEN		23.000	23.000	23.000	23.000	23.000
SUM Z		8.000	8.000	8.000	8.000	8.000
SUM Y		5.000	5.000	5.000	5.000	5.000
SUM M_4		2.000	2.000	2.000	2.000	2.000
SUM X		.445	.461	.623	.589	.564
MINERAL NAME		MAGNESIO. HORN.	TSCHERM. HORN.	FERROAN PARGASTIC HORN.		
Fe/Fe+Mg		.461	.453	.392	.428	.428

TABLE 6.8

MICROPROBE ANALYSES OF AMPHIBOLES - (CONTINUED)

		81117				
		1	2	3	4	5
SiO_2		43.55	43.32	43.79	43.00	43.30
Al_2O_3		14.46	14.24	13.30	14.25	14.68
Fe_2O_3		2.80	2.35	3.40	2.80	3.05
FeO		12.63	13.38	12.73	13.16	12.75
MgO		10.60	10.43	10.63	10.38	10.25
MnO		.31	.33	.21	.30	.31
TiO_2		.58	.81	.51	.71	.49
CaO		11.48	11.72	11.85	11.74	11.58
Na_2O		1.80	1.83	1.51	1.82	1.61
K_2O		.58	.66	.48	.61	.41
TOTAL		98.79	99.07	98.41	98.77	98.51
Z	Si_{IV}	6.350	6.328	6.422	6.304	6.333
	Al^{3+}	1.650	1.672	1.578	1.696	1.667
	Fe_{VI}	-	-	-	-	-
Y	Al^{3+}	.835	.780	.720	.766	.864
	Fe^{3+}	.308	.259	.376	.309	.336
	Ti	.064	.089	.056	.078	.054
	Fe	1.490	1.602	1.524	1.578	1.511
	Mn	-	-	-	-	-
	Mg	2.304	2.271	2.324	2.268	2.235
M_4	Mg^{2+}	-	-	-	-	-
	Fe^{2+}	.050	.032	.037	.035	.048
	Mn	.038	.041	.026	.037	.038
	Ca	1.793	1.834	1.862	1.844	1.815
	Na	.118	.093	.075	.084	.099
X	Ca	-	-	-	-	-
	Na	.391	.426	.355	.434	.381
	K	.108	.123	.090	.114	.077
OXYGEN		23.000	23.000	23.000	23.000	23.000
SUM Z		8.000	8.000	8.000	8.000	8.000
SUM Y		5.000	5.000	5.000	5.000	5.000
SUM M_4		2.000	2.000	2.000	2.000	2.000
SUM X^4		.499	.549	.445	.548	.458
MINERAL NAME		TSCHERM. HORN.	FERROAN PARGAS. HORN.	TSCHERM. HORN.	FERROAN PARGAS. HORN.	TSCHERM. HORN.
Fe/Fe+Mg		.401	.418	.402	.416	.411

TABLE 6.8

MICROPROBE ANALYSES OF AMPHIBOLES - (CONTINUED)

		8196				81103
		1	2	3	4	1
SiO_2		46.31	45.41	46.49	44.89	45.01
Al_2O_3		13.61	15.24	13.54	15.85	13.68
Fe_2O_3		1.85	2.40	1.95	2.35	2.70
FeO		8.50	10.07	8.82	10.09	9.27
MgO		13.33	11.78	12.97	11.33	13.06
MnO		.30	.19	.20	.23	.28
TiO_2		.40	.29	.39	.21	.98
CaO		11.91	11.67	11.70	11.54	11.18
Na_2O		1.33	1.39	1.23	1.40	2.30
K_2O		.19	.21	.14	.18	.34
TOTAL		97.73	98.65	97.43	98.07	98.80
Z	Si_{IV}	6.625	6.486	6.666	6.448	6.446
	Al^{3+}	1.375	1.514	1.334	1.552	1.554
	Fe_{VI}	-	-	-	-	-
Y	Al^{3+}	.920	1.051	.955	1.131	.754
	Fe^{3+}	.199	.258	.211	.254	.291
	Ti	.043	.031	.042	.023	.106
	Fe	.995	1.152	1.021	1.166	1.061
	Mn	-	-	-	-	-
	Mg	2.842	2.508	2.772	2.426	2.788
M_4	Mg^{2+}	-	-	-	-	-
	Fe^{2+}	.021	.051	.037	.045	.049
	Mn	.036	.023	.024	.028	.034
	Ca	1.826	1.786	1.798	1.776	1.715
	Na	.117	.140	.142	.151	.202
X	Ca	-	-	-	-	-
	Na	.252	.245	.200	.239	.437
	K	.035	.038	.026	.023	.062
OXYGEN		23.000	23.000	23.000	23.000	23.000
SUM Z		8.000	8.000	8.000	8.000	8.000
SUM Y		5.000	5.000	5.000	5.000	5.000
SUM M_4		2.000	2.000	2.000	2.000	2.000
SUM X		.287	.283	.226	.272	.499
MINERAL NAME		FERRO-PARGAS. HORN.		FERRO-EDENITIC HORN.	FERRO-PARGAS. HORN.	TSCHERM. HORN.
Fe/Fe+Mg		.263	.324	.276	.333	.285

TABLE 6.8

MICROPROBE ANALYSES OF AMPHIBOLES - (CONTINUED)

		81103	81120			
		2	1	2	3	4
SiO_2		45.70	44.04	45.04	43.87	43.81
Al_2O_3		13.45	14.95	14.07	14.20	14.89
Fe_2O_3		2.20	1.60	1.65	1.75	1.85
FeO		9.65	11.84	11.49	11.47	11.42
MgO		13.10	11.32	11.94	11.40	11.37
MnO		.24	.30	.28	.20	.33
TiO_2		.93	.97	.76	.73	.86
CaO		11.31	12.10	12.06	11.93	11.95
Na_2O		2.31	1.45	1.53	1.28	1.38
K_2O		.29	.87	.75	.76	.90
TOTAL		99.18	99.44	99.57	97.59	98.76
Z	Si^{IV}	6.512	6.341	6.455	6.420	6.345
	Al^{3+}	1.488	1.659	1.545	1.580	1.655
	Fe^{3+}	-	-	-	-	-
Y	Al^{VI}	.771	.879	.832	.869	.886
	Fe^{3+}	.236	.174	.178	.193	.202
	Ti	.100	.105	.082	.080	.094
	Fe	1.111	1.413	1.358	1.372	1.364
	Mn	-	-	-	-	-
	Mg	2.782	2.430	2.551	2.486	2.454
M_4	Mg^{2+}	-	-	-	-	-
	Fe^{2+}	.039	.013	.019	.031	.018
	Mn	.029	.037	.034	.025	.040
	Ca	1.727	1.867	1.852	1.870	1.854
	Na	.205	.084	.095	.073	.087
X	Ca	-	-	-	-	-
	Na	.433	.321	.330	.290	.301
	K	.053	.161	.137	.142	.166
OXYGEN		23.000	23.000	23.000	23.000	23.000
SUM Z		8.000	8.000	8.000	8.000	8.000
SUM Y		5.000	5.000	5.000	5.000	5.000
SUM M_4		2.000	2.000	2.000	2.000	2.000
SUM X		.486	.481	.467	.432	.467
MINERAL NAME		MAGNESIO HORN.	T S C H E R M A K I T I C H O R N B L E N D E S			
Fe/Fe+Mg		.292	.370	.351	.361	.361

TABLE 6.8

MICROPROBE ANALYSES OF AMPHIBOLES - (CONTINUED)

		8144	
		1	2
SiO_2		42.40	42.92
Al_2O_3		14.03	14.11
Fe_2O_3		2.50	1.40
FeO		17.50	18.24
MgO		7.80	7.53
MnO		.19	.21
TiO_2		1.17	.94
CaO		11.55	11.91
Na_2O		1.16	1.09
K_2O		1.30	1.33
TOTAL		99.15	99.68
Z	Si_{IV}	6.289	6.365
	Al^{3+}	1.711	1.635
	Fe^{3+}	-	-
Y	Al^{VI}	.753	.831
	Fe^{3+}	.281	.156
	Ti	.131	.105
	Fe	2.102	2.244
	Mn	-	-
	Mg	1.733	1.664
M_4	Mg	-	-
	Fe^{2+}	.048	.018
	Mn	.024	.026
	Ca	1.844	1.892
	Na	.084	.063
X	Ca	-	-
	Na	.251	.250
	K	.247	.252
OXYGEN		23.000	23.000
SUM Z		8.000	8.000
SUM Y		5.000	5.000
SUM M_4		2.000	2.000
SUM X		.498	.502
MINERAL NAME		FERRO-TSCHERM. HORN.	FERROAN PARGAS. HORN.
Fe/Fe+Mg		.554	.576

TABLE 6.8

MICROPROBE ANALYSES OF AMPHIBOLES

(CONTINUED)

Rock type, sample location and minerals analyzed.

8106: Fine-grained metabasite from Middle River near the mouth of Second Gold Brook; fine-grained hornblendes.

8118B: Fine-grained porphyroblastic metabasite from the south branch of Third Gold Brook; fine- to medium-grained idioblastic hornblende porphyroblasts.

81111: Fine-grained metabasite from the west branch of Fortune Brook; fine-grained hornblendes.

8129: Medium-grained metabasite from Fourth Gold Brook; medium-grained hornblendes.

8122: Fine-grained metabasite from the southern end of Egypt Highland Road; fine-grained hornblendes.

8148: Fine-grained metabasite from northern Middle River; fine-grained hornblendes.

81117: Fine-grained metabasite from the eastern reaches of Ryan Brook; fine-grained hornblendes.

8196: Fine-grained metabasite from an unnamed brook north of First Lake O'Law; fine-grained hornblendes.

81103: Fine-grained metabasite from Middle River near the mouth of Duncan Brook: fine-grained hornblendes.

81120: Fine-grained metabasite from the eastern reaches of Ryan Brook; fine-grained hornblendes.

TABLE 6.8

MICROPROBE ANALYSES OF AMPHIBOLES

(CONTINUED)

8144: Medium-grained semipelitic gneiss from Middle River north of Sarach Brook; fine- to medium-grained hornblendes concentrated in a single layer a few centimeters thick.

The most noteworthy trend shown by the hornblendes is an increase in titanium from south to north. This is associated with a similar increase in TiO_2 in metabasites (previously mentioned in Chapter 5). The increase in TiO_2 in hornblende may reflect overall compositional variations in the host rock in the sequence and/or may be a reflection of the increase in Ti in amphibole with increasing metamorphic grade noted by Laird and Albee (1981). A plot of TiO_2 in hornblende versus TiO_2 in the metabasites (Figure 6.3) shows no correlation between the two parameters, yet since sphene and ilmenite are present in only certain metabasites, it appears that both minor variations in the host rock and differences in the metamorphic grade of the metabasites are responsible for the variable TiO_2 content of the hornblendes.

Changes in the composition of calciferous amphiboles have been used in numerous studies as indicators of metamorphic pressure during metamorphism of metabasites. Features used to distinguish low-pressure from medium-pressure amphiboles include their lower Al^{vi} (Leake, 1965; Raase, 1974; Laird and Albee, 1981) and their higher Na_A contents (Graham, 1974; Holland and Richardson, 1979; Laird and Albee, 1981) and the suggestion by Brown (1975) that medium-pressure rocks may contain more glaucophane-rich amphiboles. Hynes (1982) reports no consistent dif-

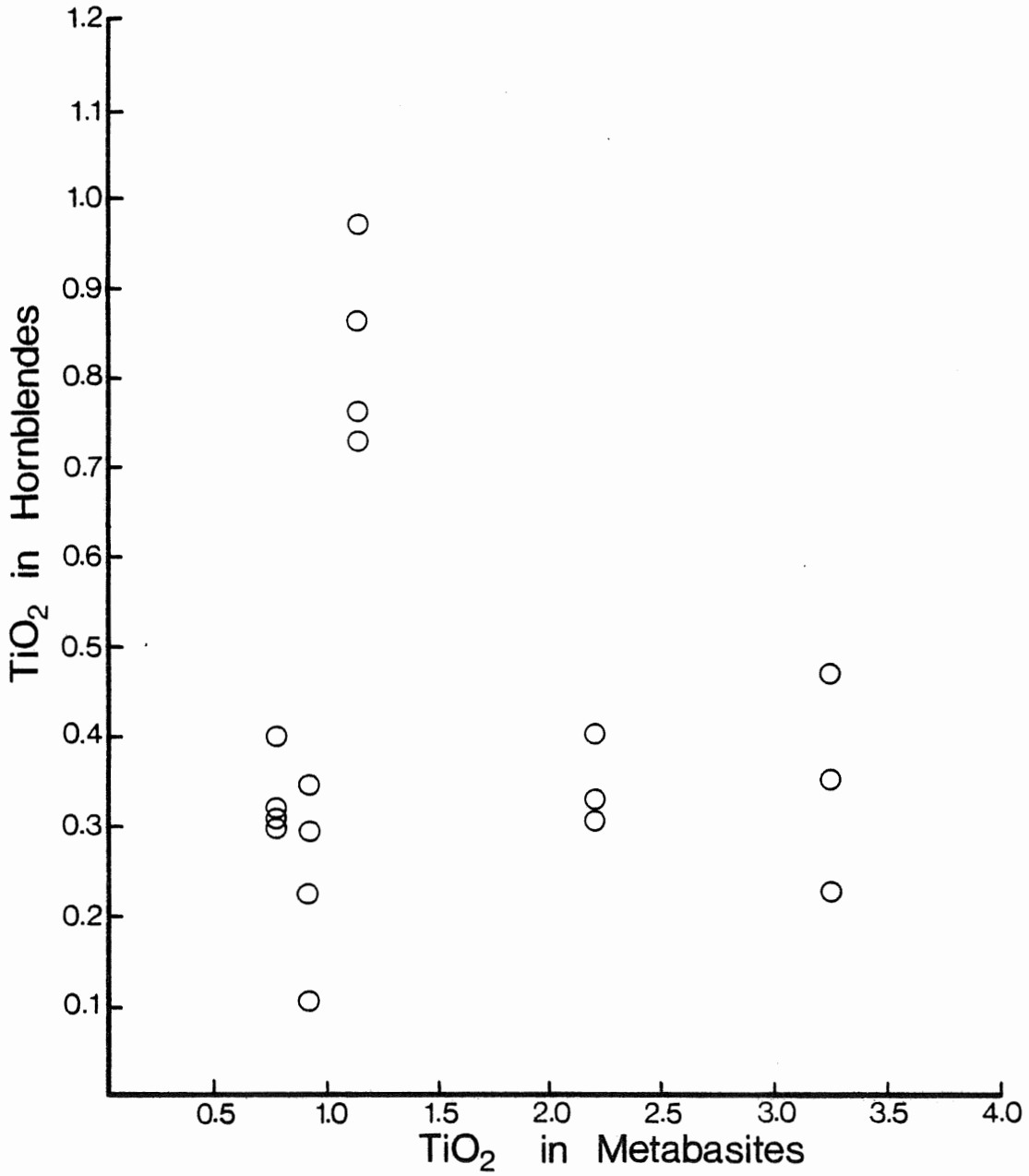

Figure 6.3 Plot of TiO_2 in hornblendes versus TiO_2 in metabasites. The lack of a relationship between the two parameters indicates that the TiO_2 content in hornblende is a function of both the metamorphic grade and the TiO_2 content of the host metabasite.

ferences in Na_B, Al^{vi} or Na_A between the two series but recognizes generally higher Ti/Al ratios in low-pressure amphiboles. Despite this lack of consensus, comparison of the hornblendes examined in this study with the Al^{vi} versus Si diagram of Raase (1974), with amphibole proportion diagrams from Laird and Albee (1981), and with the Ti versus Al diagram of Hynes (1982) indicate that the hornblendes from the Middle River metabasites formed under medium-pressure metamorphic conditions.

6.9 CALCITE ANALYSES

The analyses of calcite crystals contained in four samples of dolomitic marble, taken from the thick layer along Middle River north of Sarach Brook, are listed in Table 6.9. The number of ions in the chemical formula could not be calculated since the amount of CO_2 in calcite could not be determined with the electron microprobe. The mol percent $MgCO_3$ in calcite, used in the calcite-dolomite geothermometers discussed in the following chapter, is calculated as follows:

For each sample, for CaO and MgO,

$$\text{molecular proportion} = \frac{\text{weight percent oxide}}{\text{molecular weight}} \times 100$$

and the sum of the two values is adjusted to equal 100 percent. The adjusted percentage for the MgO molecular proportion is equal to the mol percent $MgCO_3$ in calcite

TABLE 6.9

MICROPROBE ANALYSES OF CALCITES

	8145									
	1	2	3	4	5	6	7	8	9	10
MgO	3.11	2.72	3.23	2.61	2.14	3.00	2.14	2.23	2.39	2.52
CaO	52.36	52.43	51.18	52.18	52.76	51.00	51.62	52.37	52.68	51.76
TOTAL	55.47	55.15	54.41	54.79	54.90	54.00	53.76	54.60	55.07	54.28
MoL% $MgCO_3$	7.62	6.72	8.07	6.51	5.34	7.65	5.46	5.59	5.94	6.34

8145 : Medium-grained calcites, marble from Middle River north of Sarach Brook, westernmost sample.

TABLE 6.9

MICROPROBE ANALYSES OF CALCITES - (CONTINUED)

	8252				
	1	2	3	4	5
MgO	3.8	3.47	3.09	1.26	1.93
CaO	53.15	52.14	52.93	54.05	54.23
TOTAL	56.33	55.61	56.02	55.31	56.16
MoL% $MgCO_3$	7.68	8.48	7.51	3.14	4.73

8252 : Medium-grained calcites, marble from Middle River north of Sarach Brook.

TABLE 6.9

MICROPROBE ANALYSES OF CALCITES - (CONTINUED)

	8162			8251				
	1	2	3	1	2	3	4	5
MgO	2.11	1.36	0.65	2.14	3.86	3.51	2.34	4.57
CaO	53.43	52.81	54.44	53.77	52.65	54.12	54.15	52.65
TOTAL	55.54	54.17	55.09	55.91	56.51	57.63	56.49 ,	57.22
MoL $MgCO_3$	5.20	3.44	1.64	5.25	9.25	8.27	5.67	10.77

8162 : Medium-grained calcites, marble from Middle River north of Sarach Brook, easternmost sample.

8251 : Medium-grained calcites, marble from Middle River north of Sarach Brook.

(considering the 1:1 ratio of $MgO:CO_2$ in $MgCO_3$), which is given in Table 6.9.

As mentioned in Chapter 4, the marble contains medium-grained calcite and dolomite that appear to be in textural equilibrium. Microprobe analyses of calcites from all four samples show a relatively large range of MgO content, an indication that chemical equilibrium was not reached. Nonetheless, with a sufficient number of analyses, a good approximation of the $MgCO_3$ content of the calcites can be obtained and the temperatures calculated from geothermometers may be considered more or less representative.

6.10 STAUROLITE, KYANITE AND SILLIMANITE ANALYSES

The analyses of a few crystals of staurolite and kyanite in sample 8135 and kyanite and sillimanite (fibrolite) in sample 8247 are listed in Table 6.10. The number of ions in the chemical formulas are calculated on the basis of 47 oxygens for staurolite (Baltatzis, 1979), and 20 oxygens for kyanite and sillimanite (Deer et al., 1978).

The staurolites from sample 8135 are richer in TiO_2 and poorer in MnO and MgO than those reported by Griffen and Ribbe (1973), Guidotti (1974), Baltatzis (1979) and

TABLE 6.10

MICROPROBE ANALYSES OF STAUROLITES, KYANITES AND SILLIMANITE

	8135 STAUROLITE		8135 KYANITE	8247 KYANITE		8247 SILLIMANITE
SiO_2	27.57	27.37	37.26	35.98	36.36	35.36
TiO_2	.84	.74	.09	.04	.04	.17
Al_2O_3	53.78	54.39	62.69	61.71	62.07	61.36
FeO*	13.37	13.56	.35	.30	.31	.25
MnO	.06	-	.05	-	.03	.07
MgO	1.73	1.83	-	-	-	-
CaO	-	-	-	-	-	-
Na_2O	-	-	-	-	-	-
K_2O	-	-	-	.03	.06	.23
TOTAL	97.35	97.89	100.34	98.06	98.87	97.44
Si	7.838	7.745	4.012	3.967	3.977	3.931
Al^{IV}	.162	.255	-	-	-	-
Al^{VI}	17.865	17.887	9.958	8.020	8.003	8.042
Ti	.180	.158	.007	.003	.003	.014
Fe	3.179	3.209	.023	.028	.028	.023
Mn	.014	-	.005	-	.001	.007
Mg	.733	.772	-	-	-	-
Ca	-	-	-	-	-	-
Na	-	-	-	-	-	-
K	-	-	-	.004	.008	.032
TOTAL CATIONS	29.971	30.026	12.005	12.022	12.020	12.049
Fe/Fe+Mg	.813	.806	1.000	1.000	1.000	1.000
O	47 OXYGENS			20 OXYGENS		

* Total iron as FeO.

TABLE 6.10

MICROPROBE ANALYSES OF STAUROLITES,

KYANITES AND SILLIMANITE

(CONTINUED)

Rock type, sample location and minerals analyzed.

8135: Medium-grained pelitic schist from Middle River south of the mouth of the unnamed brook between Duncan Brook and Fourth Gold Brook; coarse-grained kyanite porphyroblast, fine- to medium-grained staurolite grains.

8247: Medium-grained pelitic schist from Middle River north of the mouth of the unnamed brook between Duncan Brook and Fourth Gold Brook: medium-grained kyanite porphyroblasts, very fine-grained sillimanite (fibrolite).

Mohr and Newton (1983). Similarly, the kyanites and sillimanite from sample 8247 are also enriched in TiO_2 compared to those listed by Deer et al. (1978). These differences probably reflect compositional peculiarities of the pelitic schists and, in fact, most minerals in the rocks of the Middle River unit have relatively high titanium contents.

6.11 SUMMARY

The minerals analyzed in the low- and medium- to high-grade metasedimentary rocks have relatively homogeneous compositions that more or less resemble those listed in the literature for low- and medium- to high-grade metapelites. Major differences, as in the case of garnets from sample 8150, are probably attributable to host rock compositional variations.

In the metabasites, hornblende compositions are quite homogeneous except for variable TiO_2 contents, with higher TiO_2 in central and northern metabasites. This northward increase is probably due to a combination of host rock differences and the postulated increase in Ti in amphibole with increasing metamorphic grade (Laird and Albee, 1981). Similarly, the An content of plagioclase apparently increases in both the metabasites and metapelites from south

to north, in accordance with the postulated increase of the anorthite content in plagioclase with increasing metamorphic grade (van de Kamp, 1970; Liou et al., 1974; Tracy, 1978; Laird and Albee, 1981; Moody et al., 1983).

Postulated compositional changes in certain minerals with increasing metamorphic grade are compared to the minerals of the Middle River rocks. Muscovites from the low- and medium- to high-grade rocks appear to follow the indicated compositional changes while garnet compositions show no conclusive trends between the two assemblages. As mentioned above, the TiO_2 content of the hornblendes is controlled to some extent by metamorphic grade. Biotite analyses were obtained from medium- to high-grade rocks only and compositional differences are slight and random. Results from plagioclase analyses are inconclusive due to the small number of grains analyzed but the high An contents nonetheless reflect medium- to high-grade metamorphic conditions.

Compositional zoning in idioblastic chloritoid porphyroblasts in the low-grade phyllite sample, with increasing MgO from core to rim, follows that noted by Cruickshank and Ghent (1978). The compositional cross section of a garnet from a metasedimentary schist sample reveals two phases of "normal" zoning, with Ca and Mn decreasing

and Fe and Mg increasing from core to rim (Hollister, 1966), apparently interrupted by a "retrograde" period of garnet breakdown. This three fold sequence of crystal growth seems to indicate a polyphase metamorphic history for this particular sample which was taken from the area adjacent to the postulated tectonic break between the southern and central belts.

A comparison of the Fe/Fe+Mg ratios of coexisting muscovites, biotites and garnets and host rock for the four medium- to high-grade metapelites (Table 6.11) shows a narrow range within each mineral for each sample but reveals significant variations in the three mineral phases across the four rock samples. These variations are probably the result of differences in the bulk chemistry of the samples and in the modes of each mineral in the particular rock sample. Ionic substitution for Fe^{+2} and Mg, particularly in biotites and garnets (discussed in the following chapter) and the presence of any significant amount of Fe_2O_3 in biotite (which could not be determined by microprobe analysis), may also be responsible for some of the variability of the Fe/Fe+Mg ratios in these two minerals.

From the results obtained from the analyses of the mineral phases of the rocks of the Middle River unit, it

TABLE 6.11

Fe/Fe+Mg RATIOS
OF COEXISTING MINERALS
AND HOST ROCKS

SAMPLE:	8135	81101	8123	8150
Muscovite	0.584 to 0.583	--	0.464 to 0.493	--
Biotite	0.466 to 0.479	0.556 to 0.584	0.455 to 0.469	0.395 to 0.428
Garnet	0.816 to 0.817	0.860 to 0.864	0.773 to 0.822	0.784 to 0.822
Whole Rock	0.691	0.715	0.683	0.661

is concluded that the metamorphic grade of the assemblage has had the greatest influence on the composition of the various mineral phases, with minor compositional inhomogeneities accounted for by slight differences in the bulk chemistry of the host rock.

CHAPTER 7

METAMORPHISM

7.1 METAMORPHIC ASSEMBLAGES

The low-grade assemblage chlorite, muscovite, quartz, biotite or chloritoid characteristic of the metasedimentary schists and phyllites places the rocks occurring over the entire length of Second Gold Brook in the biotite zone of the greenschist facies. No anomalous metamorphic grade is detected in the vicinity of the old gold mine. The appearance of garnet near the mouth of Second Gold Brook corresponds to the transition from the biotite zone to the garnet zone and reflects the change from low-grade to medium-grade metamorphic conditions.

The medium-grade assemblage hornblende, plagioclase of oligoclase and andesine composition, quartz and epidote characteristic of the metabasites places this lithology in the staurolite to kyanite zone transition area. Although epidote group minerals may be retrograde phases, it appears more likely that they are part of the main assemblage since epidote and clinozoisite grains dominantly occur within quartz and plagioclase clusters and are rarely in contact with hornblende.

If the phyllites and metabasites form a continuous belt, as indicated in the proposed structural model, the metamorphic grade increases more or less steadily northward from the biotite zone in the south to the staurolite to kyanite zone near Fourth Gold Brook and the peak of metamorphism is indicated by the mineral assemblage hornblende, oligoclase/andesine, quartz and epidote of the metabasites. Throughout this low- to medium-grade sequence, the development of the various metamorphic assemblages is syntectonic to the major foliation, S_{GB1}. Similarly, the porphyroblastic minerals, chlorite, chloritoid, biotite and garnet in the metasedimentary rocks and hornblende in the metabasites, are syn- to posttectonic to S_{GB1}.

The appearance of staurolite, kyanite and minor sillimanite (fibrolite) at the mouth of the unnamed brook between Fourth Gold and Bothan brooks corresponds to the transition from the staurolite zone to the kyanite zone of the amphibolite facies. Considering the widespread occurrence of large kyanite crystals north of the unnamed brook and the comparatively minor sillimanite, apparently forming from muscovite, it is doubtful that the sillimanite represents locally higher-grade metamorphic conditions but rather may be metastable in the kyanite zone (Holdaway, 1971).

Since the staurolite and kyanite porphyroblasts are pre-tectonic to the major foliation, while garnets may be pre- or syntectonic, there appears to be no relationship between the syn- to post-tectonic porphyroblasts in the rocks of the southern belt and the relict pre-tectonic staurolite and kyanite porphyroblasts in the rocks of the central belt.

The peak of metamorphism in the central belt is indicated by the mineral assemblage muscovite, biotite, garnet, staurolite and kyanite even though it is overprinted by the lower grade assemblage muscovite, biotite and garnet.

The metamorphic mineral assemblages characteristic of the two principal lithologies of the Middle River unit are listed in Table 7.1.

Although the distribution of pelitic units is interrupted by metabasite sheets and felsic gneiss layers, and although the incoming of key metamorphic index minerals is strongly dependent on the bulk composition of the rock, two isograds are identified and positioned along Middle River (Figure 7.1). These isograds are lines representing the first appearance of certain index minerals (in this case garnet and staurolite-kyanite) or, in other words, where a specific change in mineral assemblage reflecting

TABLE 7.1

METAMORPHIC MINERAL ASSEMBLAGES IN THE ROCKS OF THE MIDDLE RIVER UNIT

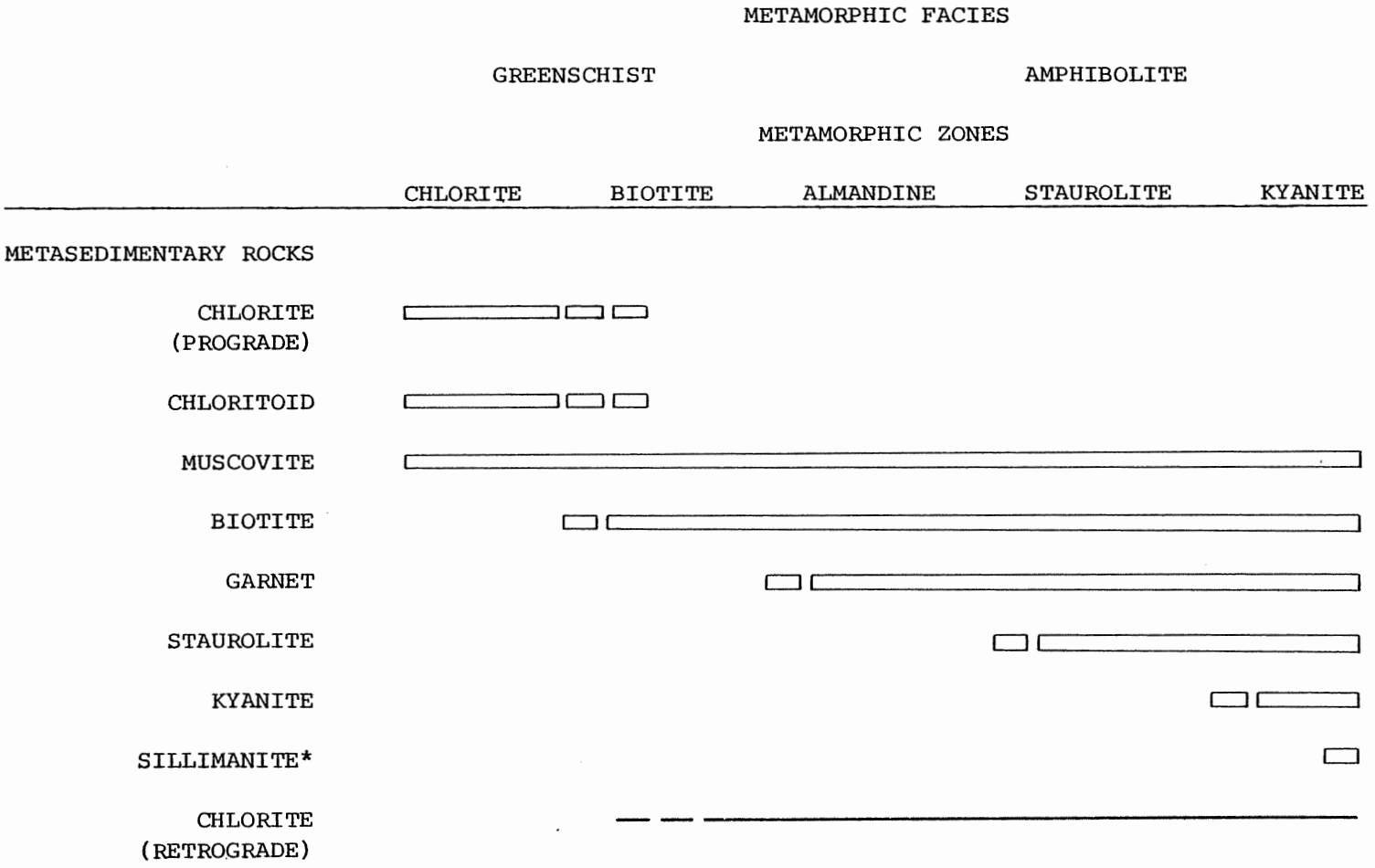

TABLE 7.1

METAMORPHIC MINERAL ASSEMBLAGES IN THE ROCKS OF THE MIDDLE RIVER UNIT - (CONTINUED)

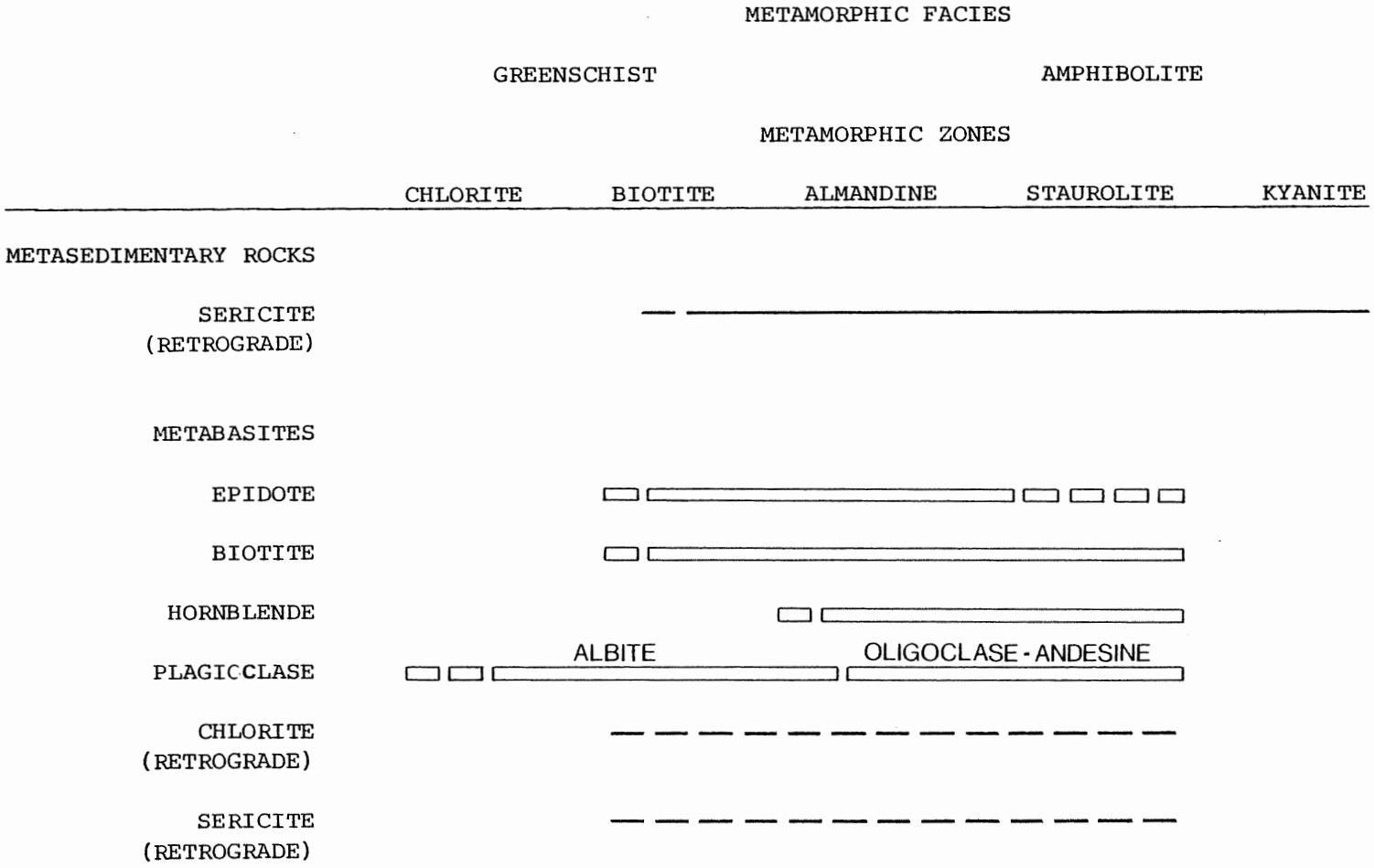

TABLE 7.1

METAMORPHIC MINERAL ASSEMBLAGES IN THE ROCKS OF THE MIDDLE RIVER UNIT - (CONTINUED)

	METAMORPHIC FACIES				
	GREENSCHIST			AMPHIBOLITE	
	METAMORPHIC ZONES				
	CHLORITE	BIOTITE	ALMANDINE	STAUROLITE	KYANITE
METABASITES					
ACTINOLITE (RETROGRADE)		- - - -	- - - -	- - - -	

* SILLIMANITE IS METASTABLE IN THE KYANITE FIELD.

SOLID LINES : ABUNDANT PHASES

DASHED LINES : MINOR PHASES

Figure 7.1 Metamorphic map of the Middle River area showing the occurrence of metamorphic index minerals and associated isograds. Locations where metastable sillimanite, pegmatite (of intrusive origin ?) and migmatite are observed are illustrated.

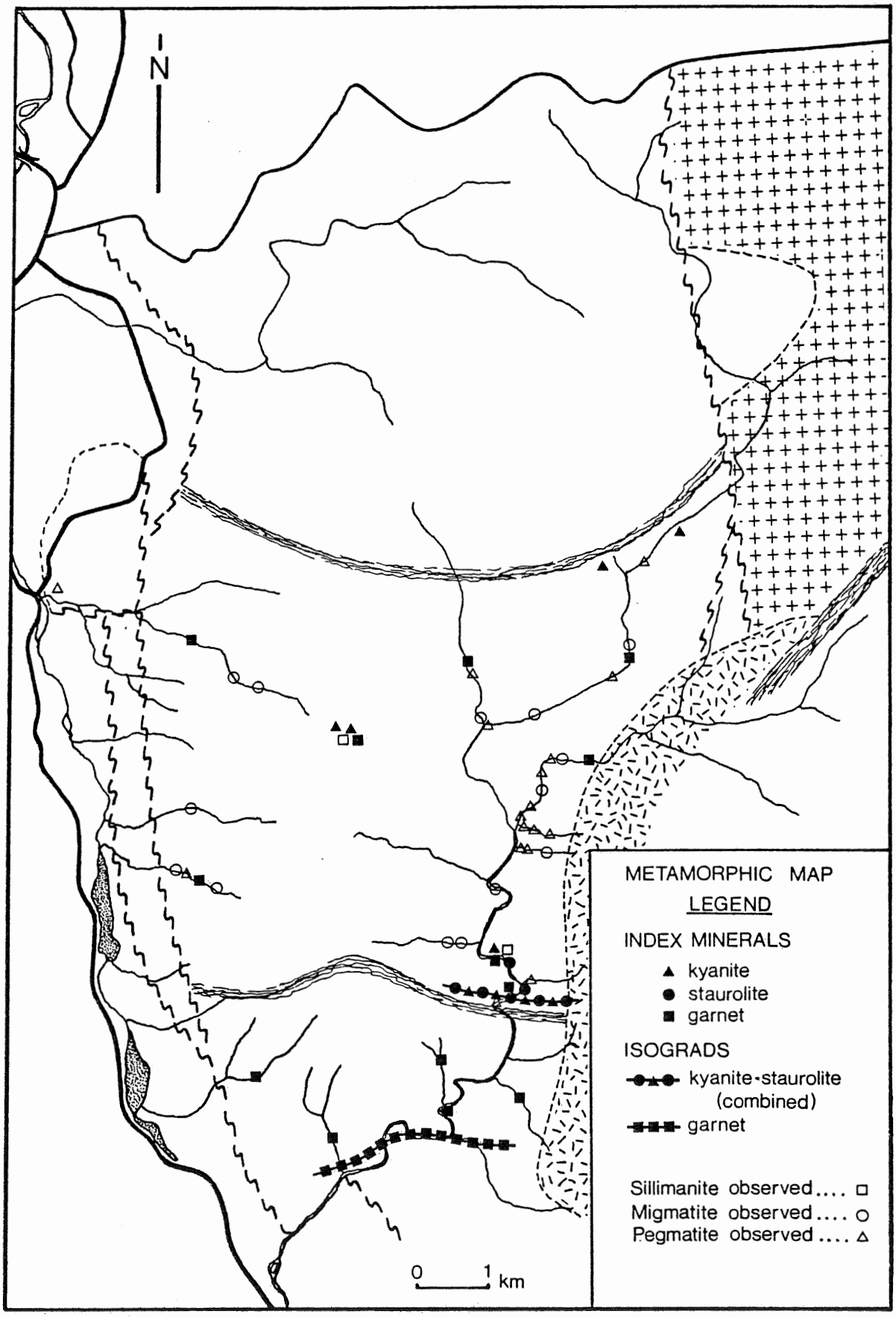
N
METAMORPHIC MAP
LEGEND
INDEX MINERALS
kyanite
staurolite
garnet
ISOGRADS
kyanite-staurolite (combined)
garnet
Sillimanite observed....
Migmatite observed....
Pegmatite observed....
0
1 km

a metamorphic reaction has taken place (Winkler, 1979). The first appearance of migmatites is included in Figure 7.1 as a further indication of the rapid increase in metamorphic grade as one progresses northward.

Even though the isograds can be defined with a certain degree of accuracy along Middle River, they cannot be extended laterally over large distances and their subsurface configuration is not known. However, the garnet isograd is roughly parallel to lithological boundaries and, although the stratigraphy of the sequence may be partly responsible for this orientation, apparently reflects the postulated south-to-north metamorphic gradient of the study area.

Ideally, prograde metamorphic reactions responsible for the formation of index minerals can be derived from petrographic observations; unfortunately, due to the small number of outcrops where staurolite and kyanite have been detected and the probability that these minerals are pretectonic to the present assemblage, this may prove difficult in this study.

7.2 CONDITIONS OF METAMORPHISM

7.2.1 Petrologic Data

Since chloritoid has been the subject of numerous

investigations (Halferdahl, 1961; Hoschek, 1969; Albee, 1972; Baltatzis, 1979; La Tour et al., 1980; Karabinos, in press), its presence in certain layers of the low-grade schists and phyllites can provide some insight into the metamorphic characteristics of these rocks.

Hoschek (1969) wrote that chloritoid is formed during the regional metamorphism of aluminum-rich sediments at about the beginning of the greenschist facies according to the reaction:

chlorite + Al-silicate (kaolinite, pyrophyllite) = chloritoid + quartz + H_2O. (1)

Other chloritoid-forming reactions discussed by Hoschek (1969) include:

chlorite + muscovite = chloritoid + biotite + quartz + H_2O (2)

which takes place at high temperatures in the greenschist facies;

chlorite + paragonite + quartz = chloritoid + albite + H_2O (3)

in rare circumstances; and

chlorite + paragonite + quartz = chloritoid + glaucophane + H_2O (4)

where the rocks are composed of various amounts of pelitic, calcareous and basic magmatic material.

The presence of large amounts of fine muscovite and chlorite in the two samples where chloritoid occurs, and throughout the schists and phyllites, favors reaction (2) but no biotite is seen in either sample. In sample 81108, which contains poorly-developed highly poikiloblastic chloritoid porphyroblasts, chlorite and a fine colorless platy mineral are reacting to produce chloritoid and fine-grained quartz. However, the absence of biotite as a reaction product indicates that reaction (2) is not responsible for the formation of chloritoid. The discrepancy may be resolved if some of the fine colorless platy minerals are not muscovite but pyrophyllite, which can be confused with sericite, especially when fine-grained (Heinrich, 1965). Therefore, with the absence of biotite in both chloritoid-bearing samples, it is concluded that chloritoid formed according to reaction (1).

The presence of chloritoid as far north as Fortune Brook, where sample 81108 was collected, indicates that maximum P-T conditions affecting these rocks did not exceed the lower amphibolite facies since chloritoid nowhere survives beyond the lower amphibolite facies (La Tour et al., 1980).

In the metabasites, the peak metamorphic conditions can be approximated from the mineral assemblage of the

rocks. The presence of oligoclase and andesine rather than albitic plagioclase reflects garnet to staurolite-kyanite grade metamorphism (van de Kamp, 1970; Harte and Graham, 1975; Laird and Albee, 1981; Moody et al., 1983). The occurrence of disseminated garnets in some of the metabasite sheets, and the compositional range of the amphiboles, hornblende to tschermakite, also indicate garnet to staurolite-kyanite zone metamorphic conditions (Harte and Graham, 1975; Laird and Albee, 1981; Moody et al., 1983).

Epidote can also be used as an indicator of peak metamorphism. Clinozoisite, present in the metabasites of the Middle River unit, can be stable up to 700°C under oxidizing conditions, in the presence of hematite and/or magnetite, at low to medium pressures (Liou, 1973), but it breaks down at considerably less than 700°C under more reducing conditions. Since the metabasites contain sphene and ilmenite rather than magnetite, epidote is probably stable up to 600-650°C at low to medium pressures (Liou, 1973; Liou et al., 1974; Moody et al., 1983), temperatures that concur with staurolite-kyanite zone conditions implied for the metabasite sheets.

The presence of staurolite in the pelitic schists north of Fourth Gold Brook is a good indicator of the

metamorphic conditions reached by these rocks. Studies by Richardson (1968), Hoschek (1969), Albee (1972), Baltatzis (1979) and Karabinos (in press) on staurolite-bearing pelitic rocks have shown that reactions leading to the formation of staurolite during progressive metamorphism include:

chlorite + muscovite = staurolite + biotite + quartz + H_2O (5)

in the case of rocks containing neither chloritoid or garnet (Hoschek, 1969);

chloritoid + Al-silicate (andalusite, kyanite) = staurolite + quartz + H_2O (6)

chloritoid + quartz = staurolite + garnet + H_2O (7)

in the case of more iron-rich compositions and the absence of biotite (Baltatzis, 1979);

chloritoid + chlorite + muscovite = staurolite + biotite + quartz + H_2O (8)

chloritoid + muscovite + quartz = staurolite + biotite + garnet + H_2O (9)

(Hoschek, 1969).

With the presence of chlorite and muscovite and isolated occurrences of chloritoid in the lower-grade metasedimentary rocks any one of these reactions could be responsible for the formation of staurolite. The problem is further compounded by the previous-

ly mentioned observation that staurolite is apparently pre-tectonic to the major foliation and appears to be breaking down to muscovite, biotite and quartz.

Kyanite, as with staurolite, appears to be pre-tectonic to the foliation of the schists and rarely breaks down to muscovite, biotite and quartz. The formation of kyanite in the high-grade rocks is therefore difficult to resolve.

Although kyanite and staurolite are rarely in contact with one another, with what appear to be gradational boundaries (Plate 24), the textural evidence for a reaction between the two minerals is inconclusive. Nonetheless, the possibility that kyanite resulted from the breakdown of staurolite does exist. Reactions involving the breakdown of staurolite to produce kyanite include:

staurolite + chlorite + muscovite = Al-silicate + biotite + quartz + H_2O (10)

at relatively low temperatures (Hoschek, 1969);

staurolite + muscovite + quartz = Al-silicate + biotite + H_2O (11)

at low and intermediate pressures (Hoschek, 1969); and

staurolite + quartz = Al-silicate + garnet + H_2O (12)

at relatively high pressures (Hoschek, 1969; Baltatzis, 1979). The combination of reactions (11) and (12) produces

Plate 24. Photomicrograph of a kyanite (ky) and staurolite (st) porphyroblast in a sample of high-grade metapelite. The contact between the two minerals appears gradational and may indicate that the two phases are linked through one of a number of possible metamorphic reactions listed in the text. (Magnification x25; plane polarized light.)

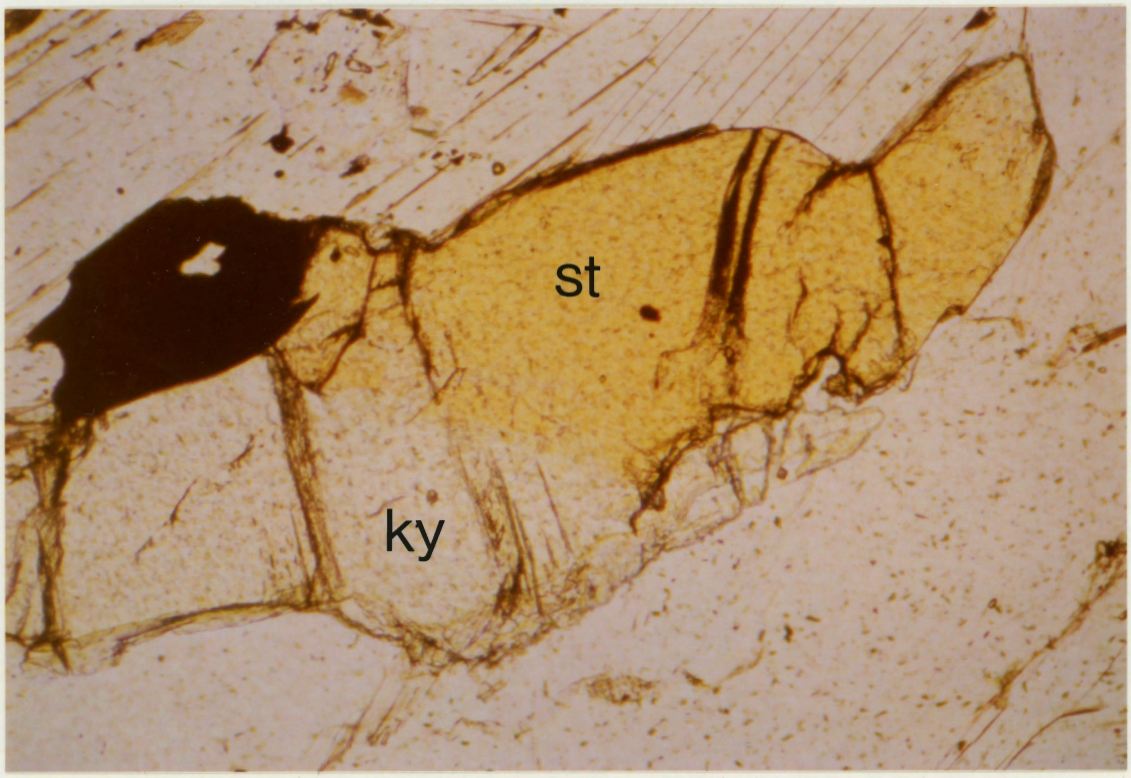
st
ky

a third reaction:

staurolite + muscovite + quartz = Al-silicate + biotite + garnet + H_2O (13)

that may take place at some intermediate pressure range (Hoschek, 1969). Alternative reactions, not involving the breakdown of staurolite, include:

Mg-rich chlorite + muscovite + quartz = kyanite + biotite + H_2O (14)

from Carmichael (1970) and

chlorite + muscovite = kyanite + phlogopite + quartz + H_2O (15)

from Bird and Fawcett (1973).

In an attempt to determine which reactions are responsible for the formation of the high-grade minerals, the mineral assemblages of the various metamorphic zones mentioned in section 7.2 are illustrated on Thompson AFM diagrams. When available, mineral analyses, listed in Chapter 6, and whole rock compositions, listed in Chapter 5, are included.

The assemblages CHL-MUSC-QTZ-BT or CHL-MUSC-QTZ-CHLTD characteristic of the biotite zone along Second Gold Brook are illustrated in Figure 7.2a. The appearance of garnet at the mouth of Second Gold Brook produces the garnet zone mineral assemblages CHL-MUSC-QTZ-BT-GNT or CHL-MUSC-QTZ-

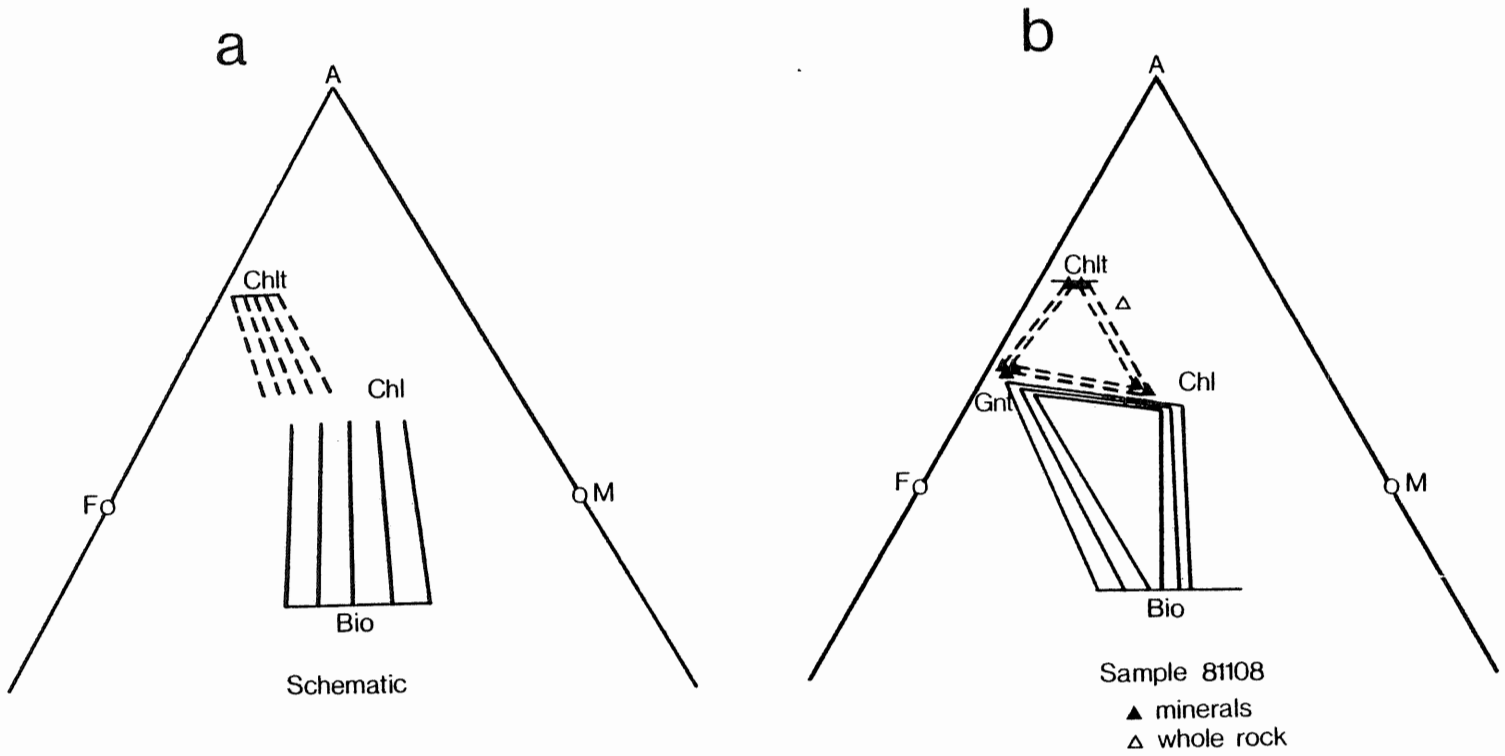

Figure 7.2 Thompson AFM diagrams for (a) mineral assemblages CHL-CHLT (dashed lines) or CHL-BT (solid lines), and (b) mineral assemblages CHL-CHLT-GNT (dashed lines) or CHL-BT-GNT (solid lines). Mineral analyses and bulk composition of sample 81108 are included in (b). The position of the bulk composition outside the mineral stability may reflect chemical disequilibrium or metasomatic alteration.

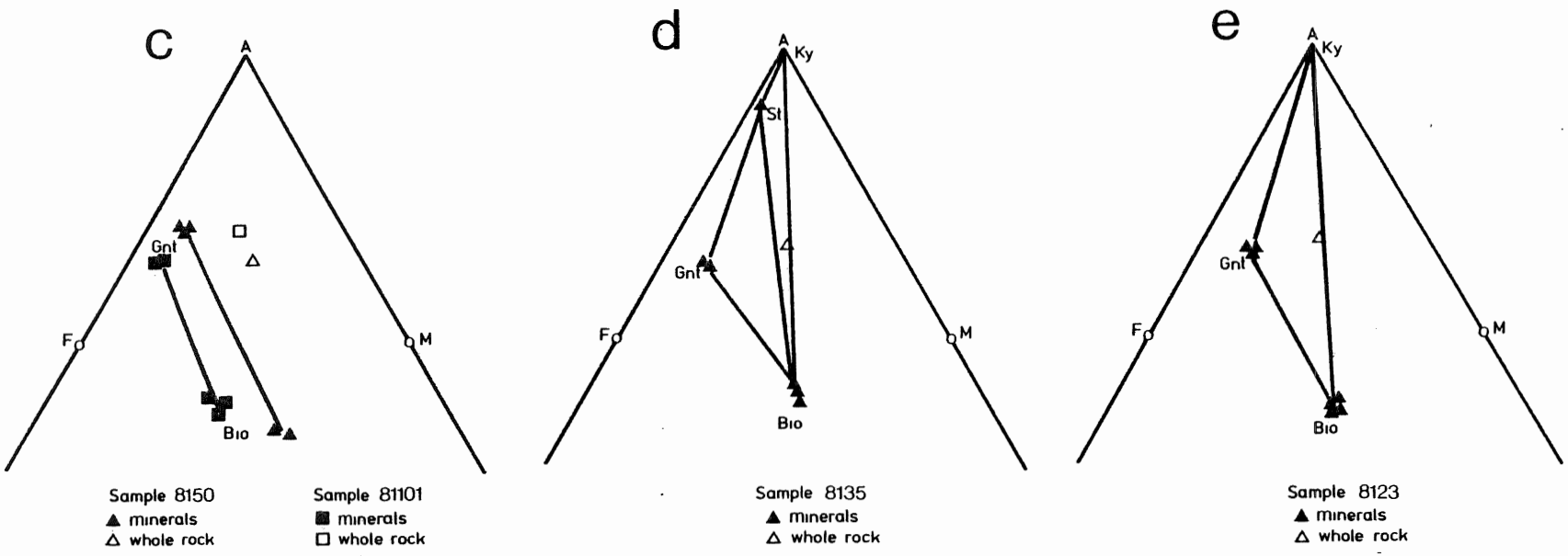

Figure 7.2 (continued) Thompson AFM diagrams for (c) mineral assemblage BT-GNT in sample 8150 and 81101, (d) mineral assemblage BT-GNT-ST-KY in sample 8135, and (e) mineral assemblage BT-GNT-KY in sample 8123.

CHLTD-GNT (sample 81108) shown in Figure 7.2b.

North of the metabasite sheets, on the other side of the postulated tectonic break, observed mineral assemblages include QTZ-MUSC-BT-PLAG-GNT (samples 8150 and 81101), QTZ-MUSC-BT-PLAG-GNT-ST-KY (sample 8135) and QTZ-MUSC-BT-PLAG-GNT-KY (sample 8123) represented in Figure 7.2c, 7.2d and 7.2e respectively.

Ideally, the whole rock compositions should plot somewhere within the field delineated by tie lines joining the various coexisting minerals in a particular assemblage, or on the tie line connecting "two-mineral" assemblages. In Figure 7.2b, the bulk composition of sample 81108 plots outside the stability field defined by chlorite-chloritoid-garnet but since both chloritoid and garnet have not reached textural equilibrium with the surrounding matrix. chemical equilibrium may not have been attained. Similarly, the bulk compositions of samples 8150 and 81101 do not plot on the tie lines joining their respective biotite-garnet pairs in Figure 7.2c. This discrepancy may be explained if the samples contain undetected kyanite, a possibility since both samples are located north of the staurolite-kyanite isograd. The addition of kyanite as a third phase would create stability fields that would include the bulk

compositions of the two samples. If the low- to medium-grade southern belt and the high-grade northern belt represent different slices from a single protolithic package, it may be assumed that the high-grade belt developed low- to medium-grade metamorphic minerals, similar to those presently observed in the low- to medium-grade rocks, during its progressive regional metamorphic evolution. With this assumption in mind, comparing Figure 7.2b and 7.2c reveals that the appearance of staurolite involves the breakdown of chlorite and chloritoid, indicating that reaction (8) may be responsible for the formation of staurolite.

The formation of kyanite cannot be resolved from the AFM diagrams. The presence of staurolite indicates that kyanite may have resulted from the breakdown of staurolite but the possibility that kyanite formed according to either reaction (14) or (15) remains.

The presence of staurolite as relict porphyroblasts in a few samples of high-grade metapelites can be useful in defining the peak P-T conditions reached by these rocks. The stability of staurolite plus quartz according to reaction (12) has been experimentally determined by Richardson (1968) at approximately 675°C. Similarly, the stability of staurolite + quartz + muscovite, reaction (11)

was established at 675 ± 15°C at 5.5 kb and 575 ± 15°C at 2 kb by Hoschek (1969). Thompson (1976) calculated the P-T curve of reaction (13) from data from Richardson (1968) and determined the upper stability of staurolite at approximately 675°C at 4 kb and about 700°C at 6 kb. However, Carmichael (1978) positioned the curve of reaction (13) about 130°C below that calculated by Thompson (1976) so that it would be consistent with the sequence and relative spacing of isograds, reflecting smooth regional pressure gradients, in well-documented metamorphic terrains. Carmichael (1978) acknowledges the inconsistency between his P-T coordinates for reaction (13) and available experimental data but nonetheless concludes that the apparently arbitrary placement of the reaction curve is consistent with a huge body of field data.

On the basis of the more concrete experimental data presented by Richardson (1968), Hoschek (1969) and Thompson (1976), coexistence of staurolite and kyanite as peak metamorphic index minerals in the pelitic rocks of the high-grade belt implies maximum temperatures between 650°C and 700°C and pressures of 6 to 8 kb. Approximate pressure-temperature paths for the progressive regional metamorphism of the pelitic assemblages of the low- to medium-grade and high-grade belts can be defined on the basis of reaction (1) for the formation of chloritoid,

reaction (8) for the development of staurolite, and, for reference, reactions (11), (12), (13) and (15) for the formation of kyanite, and by considering the following petrographic observations:

1. Cordierite is never present.
2. Kyanite is the dominant Al_2SiO_5 polymorph present and appears to represent the highest grade attained; sillimanite (fibrolite) occurs in minute amounts and may be metastable in the kyanite field rather than representing local higher-grade metamorphic conditions; andalusite is never present.

The partial retrograde breakdown of staurolite and kyanite to produce the dominant medium-grade assemblage biotite-muscovite-garnet reflects a re-equilibration of the high-grade rocks in the central belt to lower amphibolite facies conditions, converging on the lower amphibolite facies conditions of the metabasites in the low- to medium-grade southern belt.

The pressure-temperature paths obtained are schematically illustrated in Figure 7.3. The "return" path for the high-grade belt is also illustrated.

7.2.2 Geothermometry

In order to define more precisely the pressure-tempe-

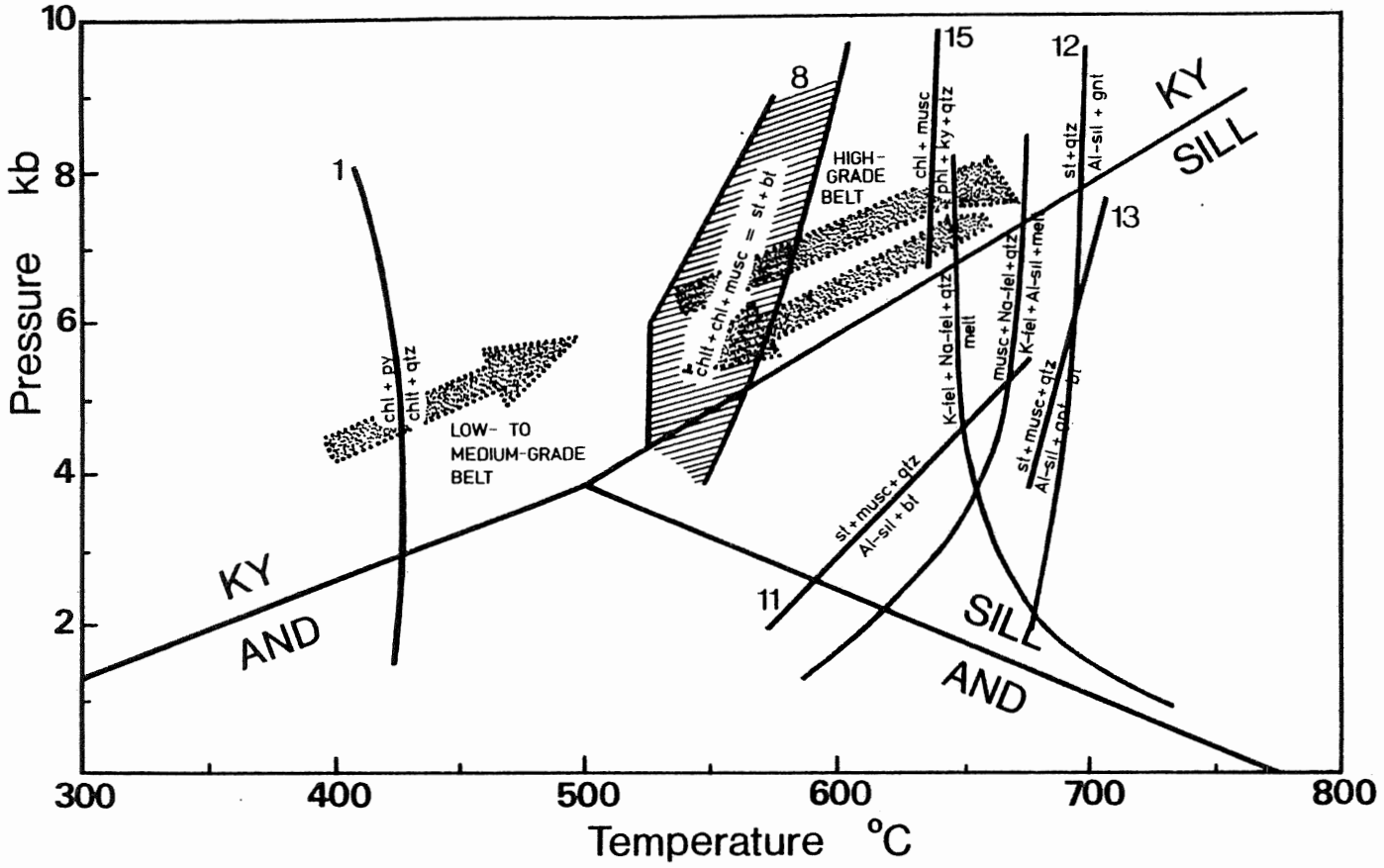

Figure 7.3 Approximate P-T paths of the low-to medium-grade and high-grade belts of the Middle River area. Triple point for the Al_2SiO_5 system according to Holdaway (1971). The reaction data are from the following sources: (1), (8) (occurring somewhere in the hachured area), (11) and (12) Hoschek (1969); (13) Thompson (1976); (15) Bird and Fawcett (A) Chatterjee and Johannes (1974); (B) Kerrick (1972).

rature conditions of metamorphism of the high-grade belt, data from selected mineral analyses from the marble layer and from pelitic schists of the Middle River unit are applied to calcite-dolomite and garnet-biotite geothermometers.

A. Calcite-Dolomite Geothermometry

The system $CaCO_3$-$MgCO_3$ has been the subject of many investigations (Graf and Goldsmith, 1955; Goldsmith et al., 1955; Goldsmith and Newton, 1969; Rice, 1977). The solubility of $MgCO_3$ in calcite has proven to be strongly temperature dependent and therefore can be used to determine the temperature at which magnesian calcite and dolomite equilibrated during regional metamorphism.

The calcite-dolomite geothermometers compiled by three different sources (Graf and Goldsmith, 1955; Goldsmith and Newton, 1969; Rice, 1977) are applied to samples from the thick dolomitic marble layer located along Middle River north of Sarach Brook. Four samples containing both calcite and dolomite (determined by staining and by electron microprobe analysis) were used. The mol percents $MgCO_3$ in calcite were calculated from microprobe data and are listed in Table 6.9. Temperatures of equilibration of coexisting calcite and dolomite were determined by using

the graphs of Graf and Goldsmith (1955) (Figure 7.4) and Goldsmith and Newton (1969) (Figure 7.5). A third set of temperatures was obtained using the equation

$$\log X^{CC}_{MgCO_3} = \frac{-1690}{T\ (^{o}K)} + 0.795$$

derived by Rice (1977) from a least square analysis of the combined data of Graf and Goldsmith (1955) and Goldsmith and Newton (1969). The temperatures obtained from all three methods are listed in Table 7.2.

The calculated temperatures cover a relatively wide range within any given geothermometer but the majority occur between 500°C and 600°C. The marble layer from which the four samples are taken is located north of the staurolite-kyanite isograd and should therefore reflect kyanite zone metamorphic temperatures, between 650°C and 700°C, mentioned previously. Results obtained from the three geothermometers do not agree with this temperature range but are consistently lower, some by as much as 200°C.

The lower temperatures may be explained when considering the apparent pre-tectonic nature of staurolite and kyanite with respect to the syntectonic biotite, muscovite and garnet assemblage. It is probable that the retrograde metamorphic conditions required for the breakdown of the high-grade minerals would produce a re-equilibration of

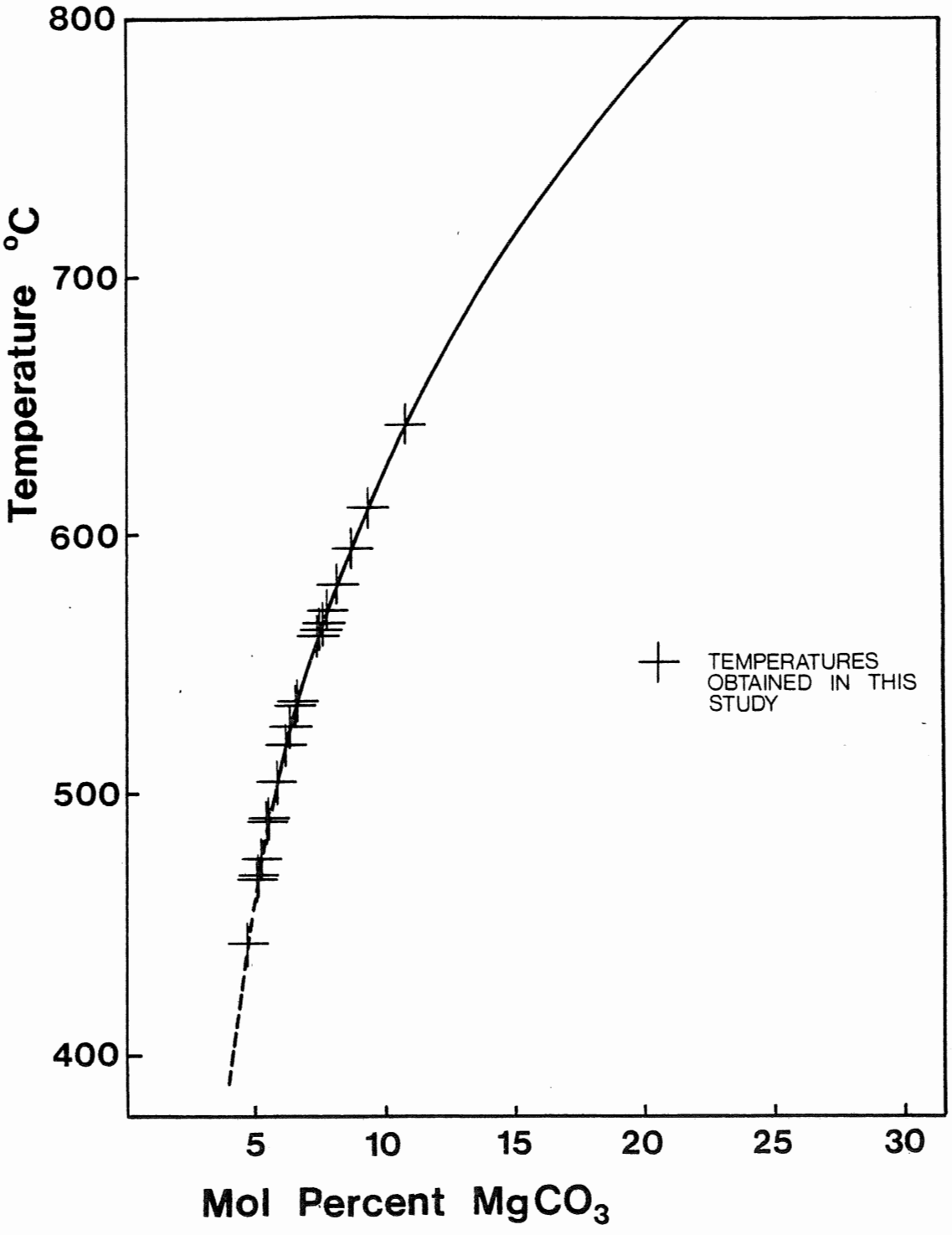

Figure 7.4 A portion of the exsolution curve in the system $CaCO_3$-$MgCO_3$, according to Graf and Goldsmith (1955). (Extrapolated below 500°C by this author.) The mol percent $MgCO_3$ are listed in Table 6.9 and the temperatures calculated, accurate to $\pm$ 25°C, are listed in Table 7.2.

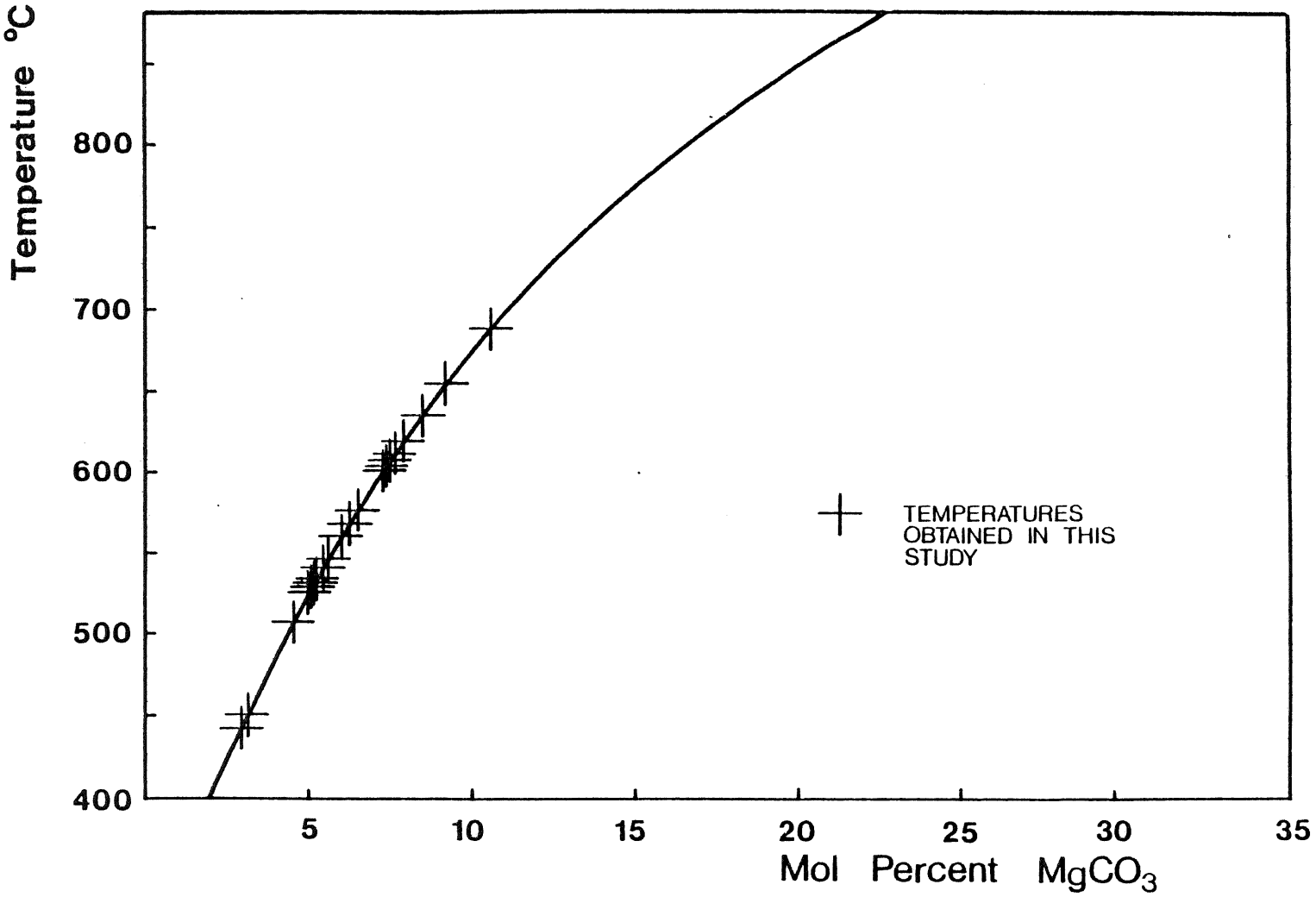

Figure 7.5 Unique polybaric calcite-dolomite soluus, according to Goldsmith and Newton (1969). The mid percent $MgCO_3$ are listed in Table 6.9 and the temperatures calculated, accurate to $\pm$ 25°C, are listed in Table 7.2.

TABLE 7.2

CALCULATED EQUILIBRIUM TEMPERATURES FROM CALCITE-DOLOMITE GEOTHERMOMETERS

		TEMPERATURES (°C)					
		GRAF AND GOLDSMITH (1955)		GOLDSMITH AND NEWTON (1969)		RICE (1977)	
SAMPLE NUMBER	NUMBER OF GRAINS	RANGE	AVERAGE	RANGE	AVERAGE	RANGE	AVERAGE
8145	10	467-584	524	536-628	574	545-622	579
8162	3	365-465	415	457-529	493	382-540	466
8251	5	466-640	558	530-692	610	541-686	612
8252	5	445-593	542	441-639	561	462-632	558

the amount of $MgCO_3$ in solid solution between coexisting calcite and dolomite, resulting in the lower equilibrium temperatures obtained, temperatures that are more consistent with the medium-grade syntectonic mineral assemblage of the surrounding metapelites.

B. Garnet-Biotite Geothermometry

Numerous studies have shown that the partitioning of iron and magnesium between coexisting garnet and biotite in an equilibrium assemblage can be used to determine the temperature at which they were last at equilibrium (Thompson, 1976; Goldman and Albee, 1977; Ferry and Spear, 1978). Of the numerous samples of pelitic schist containing both biotite and garnet, four widely separated samples were chosen on the basis of textural equilibrium between the two phases. All samples contain various concentrations of biotite, muscovite, quartz, plagioclase and garnet; in addition, samples 8135 and 8123 contain kyanite and sample 8135 contains staurolite. The four samples are located north of the staurolite-kyanite isograd.

The garnet-biotite geothermometers compiled by Thompson (1976), illustrated in Figure 7.6, Goldman and Albee (1977), shown in Figure 7.7, and Ferry and Spear (1978), represented in Figure 7.8, were applied to the four sam-

Figure 7.6 Plot of ln K_D against $1/T_K$ for the (Fe-Mg) exchange for coexisting garnet and biotite, according to Thompson (1976). Temperatures calculated, accurate to $\pm 25^{o}C$, are listed in Table 7.3.

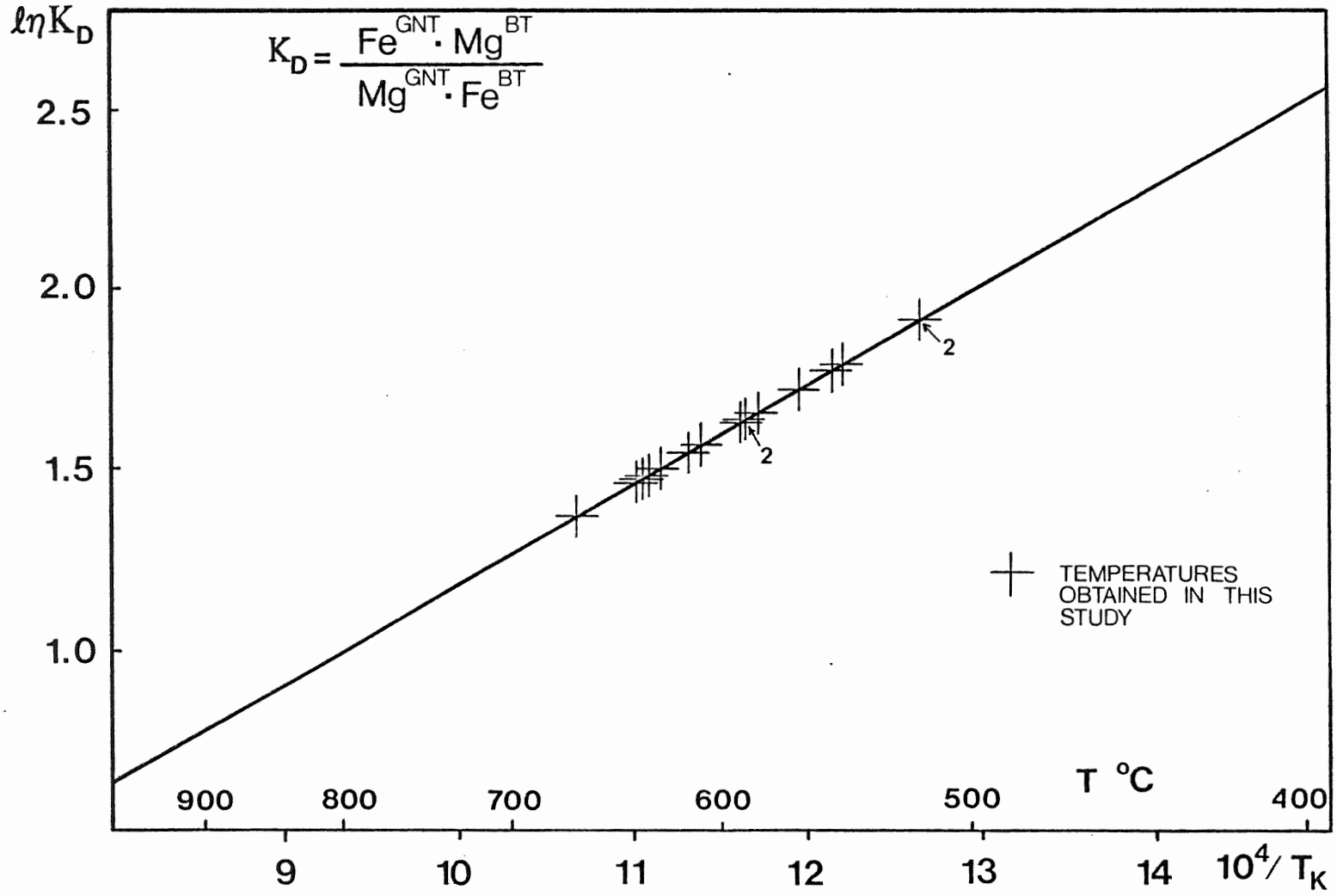
ln K_D
K_D = Fe^GNT · Mg^BT / Mg^GNT · Fe^BT
2.5
2.0
1.5
1.0
2
2
TEMPERATURES OBTAINED IN THIS STUDY
T °C
900
800
700
600
500
400
9
10
11
12
13
14
10^4/ T_K

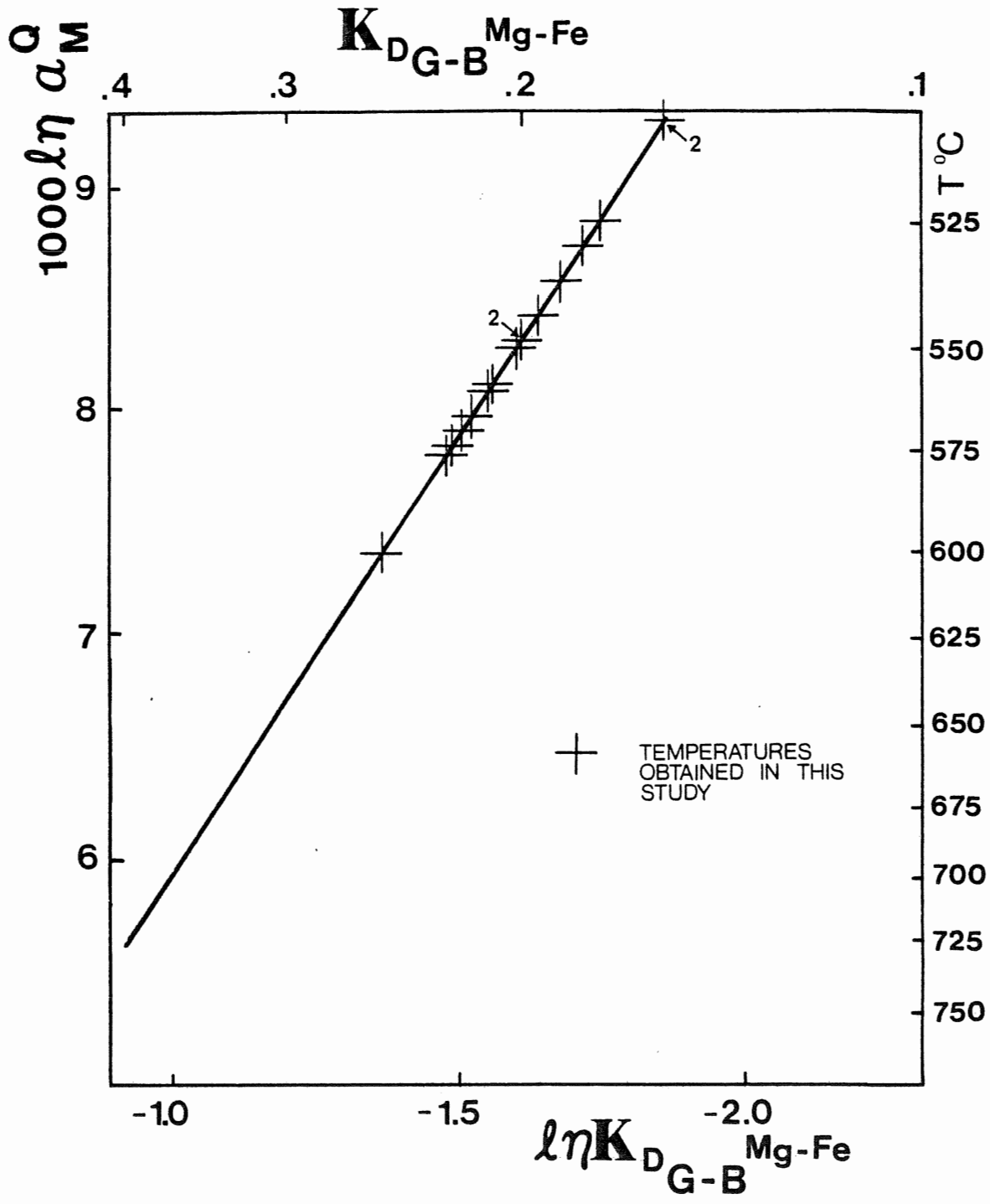

Figure 7.7 Isotopic and elemental partitioning to give an (Fe-Mg) exchange calibration between coexisting garnet and biotite, according to Goldman and Albee (1977). The temperatures calculated, accurate to ± 25°C, are listed in Table 7.3.

Figure 7.8 Ferry and Spear (1978) plot of $\ln K = \ln K\ (Mg/Fe)_{GNT}/(Mg/Fe)_{BT}$ versus $1000/T\ (^{\circ}C)$. For comparison, the Thompson (1976) and Goldman and Albee (1977) geothermometers are illustrated. The temperatures calculated, accurate to $\pm 25^{\circ}C$, are listed in Table 7.3.

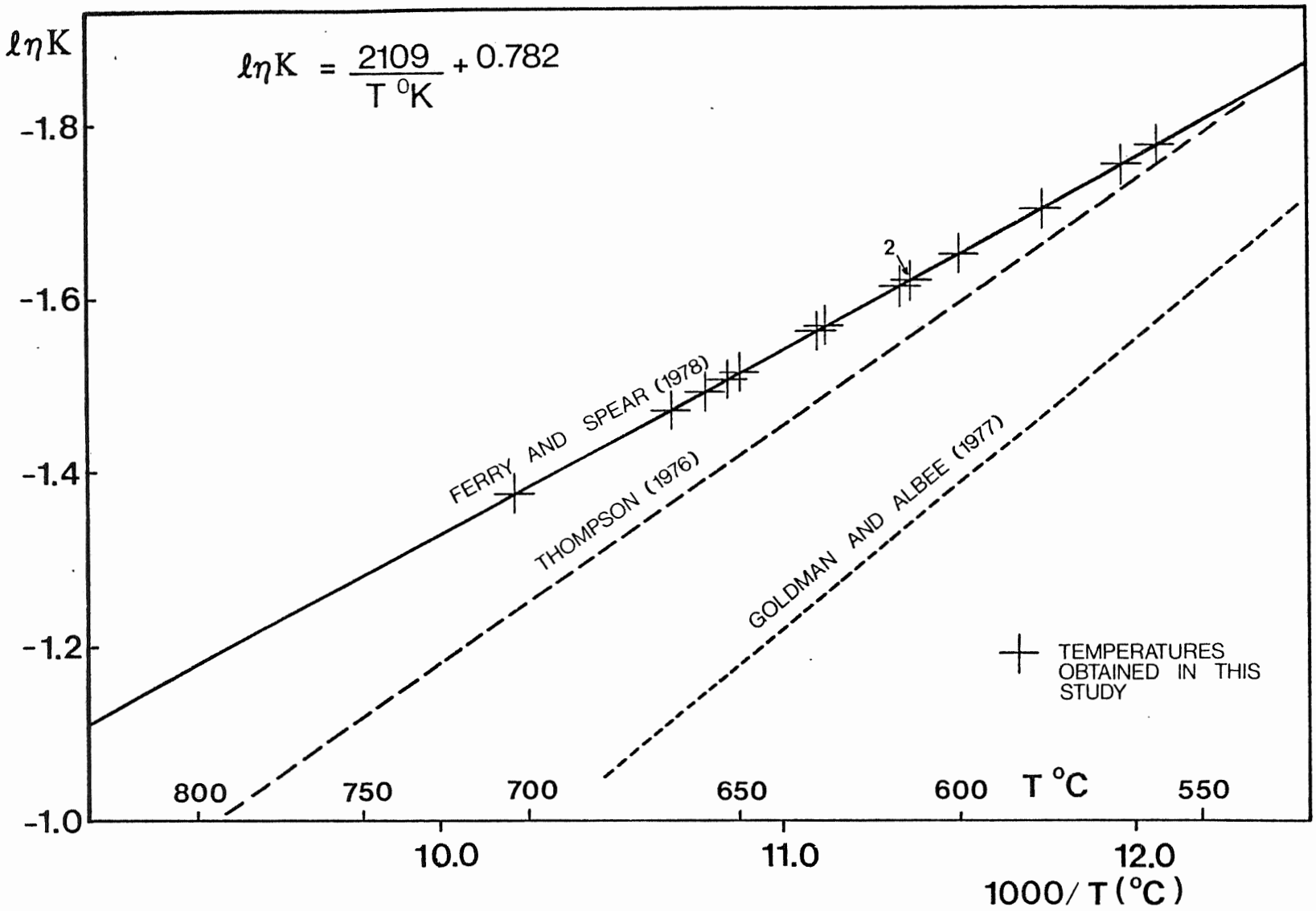
lnK
$\ln K = \frac{2109}{T\ ^{0}K} + 0.782$
-1.8
-1.6
-1.4
-1.2
-1.0
2
FERRY AND SPEAR (1978)
THOMPSON (1976)
GOLDMAN AND ALBEE (1977)
TEMPERATURES OBTAINED IN THIS STUDY
800
750
700
650
600
T °C
550
10.0
11.0
12.0
1000/ T (°C)

ples. The results are given in Table 7.3.

The apparent equilibrium temperatures obtained cover a relatively narrow range within any one of the three geothermometers and the majority are between 500°C and 600°C. Since Fe_2O_3 cannot be determined in biotite with the electron microprobe, Fe^T is used in determining K_D. The temperatures obtained must therefore be considered higher than the "true" equilibrium temperatures. Other factors which may have affected K_D include a number of compositional dependencies of the partitioning of Fe and Mg between garnet and biotite.

Goldman and Albee (1977) showed that, in garnet, K_D depends on the ideality of the Mg-Fe exchange, on the Mn and Ca content of the eight-fold position, and to a lesser degree on the amount of Fe^{+3} in the six-fold position, and that the Cr and Ti content may be important in some rocks. They also wrote that, in biotite, K_D depends not only on the ideality of the Mg-Fe exchange but also on the number of exchangeable Mg-Fe sites. Dallmayer (1974) indicated that increasing octahedral Ti, Al and Fe^{+3} would increase K_D, with Ti playing the most important role.

Ferry and Spear (1978), whose calibration was determined using synthetically produced garnets and biotites,

TABLE 7.3

CALCULATED EQUILIBRIUM TEMPERATURES FROM GARNET-BIOTITE GEOTHERMOMETERS

SAMPLE NUMBER	NUMBER OF GNT-BIO PAIRS	RANGE OF MOL mg/Fe GNT	RANGE OF MOL mg/Fe BIO	TEMPERATURES (°C) THOMPSON (1976) RANGE	THOMPSON (1976) AVERAGE	GOLDMAN AND ALBEE (1977) RANGE	GOLDMAN AND ALBEE (1977) AVERAGE
8135	1	.1186	.6096	-	594	-	544
8150	6	.1116 TO .11365	.7350 TO .7691	525-572	542	504-531	514
8123	8	.1160 TO .1592	.5924 TO .6709	561-669	619	524-600	563
81101	4	.0884 TO .0898	.4012 TO .4471	604-631	614	549-569	557

TABLE 7.3

CALCULATED EQUILIBRIUM TEMPERATURES FROM GARNET-BIOTITE GEOTHERMOMETERS - (CONTINUED)

TEMPERATURES (°C)

SAMPLE NUMBER	FERRY AND SPEAR (1978) RANGE	FERRY AND SPEAR (1978) AVERAGE	FERRY AND SPEAR (1978) $\frac{Ca+Mn}{Ca+Mn+Mg+Fe}$ GARNET	FERRY AND SPEAR (1978) $\frac{Al^{VI}+Ti}{Al^{VI}+Ti+Fe+Mg}$ BIOTITE
8135	-	599	.06	.21
8150	518-570	537	.47 TO .50	.17 TO .26
8123	559-704	634	.10 TO .14	.20 TO .32
81101	610-649	626	.12 TO .14	.21 TO .23

warned that caution should be exercised in applying their geothermometer to systems containing significant amounts of Ca, Mn or Ti. They noted that their calibration could be applied, without correction, for systems in which $(Al^{vi}+Ti)/(Al^{vi}+Ti+Fe+Mg) \leq 0.15$ in biotite and $(Ca+Mn)/(Ca+Mn+Fe+Mg) \leq 0.2$ in garnet. As can be seen in Table 7.3, the garnets of sample 8150 and the biotites of all four samples exceed the limits specified by Ferry and Spear (1978) to a degree clearly sufficient to invalidate results based on this technique.

Dallmayer (1974) and Goldman and Albee (1977) wrote that high calcium content in garnet reduces K_D, so that the calculated temperature is lower than the "true" equilibrium temperature.

Despite these drawbacks, a number of generalizations can be formulated:

1. Although the samples are widely separated geographically, the majority of equilibrium temperatures calculated are between 500°C and 600°C.
2. The temperatures are not consistent with the peak metamorphic assemblage of the high-grade pelitic rocks. Presence of staurolite and kyanite in some of the samples examined should indicate temperatures between 650°C and 700°C, as mentioned previously.

3. The temperatures closely parallel those obtained using calcite-dolomite geothermometers on the marble layer located in the midst of the four pelitic schist sample sites.

The discrepancy between the garnet-biotite equilibrium temperatures calculated and those postulated by the mineral assemblage can be resolved if the garnets and biotites (and muscovites) postdate the staurolites and kyanites or re-equilibrated during a retrograde metamorphic "event".

7.3 ORIGIN OF THE MIGMATITES AND PEGMATITES

Migmatites and pegmatite veins and pockets first appear in the high-grade pelitic and semipelitic schists and gneisses north of Fourth Gold Brook. Although its concentration increases toward the north as the granitic rocks of the Egypt Highland unit are approached, migmatite is not observed in the Egypt Highland unit itself, a further indication that the granitic rocks are not "granitized" paragneisses but deformed plutonic rocks. Similarly, very little pegmatite is detected in the Egypt Highland unit, instead, pegmatite is dominant along the lower sections of Sarach and Bothan brooks.

The thin leucosomes in the migmatites are composed of fine-grained quartz and plagioclase, are commonly concordant with the gneissossity and rarely ptygmatically folded across the foliation of the rock. The larger pegmatites, composed of fine- to medium-grained quartz, plagioclase and minor microcline, with or without coarse muscovite books, are parallel to or cut across the foliation. Although the pegmatite veins are only slightly deformed, sericitic alteration of the plagioclase is extensive. However, albite twinning is commonly preserved and optical determination shows that the plagioclase has compositions in the oligoclase range.

Four possible mechanisms can be envisioned for the development of the thin leucosomes and the larger pegmatites: in situ partial melting of the parent rock or anatexis, metamorphic segregation, igneous injection of granitic magma from outside, and "external metasomatism" involving the infiltration of a fluid from an external source into the rock (Yardley, 1978).

The peak metamorphic temperatures suggested previously (approximately 650°C to 700°C) appear to be sufficiently high for anatexis to have occurred according to "wet" melting of muscovite-bearing pelites (Tracy, 1978; Thompson and Tracy, 1979; Thompson, 1982). However, the absence

of potassium feldspar in the rocks of the Middle River unit indicates that these "granitic melting" reactions may not be applicable to the rocks of the high-grade belt. Hoschek (1976) required temperatures greater than 700°C for the experimental partial melting of biotite-plagioclase (An 50)-quartz mixtures more or less representative of the felsic gneisses of the Middle River unit. Similarly, Chatterjee and Johannes (1974) indicated that the curve of the reaction

$$\text{muscovite} + \text{Na-feldspar} + \text{quartz} = \text{K-feldspar} + Al_2SiO_5 + \text{melt} \qquad (16)$$

was located at about 675°C between 4-6 kb.

Anatectic reactions invoqued by Hoschek (1976) and Chatterjee and Johannes (1974) produce potassium feldspar as an important component in the liquid phase yet no potassium feldspar is observed in the thin leucosomes and only minor amounts of microcline are detected in the pegmatites. Mehnert (1968) wrote that in situ partial melting of the parent rock (venetic metatexis) should produce a melanosome or restite revealed as mafic rims surrounding the leucosome. Mafic rims are rarely observed adjacent to the leucosomes in the migmatites of the Middle River unit and are not detected near the larger pegmatite veins and pockets. On the basis of this evidence, it appears unlikely that the thin leucosomes and larger pegmatites were derived

from in situ partial melting.

Metamorphic segregation, either from within the rock ("internal metasomatism") or with the introduction of fluid from outside the rock ("external metasomatism") (Yardley, 1978), appears to be the most likely process responsible for the development of the migmatites. Conversely, although pegmatite veins and pockets could be the result of metamorphic segregation, it is improbable that such a mechanism could produce the large amounts of granitic material dominating the lower sections of Sarach and Bothan brooks, where pegmatite commonly makes up 75 percent of the rock. Presumably, these large, essentially undeformed, pegmatites were intruded from outside the Middle River area. The pegmatites are unrelated to the granitic rocks of the Egypt Highland unit since the latter are rarely cut by pegmatite dykes and are strongly deformed. The pegmatites are probably not related to the Bothan Brook granodiorite but lack of crosscutting relationships precludes the definition of such association.

Macdonald and Smith (1980) indicated that microgranites, aplites and pegmatites, occurring as sheets, lenses, boudins and ptygmatically folded layers in the gneisses of the Cape North Group, could best be described

as a lit-par-lit injection complex. Conversely, metamorphic segregation has been invoked by Craw (in press) to explain quartz-plagioclase leucosomes in the Cheticamp River high-grade rocks while crosscutting syntectonic granitic dykes are presumed to have been intruded from outside the area.

From the evidence presented, it is concluded that metamorphic segregation is likely responsible for the migmatites, while large pegmatite dykes were probably intruded into the Middle River rocks from outside the area.

7.4 TIMING OF METAMORPHISM

In an attempt to determine the absolute age of the metamorphism of the Middle River complex, hornblende and biotite separates were obtained from the least altered metabasite sample for $^{40}Ar/^{39}Ar$ dating. Since hornblende has a higher blocking temperature than biotite, the ages of coexisting hornblende and biotite phases should provide an indication of the rate of cooling of the sequence during post-metamorphic uplift.

Sample 81120 is from a metabasite sheet in the high-

grade pelitic and semipelitic gneisses located in the upper reaches of the southern branch of Ryan Brook. The metabasite contains fine- to medium-grained xenoblastic and rarely subidioblastic tschermakitic hornblendes that are slightly to moderately fractured; fine- to medium-grained subidioblastic to xenoblastic brown biotite flakes that contain a few minute zircon inclusions; minor quartz and plagioclase of andesine composition; and accessory sphene, ilmenite and apatite.

The hornblendes and intergranular biotites are preferentially aligned and produce a slight foliation in the rock concordant with the gneissossity of the surrounding metasedimentary rocks. Retrograde alteration is restricted to a very slight sericitization of plagioclase along grain boundaries and cleavage planes.

Although the hornblendes may have formed as a result of the medium-grade metamorphic conditions associated with the second phase of deformation, which produced the principal foliation (S_{MR2}), based on the fractured appearance of the hornblende grains, it appears more likely that the hornblendes formed during the medium- to high-grade metamorphism associated with the first phase of deformation and re-equilibrated during D_2. Conversely, although the present population of biotites may represent a relict

phase from D_1, based on the relatively fresh appearance of the biotite flakes it appears more likely that they represent a second generation phase formed during D_2.

The age spectra obtained at Dalhousie University in 1983 are illustrated if Figure 7.9. The spectrum for biotite gives a mean age of 377 ± 9 Ma for the portion of the plot between 3 and 98 cumulative percent ^{39}Ar released. The spectrum for hornblende gives a mean age of 386 ± 9 Ma for the protion of the plot between 18 and 97 cumulative percent ^{39}Ar released.

Speculation as to the meaning of the ages of cooling obtained hinges on the possibility that thermal effects associated with the Acadian orogeny, which the ages reflect, were sufficiently high to reset both the biotite and hornblende radiometric ages. Absolute ages of 401.3 ± 12.9 Ma for the West Branch North River monzogranite and 401 ± 44 Ma for the Muskrat Brook mylonite zone (Jamieson and Doucet, 1983), located a few kilometers south of the study area, indicate that plutonism and deformation occurred in the area at the time. However, as discussed in Chapter 3, the West Branch North River monzogranite appears to be in fault contact, at least locally, with the metamorphic complex and its effect on the rocks of the Middle River unit is questionable.

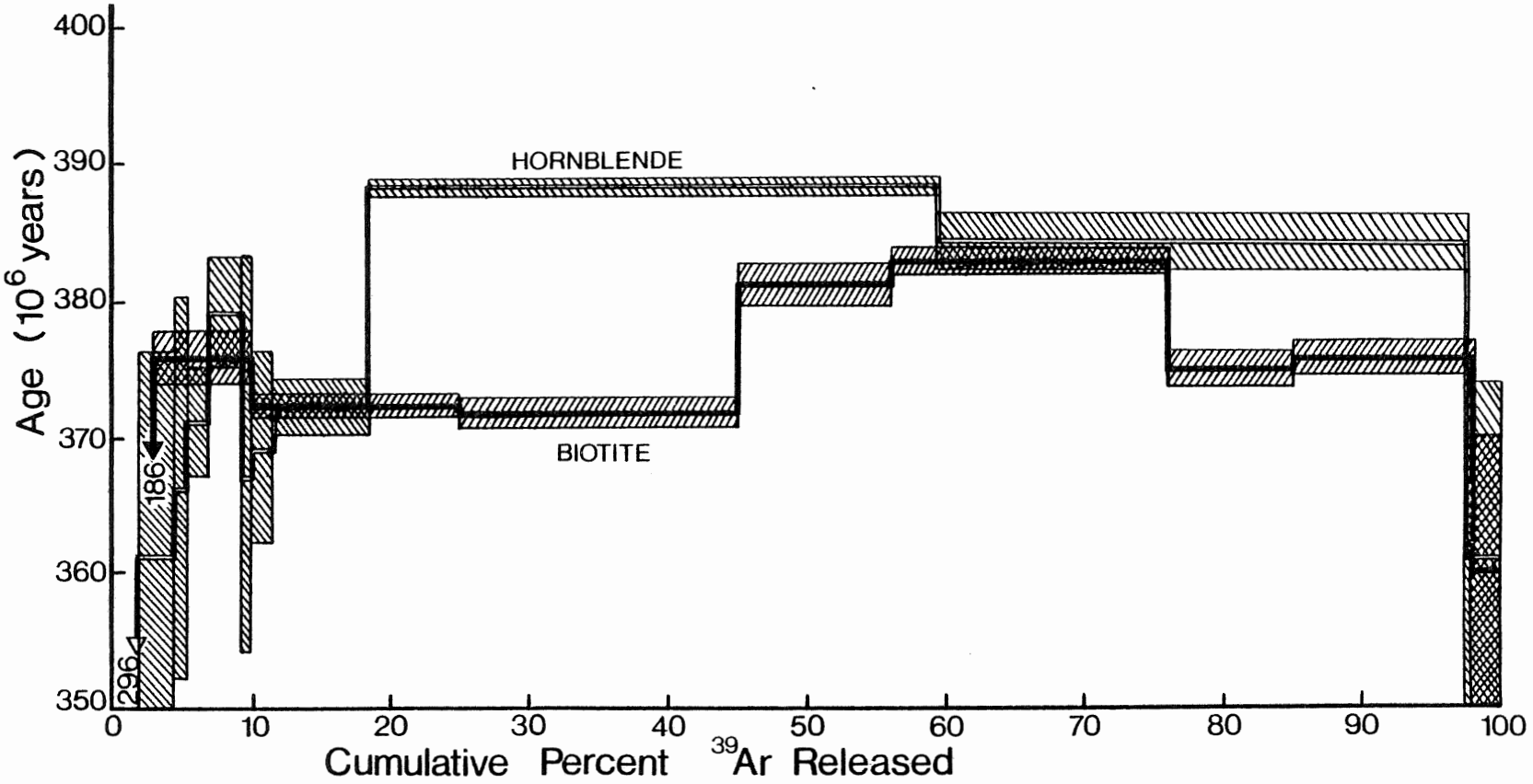

Figure 7.9 Age spectra obtained from $^{40}Ar/^{39}Ar$ radiometric dating for hornblende and biotite from metabasite sample 81120. Ages obtained are 377 ± 9 Ma for biotite and 386 ± 9 Ma for hornblende.

Similarly, it is unlikely that the deformation associated with the Muskrat Brook shear zone would be sufficiently widespread to greatly influence the Middle River complex.

The Bothan Brook granodiorite apparently cuts the Middle River complex. Although it resembles Cambrian granites found elsewhere in northern Cape Breton (Jamieson and Doucet, 1983) its age is not known. As discussed in Chapter 3, although the granodiorite appears to intrude the Middle River unit, the contact may be a fault, an extension of the fault separating the West Branch North River monzogranite from the Egypt Highland unit. The absence of any detectable contact metamorphic aureole in the metasedimentary rocks near the Bothan Brook intrusion, coupled with the possibility of a fault contact, reduces the possible effects of the granodiorite on the Middle River complex.

The Sarach Brook mylonite zone cuts, and thus post-dates, the Bothan Brook granodiorite and the West Branch North River monzogranite and may be younger than or contemporaneous with the Muskrat Brook mylonite zone. The effects of the Sarach Brook shear zone on the two intrusions are apparently restricted to a narrow band and consequently, its effects on the Middle River complex were probably not substantial enough to affect the radiometric

ages.

Even though small pegmatite veins and pockets are found along the southern branch of Ryan Brook, pegmatite does not occur within about 50 meters of the outcrop where sample 81120 was taken, and since contact metamorphic effects are not observed in the metasedimentary rocks near the margins of the pegmatites it appears unlikely that, if the pegmatites are indeed of intrusive origin, their intrusion could have affected the radiometric ages.

Therefore it appears that the more or less concordant ages obtained, 377 ± 9 Ma for biotite and 386 ± 9 Ma for hornblende, were not reset through hydrothermal alteration and reflect the timing of the cooling of the sequence during uplift following the medium-grade regional metamorphism associated with the second phase of deformation. The ages thus apparently ascribe D_2 to the Middle Devonian Acadian orogeny.

7.5 RELATIONSHIP BETWEEN METAMORPHISM AND DEFORMATION

The relative timing of the metamorphic and deformational events that have affected the Middle River complex is illustrated schematically in Figure 7.10.

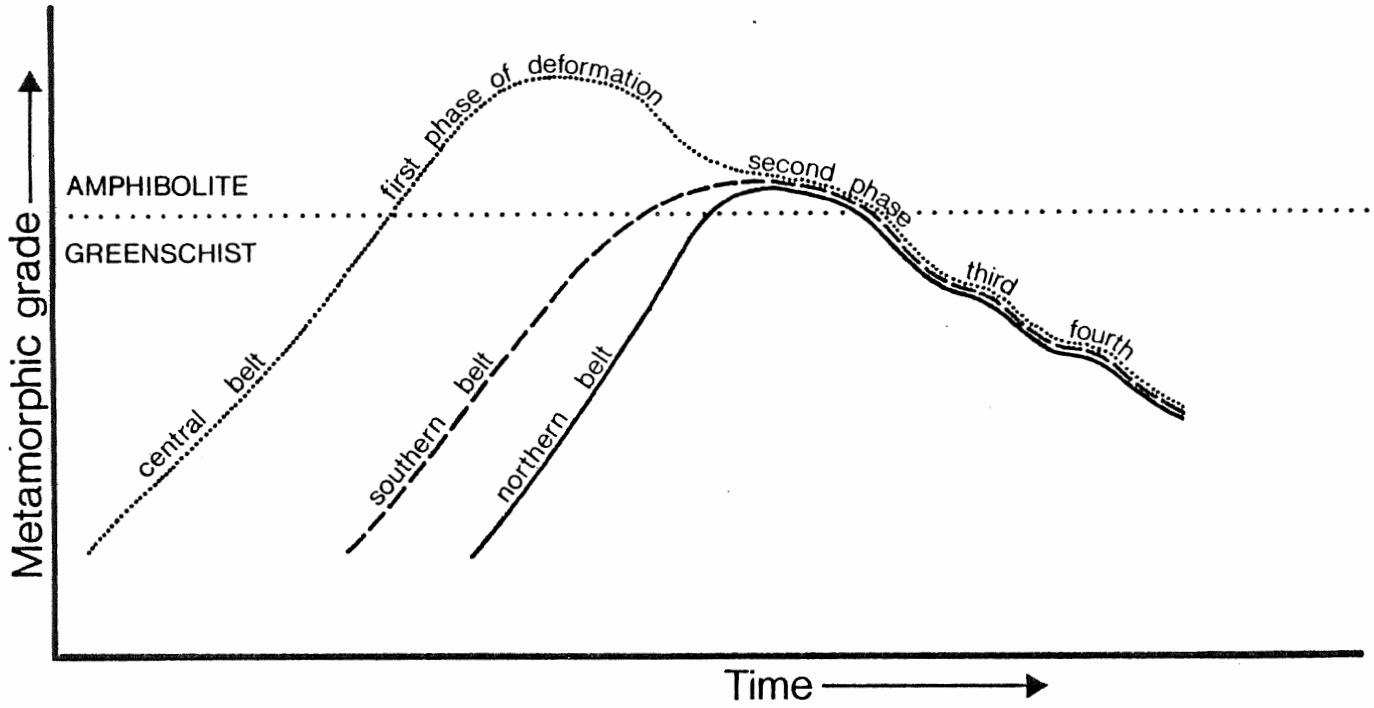

Figure 7.10 Inferred relative timing of metamorphism and deformation of the Middle River complex.

The data presented in this study show that the peak of metamorphism in the high-grade central belt, represented by relict staurolite and kyanite porphyroblasts, is pre-tectonic to the formation of the principal fabric S_{MR2} during D_2 and is therefore tentatively ascribed to the first phase of deformation, D_1, and the development of the relict isoclinally folded schistosity S_{MR1}. The absolute age of the first phase of deformation is not known but is certainly pre-Middle Devonian and may be as early as Late Precambrian if the rocks belong to the George River Group.

The peak metamorphic conditions in the southern belt, indicated by the lower amphibolite facies assemblage in the metabasites, the development of the overprinting biotite-muscovite-garnet mineral assemblage and the principal foliation in the central belt, and the deformation of the granitic rocks of the Egypt Highland unit in the northern belt, all associated with the "stacking" of the three belts, are ascribed to D_2, apparently occurring during the Middle Devonian Acadian orogeny.

Retrograde metamorphic effects, including chloritization of biotites and hornblendes and sericitization and hematization of feldspars, are widespread and apparently associated with numerous small- and large-scale shear

zones and faults. The absolute ages of the faulting and shearing are not known but they are probably Middle Devonian or younger.

7.6 SUMMARY

The data presented in this chapter can be summarized as follows:

1. The grade of metamorphism in the southern belt increases northward from the biotite zone along Second Gold Brook to the staurolite-kyanite zone in the vicinity of Fourth Gold Brook. The peak metamorphic conditions are represented by the mineral assemblage hornblende-plagioclase of oligoclase to andesine composition-epidote.
2. The grade of metamorphism in the central belt reached the kyanite zone, with P-T conditions in the range of 650°C to 700°C, but staurolite and kyanite porphyroblasts from the peak conditions are overprinted by the lower amphibolite facies assemblage muscovite-biotite-garnet.
3. Calcite-dolomite geothermometers, applied to the marble layer along Middle River north of Sarach Brook, and garnet-biotite geothermometers, applied to widely separated pelitic rocks from the high-grade central belt, gave equilibrium temperatures in the range of

500°C to 600°C, reflecting the "retrograde" lower amphibolite facies metamorphic conditions rather than the postulated peak conditions.

4. $^{40}Ar/^{39}Ar$ dating of coexisting hornblende and biotite mineral phases from a metabasite sample collected in the high-grade belt produced more or less concordant ages of 386 ± 9 Ma and 377 ± 9 Ma respectively.
5. The ages apparently reflect the timing of the cooling of the sequence during uplift following the medium-grade regional metamorphism associated with the second phase of deformation responsible for the development of the major foliation of the rocks in the study area. The ages thus appear to ascribe D_2 to the Middle Devonian Acadian orogeny.

Although the age of metamorphism of the sequence is apparently Middle Devonian, the absolute age of deposition of the rocks is not known and the entire Middle River complex may indeed be of Late Precambrian age and correlative with the George River Group.

CHAPTER 8

ECONOMIC GEOLOGY

8.1 INTRODUCTION

A detailed study of economic mineralization is considered beyond the scope of the present investigation. The objectives of the following chapter are therefore limited to a brief description of the two principal occurrences of economic mineralization in the study area: gold and minor sulphides in Second Gold Brook and copper in Nile Brook; and to report findings obtained from diamond drill holes and a number of geochemical and geophysical surveys carried out in the area in the recent past.

8.2 SECOND GOLD BROOK GOLD MINE

8.2.1 History, Development and Production

The following information is taken from Alcock (1932) and Holbrooke (1962).

Although gold in the Middle River area is first mentioned in the literature in the early 1860's, not much was done, beyond trenching, until 1906 when the

property was acquired by the Great Bras d'Or Mining Company. The company developed the principal vein, known as the Lizard vein, using extensive surface trenching and underground work, illustrated in Figures 8.1 and 8.2, on five levels on either side of the brook. Production began in 1907 and continued until early 1915 when operations ended because of World War I. Table 8.1 shows the production from these early operations. The average recovery was 0.274oz per ton although the recovery could not have been better than 70 percent considering the arsenical nature of the ore processed.

Besides the Lizard vein, there are two other mineralized zones running approximately parallel to the principal vein, one on each side. The Big Micmac lies a short distance to the south of the Lizard, the Little Micmac lies to the north.

8.2.2 Recent Work

Even though the Second Gold Brook property has basically remainded idle since the beginning of World War I, when gold production ceased, a number of companies have carried out sporadic exploration in the area since that time.

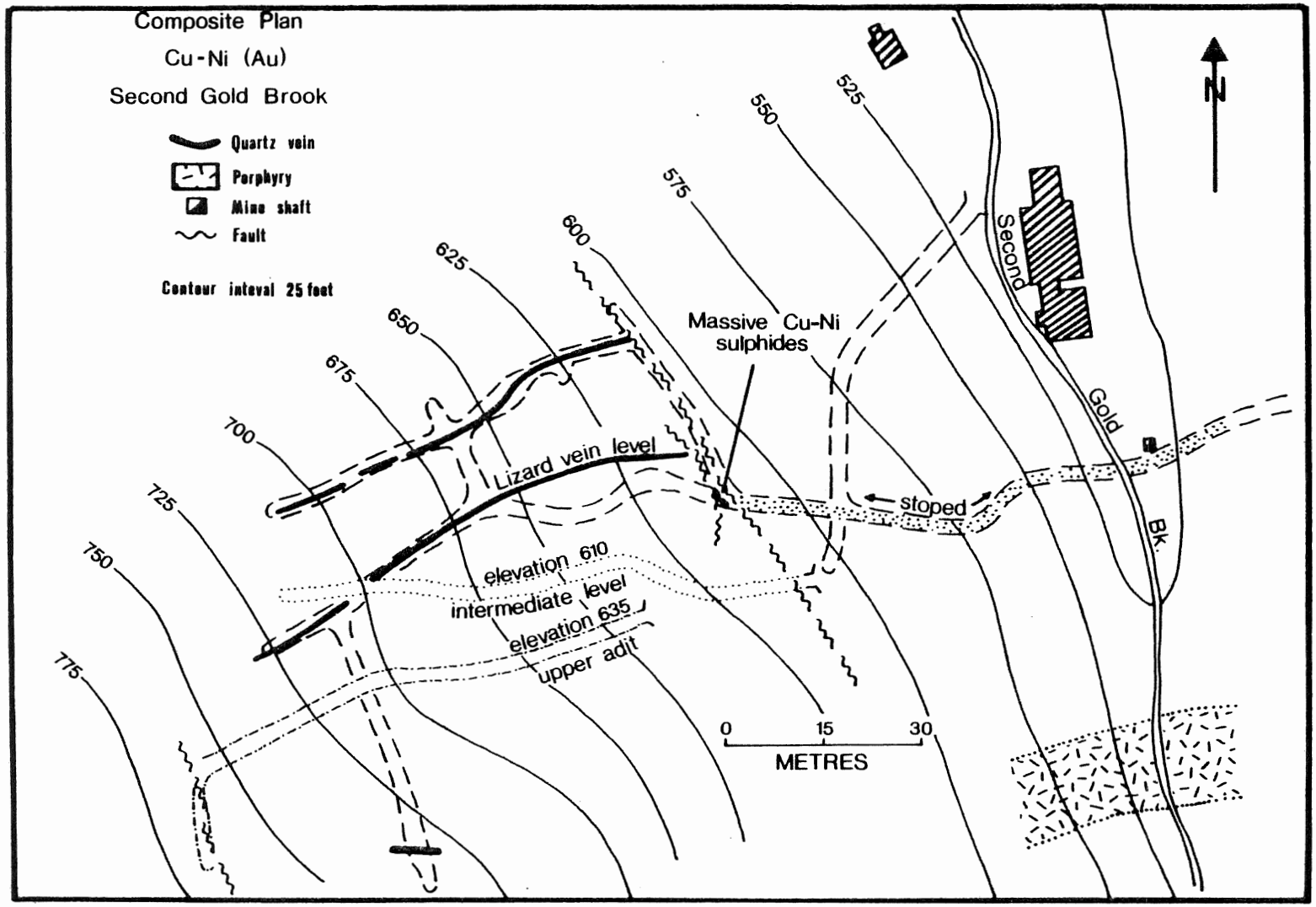

Figure 8.1 Plan section of underground workings of the Second Gold Brook gold mine (from Chatterjee, 1980).

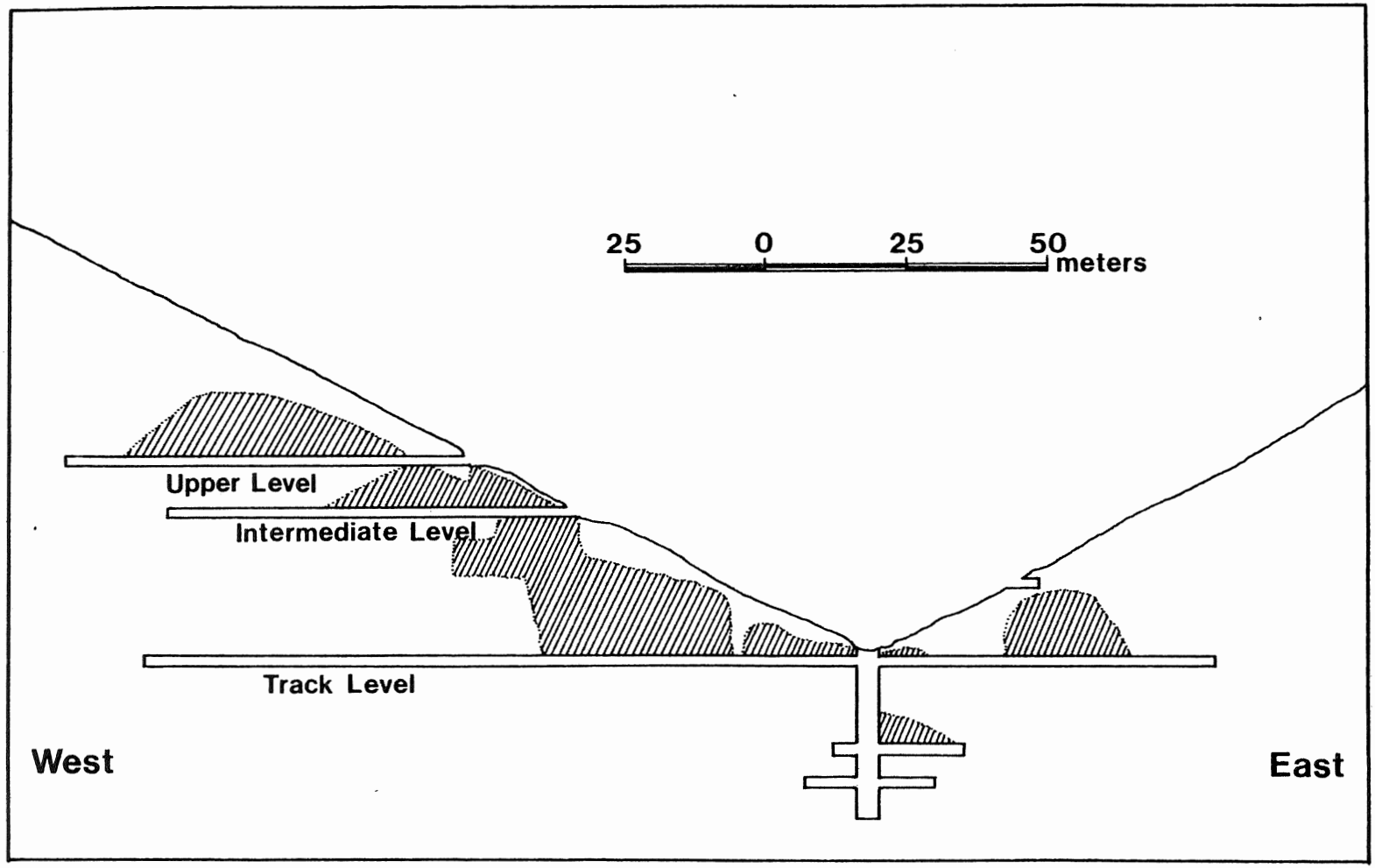

Figure 8.2 Vertical projection of underground workings on the Lizard vein; stoped areas are indicated by diagonal ruling (from Alcock, 1932).

TABLE 8.1

GOLD PRODUCTION

AT THE SECOND GOLD BROOK GOLD MINE

(From Holbrooke, 1962.)

YEAR	GOLD RECOVERED (ounces)	TONS MILLED
1908	609.5	2800
1909	700.0	1783
1910	30.2	336
1911	23.2	125
1914	262.8	775
1915	47.2	274
	1672.9	6093

In 1955, Cape Breton Metals Limited did an electromagnetic survey over the region and recovered about 500 meters of diamond drill core to investigate base metal possibilities in the vicinity of the mine. The rough terrain made interpretation impossible and the project was abandoned (Holbrooke, 1962). During 1967, Sullico Mines Limited carried out electromagnetic, induced polarization and resistivity surveys over a portion of Second Gold Brook. Two weak anomalous zones were located by the induced polarization survey and, as a result of these findings, Sullico drilled two diamond drill holes over the highest anomaly located 350 meters east of the mine shaft. The deepest hole reached a depth of 72 meters and encountered only pyrite mineralization. It was concluded that the drilling did not encounter a possible source for the anomaly.

During the months of December 1969 and January 1970, the entrance to the main level was retimbered to permit access to a small section of the adit for close examination and sampling of the sulphide mineralization (Bingley, 1970). Two geochemical soil surveys were carried out along Second Gold Brook in 1976 to determine if arsenic could be used as a pathfinder element for arsenical gold mineralization. Findings revealed a sudden increase in arsenic over the host metasedimentary rocks (Johnson,

1976). In 1981 and 1982, Dome Exploration drilled a number of diamond drill holes on the eastern flank of the brook valley, less than 100 meters from the mine shaft, but the results are unknown to this author.

8.2.3 Geology and Structure

The area is underlain by the greenschist facies metasedimentary schists and phyllites of the Middle River unit which strike east-west and dip from 35 to 50 degrees to the north. The metaconglomerate layer occurs along Second Gold Brook about 65 meters north of the mine shaft. A fine-grained quartz porphyry sill, about 20 feet (6 m) thick, reportedly occurs along Second Gold Brook 150 feet (45 m) south of the shaft (Alcock, 1932; Milner, 1936; Holbrooke, 1962). The sill is described as pale pink and shows small phenocrysts of quartz and feldspar (orthoclase and acid plagioclase) in a finely crystalline groundmass of quartz and feldspar (Alcock, 1932). Johnson (1970) reported the presence of an altered diorite sill occurring on the east side of the valley. The sill is about 45 feet (15 m) thick, strikes east-west, dips 37 degrees north, and lies approximately 50 feet (16 m) "above" the quartz porphyry sill (Johnson, 1970). The quartz porphyry sill did not attract the attention of this author and was probably categorized with numerous

other "quartzites" (mineralized quartz veins, felsic tuffs) found in the immediate vicinity of the mine. The diorite sill was not observed.

The major structural features of the area have been discussed in Chapter 3. Alcock (1932), Milner (1936) and Holbrooke (1962) described a cross fault visible in the main level 48 feet (15 m) west of where the adit joins the drift. The fault has displaced the Lizard vein and the quartz porphyry sill about 25 feet (8 m) to the right. The fault strikes northwest and dips 35° east (Holbrooke, 1962). Milner (1936) mentioned three minor faults also on the main level, each having a displacement of less than 1 foot (30 cm).

8.2.4 Mineralization

The mineralized veins are made up of stringers of white quartz that follow the structural trend of the enclosing schists and phyllites. The quartz has a weak pyrite mineralization and shows visible gold while the wallrocks are strongly mineralized by pyrite and arsenopyrite (Holbrooke, 1962). The Lizard vein pinches and swells from 1 inch (2.5 cm) to over 6 feet (2 m) in width, with an average of 3.6 feet (1.1 m), and varies in dip from vertical to nearly horizontal (Holbrooke,

1962).

The Big Micmac zone occurs along Second Gold Brook some 280 feet (85 m) south of the mine shaft. The quartz-bearing zone, about 20 feet (6 m) wide, is made up of quartz lenses up to 22 inches (55 cm) thick (Alcock, 1932). Assay results gave only a trace of gold and a trace of silver. The Little Micmac zone occurs 150 feet (46 m) north of the shaft. It is an irregularly shaped body dipping at a shallow angle to the northeast (Alcock, 1932).

Sulphide mineralization, both massive and disseminated, has also been observed in the underground workings. Bingley (1970) and Johnson (1970) described a massive nickeliferous pyrrhotite and chalcopyrite lens, about 10 feet (3 m) long and up to 2 feet (60 cm) thick, occurring along the main level (see Figure 8.2). Johnson (1970) also mentioned disseminated pyrrhotite and chalcopyrite mineralization in the surrounding wallrock.

8.2.5 Metallogenesis

Hypotheses pertaining to the origin of the gold and sulphide mineralization at Second Gold Brook are conspicuously absent from the literature. Holbrooke (1962)

indicated that the quartz porphyry sill may have had some influence on the formation of the Lizard vein. Johnson (1970) proposed the following sequence of events for the formation of the sulphide mineralization:

- Emplacement of the diorite sill containing syngenetic copper-nickel minerals.
- Faulting, and associated folding, with the emplacement of the granite pluton to the southeast (Bothan Brook granodiorite) causing remobilization of the sulphides into lens-shaped bodies along the footwall of the diorite sill.
- Later vertical strike faulting displacing the massive sulphide and channelling the auriferous solutions into veins along both the footwall and hanging wall of the sill and in open fractures into the massive sulphide lenses.

If the quartz porphyry sill is in fact a felsic tuff layer, as it appears to be from the description of Alcock (1932), it is improbable that it would have had any influence on the mineralization, having been metamorphosed prior to the emplacement of the mineralized quartz veins. The hypothesis presented by Johnson (1970) appears reasonable although it revolves around the emplacement of the Bothan Brook granodiorite to the southeast to concentrate the sulphides from the diorite sill.

Unfortunately, as discussed in Chapter 3, contact relationships between the granodiorite and the metamorphic complex are nowhere observed and it is possible that the two are faulted against each other, a possibility that would invalidate Johnson's model.

Quartz veins and sulphides are commonly associated with small shear zones found throughout the area and significant mineralization has been observed in one location along Nile Brook (see below). Whether or not the Second Gold Brook sulphide mineralization resulted from a mechanism similar to that invoked for the Nile Brook prospect is uncertain, and although the deposit is hydrothermal in origin, postdates the metamorphism of the rocks of the Middle River unit, and is affected by late faults, its origin remains unresolved.

8.3 NILE BROOK COPPER PROSPECT

8.3.1 Introduction

The Nile Brook copper showing is situated at the bottom of the deep valley carved by the north branch of Nile Brook (Figure 8.3). Although it is located less than 1 km south of Fielding Road, the showing, which was discovered in 1954, is accessible only on foot. The surface exposure, where shallow drilling and blasting have been

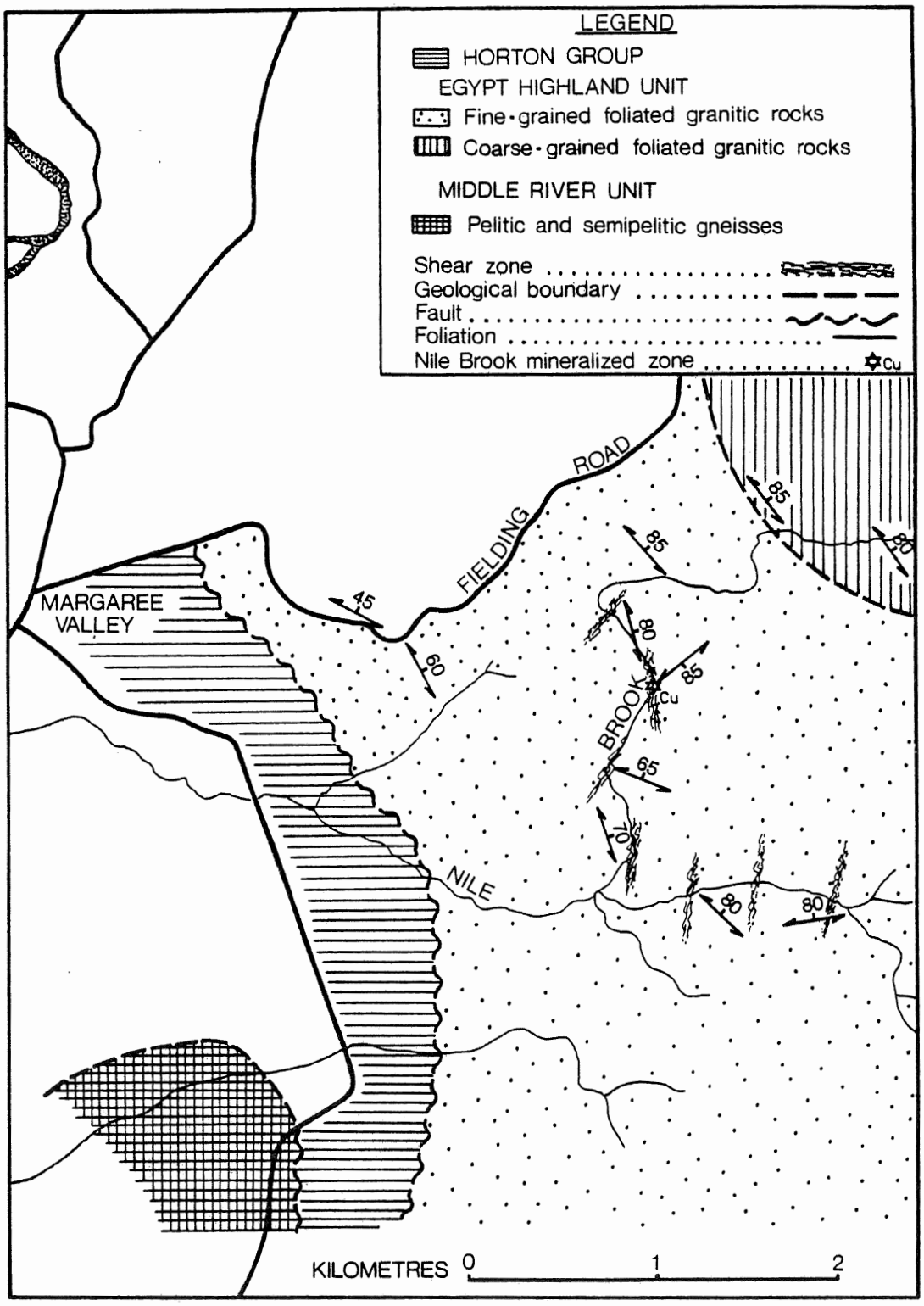

Figure 8.3 Geology and structure of Nile Brook area, showing the location of the Nile Brook copper prospect.

done, is fairly small but contrasts sharply with the surrounding granitic host rock because of the distinctive orange-brown gossan resulting from the oxidation of the sulphides.

8.3.2 Geology

The host rock is the fine-grained foliated granitic rock of the Egypt Highland unit. The quartz-plagioclase-microcline rocks strike northwest-southeast and dip steeply to the northeast. A number of small faults and narrow shear zones cut across the area and Nile Brook itself is undoubtedly controlled, to a large degree, by these structural features.

8.3.3 Mineralization

The sulphide mineralization occurs in a shear zone, marked by a fine-grained black biotite schist, which is exposed for a length of about 5 meters and whose width varies from 1 to 2 meters. The shear zone strikes northwest and dips steeply to the east. Sericitization and chloritization of the wall rock are visible as are thin epidote veinlets. The sulphides are dominantly chalcopyrite, pyrite and pyrrhotite with minor sphalerite (Chatterjee, 1980).

8.3.4 Metallogenesis

Chatterjee (1980) proposed a four stage paragenetic sequence for the formation of the deposit: metamorphism, hydrothermal activity, mineralization, and gangue alteration. The first occurred during the metamorphism of the host rock. Chatterjee (1980) indicated that argillaceous rocks were metamorphosed to the present quartz-plagioclase-microcline rocks by the intrusion of a granite pluton located less than 1 km to the east. The present study disagrees with this interpretation in that it shows that the entire region is underlain by foliated granitic rocks of igneous rather than sedimentary origin. Despite this discrepancy, the metamorphism of the protolith still represents the first stage in the paragenetic sequence. According to Chatterjee (1980), the metamorphism of the original rock was followed by a hydrothermal stage during which sericitization of plagioclase and microcline and chloritization of biotite and garnet occurred. This was followed by the sulphide mineralization stage and finally by oxidation of the sulphides to form pods, patches and veins of malachite.

Localized shearing of the granitic rocks has played an important role in the location and concentration of the mineralization, providing a favorable medium for the

channelling sulphide-bearing hydrothermal fluids and precipitation of these sulphides. The presence of numerous other shear zones in the granitic rocks along Nile Brook provides an interesting exploration target, but the small size of the shear zones limits the probability of the discovery of a deposit of economic significance.

8.4 SARACH BROOK MINERALIZATION

In 1978, St. Joseph Exploration Limited carried out an extensive geochemical survey along Sarach Brook and confirmed previous results indicating zinc and lead anomalies in the area. The company drilled two diamond drill holes in the area in 1981 but encountered only disseminated pyrite and galena mineralization in the high grade gneisses.

8.5 REGIONAL ECONOMIC SIGNIFICANCE

The Middle River area forms the southern half of an inferred metallogenic "domain" on the Metallogenic Map of Nova Scotia compiled by Chatterjee (1983). The "domain", about 15 km wide and 60 km long, extends from the town of Upper Middle River in the south to Cheticamp in the north. In the Middle River region, disseminated copper, silver and gold mineralization of hydrothermal

origin dominates while massive copper, zinc and gold mineralization, mostly of volcano-sedimentary origin, predominates east of Cheticamp. The polymetallic deposits are hosted, for the most part, in Precambrian volcano and volcano-sedimentary rocks.

The majority of the deposits in the "domain" are in the Precambrian metallotect (defined as a period of time during which a particular metallogenic process dominates; Chatterjee, pers. comm., 1983), which includes the George River, Fourchu and Georgeville Groups and rocks of the Mt. Thom and Bass River Complexes, Basement Complex and undifferentiated schists and gneisses. Most of the deposits are also closely associated with a number of pre-Devonian and Devono-Carboniferous intrusive complexes including diorite, granodiorite, granite, leucomonzogranite and aplite bodies.

From the data compiled by Chatterjee (1983), there appears to be a relationship between the Precambrian metallotect underlying most of the Cape Breton Highlands and pre-Devonian and Devono-Carboniferous intrusions in governing the location of economic mineralization. Although the data are, by necessity, generalized and simplified, the relationship indicates that, in the search for economic mineralization, particular attention should be paid to areas where Precambrian metasedimentary

and metavolcanic rocks are intruded by pre-Devonian and Devono-Carboniferous intrusions. The present study also indicates that localized shearing may also play a part in the concentration of sulphide mineralization.

CHAPTER 9

CONCLUSIONS AND RECOMMENDATIONS FOR FUTURE WORK

9.1 CONCLUSIONS

The main goals of this study were to describe the petrology and geochemistry of the rocks of the Middle River area and to provide some insight into the metamorphic history of the sequence. The following conclusions are presented:

1. The original lithologies present in the Middle River assemblage prior to regional metamorphism are the following:
   - For the Middle River unit, the thick sequence of schists and phyllites, micaceous schists and felsic gneisses, and dolomitic marbles indicates the deposition of interlayered fine-grained shales, mudstones and siltstones, with some carbonates, interbedded with coarser grained impure sandstones and rare, but relatively pure limestones. The deposition of these sediments was interrupted for a short interval by the introduction of cobble-size fragments of various rock types to produce a thin conglomerate layer. Sedimentation was repeatedly

interrupted by volcanism and deposition of felsic and mafic tuffs and rhyolite flows. The rocks may therefore represent a back-arc basin sedimentary package, interrupted by volcanism, deposited during Hadrynian to Cambrian times, according to the model suggested by Bird and Dewey (1970) and Helmstaedt and Tella (1973) that Cape Breton Island was part of a Hadrynian island arc system.

- For the Egypt Highland unit, composed of interlayered fine- and medium-grained foliated granitic rocks, an intrusive origin is indicated and the unit probably represents a granitic pluton, or plutons, emplaced prior to the deposition of the sedimentary rocks of the Middle River unit.

2. The sedimentary package that would eventually become the central high-grade belt was subjected to regional metamorphism up to the upper amphibolite facies, which produced an early foliation (S_{MR1}), with perhaps the formation of thin leucosomes through metamorphic segregation. This assemblage was subsequently stacked against an essentially undeformed interlayered volcano-sedimentary sequence during a second phase of deformation which produced the phyllitic schistosity (S_{GB1}) in the low- to medium-grade belt and the overprinting principal foliation (S_{MR2}) in the high-grade belt. The stacking process brought

the granitic rocks of the Egypt Highland unit, perhaps representing the "basement complex" of the sequence, into contact with the high-grade belt and may be responsible for the formation of the large-scale east- and west-plunging folds in the high-grade belt. Metamorphism of the assembled belts, with P-T conditions up to the lower amphibolite facies, was contemporaneous with the stacking of the three belts. Subsequent east-west folding resulted in the formation of the fine crenulation cleavage (S_{GB2}) along Second Gold Brook, of mesoscopic folds and kinks in all three belts and of a large-scale antiform west of Second Gold Brook. The southward and upward displacement of the Middle River metamorphic complex along the Sarach Brook mylonite zone and parallel north-south trending faults produced the observed structural configuration of the area.

3. The more or less concordant $^{40}Ar/^{39}Ar$ ages of 386 ± 9 Ma for hornblende and 377 ± 9 Ma for coexisting biotite from a metabasite from the high-grade central belt assign the cooling following the second phase of deformation to the Middle Devonian Acadian orogeny.
4. The principal east-west fabric of the rocks of the Middle River area is at a high angle to the predominantly north-south to northeast-southwest structural

trend of the Cape Breton Highlands. The rotation of the foliation from a north-south orientation in the northern Highlands (Cheticamp River, Cape North and Ingonish regions) to an east-west direction in the Middle River area may be due to movement of the complex along late shear zones such as the Sarach Brook and Muskrat Brook mylonite zones located to the east and south of the study area respectively.

5. The rocks of the Middle River metamorphic complex are lithologically similar to the assemblages studied by Macdonald and Smith (1980) in the Cape North area, and by Currie (in press) in the Jumping Brook region. Macdonald and Smith (1980) tentatively correlated the metasedimentary and metavolcanic rocks with the George River and Fourchu Groups respectively, while Currie (in press) ascribed a lower Paleozoic age to the sequence north of Cheticamp. The structural configuration of the Middle River complex closely resembles that of the Cheticamp River area examined by Craw (in press). Clearly, more detailed comparative work must be done between these areas before definitive stratigraphic relationships are formulated and a broad tectonic model for the Cape Breton Highlands is developed.
6. The conclusions derived from the present study are markedly different from the interpretation of the

Middle River area on the Tectonic Map of Nova Scotia compiled by Keppie (1982), where the rocks of the southern belt are correlated with the George River Group while those of the central belt are classified as Helikian to Hadrynian gneisses of unknown origin. The results obtained during the course of this study indicate that the rocks of the southern and central belts have undergone different deformation histories, but correlation of any part of the Middle River metamorphic complex with the George River Group is uncertain since the absolute age of the rocks is not known.

9.2 RECOMMENDATIONS FOR FUTURE WORK

In the course of this study, a number of possible research projects became evident. These are:

1. The study of the petrology and geochemistry of the rocks north of Fielding Road to determine the extent of the granitic rocks of the Egypt Highland unit and the West Branch North River monzogranite and possibly establish a more definite contact relationship between these two lithologies.
2. The detailed geochemical analysis, for both major and trace elements, of the metabasites of both the south and central belts in order to define possible compo-

sitional differences that might indicate distinct magma sources, and thus substantiate the postulated tectonic and possible chronologic break between the two belts.

3. The detailed investigation of compositional zoning in garnets to further document the observed break in the compositional zoning of a garnet from sample 8130 and to establish whether or not compositional zoning occurs in other garnets in the medium- and high-grade rocks.
4. The application of garnet-plagioclase-quartz-aluminum silicate, muscovite-quartz-plagioclase-aluminum silicate and staurolite-quartz-garnet-aluminum silicate geothermometers (discussed in Ferry, 1980) to appropriate samples from the high-grade pelitic rocks of the central belt to further document the calculated "retrograde" lower amphibolite facies temperatures obtained from calcite-dolomite and garnet-biotite geothermometers.
5. The petrological and geochemical comparison of the metasedimentary and metavolcanic rocks from the Cape North, Jumping Brook, Cheticamp River and Middle River areas to determine similarities and discrepancies between these various assemblages to establish possible stratigraphic relationships.

REFERENCES

Albee, A.L. (1972). Metamorphism of pelitic schists: reaction relations of chloritoid and staurolite. Geol. Soc. America Bull., 83: 3249-3268.

Alcock, F.J. (1932). Middle River gold field, Victoria County, Nova Scotia. Geol. Surv. Canada, Summary Report, 1932 Part D, 58-68.

Atherton, M.P. (1968). The variation in garnet, biotite and chlorite in medium grade pelitic rocks from the Dalradian of Scotland, with particular reference to the zonation in garnet. Contr. Mineral. Petrol., 18: 347-371.

Atherton, M.P., Smith, R.A. (1979). Chloritoid-staurolite assemblages from Barrow's Zones in Central Perthshire, Scotland. Geol. Mag., 116: 469-476.

Baltatzis, E. (1979). Staurolite-forming reactions in the eastern Dalradian rocks of Scotland. Contrib. Mineral. Petrol., 69: 193-200.

Barr, S.M., O'Reilly, G.A. and O'Beirne, A.M. (1979). Geochemistry of granitoid plutons of Cape Breton Island. Nova Scotia Department of Mines and Energy, Report 79-1, 109-141.

Bingley, J.M. (1970). Sulphide mineralization - Middle River gold mine Middle River, Victoria County, Nova Scotia. Nova Scotia Department of Mines and Energy, Assessment Report 11K/02C 21-Q-12(06).

Bird, J.M., Dewey, J.F. (1970). Lithosphere plate-continental margin tectonics and the evolution of the Appalachian orogen. Geol. Soc. America Bull., 81: 1031-1060.

Bird, G.W., Fawcett, J.J. (1973). Stability relations of Mg-chlorite-muscovite and quartz between 5 and 10 kb water pressure. J. Petrol., 14: 415-428.

Bouvier, J.L., Gupta, J.G., Abbey, S. (1972). Use of an "Automatic Sulphur Titrator" in rock and mineral analysis: determination of sulphur, total carbon, carbonate and ferrous iron. Geol. Surv. Canada, Paper 73-21, 22 pp.

Brock, K.J. (1972). Genesis of Garnet Hill skarn, Calavaras County, California. Geol. Soc. America Bull., 83: 3391-3404.

Brown, E.H. (1975). A petrogenetic grid for reactions producing biotite and other Al-Fe-Mg silicates in the greenschist facies. J. Petrol., 16: 258-271.

Carmichael, D.M. (1970). Intersecting isograds in the Whetstone Lake area, Ontario. J. Ptrol., 11: 147-181.

Carmichael, D.M. (1978). Metamorphic bathozones and bathograds: a measure of the depth of post-metamorphic uplift and erosion on a regional scale. Am. Jour. Sci., 278: 769-797.

Chatterjee, A.K. (1980). Mineralization and associated wall rock alteration in the George River Group, Cape Breton Island, Nova Scotia. Unpublished Ph.D. thesis, Dalhousie University, 197 pp.

Chatterjee, A.K. (1983). Metallogenic map of the province of Nova Scotia. Nova Scotia Department of Mines and Energy.

Chatterjee, N.D., Johannes, W. (1974). Thermal stability and standard thermodynamic properties of synthetic $2M_1$-muscovite, $KAl(AlSi_3O_{10}(OH)_2)$. Contrib. Mineral. Petrol., 48: 89-114.

Cooper, A.F. (1972). Progressive metamorphism of metabasic rocks from the Haast Schist Group of southern New Zealand. J. Petrol., 13: 457-492.

Cormier, R.F. (1972). Radiometric ages of granitic rocks, Cape Breton Island, Nova Scotia. Can. J. Earth Sci., 9: 1074-1086.

Cox, K.G., Bell, J.D. and Pankhurst, R.J. (1979). The interpretation of igneous rocks. George Allen and Unwin, London, 450 pp.

Craw, D. (1983). Tectonic stacking of metamorphic zones in Cheticamp River area, Cape Breton Highlands, Nova Scotia. (In press.)

Cruickshank, R.D., Ghent, E.D. (1978). Chloritoid-bearing pelitic rocks of the Horsethief Creek Group, southeastern British Columbia. Contrib. Mineral. Petrol., 65: 333-339.

Currie, K.L. (1975). Studies of granitoid rocks in the Canadian Appalachians. Geol. Surv. Canada, Paper 75-1, 265-270.

Currie, K.L. (1977). A note on post-Mississippian thrust faulting in northern Cape Breton Island. Can. J. Earth Sci., 14: 2937-2941.

Currie, K.L., Loveridge, W.D. and Sullivan, R.W. (1982). A U-Pb age on zircon from dykes feeding basal rhyolitic flows of the Jumping Brook complex, northwestern Cape Breton Island, Nova Scotia. in Current Research, Part C, Geol. Surv. Canada, Paper 82-1C, 125-128.

Currie, K.L. (1983). Relations between metamorphism and magmatism near Cheticamp, Cape Breton Island. (In press.)

Dallmayer, R.D. (1974). The role of crystal structure in controlling the partitioning of Mg and Fe^{2+} between coexisting garnet and biotite. Am. Mineral., 59: 201-203.

Deer, W.A., Howie, R.A. and Zussman, J. (1966). An introduction to the rock-forming minerals. Longman Group Limited, London, 528 pp.

Delahay, S.C. (1979). Metamorphism of the George River Group; Gold Brook, Victoria County Cape Breton Island, Nova Scotia. Unpublished B.Sc. thesis, Dalhousie University, 84 pp.

Evans, B.W., Guidotti, C.V. (1966). The sillimanite-potash feldspar isograd in western Maine, U.S.A. Contrib. Mineral. Petrol., 12: 25-62.

Evans, B.W., Leake, B.E. (1960). The composition and origin of the striped amphibolites of Connemara, Ireland. J. Petrol., 1: 337-363.

Ferry, J.M. (1980). A comparative study of geothermometers and geobarometers in pelitic schists from south-central Maine. Am. Mineral., 65: 720-732.

Ferry, J.M., Spear, F.S. (1978). Experimental calibration of the partitioning of Fe and Mg between garnet and biotite. Contrib. Mineral. Petrol., 66: 113-117.

Friedman, G.M. (1959). Identification of carbonate minerals by staining methods. J. Sed. Petrol., 29: 87-97.

Goldman, D.S., Albee, A.L. (1977). Correlation of Mg/Fe partitioning between garnet and biotite with $^{18}O/^{16}O$ partitioning between quartz and magnetite. Am. Jour. Sci., 277: 750-767.

Goldsmith, J.R., Graf, D.L. and Joensuu, O.I. (1955). The occurrence of magnesian calcites in nature. Geochim. Cosmochim. Acta, 7: 212-230.

Goldsmith, J.R., Newton, R.C. (1969). P-T-X relations in the system $CaCO_3$-$MgCO_3$ at high temperatures and pressures. Am. Jour. Sci., 267-A: 160-190.

Graf, D.L., Goldsmith, J.R. (1955). Dolomite-magnesian calcite relations at elevated temperatures and CO_2 pressures. Geochim. Cosmochim. Acta, 7: 109-128.

Graham, C.M. (1974). Metabasite amphiboles of the Scottish Dalradian. Contrib. Mineral. Petrol., 47: 165-185.

Griffen, D.T., Ribbe, P.H. (1973). The crystal chemistry of staurolite. Am. Jour. Sci., 273: 479-495.

Guidotti, C.V. (1970). The mineralogy and petrology of the transition from the lower to upper sillimanite zone in the Oquossoc area, Maine. J. Petrol., 11: 277-336.

Guidotti, C.V. (1974). Transition from staurolite to sillimanite zone, Rangeley quadrangle, Maine. Geol. Soc. America Bull., 85: 475-490.

Halferdahl, L.B. (1961). Chloritoid: its composition, X-ray and optical properties, stability, and occurrence. J. Petrol., 2: 49-135.

Harte, B., Graham, C.M. (1975). The graphical analysis of greenschist to amphibolite facies mineral assemblages in metabasites. J. Petrol., 16: 347-370.

Heinrich, E.W. (1965). Microscopic identification of minerals. McGraw-Hill, New York, 414 pp.

Helmstaedt, H., Tella, S. (1972). Structural history of pre-Carboniferous rocks in parts of eastern Cape Breton Island. Geol. Surv. Canada, Paper 71-1, Part A, 7-10.

Helmstaedt, H., Tella, S. (1973). Pre-Carboniferous structural history of southeastern Cape Breton Island. Maritime Sed., 9: 88-99.

Hey, M.H. (1954). A new review of the chlorites. Min. Mag., 30: 277-292.

Holbrooke, G.L. (1962). Report on Gold Brook Property, Cape Breton, Nova Scotia. Nova Scotia Department of Mines and Energy, Assessment Report 11K/02C 21-Q-12(03).

Holdaway, M.J. (1971). Stability of andalusite and the aluminum silicate phase diagram. Am. Jour. Sci., 271: 97-131.

Holland, T.J.B., Richardson, S.W. (1979). Amphibole zonation in metabasites as a guide to the evolution of metamorphic conditions. Contrib. Mineral. Petrol., 70: 143-148.

Hollister, L.S. (1966). Garnet zoning: an interpretation based on the Rayleigh fractionation model. Science, 154: 1647-1651.

Hoschek, G. (1967). Untersuchungen zum stabilitatsbereich von chloritoid und staurolith. Contrib. Mineral. Petrol., 14: 123-162.

Hoschek, G. (1969). The stability of staurolite and chloritoid and their significance in metamorphism of pelitic rocks. Contrib. Mineral. Petrol., 22: 208-232.

Hoschek, G. (1976). Melting relations of biotite + plagioclase + quartz. Neues Jahrbuch Fur Mineralogie Monatshefte, 79-83.

Hughes, C.J. (1973). Late Precambrian volcanic rocks of Avalon, Newfoundland - a spilite/keratophyre province: recognition and implications. Can. J. Earth Sci., 10: 272-282.

Hynes, A. (1982). A comparison of amphiboles from medium- and low-pressure metabasites. Contrib. Mineral. Petrol., 81: 119-125.

Jamieson, R.A. (1981). The geology of the Crowdis Mountain volcanics, southern Cape Breton Highlands. in Current Research, Part C, Geol. Surv. Canada, Paper 81-1C, 77-81.

Jamieson, R.A., Craw, D. (1983). Reconnaissance mapping of the southern Cape Breton Highlands - a preliminary report. in Current Research, Part A, Geol. Surv. Canada, Paper 83-1A, 263-268.

Jamieson, R.A., Doucet, P. (1983). The Middle River - Crowdis Mountain area, southern Cape Breton Highlands. in Current Research, Part A, Geol. Surv. Canada, Paper 83-1A, 269-275.

Jeffery, P.G. (1970). Chemical methods of rock analysis (1st ed.). Oxford, New York, Pergamon Press, 509 pp.

Johnson, C.G. (1970). The Gold Brook copper-nickel prospect, an exploration proposal. Nova Scotia Department of Mines and Energy, Assessment Report 11K/02C 21-Q-12(11).

Johnson, C.G. (1976). Report on the soil sample survey for arsenic at Second Gold Brook, Victoria County, Nova Scotia. Nova Scotia Department of Mines and Energy, Assessment Report 11K/02C 04-Q-12(01).

Karabinos, P. (1983). Polymetamorphic garnet zoning from southeastern Vermont. (In press.)

Kelley, D.G. (1967). Baddeck and Whycocomagh map areas. Geol. Surv. Canada, Memoir 351, 65 pp.

Keppie, J.D. (1979). Geological map of the province of Nova Scotia. Nova Scotia Department of Mines and Energy.

Keppie, J.D. (1982). Tectonic map of the province of Nova Scotia. Nova Scotia Department of Mines and Energy.

Keppie, J.D., Smith, P.K. (1978). Compilation of isotopic age data of Nova Scotia. Nova Scotia Department of Mines and Energy, Report 78-4, 101 pp.

Kerrick, D.M. (1972). Experimental determination of muscovite + quartz stability with $P_{H_2O} < P_{Total}$. Am. Jour. Sci., 272: 946-958.

Laird, J., Albee, A.L. (1981). Pressure, temperature and time indicators in mafic schists: their application to reconstructing the polymetamorphic history of Vermont. Am. Jour. Sci., 281: 127-175.

La Tour, T.E., Kerrich, R., Hodder, R.W. and Barnett, R.L. (1980). Chloritoid stability in very iron-rich pillow lavas. Contrib. Mineral. Petrol., 74: 165-173.

Leake, B.E. (1964). The chemical distinction between ortho- and para-amphibolites. J. Petrol., 5: 238-254.

Leake, B.E. (1965). The relationship between tetrahedral aluminum and the maximum possible octahedral aluminum in natural calciferous and sub-calciferous amphiboles. Am. Mineral., 50: 843-851.

Leake, B.E. (1978). Nomenclature of amphiboles. Am. Mineral., 63: 1023-1052.

Liou, J.G. (1973). Synthesis and stability relations of epidote, $Ca_2Al_2FeSi_3O_{12}(OH)$. J. Petrol., 14: 381-413.

Liou, J.G., Chen, P.Y. (1978). Chemistry and origin of chloritoid rocks from eastern Taiwan. Lithos, 11: 175-187.

Liou, J.G., Kunyioshi, K. and Ito, K. (1974). Experimental studies of the phase relations between greenschist and amphibolite in a basaltic system. Am. Jour. Sci., 274: 613-632.

Macdonald, A.S., Smith, P.K. (1980). Geology of Cape North area, northern Cape Breton Island, Nova Scotia. Nova Scotia Department of Mines and Energy, Paper 80-1, 60 pp.

MacKay, R.M. (1981). Whole rock analysis using the electron microprobe. Unpublished B.Sc. thesis, Dalhousie University, 84 pp.

Mather, J.D. (1970). The biotite isograd and the lower greenschist facies in the Dalradian rocks of Scotland. J. Petrol., 11: 253-275.

Mehnert, K.R. (1968). Migmatites and the origin of granitic rocks. Elsevier, New York, 393 pp.

Miller, C.F., Stoddard, E.F., Bradfish, L.J. and Dollase, W.A. (1981). Composition of plutonic muscovite: genetic implications. Can. Mineral., 19: 25-34.

Milligan, G.C. (1970). Geology of the George River Series, Cape Breton. Nova Scotia Department of Mines, Memoir 7, 111 pp.

Milner, R.L. (1936). Report on the Middle River gold mine. Nova Scotia Department of Mines and Energy, Assessment Report 11K/02C 21-Q-12(01).

Miyashiro, A. (1953). Calcium-poor garnet in relation to metamorphism. Geochim. Cosmochim. Acta, 4: 179-208.

Miyashiro, A., Shido, F. (1973). Progressive compositional change of garnet in metapelite. Lithos, 6: 13-20.

Mohr, D.W., Newton, R.C. (1983). Kyanite-staurolite metamorphism in sulphide schists of the Anakeesta Formation, Great Smoky Mountains, North Carolina. Am. Jour. Sci., 283: 97-134.

Moody, J.B., Meyer, D. and Jenkins, J.E. (1983). Experimental characterization of the greenschist/amphibolite boundary in mafic systems. Am. Jour. Sci., 283: 48-92.

Murray, D.L. (1977). The structural relationship between rocks of the George River and Fourchu Groups in the Ingonish River - Clyburn Brook area, Cape Breton Island, Nova Scotia. Unpublished M.Sc. thesis, Queen's University, 63 pp.

Neale, E.R.W., Kennedy, M.J. (1975). Basement and cover rocks at Cape North, Cape Breton Island, Nova Scotia. Maritime Sed., 11: 1-4.

Niggli, P. (1954). Rocks and mineral deposits. W.H. Freeman, San Francisco, 559 pp.

Raase, P. (1974). Al and Ti contents of hornblende, indicators of pressure and temperature of regional metamorphism. Contrib. Mineral. Petrol., 45: 231-236.

Ramsey, C.R. (1973). Controls of biotite zone mineral chemistry in Archean meta-sediments near Yellowknife, Northwest Territories, Canada. J. Petrol., 14: 467-488.

Rice, J.M. (1977). Progressive metamorphism of impure dolomitic limestone in the Marysville aureole, Montana. Am. Jour. Sci., 277: 1-24.

Richardson, S.W. (1968). Staurolite stability in a part of the system Fe-Al-Si-O-H. J. Petrol., 9: 467-488.

Spry, A. (1969). Metamorphic textures. Pergamon Press, New York, 350 pp.

Sturt, B.A. (1962). The composition of garnets from pelitic schists in relation to the grade of regional metamorphism. J. Petrol., 3: 181-191.

Thompson, A.B. (1975). Calc-silicate diffusion zones between marble and pelitic schist. J. Petrol., 16: 314-346.

Thompson, A.B. (1976). Mineral reactions in pelitic rocks: II. Calculation of some P-T-X (Fe-Mg) phase relations. Am. Jour. Sci., 276: 425-454.

Thompson, A.B. (1982). Dehydration melting of pelitic rocks and the generation of H_2O-undersaturated granitic liquids. Am. Jour. Sci., 282: 1567-1595.

Thompson, A.B., Tracy, R.J. (1979). Model systems for anatexis of pelitic rocks: II. Facies series melting and reactions in the system $CaO-KAlO_2-NaAlO_2-Al_2O_3-SiO_2-H_2O$. Contrib. Mineral. Petrol., 70: 429-438.

Thompson, A.B., Tracy, R.J., Lyttle, P.T. and Thompson, J.B. Jr. (1977). Prograde reaction histories deduced from compositional zonation and mineral inclusions in garnet from the Gassetts schist, Vermont. Am. Jour. Sci., 277: 1152-1167.

Tracy, R.J. (1978). High grade metamorphic reactions and partial melting in pelitic schist, west-central Massachusetts. Am. Jour. Sci., 278: 150-178.

Tracy, R.J., Robinson, P. and Thompson, A.B. (1976). Garnet composition and zoning in the determination of temperature and pressure of metamorphism, central Massachusetts. Am. Mineral., 61: 762-775.

Van de Kamp, P.C. (1970). The green beds of the Scottish Dalradian series: geochemistry, origin, and metamorphism of mafic sediments. J. Geol., 78: 281-303.

Vidale, R. (1969). Metasomatism in a chemical gradient and the formation of calc-silicate bands. Am. Jour. Sci., 267: 857-874.

Volborth, A. (1969). Elemental analysis in geochemistry. Elsevier, Amsterdam, New York, 373 pp.

Weeks, L.J. (1954). Southeast Cape Breton Island, Nova Scotia. Geol. Surv. Canada, Memoir 277, 112 pp.

Weibe, R.A. (1972). Igneous and tectonic events in northeastern Cape Breton Island, Nova Scotia. Can. J. Earth Sci., 9: 1262-1277.

Weibe, R.A. (1973). Precambrian rocks of Cape Breton Island. Maritime Sed., 9: 100-101.

Winkler, H.G.F. (1979). Petrogenesis of metamorphic rocks (5th ed.). Springer, Berlin, Heidelberg, New York, 348 pp.

Yardley, B.W.D. (1978). Genesis of the Skagit Gneiss migmatites, Washington, and the distinction between possible mechanisms of migmatization. Geol. Soc. America Bull., 89: 941-951.

Yardley, B.W.D., Leake, B.E. and Farrow, C.M. (1980). The metamorphism of Fe-rich pelites from Connemara, Ireland. J. Petrol., 21: 365-399.

APPENDIX I

ANALYTICAL METHODS

(i) Sample Preparation

Each rock sample weighed about 200 g. A piece of the sample was broken into small chips with a hydraulic press and a ceramic jaw crusher. Between 25 and 50 g of powder were recovered after grinding the rock fragments in a tungsten carbide vessel secured to a swing mill.

(ii) Electron Microprobe Analysis

The following procedure (according to MacKay, 1981) was used for each sample:

(1) 200 g of rock powder (100 μm) is mounted on a 5 cm x 1.5 cm molybdenum strip and fused between two electrodes in the bell jar of a vacuum coating unit. A vacuum of better than 10^{-3} torr is obtained. Nitrogen gas is permitted to flow in and out of the bell jar.

(2) The resulting glass is crushed and selected chips are mounted in an epoxy block.

(3) The electron microprobe is operated at 75 kv with a current of 5 nanoamperes. The sample is

rastered over an area of 50 μ^2.

(4) Five analyses were obtained and averaged for each sample.

(iii) Determination of total H_2O and H_2O^-.

(Using the Penfield tube technique modified after Volborth, 1969.)

A dry flux, consisting of PbO_2:$PbCr_2O_4$:$NaWO_4$ = 2:1:1 was added and thoroughly mixed with 0.50 g of rock sample powder. The mixture was placed in a Penfield tube and heated. The weight of the extracted water represents total H_2O. To determine H_2O^-, 1.0 g of sample powder was carefully weighed before and after dessication.

(iv) Determination of CO_2.

(Using the automatic CO_2 titration method, Bouvier et al., 1972.)

Between 0.25 and 0.50 g of rock sample powder was heated with HCl for 5 minutes. Water and sulphur dioxide vapor are removed from the fumes. The remaining gas is automatically titrated with sodium methylate. The percentage of CO_2 is calculated by multiplying the burette reading by a factor derived from the analysis of a standard rock sample.

(v) FeO Determination.

(Using the Wilson technique of cold acid decomposition and visual titration, Jeffery, 1970.)

Ammonium metavadanate solution and hydrofluoric acid were added to 0.50 g of rock sample powder in a polyethylene flask. The solution was blended for 48 hours until homogenized. An acid mix, consisting of H_3PO_4:H_2SO_4:H_2O = 1:2:2, was added to each flask. The mixture was then transferred to a beaker by washing it with a 5 percent boric acid solution. Ferrous ammonium sulphate and barium diphenylamine indicator were added and the solution was titrated with potassium dichromate to a purple end-point. The weight percent FeO is then calculated by subtracting a standard factor from the burette reading and subtracting the resulting value from the weight percent FeO of the microprobe analysis.

APPENDIX II

PETROGRAPHIC SUPPLEMENT

The 32 samples from which individual mineral analyses were obtained and 7 additional samples for which only whole rock analyses were obtained are described. The sample locations are illustrated on the Sample Location Map in the pocket at the back of this study. Mineral abbreviations used are:

mus - muscovite
plag - plagioclase
gnt - garnet
bt - biotite
ep - epidote
hb - hornblende
qz - quartz
ser - sericite
micr - microcline
st - staurolite
ox - oxides, includes pyrite, chalcopyrite and minor magnetite
sph - sphene
chl - chlorite
chlt - chloritoid
ap - apatite
rt - rutile
zr - zircon
ilm - ilmenite
cc - calcite
ky - kyanite

Mineral abundance is approximate except where modal percentages were obtained for certain rocks.

Lithology	Number	Mineralogy	Fabric
phyllites	8223	qz(25%), chl(25%), mus(15%), cc(15%), bt(10%), ilm(5%), plag(5%)	pronounced S_{GB1} (chl, mus) with qz granules and plag clasts in a fine qz-chl-mus matrix; rare bent or kinked bt
	8220	mus(80%), qz(10%), chlt(5%), ilm(5%)	pronounced S_{GB1} (mus) with porph. idiobl. chlt with straight incl. trails of qz and ilm continuous with matrix; chlt are parallel to or at angle with S_{GB1}
	8218	qz(50%), mus(30%), chl(10%), plag(5%), ilm(5%)	pronounced S_{GB1} (mus, chl) with qz granules and plag clasts in a fine qz-mus-chl matrix
	81108	qz(40%), chl(35%), mus(5%), gnt(5%), ilm+ap+sph(5%)	pronounced S_{GB1} (chl, mus) with poikiloblastic porph. chlt and gnt with straight incl. trails of qz and ilm conti-

Lithology	Number	Mineralogy	Fabric
			nuous with matrix
	8130	qz(45%), mus(15%), plag(15%), bt(10%), gnt(10%), ox(5%), tourmaline+zr+ap<1% retrograde: ser, chl	pronounced S_{GB1} (mus, bt) with porph. gnt with circular incl. trails of qz and ox in core and incl.-free rims; chl replaces bt along cleavages; plag sericitized slightly
metabasites	8106	hb(45.4%), qz(24.7%), bt(17.1%), ilm(8.5%), ep(4.3%)	slight S_{GB1} (hb, bt) with porph. hb with random incl. of qz and ilm in a qz-hb-bt matrix; slight orientation of hb porph.
	8118b	qz(32.3%), bt(35.6%), hb(23.7%), ep(6%), ilm(2.5%), cc<1% retrograde: chl	slight S_{GB1} (bt) with porph. hb, rarely poikiloblastic with random incl. of qz and ilm in a qz-bt matrix; chl replaces bt along cleavages and boundaries

Lithology	Number	Mineralogy	Fabric
	8103	hb(58.9%), plag(20.7%) qz(10.3%), ox(6.9%), cc(1.8%), bt(1.4%) <u>retrograde</u>: ser	slight S_{GB1} (hb, bt); fine hb in a qz and plag matrix; plag sericitized slightly
	8113	hb(56.3%), qz(23.6%), ox(13.0%) <u>retrograde</u>: chl(7.1%)	slight S_{GB1} (chl); poikiloblastic hb with random incl. of qz and ilm; chl replaces hb along grain boundaries
	8114a	hb(66.7%), plag(11.4%) qz(10.9%), ox(7.7%), ep(2.9%), cc(0.4%) <u>retrograde</u>: ser	no apparent foliation; poikiloblastic hb with random incl. of qz and ilm; plag sericitized slightly
	8115	hb(67.6%), qz(20.0%), ox(12.2%), plag(0.2%) <u>retrograde</u>: ser	no apparent foliation; poikiloblastic hb with random incl. of ilm; minor Fe-oxide alt.; plag sericitized slightly

Lithology	Number	Mineralogy	Fabric
	81109	hb(63.2%), ox(17.4%), plag(15.9%), qz(1.7%) ep(1.5%), cc(0.3%) <u>retrograde</u>: ser	slight S_{GB1} (hb); rarely poikiloblastic hb with random incl. of ilm; plag sericitized very slightly
	8128	hb(48.5%), qz(31.1%), ox(10.0%), cc(8.0%), bt(1.3%) <u>retrograde</u>: chl(1.1%)	moderate S_{GB1} (hb, bt); poikiloblastic hb with random incl. of qz and ilm; chl replaces hb and bt along grain boundaries and cleavages
	81111	hb(66.1%), qz(19.4%), ox(12.4%), ep(2.1%) <u>retrograde</u>: chl	slight S_{GB1} (hb); rarely poikiloblastic hb with random incl. of qz and ilm; chl rarely replaces hb along cleavages and boundaries

Lithology	Number	Mineralogy	Fabric
	8129	hb(69.4%), qz(18.3%), ilm(10.0%), cc(0.8%). ep(0.1%) retrograde: chl(1.4%)	no apparent foliation; cc as vein-filling material; minor hematite alt. along fractures; chl rarely replaces hb along boundaries
	8122	hb(55%), plag(An 40-46)(20%), qz(10%), ep(10%), ilm+sph+gnt (5%) retrograde: ser	slight S_{GB1} (hb) poikiloblastic gnt with random incl. of qz and sph; minor hematite alt. along fractures; plag sericitized slightly
	81103	hb(75.1%), plag(An 33-35)(21.7%), rt (2.5%), bt+ap(0.7%) retrograde: ser	slight S_{GB1} (hb) rarely poikiloblastic hb with random incl. of plag and rt; plag sericitized slightly

Lithology	Number	Mineralogy	Fabric
	8196	hb(47.9%), qz(11.2%), plag(5.5%), sph+ox (0.7%), tourmaline+ ep<1% retrograde: chl(34.7%) ser	slight S_{GB1} (chl); extensive chloritization of hb; plag sericitized extensively
	81117	hb(55%), plag(An 27-29)(30%), bt(10%), ilm(5%), rt+ap<1% retrograde: ser, chl	moderate S_{GB1} (hb, bt); rarely poikiloblastic hb with random incl. of plag and ilm; plag sericitized very slightly; minor chloritization of bt along boundaries
	81120	hb(59.7%), plag(An 46-49)(29.1%), sph+ ap+ox+zr(3.9%), bt (6.7%), qz(0.6%) retrograde: ser	pronounced S_{GB1} (hb, bt); sph rarely with rt core, replacing rt; plag sericitized slightly
	8148	hb(55%), qz(25%), plag(An 20-26)(10%), bt(5%), cc+sph+ap+ox (5%) retrograde: chl, ser	moderate S_{GB1} (hb, bt); cc as vein-filling material; plag sericitized very slightly; minor

Lithology	Number	Mineralogy	Fabric
			chloritization of bt along boundaries
Pelitic Schists and Gneisses	8135	qz(36.9%), bt(24.3%), mus(23%), gnt(9.2%), ky(3%), st(1.6%), tourmaline+ox+zr+ap(2%) retrograde: ser	pronounced S_{MR2} (mus, bt); poikiloblastic gnt with random incl. of qz and ox; ky and st breaking down to ser and qz along boundaries
	81101	qz(59.6%), plag (17.7%), bt(14.2%), mus(7.1%), gnt(1.2%), sph(0.1%), ox(0.1%) retrograde: ser	moderate S_{MR2} (mus, bt); poikiloblastic gnt with random incl. of qz; plag sericitized very slightly
	8247	mus(60%), gnt(10%), bt(10%), plag(5%), ky(5%), st(5%), qz (5%), sill+ox+sph+tourmaline 1% retrograde: chl, ser	moderate S_{MR2} (mus, bt); poikiloblastic gnt porph. with random incl. of qz and ox; ky and st breaking down to ser, bt and qz; slight chloritization of bt and gnt along

Lithology	Number	Mineralogy	Fabric
			boundaries and fractures in gnt
	8123	bt(37.8%), qz(29.4%), plag(18.4%), gnt (5.2%), mus(4.9%), ky(4.3%), zr 1% <u>retrograde</u>: ser	moderate S_{MR2} (bt, mus); gnt porph. without incl.; poikiloblastic bt with random incl. of qz and plag; ky breaking down to ser, bt and qz; plag sericitized very slightly
	8238	qz(40%), bt(15%), ky(15%), mus(10%), gnt(10%), plag(5%), ox+rt+sill(5%)	pronounced S_{MR2} (bt, mus); gnt porph. without incl.; ky breaking down to bt and qz
	8140	bt(36.3%), plag(An 24-30)(33.1%), qz (29.3%), gnt(1%), zr+ap+ox(0.3%)	moderate S_{MR2} (bt); gnt porph. with random incl. of qz, bt and ox
	8144	plag(An 25-34)(40%), qz(30%), bt(10%), hb(10%), gnt(5%), ox+ap+sph+zr(5%) <u>retrograde</u>: chl, ser	moderate S_{MR2} (bt); compositional layering (bt/hb) parallel to S_{MR2}; poiki-

Lithology	Number	Mineralogy	Fabric
			loblastic hb with random incl. of sph; plag sericitized very slightly; very slight chloritization of bt
	8150	qz(36.3%), bt(26.4%), plag(An 28-45)(16.9%) gnt(12.7%), mus(3.2%) ox+rt+zr+sph(3.8%) <u>retrograde</u>: chl(0.7%) ser	moderate S_{MR2} (bt, mus); poikiloblastic gnt porph. with random incl. of bt, qz, ox and sph; plag sericitized very slightly; very slight chloritization of bt
Marble	8145	calcite+dolomite (80%), qz(10%), plag (5%), phlogopite+ tremolite+diopside+ sph+talc(5%)	compositional layering (cc/dolomite) parallel to contact between marble and metapelites; the marble is separated from the gneisses by a thin layer of phlog+talc

Lithology	Number	Mineralogy	Fabric
			(gneiss side) and tre+diop (marble side)
	8162	calcite+dolomite (60%), tremolite (20%), mus(20%)	compositional layering (calc+ dol/tre+mus) parallel to contact between marble and meta-pelites
	8251	calcite+dolomite (99%), mus(1%)	compositional layering (cc/ dolomite) paral-lel to contact between marble and metapelites
	8252	calcite+dolomite (95%), mus(5%)	compositional layering (cc/ dolomite) paral-lel to contact between marble and metapelites
Granitic rocks of the Egypt Highland unit	8174	qz(30%), plag(An 6-10)(30%), micr (25%), sph(5%), ox+ap(5%) retrograde: ser, chl	slight S_{EHU} (mus, chl); very minor myrmekite development bet-ween qz and plag which is serici-

Lithology	Number	Mineralogy	Fabric
			tized slightly; total chloriti-zation of bt(?)
	8177	qz(30%), plag(An 26-28)(25%), micr (25%), sph(5%), ox+ap 1% retrograde: chl(15%) ser	very slight S_{EHU} (chl); micr augen with plag incl.; plag se-ricitized exten-sively; total chloritization of bt(?)
	8190	micr(35%), qz(30%), plag(An 2-3)(25%), ox(5%), mus+sph+ap (5%) retrograde: chl, ser	no apparent fo-liation; coarse micr with plag incl.; plag se-ricitized mode-rately; moderate sericitization of micr; total chloritization of bt(?)
	8191	micr(55%), qz(20%), plag(An 2-9)(20%), ox+mus+sph+ap(5%) retrograde: chl, ser	no apparent fo-liation; coarse micr with plag incl.; plag se-ricitized mode-rately; total chloritization of bt(?)

Lithology	Number	Mineralogy	Fabric
Bothan Brook granodiorite	8248	plag(An 1-2)(48.2%), qz(34.8%), micr (12.4%), ox(2.9%), mus(0.3%) retrograde: chl(1.4%) ser	no apparent foliation; plag sericitized extensively; micr sericitized moderately; total chloritization of bt(?); minor hematite alteration along fractures

61°00'
46°23'

60°48'
46°23'

MARGAREE VALLEY

MARGAREE CENTRE

FIELDING ROAD

Nile Br.

Ryan Br.

Florinar Br.

MIDDLE RIVER

D

R

UM

?

Duncan Br.

Bothan Br.

Sarach Br.

HIGHLAND ROAD

Lakes O' Law

CABOT TRAIL

Fortune Br.

Gold Falls

Fourth Gold Br.

Third Gold Br.

Second Gold Br.

MIDDLE RIVER

N

SCALE 1:25,000

Meters 500 0 0.5 1 1.5 2 2.5 3 Kilometers

LOCATION MAP

CAPE BRETON ISLAND

MAP AREA

0 40 Km

MIDDLE RIVER GEOLOGICAL MAP

LEGEND

CARBONIFEROUS

HORTON GROUP : conglomerate, sandstone

DEVONIAN

West Branch North River monzogranite

DEVONIAN OR EARLIER

Bothan Brook granodiorite

LATE PRECAMBRIAN (?)

Egypt Highland Unit

Coarse-grained foliated granitic rock

Fine-grained foliated granitic rock

Middle River Unit

Metasedimentary schists and phyllites (rare felsic tuff layers)

Metaconglomerate

Metabasite

Meta-rhyolite

Metasedimentary gneisses (micaceous schists and felsic gneisses)

Marble

Fault (defined, approximate, assumed) .....

Geological boundary (defined, approximate, assumed) ...

Shear zone .....

Road (paved, gravel) .....

Dyke (D: diabase ; R: rhyolite ; UM: ultramafic) .....

Mine (abandoned) .....

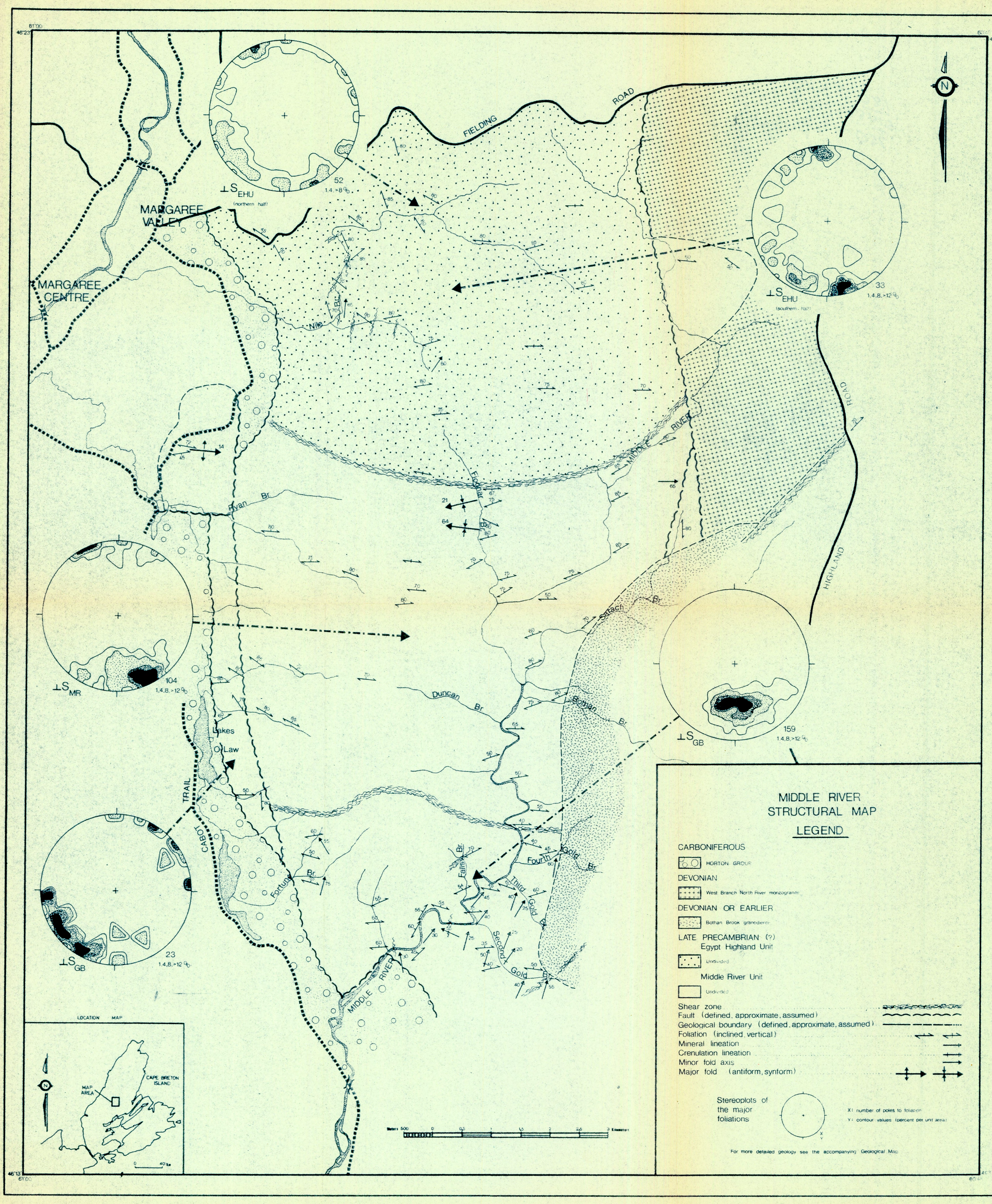

MIDDLE RIVER
STRUCTURAL MAP
LEGEND
CARBONIFEROUS
HORTON GROUP
DEVONIAN
West Branch North River monzogranite
DEVONIAN OR EARLIER
Bothan Brook granodiorite
LATE PRECAMBRIAN (?)
Egypt Highland Unit
Undivided
Middle River Unit
Undivided
Shear zone
Fault (defined, approximate, assumed)
Geological boundary (defined, approximate, assumed)
Foliation (inclined, vertical)
Mineral lineation
Crenulation lineation
Minor fold axis
Major fold (antiform, synform)
Stereoplots of the major foliations
X: number of poles to foliation
Y: contour values (percent per unit area)
For more detailed geology see the accompanying Geological Map
MARGAREE VALLEY
MARGAREE CENTRE
FIELDING ROAD
HIGHLAND ROAD
CABOT TRAIL
MIDDLE RIVER
Nile Br.
Ryan Br.
Duncan Br.
Bothan Br.
Satach Br.
Lakes O'Law
Fortune Br.
Falls Br.
Second Gold Br.
Third Gold Br.
Fourth Gold Br.
⊥S EHU (northern half) 52 1,4,>8 %
⊥S EHU (southern half) 33 1,4,8,>12 %
⊥S MR 104 1,4,8,>12 %
⊥S GB 159 1,4,8,>12 %
⊥S GB 23 1,4,8,>12 %
LOCATION MAP
CAPE BRETON ISLAND
MAP AREA
0 40 km
Meters 500 0 0.5 1 1.5 2 2.5 3 Kilometers
61°00' 46°23'
46°13' 61°00'